Aromatic Transformations Facilitated by 6–Coordination to Ruthenium (II)

LUKE JAMIE WILLIAMS

Durham University
Department of Chemistry

Aromatic Transformations Facilitated by η^6–Coordination to Ruthenium (II)

Luke J Williams

A thesis submitted for the degree of Doctor of Philosophy

July 2022

Abstract

Over the last 70 years the chemistry of η^6-arene transition metal complexes has been extensively developed, with the enhancement of aromatic reactivity through complexation being applied to extensive number of different synthetic targets. On η^6-complexation to a metal, a C_6-aromatic ring becomes much more susceptible to nucleophilic attack (S_NAr), while the deprotonation of both aromatic and benzylic sites is made much more facile than for free arenes. Furthermore, the activating ML_n fragment blocks the face of the aromatic ring it is bound to, meaning any attacks on the ring are inherently directed towards the free face, thus giving some steric control over the reactivity. Since the turn of the millennium, a resurgence in this field of organometallic chemistry has occurred with the realisation of metal-catalysed aromatic transformations *via* transient η^6-coordination of the arene. Through an arene exchange process, the bound transformed aromatic ring can exchange with the starting material to regenerate the initial η^6-arene complex, giving catalytic turnover. In this thesis, four projects exploring the reactivity of η^6-arene complexes of ruthenium(II), their arene exchange and finally ruthenium-catalysed aromatic transformations *via* transient coordination.

The first project described is the attempted nucleophilic fluorination and difluoromethylations of arenes bound η^6- to an activating $[RuCp]^+$ fragment. The complex $[(\eta^6\text{-}C_6H_6)RuCp]^+$ was reacted with a series of different nucleophilic sources of fluoride, with only TBAF exhibiting any sort of reactivity. Due to the presence of moisture in the reaction, addition of a hydroxy group to the ring occurred, resulting in the formation of an η^5-cyclohexadienyl (Meisenheimer) complex, which proved too unstable to isolate, while attempts at *in-situ* oxidation of the ring resulted in decomposition of the complex. Difluoromethylation of the complex $[(\eta^6\text{-}C_6H_5CN)RuCp]^+$ using the reagent CF_2HSiMe_3 in the presence of base and fluoride resulted in *ortho*-addition of a hydroxy group to the bound benzonitrile ring, giving another Meisenheimer complex. Unlike the previous one, this complex was sufficiently stable under ambient conditions to be isolated and characterised, while attempts to oxidise the ring resulted in formation of a free arene, most likely to be 2-cyanophenol.

The next project revolves around an enolate S_NAr reaction of the aromatic ring in the complexes $[(C_6H_5X)RuCp]^+$ (where X = leaving group), resulting in the formation of bound 2-aryl-1,3-diones. The presence of methyl groups *ortho* to the leaving group hindered the reaction significantly, as an increased temperature was required to facilitate S_NAr. Experiments on rings containing multiple different leaving groups were used to establish the chemoselectivity of the

S_NAr on the bound ring, while a broad range of cyclic diones were successfully tested under the reaction conditions. Following the S_NAr transformation, the free aromatic product could be liberated from the ruthenium centre by irradiating an acetonitrile solution of the complex with UV light. While attempts to translate the enolate S_NAr into a process catalytic in ruthenium were unsuccessful, a one-pot stepwise synthesis of the free aromatic product, in which the activating $[RuCp]^+$ fragment could be recycled was achieved.

The arene exchange of the complexes $[(\eta^6\text{-arene})RuCp(*)]^+$ with hexamethylbenzene were investigated and the effects of changing the temperature and irradiating the system were established. Also, the tether-assisted arene exchange of a library of sandwich complexes containing Cp rings functionalised with tethered coordinating groups was explored, and enhanced rates of arene exchange were observed for some of the tether complexes.

Finally, two ruthenium-catalysed aromatic transformations proposed to occur *via* temporary η^6-coordination were explored and optimised. The first was a previously established catalytic S_NAr amination of 4-chlorotoluene, where the complexes bearing tethered coordinating groups were tested for their activity. A stoichiometric study on the S_NAr amination with morpholine proved the existence of the suspected resting state of the catalytic cycle, $[(\eta^6\text{-N(4-tolyl)morpholine})RuCp]^+$. Next, a ruthenium-catalysed hydrodeiodination of aryl iodides was further optimised with shorter reaction times under microwave heating. Further experiments were performed on iodoarenes functionalised with electron-donating or electron-withdrawing groups to obtain insight on the reaction mechanism and infer the nature of charge build-up in the transition state.

Declaration

The work described in this thesis was undertaken at the Department of Chemistry, Durham University between October 2018 and March 2022. All the work reported is my own, except where specifically stated otherwise. No part has previously been submitted for a degree at this or any other university.

Statement of Copyright

Acknowledgements

James Walton. Thank you so much for all your help and guidance over the last 4 years, I wouldn't be half the chemist or person I am today without you. Through all the difficult times when my none of my chemistry was working, your enthusiasm and optimism kept me motivated and believing that it would be worth it in the end. I am extremely proud of everything we have managed to achieve over the course of this project, and I hope you are too; thank you again for making it all possible.

Yunas Bhonoah. I really appreciate supervising me during my placement at Syngenta, I learnt so much in those three months. Thank you for your guidance during that time, in particular for your contributions to the enolate S_NAr project, our paper would not have been possible without you.

Dr Paul McGonigal. Thank you for all the useful and insightful research advice you've given me in group meetings, I really appreciate it. I am extremely grateful for the opportunity to work in your group for a short period, I am still learning so much.

Prof. Martin Bryce. Thank you for giving me the opportunity to work in your group for a short period while I was writing up, I have learned a lot working with you.

Aisha Bismillah. A great housemate, mentor and one of my closest friends. You have been here for almost my whole time in Durham, thank you so much for all the special memories, both on big nights out, watching TV shows together, and just chatting and being there for me when I needed someone to talk to. I can't imagine where I would be without you.

Atreyee Mishra. An amazing labmate and friend, I feel so lucky to have shared my PhD journey with you. Through all the good and scuffed times, late nights in the lab and everything else. Thank you so much for all the advice you given me, both chemistry and general life, and also for helping me become a much better communicator! You have made my PhD experience so much better and for that I'll always be grateful. I wish you all the very best for the future, you're going to do amazing things.

Akkharadet Piyasaengthong (Rak). I really appreciate all the long chats in the lab when I was stuck, your motivation and love for chemistry really inspired me to carry on during the difficult times. Outside the lab, your motivational talks helped me so much with my general life, I will miss our regular chats about football and comparing our fantasy teams.

CG108 & CG235. Thank you to all the friends I have made in the Walton, McGonigal and Avestro groups, both current and previous, for all your continued support over the years. In-particular I'd like to thank Beth, David, Marcus, Promeet, Will, Ho Chi, Juliet, Senthil, Burhan, Rob, Ash, Andrew, Abhijit, Phil, and Kas. I wish you all the very best in the future.

CG104. Thank you to Rebecca, Saliha, Suman and Luke from Bryce group for all the support during my short stay in the lab. I learned so much during my time in CG104 and have so many great memories both in and out of the lab, here's to making more soon!

Durham chemistry analytical staff. I would like to thank all the members of the analytical services at Durham, in particular Juan Aguilar, Dmitry Yufit, David Parker and Peter Stokes. My PhD has relied heavily on analytical techniques such as NMR, mass spec and X-ray crystallography, thank you all for maintaining the analytical services and making them so easily accessible.

Bonus Werthers. The late-night calls, cube weekends, trips to events, bizarre griefs, visits to Bob's Tavern and so much more. I feel so lucky to have met such an amazing group of friends through going to Pokémon card tournaments and I can't imagine my life without you all. Special thanks to Tim also for helping to plot some of the data used in this thesis, and for always being there.

My loving Family. My siblings, Ellie, Heidi and Rhys. Thank you for all your love and support over the years, I really do appreciate it, even if we don't get to see each other often. Mum, Dad and Nanny, I wouldn't be where I am today without your eternal love and guidance. I love you all so much.

List Of Abbreviations

Ac	acetate
Acac	acetylacetonate anion
Ad	adamantane
Ar	aryl
Bu	butyl
Boc	tert-butyloxycarbonyl
CMD	concerted metalation deprotonation
COD	cyclooctadiene
COSY	correlation spectroscopy
Cp	cyclopentadiene
Cp*	pentamethylcyclopentadiene
d	doublet
DBU	1,8-diazabicyclo[5.4.0]undec-7-ene
DBN	1,5-diazabicyclo[4.3.0]non-5-ene
DCM	dichloromethane
DCE	dichloroethane
dd	doublet of doublets
ddd	doublet of doublets of doublets
dq	doublet of quartets
DDQ	2,3-dichloro-5,6-dicyano-1,4-benzoquinone
ddq	doublet of doublets of quartets
ddt	doublet of doublets of triplets
DMF	dimethylformamide

DFT	density functional theory
DIPEA	diisopropylethylamine
DPPPent	1,3-bis(diphenylphosphino)propane
dt	doublet of triplets
EDG	electron donating group
ESI	electrospray ionisation
Equiv	equivalent
Et	ethyl
EWG	electron withdrawing group
FG	functional group
High Res	high resolution
HOMO	highest occupied molecular orbital
HPLC	high performance liquid chromatography
hν	irradiation
In situ	in the original place
k_{obs}	observed rate constant
LUMO	lowest unoccupied molecular orbital
m	multiplet
m	meta
Mass Spec	mass spectrometry
Me	methyl
MW	microwave
NMR	nuclear magnetic resonance
NOESY	nuclear Overhauser effect spectroscopy
OMs	mesylate

ORTEP	oak ridge thermal-ellipsoid plot program
o	*ortho*
p	para
PET	positron emission tomography
Ph	phenyl
Pr	propyl
q	quartet
qdd	quartet of doublets of doublets
RT	room temperature
s	singlet
sept.	septet
SM	starting material
SET	single electron transfer
S_EAr	electrophilic aromatic substitution
S_NAr	nucleophilic aromatic substitution
t	triplet
TBAF	tetrabutylammonium fluoride
TEMPO	2,2,6,6-tetramethyl-1-piperidinyloxy
OTf	triflate
OTs	tosylate
TIPS	triisopropylsilyl ether
tt	triplet of triplets
td	triplet of doublets
tdd	triplet of doublet of doublets
TFA	trifluoroacetic acid

THF	tetrahydrofuran
TMS	trimethylsilane
UV	ultraviolet
Δ	Heating
α	alpha
δ	delta
η	eta
π	pi
σ	sigma

Table of Contents

Chapter 1:

Introduction to Transition Metal π-Arene Complexes and Their Chemistry

1.1. The Chemistry of Benzene Rings

Aromatic rings have been comprehensively studied for several hundred years, with their properties and reactivity being of high significance in both civilisation and nature. For example, the four small-molecule pharmaceuticals shown in figure 1.1 are amongst the best-selling pharmaceuticals in 2020, and each contains at least one substituted benzene ring. Consequently, new processes by which aromatic rings may be functionalised are always highly desirable.

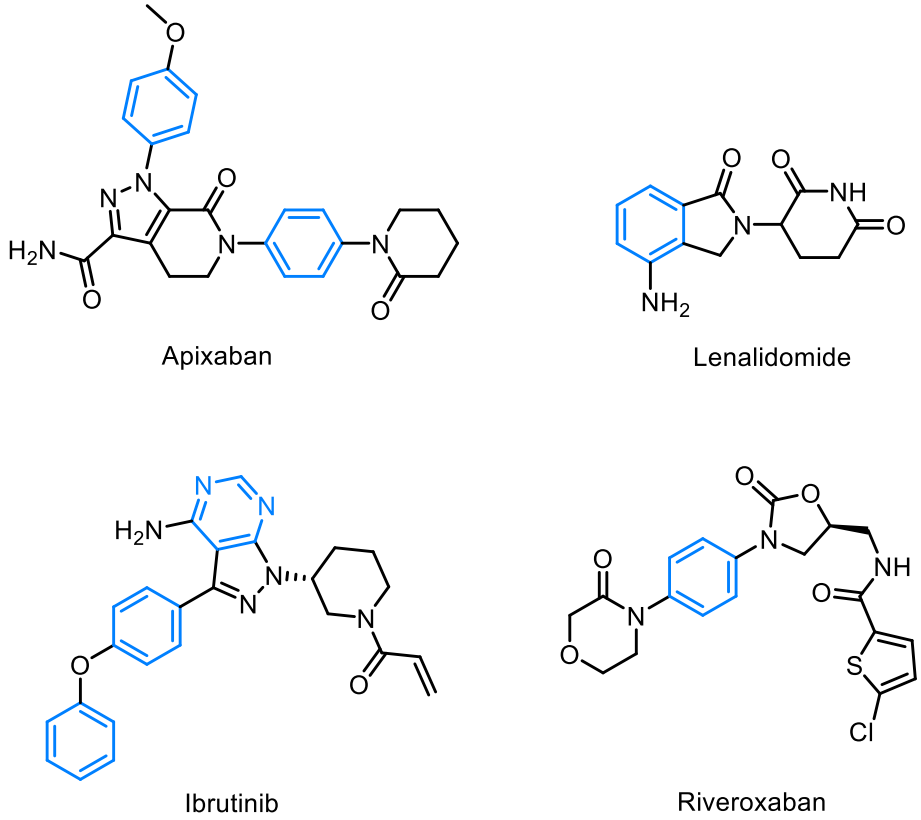

Figure 1.1. *Chemical structures of the pharmaceuticals Apixaban (anticoagulant), Lenalidomide (treatment of multi myeloma and myelodysplastic syndromes), Ibrutinib (anticancer treatment) and Riveroxaban (Anticoagulent).*

Due to the delocalised electron density both above and below the plane of a benzene ring, they are usually very electron-rich systems, leaving them prone to attack by electrophiles. A common transformation which capitalises on this property is electrophilic aromatic substitution (S_EAr), which proceeds via temporary loss of aromaticity in the ring. The first step of the S_EAr mechanism (figure 1.2) involves addition of the electrophile to the ring, resulting in formation of a carbocation, which is stabilised by resonance involving the two remaining C=C double

bonds. A simple deprotonation of the cation facilitates the restoration of aromaticity in the ring, and the final substituted product is formed.

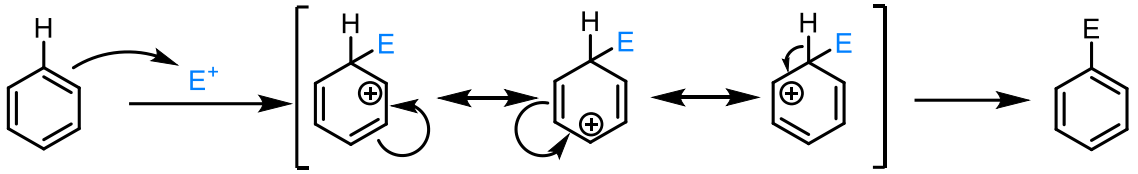

Figure 1.2. *General mechanism of electrophilic aromatic substitution (S_EAr).*

Because of their simplicity and versatility, S_EAr reactions have been widely carried out to add many different functionalities to benzene rings, such as halides, alkyl and acyl groups. Moreover, certain functional groups can be used to control the regioselectivity of an S_EAr reaction, with electron-donating groups (EDGs) generally promoting *ortho*/*para* substitution and electron-withdrawing groups (EWGs) promoting *meta*-substitution. Another common method by which functionalities can be added to benzene rings is nucleophilic aromatic substitution, S_NAr. This process occurs via attack of a nucleophile on the ring to form a Meisenheimer intermediate, followed by elimination of a leaving group to give the aromatic product. Benzene rings are not typically electrophilic due to the delocalised electron density above and below the plane of the ring repelling any incoming nucleophiles. Furthermore, the C-X bond, where X is a leaving group, must be sufficiently polarised to facilitate nucleophilic attack on the ring. As a result, S_NAr reactions are typically limited to electron-poor phenyl rings which bear one or more electron withdrawing groups (EWGs), which increase the polarity of the ring, as well as stabilising the negatively charged Meisenheimer intermediate which forms (figure 1.3).

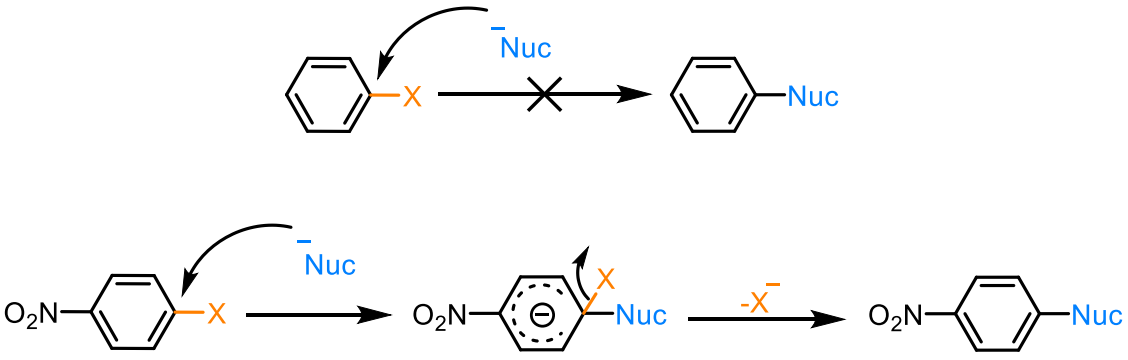

Figure 1.3. *General mechanism of nucleophilic aromatic substitution (S_NAr), facilitated by the presence of a covalent electron-withdrawing group (EWG).*

However, these electron-withdrawing groups may not be desired in the target compound, meaning further steps must be taken to remove them following the S_NAr reaction. For example, a nitro group is a strong EWG which is excellent at promoting S_NAr processes, but removal requires multiple steps, including reduction to an amine followed by deamination, meaning the overall yield and efficiency of the synthesis are both impacted. As a result, a functional group which facilitates ring transformations and can be added or removed selectively is highly desirable. One such functionality which meets these criteria are π-arene complexes of metals.

1.2. Properties and Reactivity of Metal π-Arene Complexes

While π-arene complexes of metals have been known for over 100 years, their structure and properties were not fully understood until E. O Fischer synthesised the complex, bis(benzene)chromium, $[(\eta^6\text{-}C_6H_6)_2Cr]$ in 1955.[1] Since this study was published, complexes of this nature have received intense synthetic interest due to the profound change a metal centre has on the reactivity of the aromatic ring. Due to the nature of the η^6-bond, metal centres have an electron-withdrawing effect on the π-system of the aromatic ring, like having one or multiple covalent electron-withdrawing groups mentioned above. Consequently, π-coordinated arene rings are susceptible to attack from nucleophiles, while also being deactivated towards electrophilic attack. Additionally, π-coordination to a metal enhances the ring's ability to stabilise a negative charge, promoting formation of the Meisenheimer intermediate of the S_NAr process, as well as making deprotonation of both the aromatic and benzylic positions of the ring more facile (figure 1.4). Finally, binding of a metal fragment to one face of an aromatic ring blocks that face from reagents, and any attacks on the ring are directed to the free face.

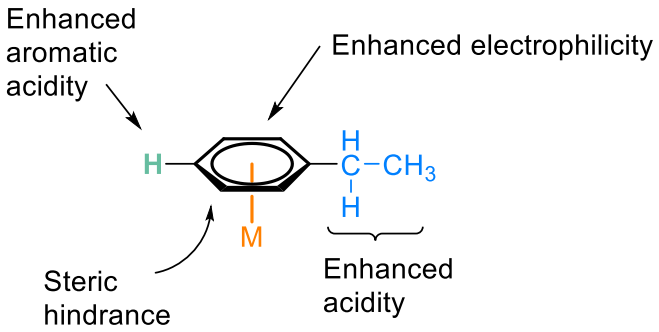

Figure 1.4. *Enhancement of reactivity on η^6-coordination of an arene to a metal centre*

The η^6-bond between an aromatic ring and a metal centre is naturally strong. The molecular orbital interactions between the π-system of an aromatic ring and the d-orbitals of a transition metal are shown in figure 1.5 below.

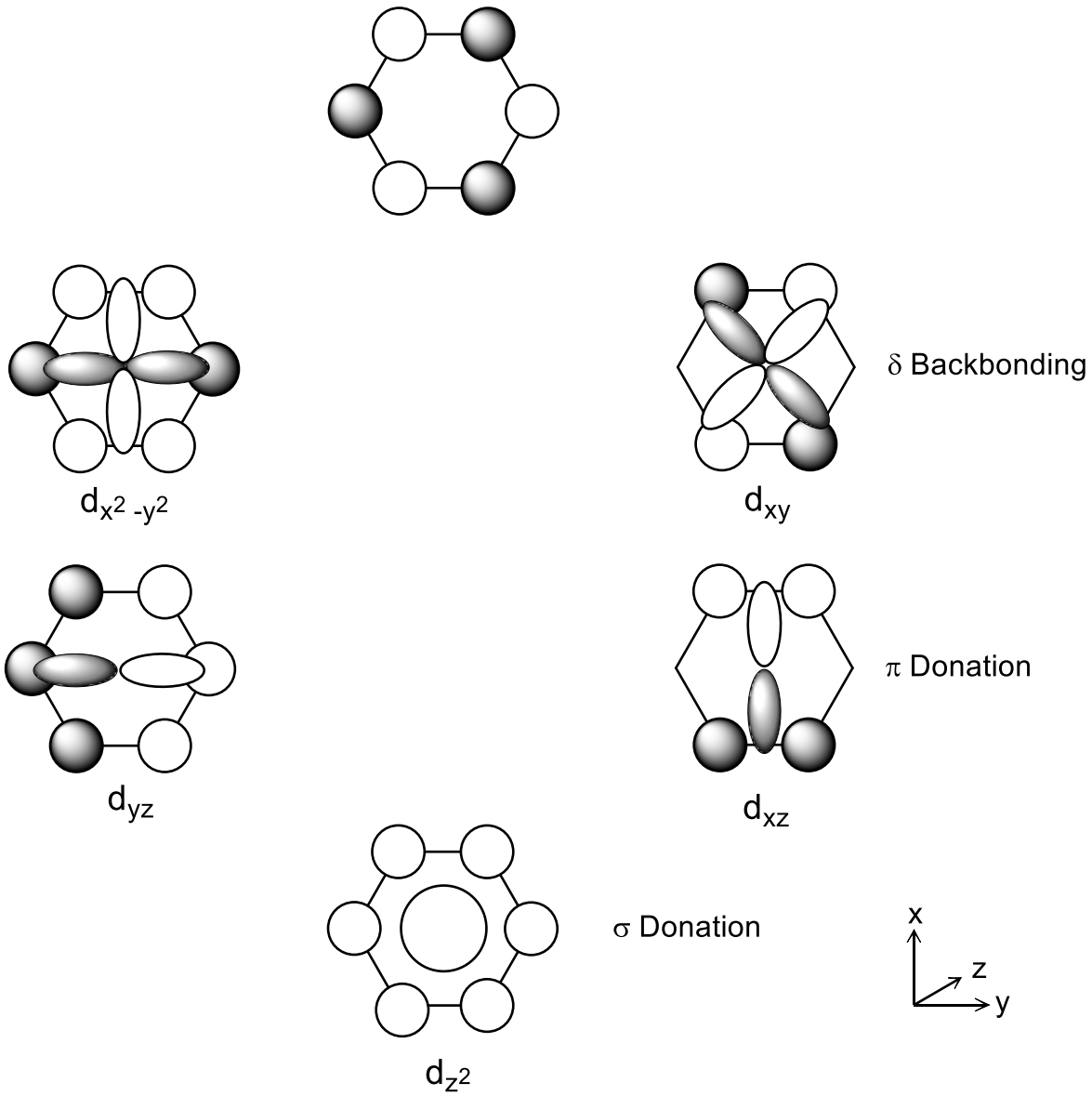

Figure 1.5. *Bonding interactions between the molecular orbitals of the π-system in benzene and d orbitals of a transition metal*

Firstly, the strongest interaction is the σ-donation from the lowest energy molecular orbital of benzene to a metal's d_z^2 orbital. Next, the highest occupied molecular orbitals (HOMOs) donate to the corresponding d orbitals (d_{xz} and d_{yz}) in a π-interaction. Finally, a weaker δ-back bonding interaction exists between the filled d orbitals of the metal ($d_x^2{}_{-y}^2$ and d_{xy}) and the lowest unoccupied molecular orbital (LUMO) of the aromatic ring. In combination, these three

interactions create a very strong bond between the arene and the metal, with the more significant donations being from the ring to the metal, hence reduced electron density remaining on the ring.

1.3. Reactions of Arene π-Complexes

In this section, the broad range of transition metal π-arene complexes and their utility towards organic synthesis will be discussed. Until now, many reviews have discussed the synthetic and catalytic relevance of various complexes using Group 6-9 metals,[2–5] with a number of examples outlined herein.

1.3.1. Reactions Using Chromium and Molybdenum (Group 6)

Generally, π-complexes of Group 6 metals are synthesised as tricarbonyl M(0) complexes, with the general formula [(η^6-arene)M(CO)$_3$] (where M = Cr, Mo). Widespread synthetic methodologies of such complexes include thermolysis of [M(CO)$_6$] in the presence of the desired arene, or via arene exchange of precursor π-arene compounds (figure 1.6),[6,7] with the latter preferred for the installation of electron-poor arenes such as nitrobenzene, where direct thermolysis is not possible.

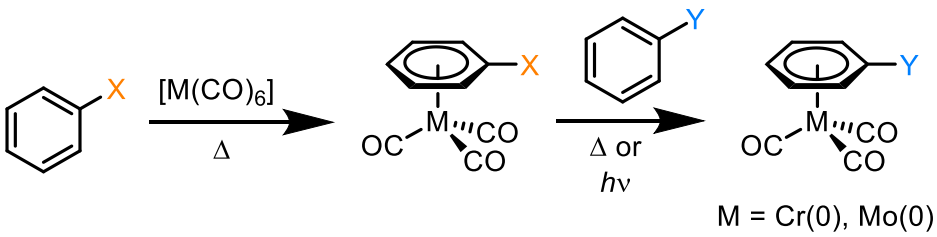

Figure 1.6. *Thermolytic synthesis of the complex [(η^6-arene)M(CO)$_3$] and synthesis via arene exchange, where M = Cr(0), Mo(0)*

Due to the facile and relatively cheap synthesis of its π-arene complexes, chromium is one of the most extensively used metals in the transformation of aromatic rings. One of the first such examples of an aromatic transformation was a nucleophilic addition to η^6-bound styrene rings, reported by Semmelhack in 1980 (figure 1.7).[8] Such addition reactions were of interest due to the relatively poor yields of previous β-addition reactions to η^6-arenes.

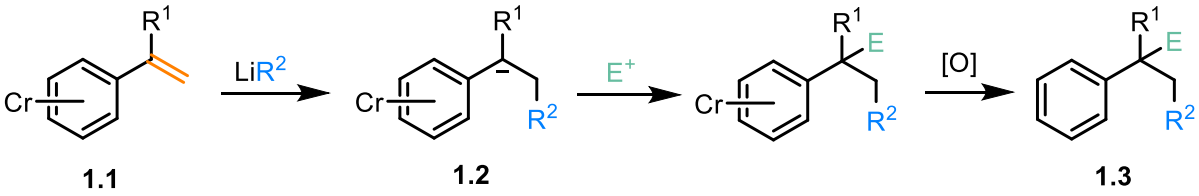

Figure 1.7. *General reaction procedure for the nucleophilic addition to styrene, trapping with an electrophile and then oxidation to give the free arene.*

In this example, the reaction occurs *via* addition of the 'R⁻' nucleophile to the alkene bond in Cr complex **1.1**. The resulting anionic intermediate **1.2** is stabilised by the presence of the electron-withdrawing $Cr(CO)_3$ fragment. Addition of an electrophile, followed by oxidation to remove the metal gave the racemic phenyl alkane **1.3** in moderate to high yields, with the reaction showing high tolerance with respect to several different lithiated alkyl nucleophiles and trapping electrophiles. Such a transformation illustrated a new and efficient way of forming new C-C bonds close to aromatic rings.

In 1979, K.C Nicolaou and co-workers demonstrated the lithiation of a π-arene chromium complex (**1.4**, figure 1.8A). Subsequent addition of a ketone electrophile to the η^6-bound ring and quenching of the resultant carbanion generated intermediate **1.5**. Following this, treatment with lithium diisopropylamide (LDA) generated a nucleophilic carbanion centre adjacent to the nitrile group of the alkyl chain, which resulted in ring closure and dearomatization of the η^6-bound arene.[9] The ring was rearomatized and liberated from the Cr centre on oxidation with elemental iodine to generate the final tetralin derivative **1.6** in a yield of around 50%. In the same work, a similar lithation procedure was used to ring open γ-butyrolactone (figure 1.8B), then spontaneous ring closure occurred via S_NAr displacement of fluoride at the adjacent carbon in the aromatic ring. Rearomatization *via* oxidation with iodine to give the resulting free heterocycle **1.7** in a yield of 48%.

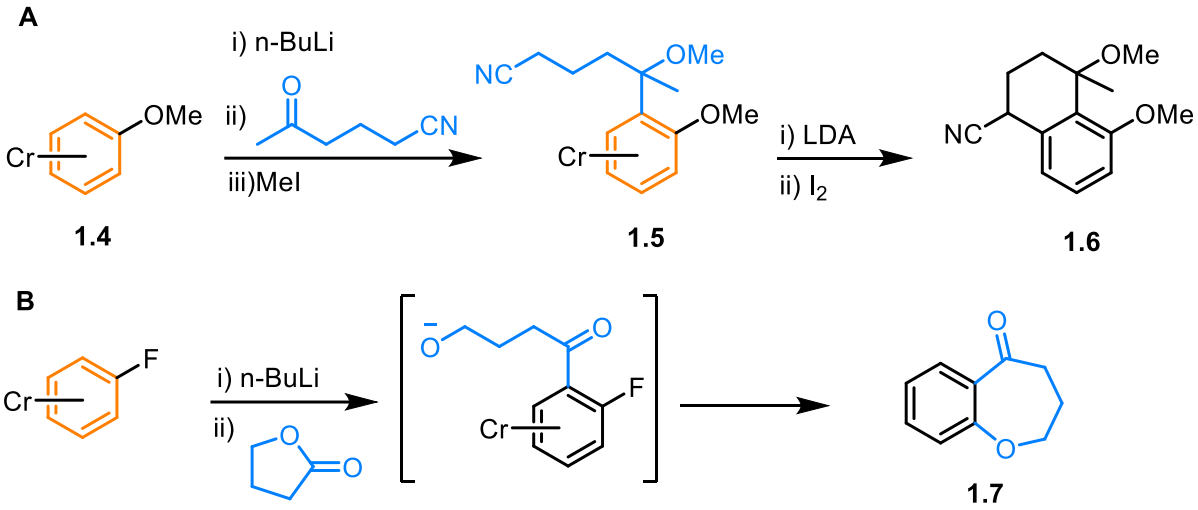

Figure 1.8. *(A). Lithiation and alkylation of anisole bound η^6 to Cr, followed by cyclisation of the arene and oxidation to form the free bicyclic compound. (B). Lithiation of η^6 bound fluorobenzene and subsequent ring opening of γ-butyrolactone, then spontaneous ring closure by nucleophilic aromatic substitution.*

In a similar process, Houghton demonstrated another intramolecular cyclisation via S_NAr of an arene bound η^6- to a Cr(0) centre (figure 1.9). Here, a bound arene bearing a linear propyl alcohol chain (**1.9**) was treated with a strong base, generating the alkoxide nucleophile. Ring closure *via* S_NAr displacement of the fluorine resulted in the formation of the expected η^6-bound heterocycle **1.10**. Oxidation gave the free chroman derivative **1.11** in an overall yield of 75% (figure 1.19).[10]

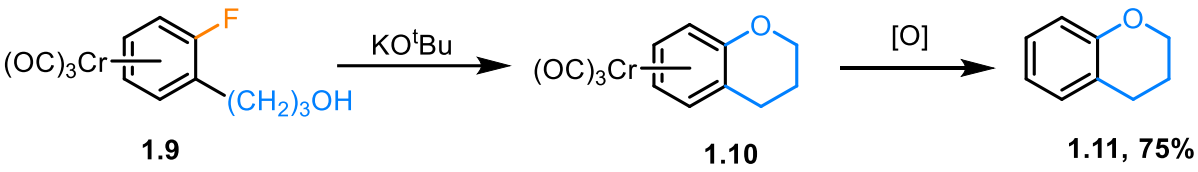

Figure 1.9. *Synthesis of chroman by Houghton et al., via deprotonation of the hydroxy group followed by intramolecular S_NAr and finally oxidation to give the free arene.*

More recent developments in the reactivity of these triscarbonyl chromium(0) aryl halide complexes have revolved around aromatic C-H activation using bimetallic catalysis. In 2013, Larossa and co-workers published a procedure for the C-H arylation of chromium π-aryl fluorides (**1.12**), facilitated by the presence of a Pd(0) catalyst (figure 1.10).[11] The C-H activation process was initially proposed to be a Pd(II)-mediated concerted metalation-deprotonation (CMD) step, though later studies indicated that the CMD was actually facilitated

by an Ag(I) species (figure 1.10B).[12] For several different aryl fluorides and aryl iodides, the Pd-catalysed arylation reaction gave the coupled products (**1.13**) in generally excellent yields.

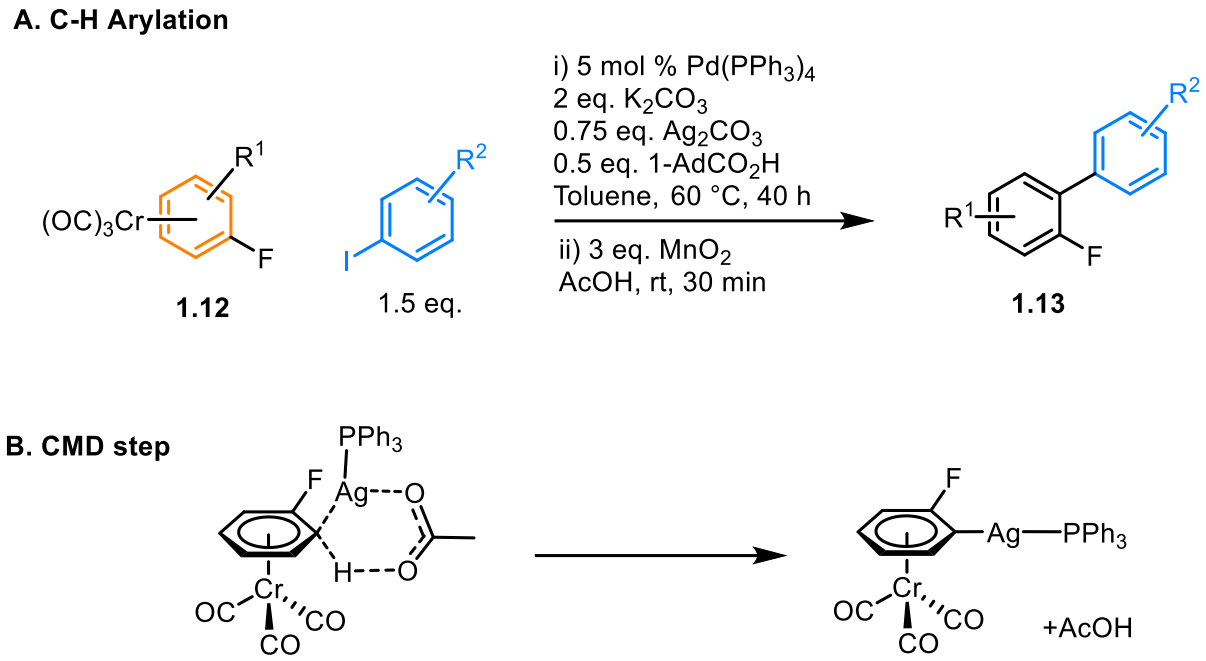

Figure 1.10. *C-H arylation of fluoroarenes coordinated η⁶- to Cr(0) and the Pd(II)-mediated concerted metalation-deprotonation (CMD) step of the arylation.*

A follow up study by the same research group was done to test the reactivity of a series of Cr η⁶-anisoles towards the Pd-catalysed arylation mentioned above. Similar to the previous work, the C-H arylation occurred *ortho* to the methoxy directing group in moderate to excellent yields for a number of methoxy-substituted arenes (**1.14**, figure 1.11).[13] Furthermore, η⁶-coordination to chromium here not only increased the reactivity of the arene, but also made the arylation much more selective for *ortho*-arylation over *meta*- or *para*-, compared to the C-H activation of a free arene.

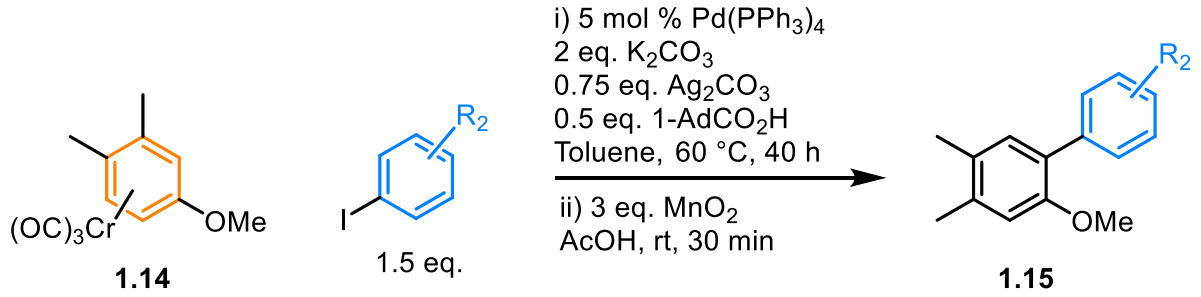

Figure 1.11. *C-H arylation of methoxy-substituted arenes reported by Larrosa et al.*

Molybdenum π-arene complexes are not as widely studied as their chromium counterparts due to several reasons. One limitation of Mo is that complex synthesis is generally more difficult due to the requirement of longer reaction times and higher temperatures for the η^6-coordination of an arene,[14] as well as their sensitivity to air. Furthermore, arenes bound to Mo are much more labile than Cr, and arene exchange rates for Mo π-arene complexes at 60 °C are comparable to that of analogous Cr complexes at 150 °C.[15] This property has facilitated the synthesis of a much greater range of π-arene complexes bound to molybdenum, although the stability isn't as high as with Cr, which further limits the development of the chemistry of Mo η^6-arene complexes.

Despite the issues, Kundig reported a reaction in which two new carbon-based substituents were introduced into the same ring in the Mo π-arene complex **1.16** via a trans-addition across an alkene bond (figure 1.12).[16] The first step of the process is the nucleophilic attack of a lithium dithiane on the ring, resulted in formation of an η^5-coordinated Meisenheimer-type anion **1.17**. Introduction of an alkene into the system results in displacement of one CO ligand, resulting in **1.18**, a Mo complex bound to both an η^3-allyl and η^5-cyclohexadienyl ligand. A CO atmosphere allows the complex to undergo an intramolecular reaction in which the allyl and cyclohexadienyl ligands react to form a free, doubly substituted cyclohexadiene ring **1.19**, in a stereoselective manner.

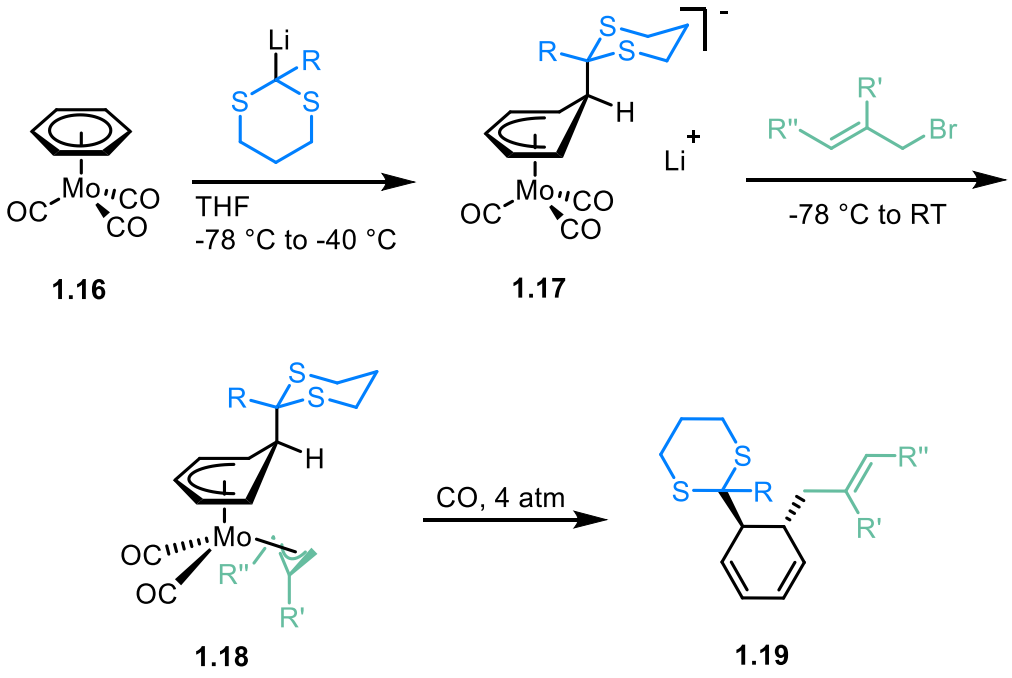

Figure 1.12. *Selective trans-addition of two substituents across a benzene double bond in the complex [(η^6-benzene)Mo(CO)$_3$].*

1.3.2. Reactions Using Manganese, Rhenium and Technetium (Group 7)

Similar to the Group 6 metals, π-arene complexes of Mn(I) are generally synthesised as half-sandwich complexes of the formula $[(\eta^6\text{-arene})Mn(CO)_3][X]$ (where X = PF_6 or BF_4) from the thermolysis of $[Mn(CO)_5]$, or via photolysis of an existing π-arene complex. However, due to the strongly electron-withdrawing nature of the $[Mn(CO)_3]^+$ fragment, electron-poor arene rings containing substituents such as nitro-, α-keto- or trifluoromethyl- groups are not able to form stable complexes, limiting the scope of complexes which can be synthesised. Generally, π-arene complexes of Mn(I) are very reactive towards attack by many different nucleophiles, such as Grignard reagents, organolithiums, hydrides, amines and alkoxides. For instance, the Pearson group have studied extensively the synthesis of aryl ethers from aryl chlorides bound to the cationic Mn(I) tricarbonyl fragment (**1.21**),[17–20] and have applied these reactions towards the synthesis of various derivatives of ristocetin-A (**1.22**, figure 1.13), which is used as an antibiotic drug. [20,21]

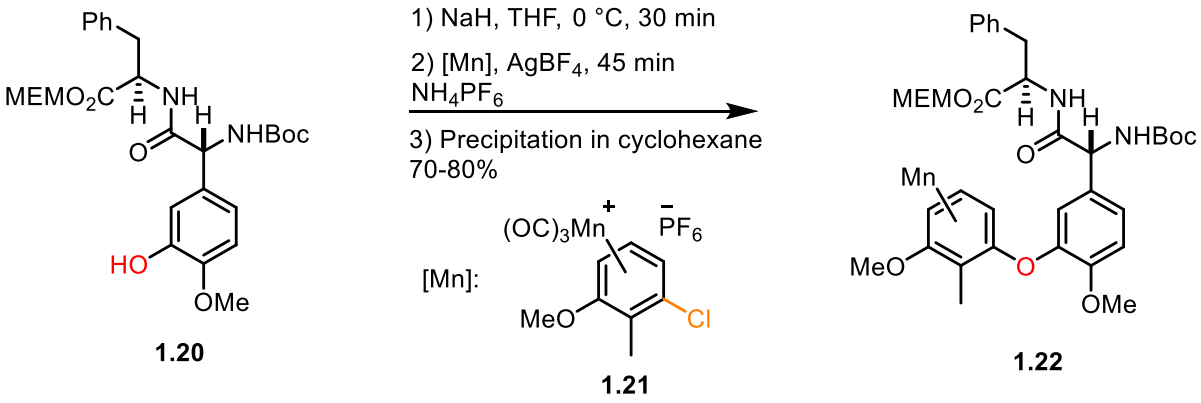

Figure 1.13. *Synthesis of an aryl ether, facilitated by coordination of an aryl chloride to* $[Mn(CO)_3]^+$*, modified by Pearson et al.* [20, 21]

A key advantage of the highly enhanced electrophilicity of arene rings bound to an $Mn(CO)_3^+$ fragment is that the η^5-Meisenheimer intermediate, formed by addition of a nucleophile to the ring, is stable enough to isolate and characterise. This opens such complexes to not only substitution reactions, but addition reactions as well. Often, multiple addition reactions are possible on the same η^5-bound ring. One such example of this was reported by Sweigart *et al.* in 1982.[22] In this work, the aromatic ring in complex **1.23** was subjected to attack by an alkyl Grignard reagent, resulting in formation of a neutral η^5-cyclohexadienyl complex (**1.24**, figure

1.14). To activate this complex towards further nucleophilic attack, one of the CO ligands was replaced with NO^+, resulting in formation of cationic complex **1.25**, where the electron-withdrawing effect of the metal fragment had been increased. Exposure of the reactivated Mn(I) complex **1.25** to various nucleophiles resulted in formation of η^4-cyclohexadiene complexes **1.26A** and **1.26B**, whereas reaction $P(OMe)_3$ resulted in complex **1.27** *via* ligand substitution.

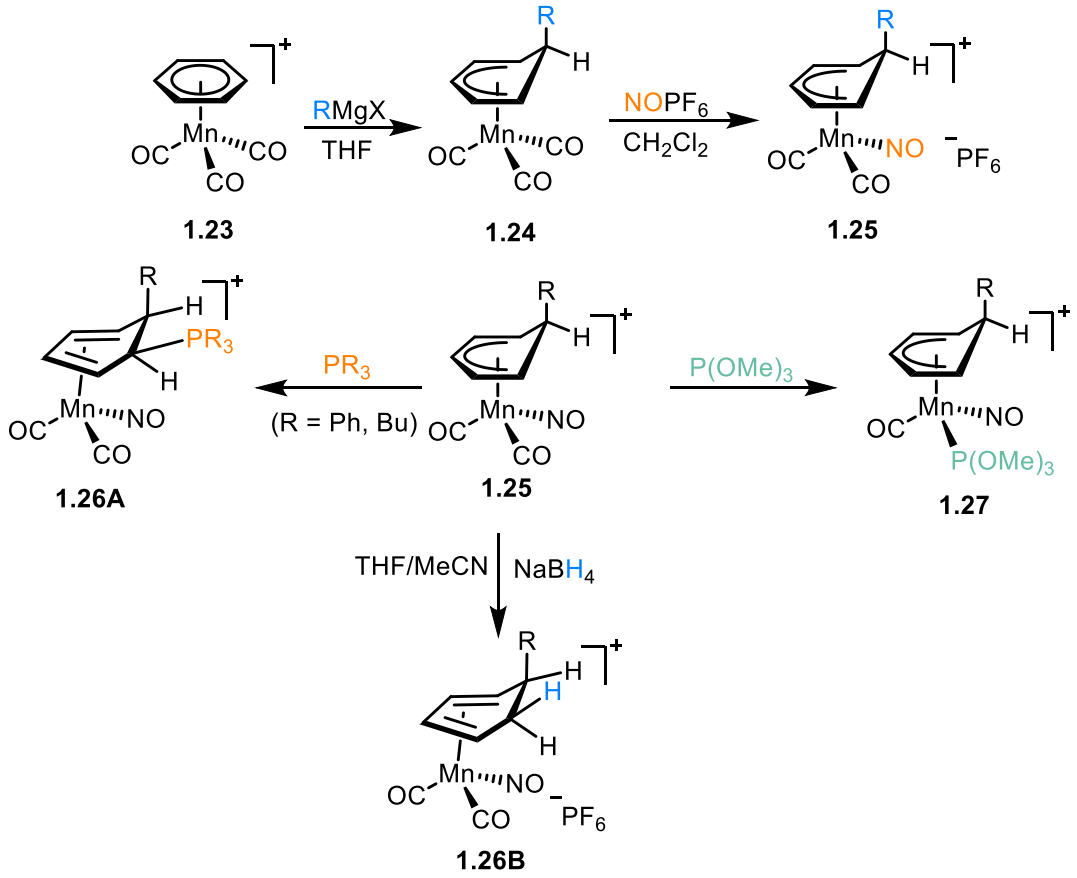

Figure 1.14. *Formation and reactivity of a Mn(I) η^5-Meisenheimer intermediate, reported by Sweigart et al.*

In a more recent study, Rose and co-workers used an $[\eta^6$-arene$)Mn(CO)_3]^+$ framework to facilitate the enantioselective syntheses of substituted cyclohexenones from a series of *meta*-substituted anisole derivatives.[23] Coordination of a 1,3-disubstituted arene to $[Mn(CO)_3]^+$ results in formation of a pair of complexes (**1.28**) which exhibit planar chirality. Reaction of these complexes with enantiopure (D)-(+)-camphor and LDA forms a pair of diastereomeric η^5-Meisenheimer complexes (**1.29**), which could be separated using chromatography (figure 1.15A). Removal of the camphor auxiliary by reacting with $AgBF_4$ and $SiMe_3Cl$ resulted in the re-aromatization of the bound ring, giving each precursor complex as a separated enantiomer,

which could both be converted to their enantiopure cyclohexenones within 3 steps. In another study, the reaction of a variety of different nucleophiles to Meisenheimer complex **1.30** resulted in addition to the position adjacent to the sp^3 carbon (**1.31**, figure 1.15B).[24] These η^4-cyclohexadiene complexes were then converted to a series of chiral cycohexenones (**1.32**) *via* reaction with $FeCl_3$ in acid. Another related report demonstrated the synthesis of a series of stemofurans via the nucleophilic substitution of hydrogen in complexes of the form $[(\eta^6\text{-arene})Mn(CO)_3]^+$ with benzofuran. [25]

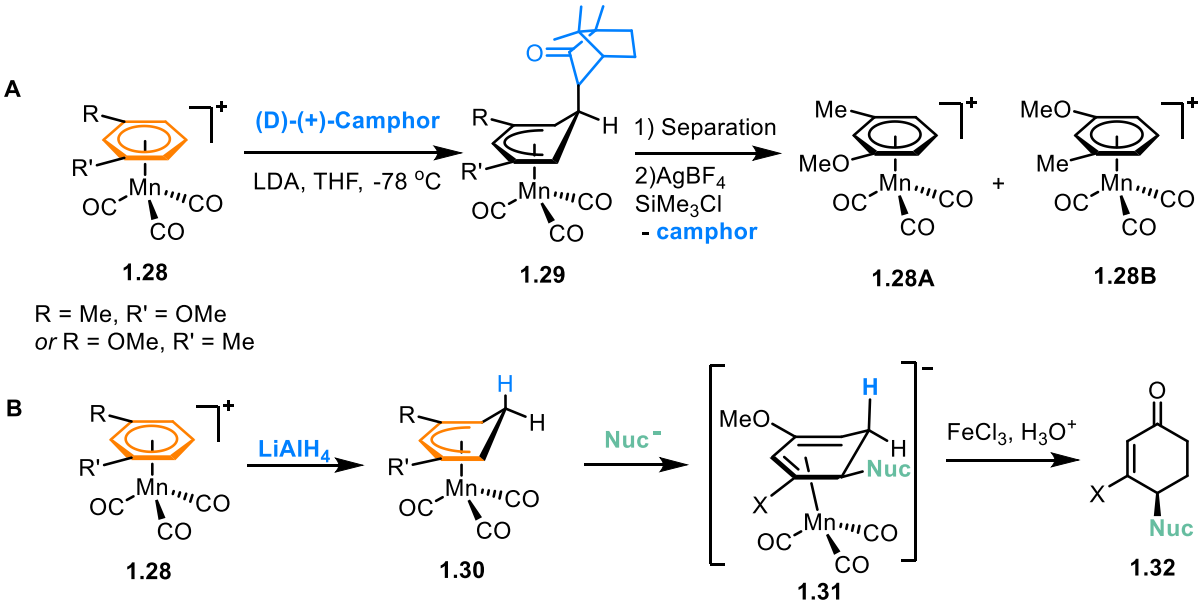

Figure 1.15. *Resolution of chiral Mn(I) π-arene complexes, and subsequent conversion into enantiopure substituted cyclohexanones*

Unlike their Mn(I)-based counterparts, there are very few examples of π-arene complexes of Tc(I), with their development limited by the radioactivity and short half-life of ^{99}Tc, although its sandwich complexes have been studied for their activity in biomimetic imaging.[26] In a rare example by Alberto and co-workers, a S_NAr hydroxylation of the sandwich complex $[(\eta^6\text{-}C_6H_5Br)Tc(\eta^6C_6Me_6)]^+$ (**1.33**, figure 1.16A) was described, resulting in formation of the η^6-phenol Tc complex **1.34**.[27] The analogous Re sandwich complex **1.35** was also subjected to the hydrolysis conditions, where it was found to undergo a ring contraction, rather than substitution, when a high concentration of hydroxide was used. A mechanism for such a transformation was proposed based on the positions of H/D exchange in a deuterated experiment. First, attack of OD^- on the ring in complex **1.35** takes place to give the coordinated Meisenheimer complex **1.36**, where H/D exchange occurs in the positions adjacent to the quaternary carbon. The final step was found to be dependent on the relative hydroxide

concentration. When $[OD]^-$ was high, ring contraction occurred, resulting in an η^5-coordinated cyclopentadienyl ring bearing an α-keto group (**1.37**). However, a low concentration of $[OD]^-$ resulted in formation of the phenol complex **1.38**. It is also worth noting that all ring contraction attempts on the coordinated phenol ring were unsuccessful, even under forcing conditions.

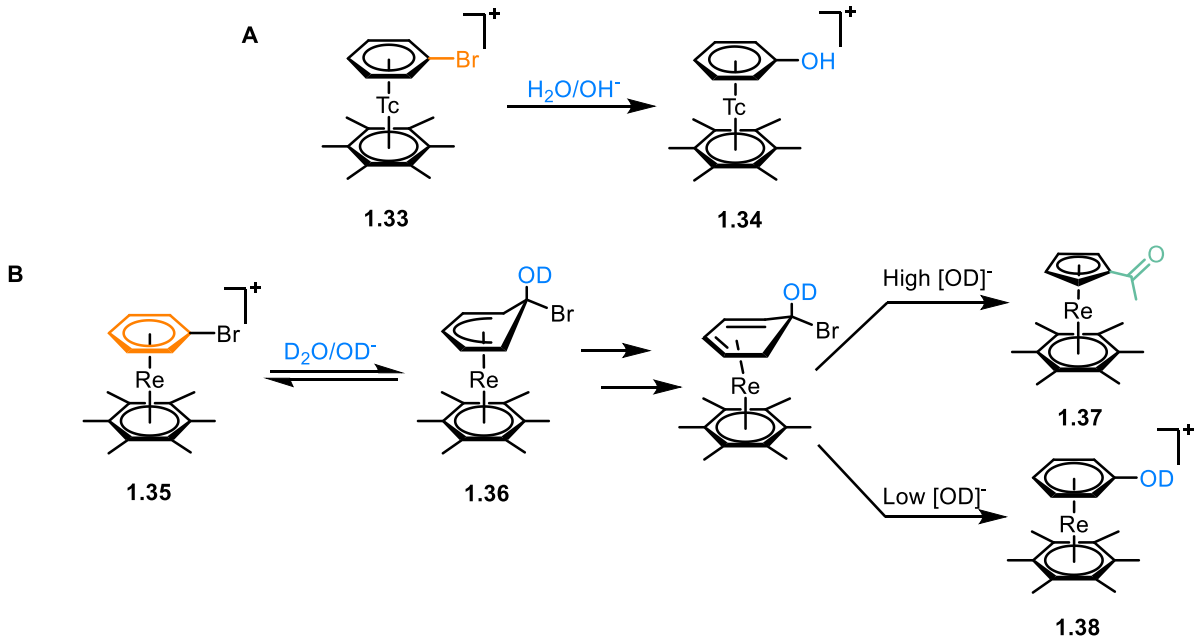

Figure 1.16. *A) S_NAr hydroxylation of $[(\eta^6\text{-}C_6H_5Br)Tc(\eta^6\text{-}C_6Me_6)]$ and B) Nucleophilic hydroxylation of $[(\eta^6\text{-}C_6H_5Br)Re(\eta^6\text{-}C_6Me_6)]$, followed by either elimination of Br^- to form the S_NAr product or ring contraction, depending on hydroxide concentration.*

In a more recent study, the sandwich complex $[Re(\eta^6\text{-}C_6H_6)_2]^+$ (**1.39**) was functionalised with a polypyridyl group, via lithiation of the bound ring with LDA, followed by nucleophilic attack on the keto group of the polypyridyl compound (**1.40**, figure 1.17).[28] Coordination of the catalytically active metal, Co(II), to the polypyridyl moiety of **1.40** gave rise to a bimetallic complex **1.41**, which was active in the photocatalytic reduction of protons to H_2 gas. Here, the presence of a Re sandwich enhanced catalytic performance by adding further structural support and stability, while also increasing the aqueous solubility of the complex and adding further resistance to deactivating redox pathways.

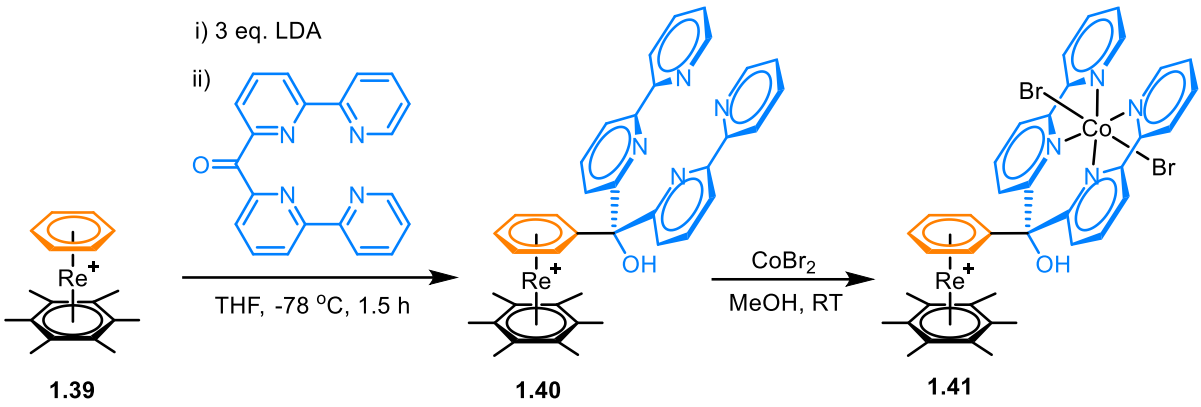

Figure 1.17. *Functionalisation of benzene in $[Re(\eta^6\text{-}C_6H_6)_2]^+$, followed by synthesis of a bimetallic Re-Co catalyst*

1.3.3. Reactions Using Iron and Ruthenium (Group 8)

π-Arene complexes of the Group 8 metals are usually synthesised as sandwich compounds, with the general formula $[(\eta^6\text{-arene})M(\eta^5\text{-cyclopentadienyl})]^+$ (where M = Fe, Ru). Synthesis of Fe complexes can be quite a challenging process since it usually requires the use of ferrocene as the source of $FeCp^+$, with a strong Lewis acid, such as $AlCl_3$, necessary to remove one of the Cp rings. Presence of the Lewis acid makes the synthesis of complexes with alkyl-substituted arenes difficult, due to the competing Friedel-Crafts rearrangements, while electron-poor and heteroarenes are not tolerated under these harsh reaction conditions at all, making the available scope of complexes extremely narrow. As an alternative, Kundig proposed the synthesis of such complexes via $[(\eta^6\text{-arene})FeCp]$, where the arene is a weakly binding polyaromatic such as pyrene, which can be converted to otherwise inaccessible complexes via arene exchange.[29] More recently, Driess and co-workers evaded the use of ferrocene as a precursor by synthesising an Fe(0) complex, $[(\eta^6\text{-arene})Fe^0L]$ (**1.42**, where L = bulky chelating 1,1'-bis(silylenyl) ferrocene moiety), via iron(II) halide salts under reducing conditions (figure 1.18).[30]

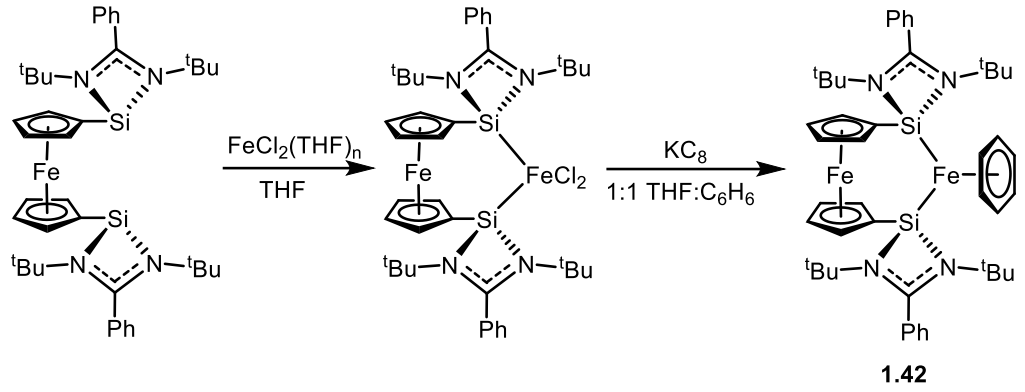

Figure 1.18. *Synthesis of an Fe(0) π-benzene complex from $FeCl_2$ and a disilenylferrocene ligand.*

In contrast to iron, π-arene complexes of ruthenium of the general formula $[(\eta^6\text{-arene})RuCp]^+$ are very easily synthesised, mainly from one of two main routes. The first pathway is from reacting the commercially available piano-stool complex **1.43**, with an arene in a non-coordinating, non-aromatic solvent, resulting in formation of the desired Ru sandwich complex **1.44** (figure 1.19A). This direct synthetic pathway tolerates any arenes, including electron-poor aromatics which are unusable in most other methods.[31,32] The second pathway is possible by reacting the dimeric chloro-bridged complex **1.45** in the presence of coordinating ligands or a source of Cp^- and a polar solvent (figure 1.19B). This reaction is also very mild and high yielding in complexes of the formulae $[(\eta^6\text{-arene})RuL_2Cl]^+$ (**1.46**) or $[(\eta^6\text{-arene})RuCp]^+$(**1.44**),[33,34] but is limited by the small number of commercially available dimer precursors.

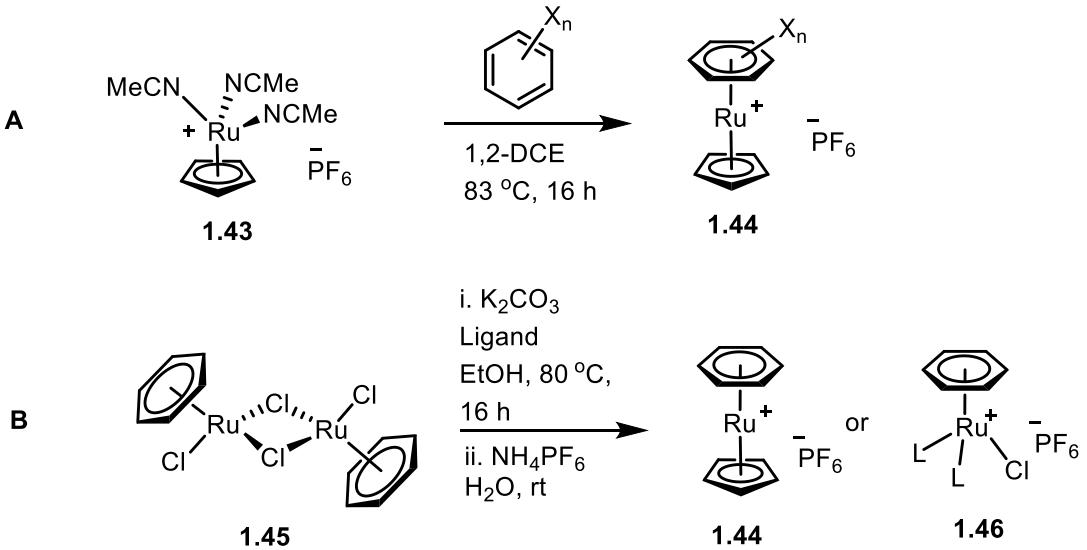

Figure 1.19. *Synthesis of Ru complexes, $[(\eta^6\text{-arene})RuCp][PF_6]$, from A) $[(NCMe)_3RuCp][PF_6]$ or B) Benzeneruthenium chloride dimer*

Group 8 metal π-arene complexes have a similar array of reactions available to them as the previously mentioned metals, with the CpM^+ (M = Fe, Ru) fragment being slightly more activating than $Cr(CO)_3$, while being much less toxic.

For instance, a study conducted by C. C. Lee *et al*. found that reacting 1,2-dichlorobenzene complex **1.47** with bis-heteroatom nucleophiles resulted in formation of new benzo-fused heterocycles via two nucleophilic substitution steps.[35] These reactions worked with varying levels of success, depending on the nature of the nucleophilic groups, with recorded yields of 23-82%. The heterocycle was freed by thermolysis from the FeCp fragment, again to varying degrees of success. Later, Woodgate and co-workers synthesised a library of dibenzo[b,e][1,4]dioxin derivatives (**1.48**) from a similar reaction between Fe complex **1.47** and a series of substituted 1,2-benzenediols (figure 1.20). [36,37]

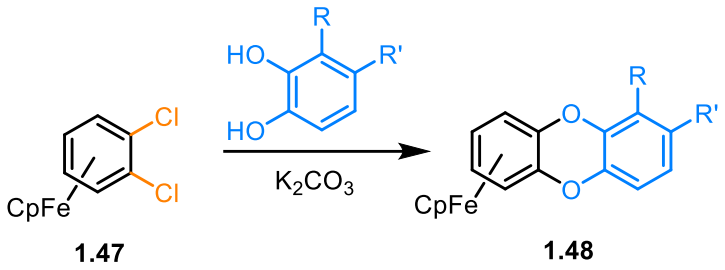

Figure 1.20. *Double S_NAr between [(η^6-1,2-dichlorobenzene)FeCp]$^+$ and various substituted 1,2-benzenediols*

One of very few 21st century examples of FeCp scaffolds being used to facilitate aromatic transformations is the synthesis of a number of unsymmetrically substituted, sterically congested benzophenones (**1.50**, figure 1.21A) *via* S_NAr of Fe π-arene complex **1.49**.[38] In a rare example of a hetereogeneous reaction involving π-arene intermediates, a piperazine nucleophile was tethered to a solid-support phase before S_NAr coupling to the η^6-bound arene in complex **1.51** (figure 1.21).[39] The resultant immobilised complexes (**1.52**) were then subjected to further nucleophilic substitution reactions, before irradiation in the presence of phenanthroline was used to remove the FeCp moiety, leaving a series of aniline derivatives **1.53** tethered to the solid support.

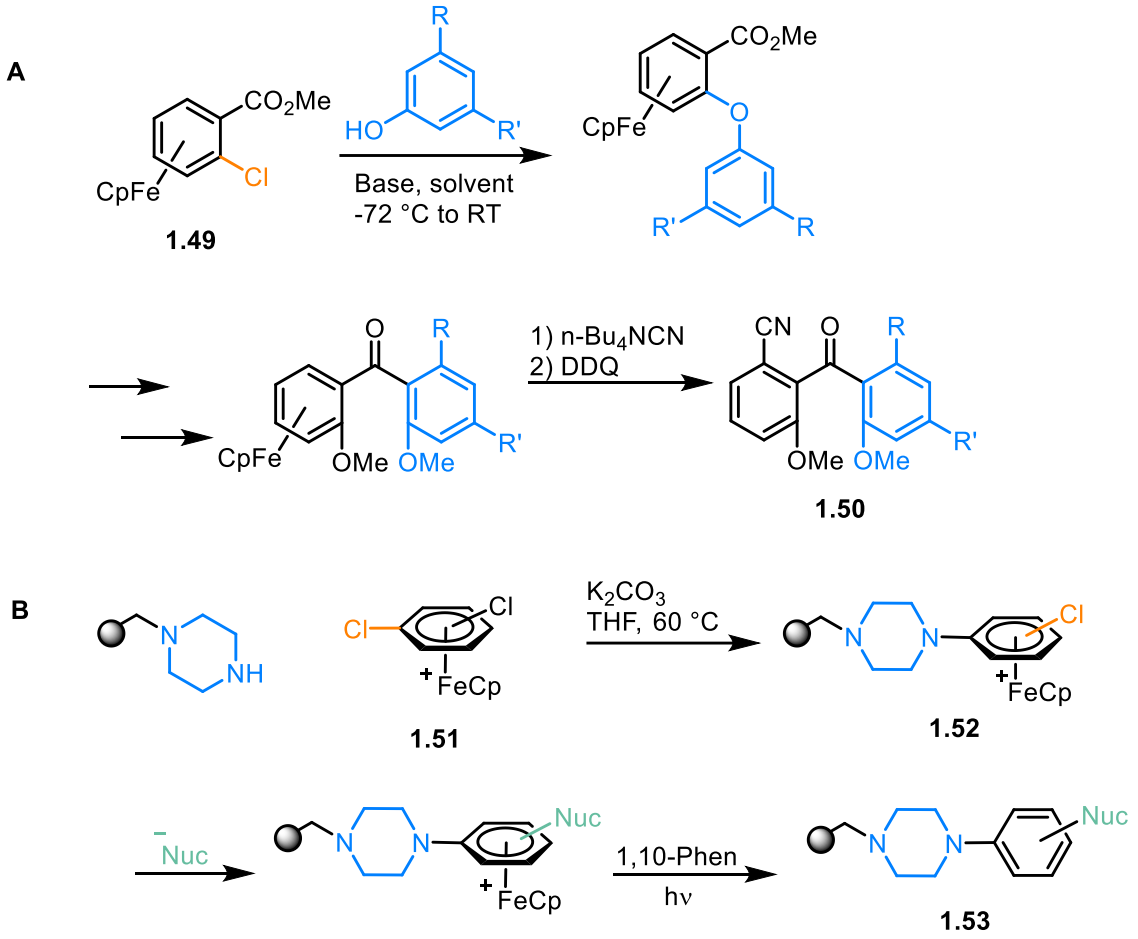

Figure 1.21. *A) FeCp-mediated synthesis of unsymmetrical benzophenone derivatives and B) FeCp-mediated S_NAr tethered to solid support phase, with subsequent photolytic liberation of the arene.*

Since the turn of the 21st century, Ru π-arene complexes have become much more commonly used than their Fe counterparts, mainly due to their much more convenient synthesis and de-complexation methods which outweigh the higher cost of Ru.

In the early 2000s, Pigge and co-workers reported a series of studies where spirolactam ring **1.56** was prepared via intramolecular attack of a 1,3-dicarbonyl enolate on the Ru π-arene complex **1.54** (figure 1.22).[40–43] Interestingly, despite the presence of a chloride leaving group on the ring, nucleophilic attack occurs exclusively on the alkyl-substituted carbon,[40] resulting in formation of the Meisenheimer complex **1.55**, which contains a 5-membered spirolactam core. Following alkylation, $CuCl_2$-mediated demetalation gave the free enantiopure spirolactam **1.56**.[41] In a follow-up study, another spirolactam was synthesised stereoselectively over two steps, first was an intramolecular cyclisation followed by a Horner-Wadsworth-Emmons olefination, and finally demetalation to give the enantiopure spirolactam. [42,43]

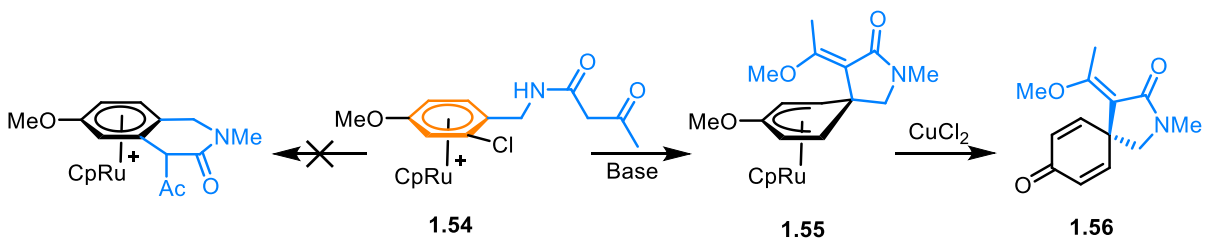

Figure 1.22. *Ru-mediated synthesis of an enantiopure spirolactam*

An interesting practical application of Ru π-complexes was published by Ritter *et al.*, in 2017, where η^6-bound phenol rings (**1.57**) were fluorinated with ^{18}F-labelled Phenofluor (**1.58**, figure 1.23). Arenes labelled with ^{18}F have applications in positron emission tomography (PET), with fluorine particularly useful for monitoring drug disposition and *in-vivo* biochemical interactions due to the prevalence of fluorine in pharmaceuticals. While fluorination with Phenofluor has already been demonstrated in free electron-poor arenes,[44] the use of a $RuCp^+$ fragment to activate the ring has expanded the scope of arenes which can be fluorinated. Furthermore, the Ru-mediated fluorination reaction appears to reduce the number of side products formed, increasing the yield and efficiency of the reaction. [45]

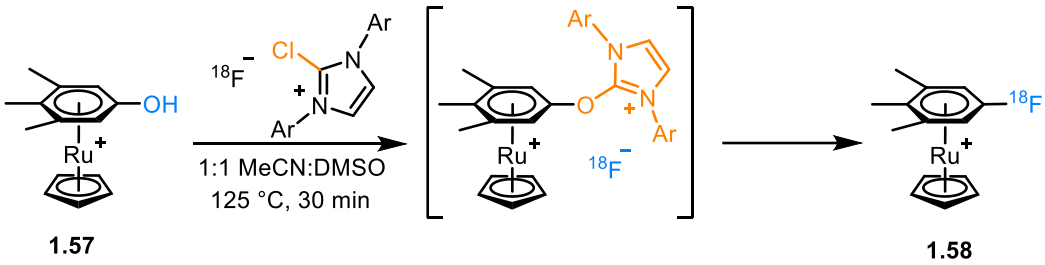

Figure 1.23. *Ru-mediated deoxyfluorination with ^{18}F-labelled Phenofluor.*[45]

In recent years, work in the Walton group has revolved around the reactivity of π-arene ruthenium complexes. One such reaction developed is a nucleophilic trifluoromethylation of nitrobenzene in **1.59** using Ruppert's reagent, Me_3SiCF_3 (figure 1.24).[46] In this reaction, two products were observed in equal quantities. First, the S_NAr product **1.60**, where the trifluoromethyl nucleophile simply displaced the nitro group was described. Photolysis of complex **1.60** gave a quantitative amount of free α,α,α-trifluorotoluene (figure 1.24, pathway A). The second product, a coordinated Meisenheimer complex **1.61**, formed by attack of the CF_3-nucleophile on C-H bond *ortho* to the chloro group was observed. Treatment of **1.61** with a strong oxidant, DDQ, both re-aromatized the ring and demetalated it, resulting in the

formation of free 1-nitro-2-trifluoromethylbenzene (figure 1.24, pathway B).[46] Reactions of the trifluoromethylating agent with other coordinated arenes, such as benzonitrile or chlorobenzene, resulted in preference for nucleophilic attack *ortho* to the nitro group.

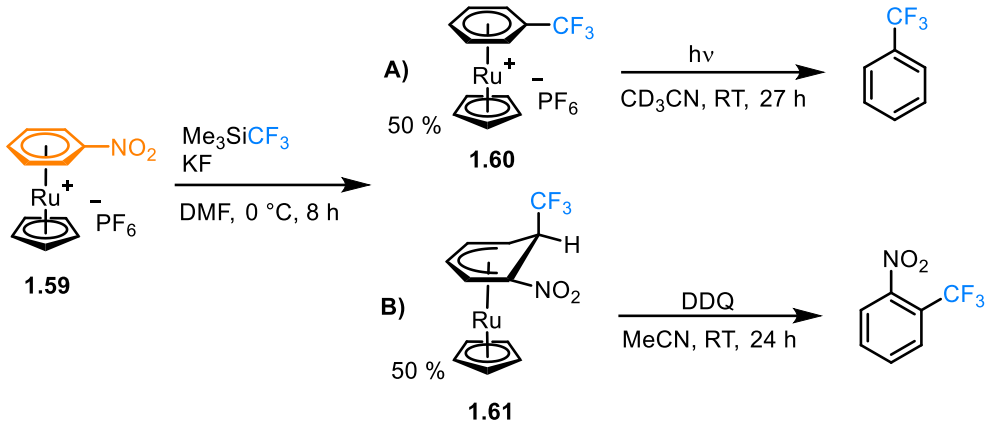

Figure 1.24. *Nucleophilic trifluoromethylation of an electron-deficient arene, followed by either A) photolysis of the S_NAr product or B) Oxidative demetalation of the coordinated Meisenheimer intermediate*

Another example builds upon the pioneering work by Larrosa, who demonstrated a bimetallic C-H activation of arenes coordinated to $Cr(CO)_3$ (figure 1.10), whereas Walton *et al.* showed the potential for a similar C-H activation process in complexes of the formula $[(\eta^6\text{-arene})RuCp]^+$.[47] In this reaction, both Pd and Ag are necessary for product formation; firstly the silver mediates C-H activation of the ring in complex **1.62A** via a CMD process (figure 1.25). Then, the aryl ligand is transmetalated to the Pd(II) centre, where the Ru-bound product arene (**1.62B**) is reductively eliminated. As with the trifluoromethylation work, the bound arene could be liberated from RuCp via a photolysis reaction, which also forms a quantitative amount of the complex $[CpRu(NCCD_3)_3]^+$, highlighting the feasibility of recovering the Ru fragment for further use.

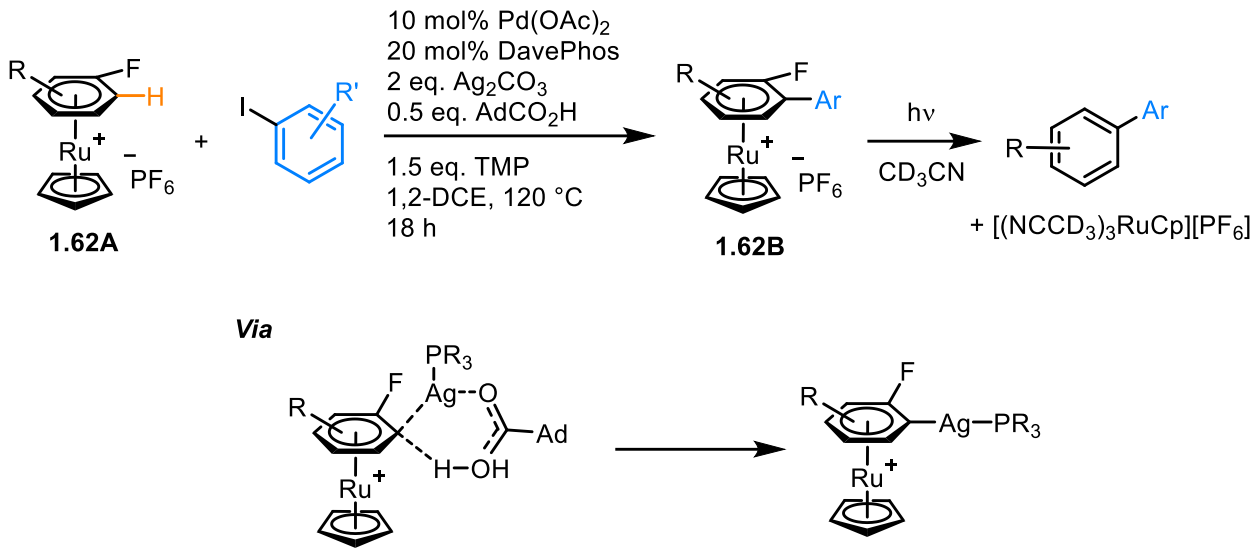

Figure 1.25. *Aromatic C-H arylation mediated by bimetallic Ag(I)/Pd(0) catalysis via a concerted deprotonation-metalation (CMD) mechanism*

1.3.4. Reactions Using Cobalt, Rhodium, and Iridium (Group 9)

Typically, cobalt diene complexes such as **1.63**, [(η^3-cyclooctenyl)Co(η^2,η^2-COD)] (where COD = cyclooctadiene) are converted to Co π-arene complexes (**1.64**) via hydrogenation of a coordinated alkene in the presence of the desired arene (figure 1.26). Generally, more electron-rich arene rings lead to higher yields from such reactions.[48] More recently, cobalt complexes bearing the diene ligand tetramethylcyclobutadiene (Cb*) have gained popularity as the [CoCb*] fragment is isolobal with [FeCp*], making the fragment highly resistant to undesired substitution reactions.[49]

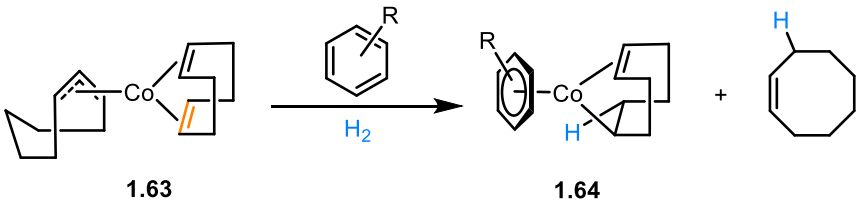

Figure 1.26. *Synthesis of complexes of the form [(η^6-arene)Co]$^+$ via hydrogenation of alkenyl ligands*

Rhodium and iridium have very similar properties and share a lot of chemistry. π-Arene complexes of the form [(η^6-arene)M(PR_3)$_2$]$^+$ can be prepared by reacting the halogen-bridged dimer complex [M(PR_3)$_2$]$_2$(μ-X)$_2$ (where M = Rh, Ir and X = bridging halogen) with the desired arene under fairly mild conditions.[50,51]

Despite their straightforward synthesis and the abundance of Rh and Ir π-arene complexes in existence, there are very few examples where the arene is undergoing a transformation while bound η^6- to the metal. One study explores the reactivity of the bound ring in the complex [(η^6-arylfluoride)RhCp'] (where Cp' = tetramethyl(ethyl) cyclopentadienyl) towards a series of different nucleophiles.[52] For example, hydroxide attacks the arene C-F bond in complex **1.65** *via* a S_NAr hydroxylation reaction, resulting in the formation of complex **1.66** (figure 1.27). However, more reactive alkyllithium nucleophiles, such as $LiCH(CO_2Et)_2$, tend to attack one of the unsubstituted C-H bonds in **1.65**, leading to formation of an η^5-Meisenheimer intermediate **1.67**. This complex was then oxidatively demetalated *in-situ* using trifluoroacetic acid (TFA) and $MeNO_2$ to give the free arene **1.68** and another Rh complex, also illustrating the non-destructive nature of the demetalation process.

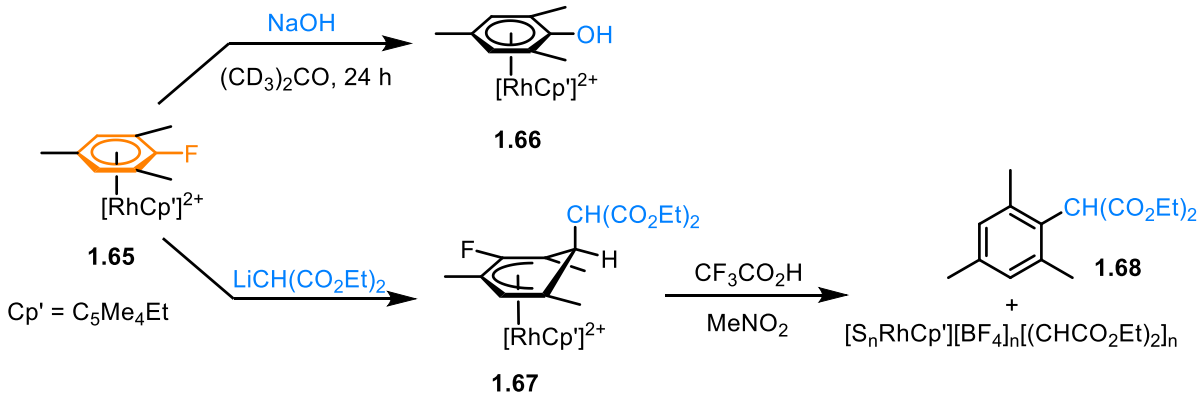

Figure 1.27. *Reactivity of the complex [(η^6-1-fluoro-2,4,6-trimethylbenzene)RhCp']$^{2+}$ (where Cp' is tetramethyl(ethyl) cyclopentadienyl) with various different nucleophiles.* [52]

The only example of the reactivity of an iridium π-arene complex involved the oxidation of the benzene ring in the complex [(η^6-C_6H_6)IrCp]$^{2+}$ (**1.69**) to an η^5-cyclohexadienyl oxide intermediate **1.70**. Treatment of **1.70** with a strong acid, $HBF_4.OEt_2$ resulted in formation of free phenol and the piano-stool complex [$(NCMe)_3$IrCp*]$^{2+}$ (**1.71**, figure 1.28).[53] While this process was stoichiometric in Ir, the researchers demonstrated how the complex **1.71** could be isolated and recycled for further use.

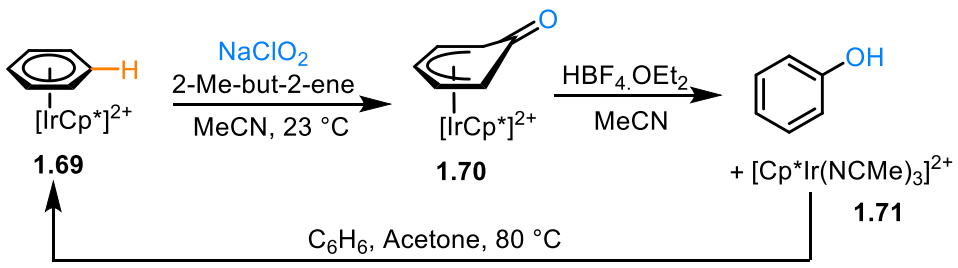

Figure 1.28. *Hydroxylation of benzene mediated by Ir^{III} and recovery of the metal fragment.*

1.4. Arene Exchange

In section 1.3, all examples of metal-mediated transformations of arenes discussed use a stoichiometric amount of metal, with most examples using decomplexation procedures which either destroy the metal fragment, or render it deactivated. This is not only inefficient in terms of atom economy and material cost, but also adds an additional step to any aromatic transformation. For these reasons, it is highly desirable to make any aromatic transformation catalytic in the activating metal, in which η^6-coordination is transient, with free exchange of one arene for another feasible. A general catalytic cycle was proposed by Semmelhack (figure 1.29),[54] whereby an S_NAr transformation of an aromatic ring coordinated η^6- to an activating metal is followed by arene exchange, regenerating the initial π-arene complex. In this reaction cycle, the rate determining step is arene exchange, making the resting state of the catalysis the η^6-bound S_NAr product.

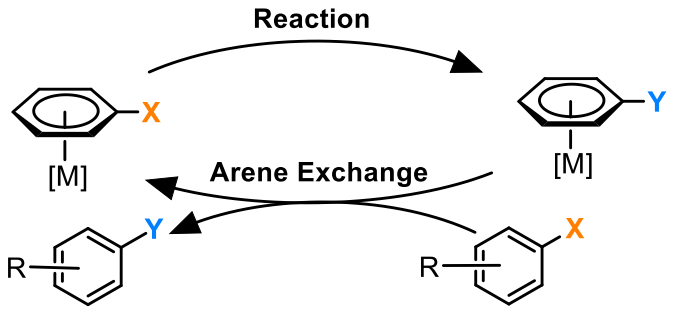

Figure 1.29. *General cycle for an arene transformation catalytic in [M].*

1.4.1. Known Arene Exchange Mechanisms

Arene exchange is the rate-limiting step in a catalytic cycle for aromatic transformations which go via transient η^6-coordination because of the nature of its mechanism. The 'unzipping' mechanism (figure 1.30) was proposed by Traylor and co-workers in the 1980s after extensive amounts of work studying the kinetics of arene exchange reactions.[55–57]

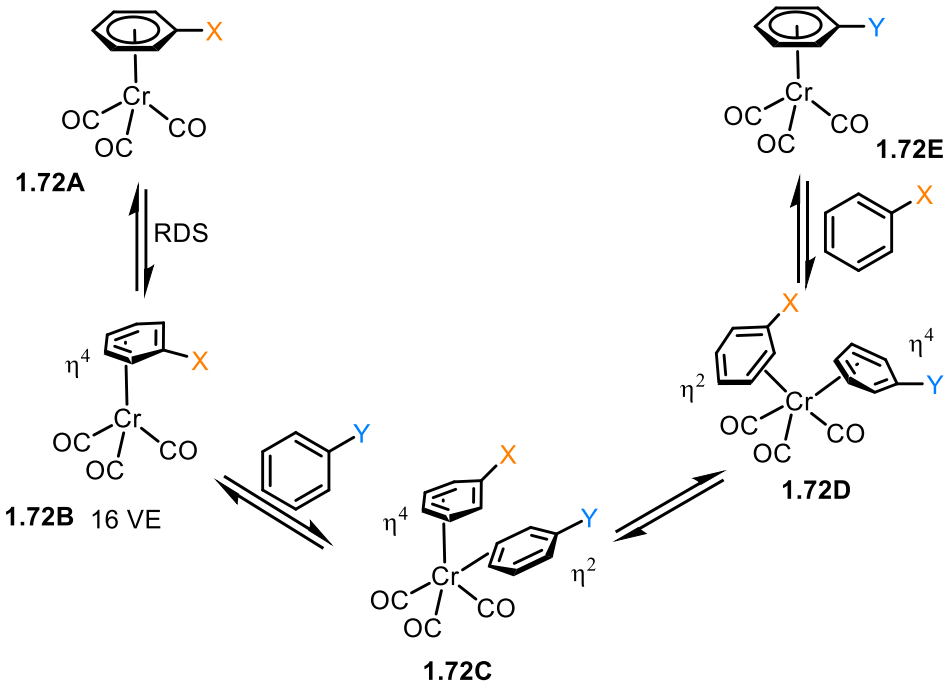

Figure 1.30. *'Unzipping' mechanism of arene exchange.*

The first and rate-limiting, step of this mechanism is a ring slip of the outgoing arene in complex **1.72A** from η^6 to η^4 (**1.72B**). This step is very slow because of the loss of electron-density around the metal centre, going from 18 to 16 valence electrons, which naturally leads to a significant loss in stability. Following the initial ring slip, the vacant coordination site can be occupied by the incoming arene in an η^2-interaction. It has also been demonstrated that the use of coordinating solvents can stabilise complex **1.72B** by coordinating to the metal and temporarily restoring the 18 valence electron count.[34,54] Alternatively, the first step can be catalysed by a metal complex, either through self-catalysis or presence of an additional complex. This catalysis was proposed to occur with species of the form [(η^6-arene)Cr(CO)$_3$] (**1.72A**), where a carbonyl ligand from another complex can temporarily coordinate to the metal centre of the η^4 intermediate (**1.73**, figure 1.31), acting as a bridging ligand.

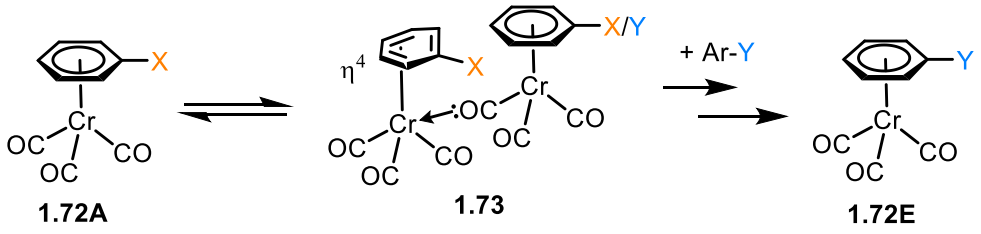

Figure 1.31. *Arene exchange catalysed by a second [(η^6-arene)Cr(CO)$_3$] complex.*

After the incoming arene coordinates to the metal centre, it can shift to η^4-coordination, while the outgoing arene swaps to η^2. The final step involves the incoming arene binding η^6- to the metal, while the original arene gets completely displaced. Every step of this mechanism is reversible, so it is desirable to have a large excess of the incoming arene in order to drive the equilibrium towards the desired complex.

1.4.2. Dependence of Incoming and Outgoing Arene on the Rate of Arene Exchange

The rate of arene exchange always depends on the outgoing arene, and when there is no catalyst present, the incoming arene too.[58] Naturally, more electron-rich arenes bind more strongly to metal centres, and so rate of arene exchange reactions for complexes of the form [(η^6-arene)$Cr(CO)_3$] will coalesce with the relative thermodynamic stabilities of the complexes (figure 1.32).[59,60]

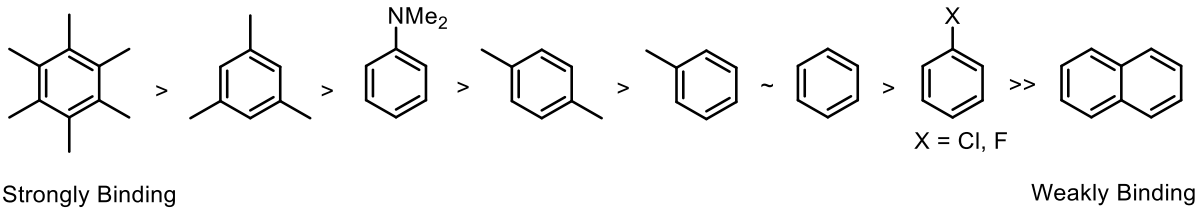

Figure 1.32. *Relative order of stability of [(η^6-arene)$Cr(CO)_3$] complexes*

Arene exchange of complexes [(η^6-arene)RuCp]$^+$ has also been studied in detail. In these species, the capping arene is particularly labile when it is a polyarene,[61–63] such as naphthalene, as aromaticity is retained when the η^6 to η^4 haptotropic shift occurs (figure 1.33). This lability has been exploited as a means to synthesise novel complexes of the formula [(η^6arene)RuCp]$^+$.[64–66] However, for C_6-aromatic rings, all aromaticity is lost when the ring slips to η^4, reducing the stability of the intermediate and hence exchange is much slower. Finally, when the incoming arene contains multiple aromatic rings, initially the least sterically hindered ring will bind to form the kinetic product. The reversibility of the haptotropic shifts then allows for conversion into the thermodynamic product, in which the more electron-rich arene ring will bind to the Ru centre.[67,68]

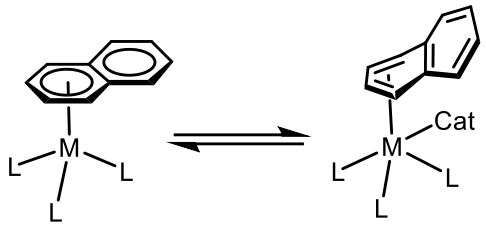

Figure 1.33. *Haptotropic shift in π-naphthalene ML_3 complexes*

1.4.3. Tether-Accelerated Arene Exchange

As was mentioned previously, the simplest way to increase the rate of arene exchange is to stabilise the η^4-intermediate formed in the rate-determining step, by addition of a coordinating solvent or catalytic ligand. Another way of doing this is to modify one or more of the spectator ligands in the complex, incorporating an intramolecular coordinating group, which can easily coordinate to the metal centre when necessary. The first example of this chemistry was a methacrylate ligand, primarily bound to the Cr centre by η^2-coordination through the alkene moiety (**1.74A**, figure 1.34A). However, this ligand could easily alter its hapticity, as the carbonyl oxygen could also coordinate the metal centre on arene ring slip, temporarily forming complex **1.74B**.[69] The effect of this stabilisation proved significant, as it facilitated room-tempertature arene exchange, whereas the non-tether chromium complex, [(η^6-arene)$Cr(CO)_3$] required a temperature of 170 °C to undergo arene exchange.[57]

Semmelhack later published work where a series of coordinating groups, L, tethered to the ligand tris(pyrrole)phosphine were tested for their effects on the rate of arene exchange (figure 1.34B).[70] After a significant amount of kinetic analysis, a clear trend emerged where ligands with higher donating ability proved more effective at accelerating arene exchange (table 1.1). In further kinetic analysis on the arene exchange of **1.75A** (L = CO_2Me) calculated transition state data for $\Delta H^{\ddagger}$ = 22 kcal mol^{-1} and $\Delta S^{\ddagger}$ = -2.8 $kcal^{-1}$, indicated a dissociative transition state for the arene exchange, as well as a dependence of the rate on both the outgoing and incoming arenes. This means that the kinetics in this reaction are sensitive to which system is under analysis, and general mechanistic descriptions, such as that in figure 1.30, are not always perfectly accurate.

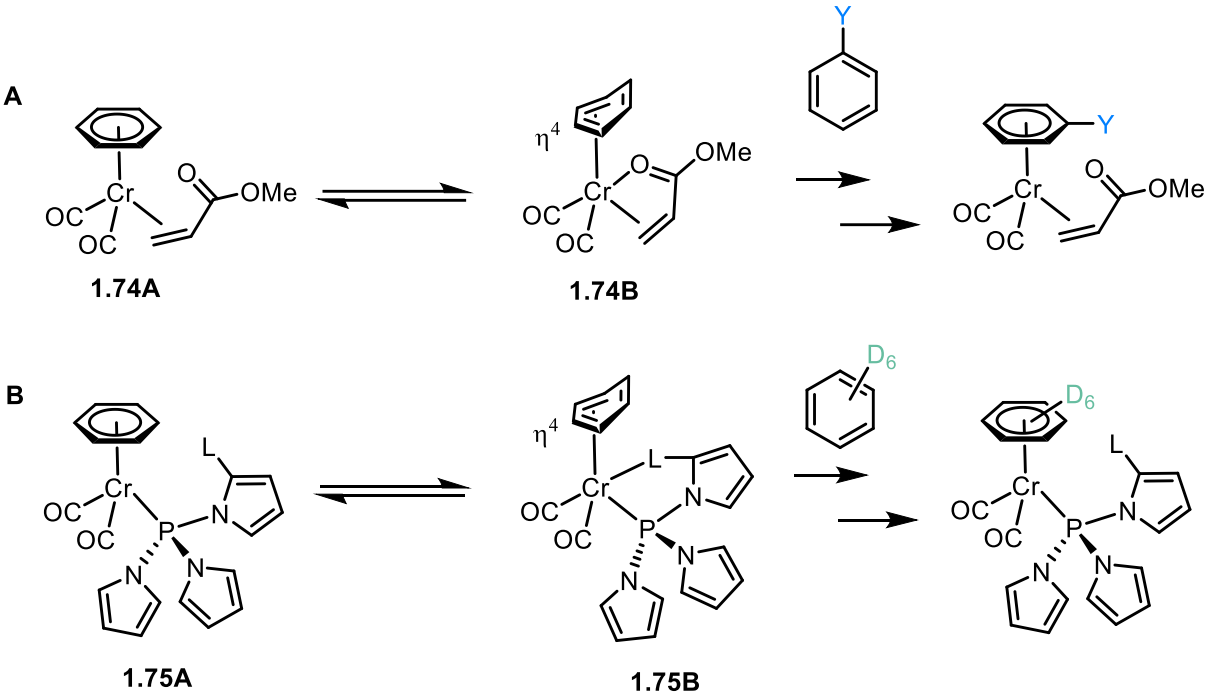

Figure 1.34. *Arene exchange catalysed by an intramolecular tether*

Table 1.1. *Exchange half-lives with different L groups at specified temperatures*

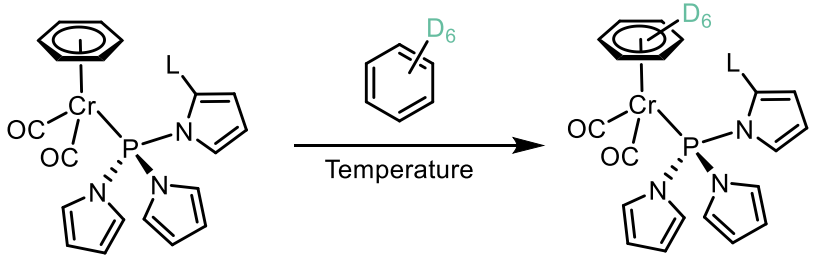

Substituent L	Temperature /°C	Exchange Half-life /h	Substituent L	Temperature /°C	Exchange Half-life /h
CO_2Me	70	0.5	CO_2Me	23	115
SMe	70	8.7	$CONMe_2$	22	9
SPh	70	30.6	2-Pyridine	22	8
SF_3	70	>150			

More recently, tethered coordinating groups were demonstrated to accelerate the rate of arene exchange in Ru complexes, where Walton *et al.* synthesised a series of complexes, [(η^6-*p*-cymene)Ru(Cp-L)]$^+$ (where Cp-L is a cyclopentadienyl ring functionalised with a donating group, L) and compared their rates of arene exchange with non-tether complexes.[34] Unsurprisingly, the rate of arene exchange was found to depend strongly on the donating ability

of the tethered coordinating group, with the 2-pyridyl tether complex **1.76A** performing the best, giving an 18-fold increase in the rate of arene exchange. .

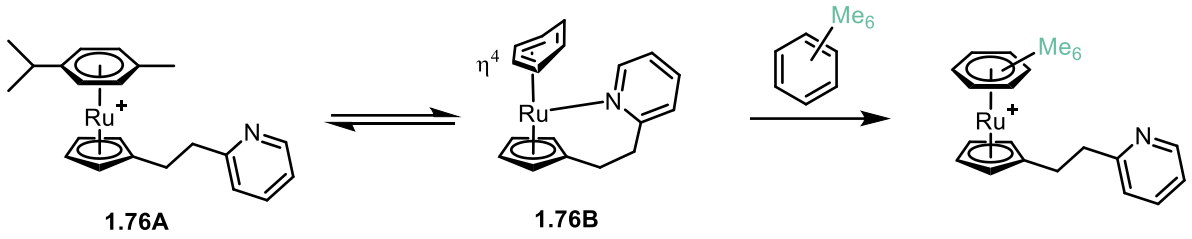

Figure 1.35. *Arene exchange in the complex [(η^6-p-cymene)Ru(Cp-Pyr)]$^+$, catalysed by an intramolecular pyridine ring.*

1.4.4. Photocatalytic Arene Exchange

As discussed in section 1.3 of this review, UV light has been used frequently to liberate arenes from the metal centre, particularly in [FeCp]$^+$ and [RuCp]$^+$ systems.[71,72] Generally, photolytic liberation of an arene leads to free coordination sites on the metal, which can be occupied by coordinating solvent molecules such as MeCN or by another arene. An early example of this was demonstrated by Woodgate *et al.*,[37] where the S_NAr of complex η^6-chlorobenzene complex **1.77** with morpholine gave the Ru-bound product **1.78**, and then photolysis using UV light (Rayonet photoreactor, 300 nm) gave quantitative yields of both free N-phenylmorpholine and complex by-product, [(NCMe)$_3$RuCp]$^+$ (**1.43**, figure 1.36).

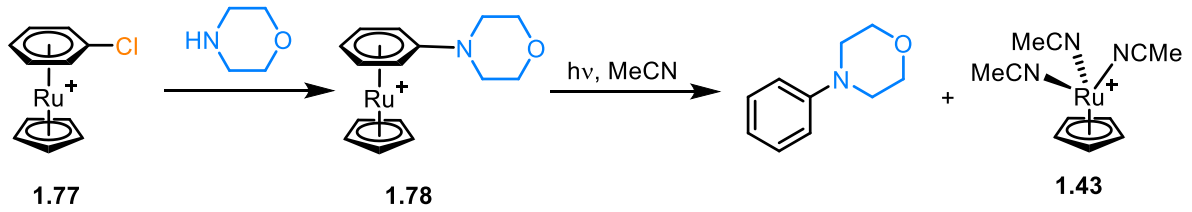

Figure 1.36. *S_NAr reaction of a Ru π-arene complex, followed by photolysis to liberate the free arene.*

The analogous complex, [(η^6-arene)FeCp]$^+$ (**1.79**, figure 1.37A), undergoes photolysis (sunlight or 100 W mercury lamp), at -40 °C in acetonitrile to give the free arene and the piano-stool Fe complex **1.80**[73] which at room temperature is susceptible to further solvolysis reactions, resulting in formation of [(NCMe)$_6$Fe]$^{2+}$ and ferrocene. In a non-coordinating solvent

such as CH_2Cl_2, photocatalytic arene exchange to complex **1.81** is possible provided the incoming arene is more electron-rich than the outgoing ring.[74]

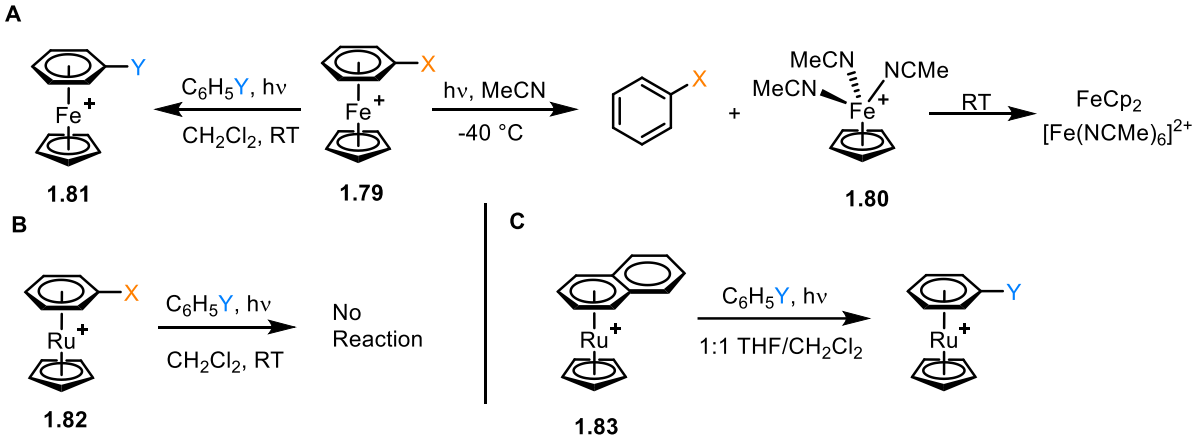

Figure 1.37. *Photocatalytic reactions of Fe and Ru π-arene complexes.*

However, under the same reaction conditions the Ru analogue[(η^6-arene)RuCp]$^+$ (**1.82**, figure 1.37B), does not undergo any arene exchange at all. Photocatalytic arene exchange is possible for Ru sandwich complexes **1.83**, where the outgoing arene is a polyaromatic. For example, arene exchange for the complex [(η^6-DBT)RuCp]$^+$ (DBT = dibenzothiophene) was measured in the presence of 1 eq. of an incoming arene at room temperature, under UV light (450 W low-pressure immersion lamp).[75] Unsurprisingly, more electron-rich arenes such as mesitylene and toluene gave the best conversions, whereas naphthalene did not exchange much with DBT. In another study, the complex [(η^6-naphthalene)RuCp]$^+$ was subjected to photocatalytic arene exchange conditions (650 W mercury lamp), where a conversion of 10% was measured for benzene as the incoming arene in CH_2Cl_2 solvent.[76] The conversion was increased to 33% when the coordinating $CF_3SO_3^-$ anion was added, then complete arene exchange was achieved by adding coordinating co-solvents to the reaction. Under the optimised conditions, the naphthalene complex was reacted with the more electron-rich arene, hexamethylbenzene, though a conversion of only 10% was observed. This result is likely due to the steric hindrance of an incoming bulky arene, highlighting the balance between electronic and steric effects that govern the arene exchange process.

The photolysis of complexes [(η^6-arene)MCp]$^+$ (where M = Fe, Ru) is proposed to occur via formation of a metal-centred photoexcited state, in which an electron is promoted to the d_Z^2 orbital from either the d_{XZ} or d_{YZ} orbital, ultimately resulting in elongation of the metal-arene

bond as well as a build-up of negative charge on the arene.[77] As a consequence, the metal centre in complex **1.84A** is open to nucleophilic attack from either a coordinating solvent molecule or incoming arene, which leads to formation of an η^4-intermediate **1.84B** (figure 1.38). Following this, the arene is rapidly liberated from the metal fragment, is accompanied by formation of either a solvated complex or another sandwich complex, depending on the reaction conditions.

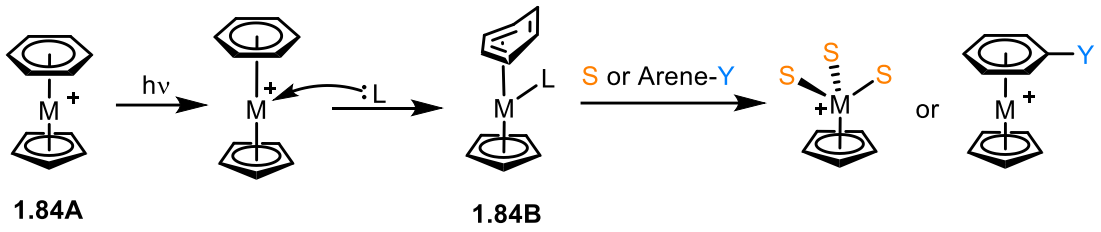

Figure 1.38. *Mechanism of photocatalytic arene exchange for either another arene or coordinating solvent molecules, where M = Fe, Ru*

1.5. Metal-Catalysed Aromatic Transformations via Transient η^6-Coordination

As previously mentioned, most aromatic transformations mentioned in this review require a stoichiometric amount of the activating metal, which is highly wasteful and therefore, the development of protocols using a catalytic amount of metal is essential. The key to making aromatic transformations catalytic in the activating metal is combining the arene transformation step with arene exchange. This is problematic however, as properties that enhance the aromatic ring's reactivity, such as a stronger π interaction (and therefore stronger electron-withdrawing effect), will naturally disfavour the arene exchange step; while a weaker π interaction promotes arene exchange but the on-ring reactivity is reduced. Therefore, a fine balance is required to make any reactions catalytic in metal, and up until now, there are a limited number of examples of catalysis. All examples discussed in this chapter will be divided into types of reaction occurring.

1.5.1. Catalytic Reactions at an Aromatic Carbon Centre

There are several reports in which a catalytic amount of metal has mediated a nucleophilic substitution reaction of an aromatic ring. The first ever example of this type of catalysis was reported in 1980 by Houghton, in which the complex $[(\eta^6\text{-}C_6H_6)Rh(C_5Me_4Et)]^{2+}$ was used to catalyse the intramolecular cyclisation of 3-(2-fluorophenyl) propanols (**1.85A**) to form chroman derivatives (**1.85B**, figure 1.39A). [78]

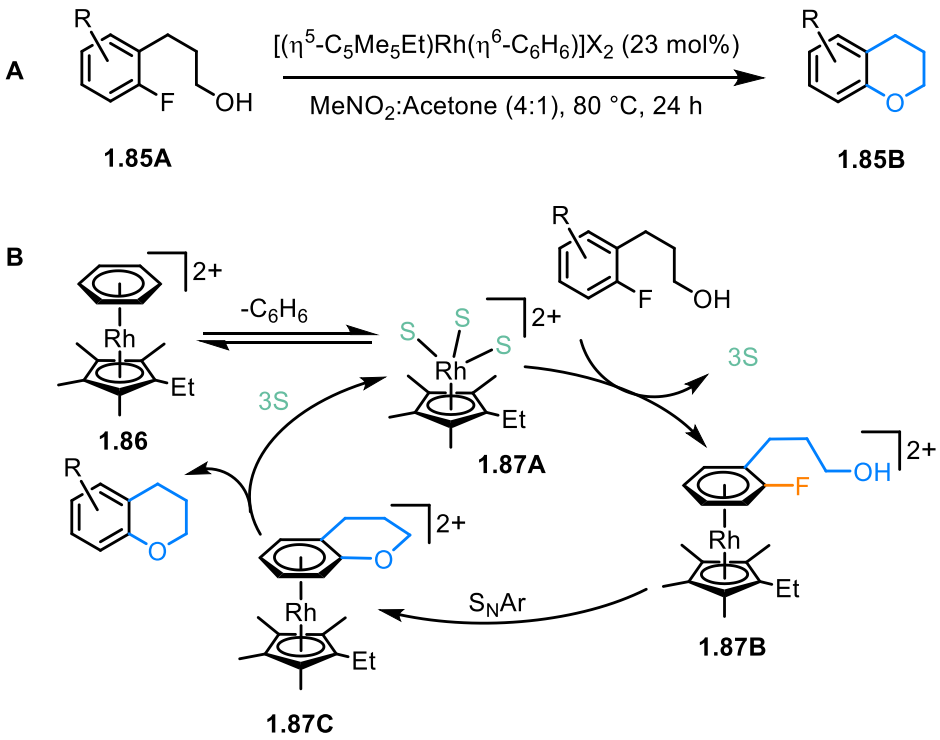

Figure 1.39. *Catalytic cycle for the mechanism of Rh(III)-catalysed intramolecular cyclisation.*

^{1}H NMR spectroscopy was used to derive the proposed mechanism (figure 1.39B), which initiates *via* solvolysis of the pre-catalyst **1.86**, forming the active species $[(S_3Rh(\eta^5\text{-}C_5Me_4Et)]^{2+}$ (**1.87A**, where S = solvent), followed by formation of η^6-fluoroarene **1.87B** and loss of the solvent ligands. The RhCp' centre is sufficiently activating such that the neutral alcohol partakes in the intramolecular S_NAr cyclisation to **1.87C**. Finally, the catalytic cycle is completed *via* solvolytic liberation of the free chroman. A noteworthy feature of this catalysis is that the identity of the counter-anion appeared to influence the reaction conversion – PF_6 salts gave a 55% conversion after 24 hours, whereas the BF_4 salts only gave 33% in the same amount of time.[78] A likely reason for this is that PF_6 can decompose under the reaction conditions, forming F^- anions, which themselves can act as catalysts in the arene exchange step.

While the scope of this catalysis was limited to only a few arenes, further tests revealed that an intermolecular process was also feasible, with a system containing fluorobenzene and methanol successfully generating anisole.

This process remained the only example of metal catalysed S_NAr for decades, until 2010 when Shibata published a report on the Ru-catalysed S_NAr reaction of unactivated aryl fluorides with secondary amines. In the initial studies, a precatalyst system containing [Ru(COD)(2-methylallyl)$_2$], DPPPent and TfOH, was employed and generated coupled aryl amines in up to 79% yields (figure 1.40A).[79] Recently, Schley and Mueller carried out a detailed mechanistic study of the reaction of fluorobenzene and morpholine under Shibata's initial conditions. Here, product inhibition was observed, as the morpholino-substituted arene ring binds more strongly to the Ru centre than fluorobenzene (figure 1.40B).[80] An equilibrium constant of 2 x 10^3 for arene exchange (**1.89A** ⇌ **1.89B**) was calculated, indicating the magnitude by which the rate of the desired arene exchange (**1.89B** → **1.89A**) is limited. Furthermore, the resting state of the catalytic cycle was revealed to be a previously unknown inactive Ru hydride species **1.88**, which is reactivated through reaction with the Et_3N/Et_3SiH additives.

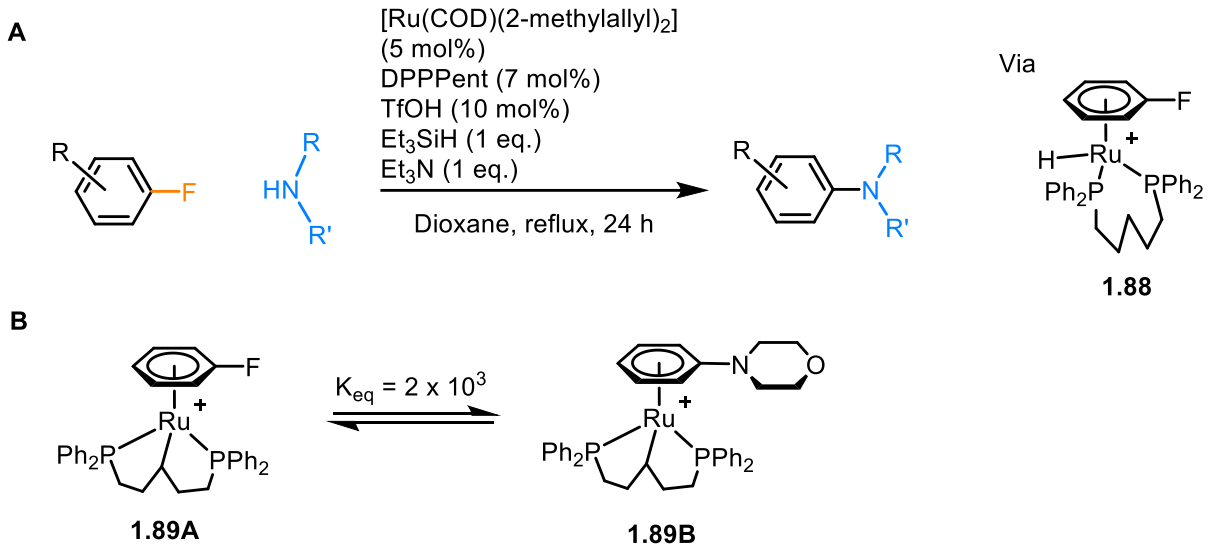

Figure 1.40. *A) Ru-catalysed amination of aryl fluorides, which goes via a Ru(II)-hydride species, and B) equilibrium between the π-fluorobenzene and π-morpholinobenzene complexes established by Schley and Mueller.*

After further optimisation by Shibata, a more bench-stable catalytic system of [Ru(η^6-C_6H_6)Cl_2]$_2$ alongside electron-poor monodentate phosphine ligands such as P(*p*-C_6H_4F)$_3$ was found to increase the yields past 80% (figure 1.41A).[81] Mechanistic insight was gained from

the use of *in-situ* ^{1}H NMR spectroscopy, which implied the resting state of the catalytic cycle to be an η^6-fluorobenzene ruthenium species **1.90A**, implying that the rate determining step of the reaction was S_NAr (**190A → 190B**), rather than arene exchange. Further evidence for slow S_NAr was found from the increase in catalytic performance for more electron-poor phosphine ligands.

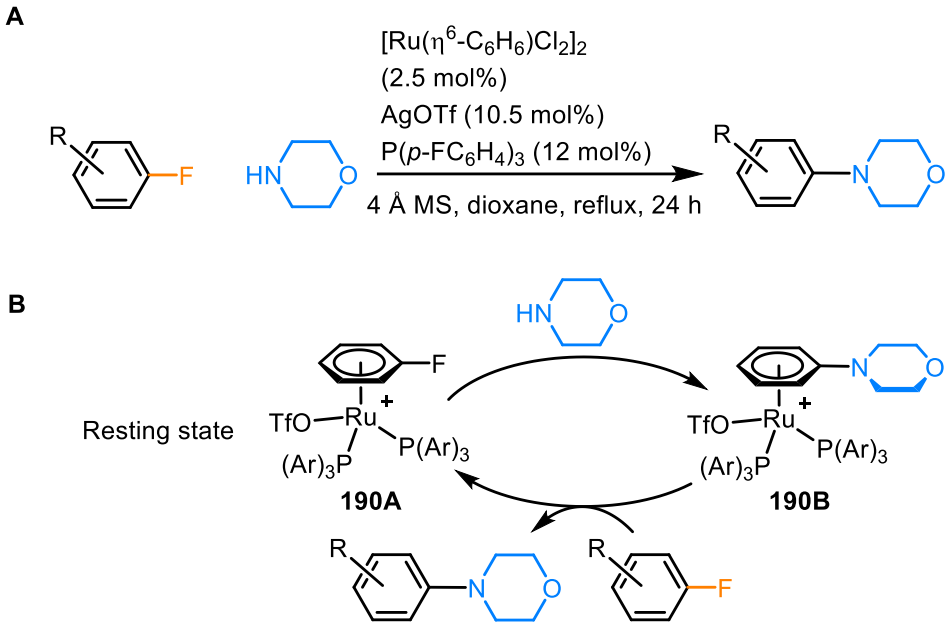

Figure 1.41. *Shibata's optimised catalytic amination of fluoroarenes*

In 2020, Shi and co-workers presented a similar study for Ru-catalysed coupling of aryl fluorides to amines under mild reaction conditions (Figure 1.42A). Here, a series of aryl fluorides bearing electron-donating or neutral substituents, were the limiting reagent, which leads to a rate-limiting arene exchange step.[82] To increase the rate of arene exchange, a ruthenium catalyst **191A**, containing one bidentate phosphine ligand and one monodentate phosphine ligand was used. Following rapid S_NAr conversion to the resting state **191B** (Figure 1.42B), arene exchange was accelerated through transient bidentate coordination of the second phosphine ligand (**191C**), which stabilises the formation of the η^4 intermediate of arene exchange. Evidence for this accelerated arene exchange was given by using a similar catalytic system **192**, where the hemi-labile group was not present, and no arene exchange occurred (figure 1.42C).[82]

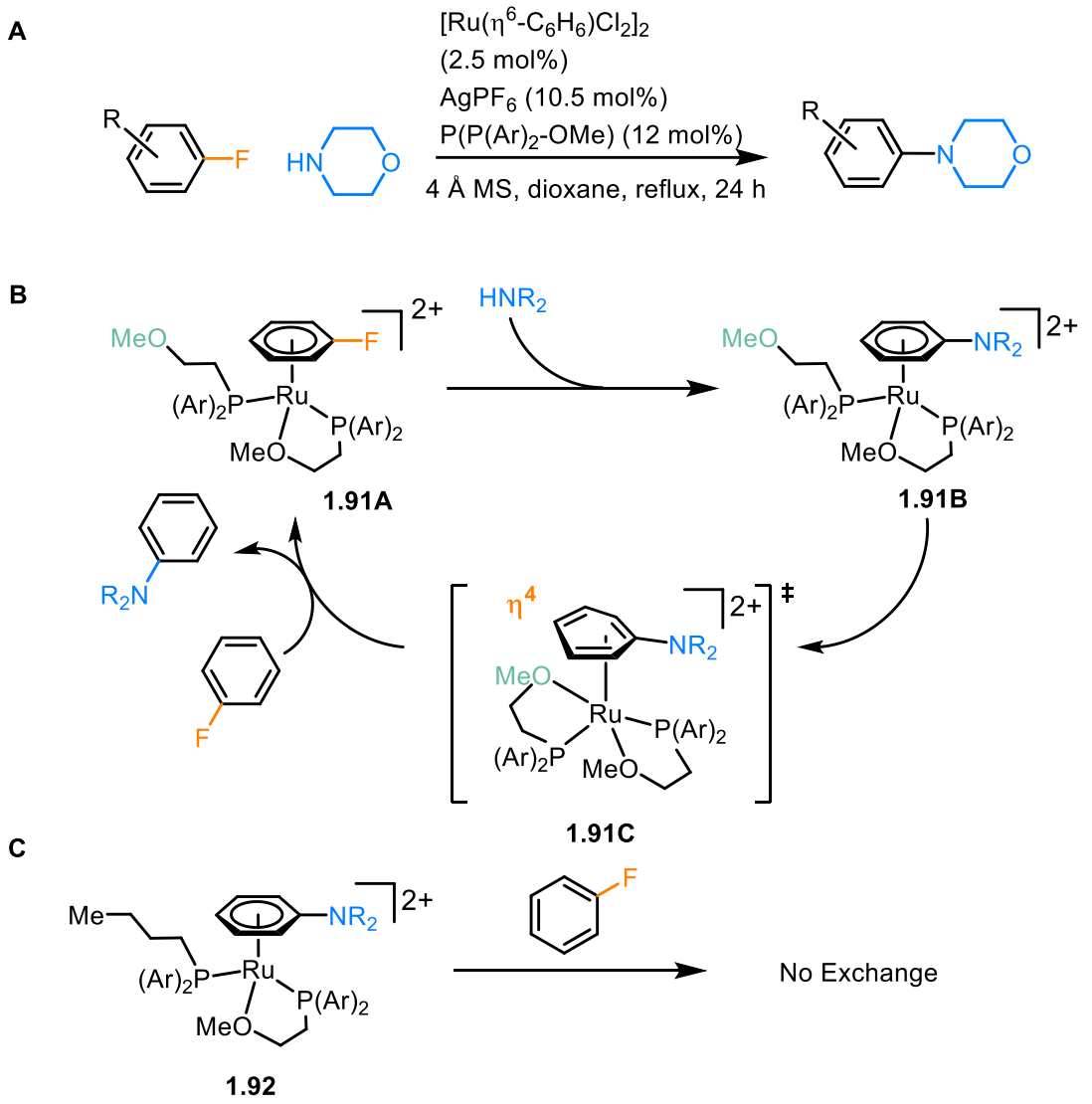

Figure 1.42. *Ru-catalysed amination of fluoroarenes, using a hemilabile phosphine tether ligand to facilitate arene exchange (where Ar = 4-methoxyphenyl).*

In the same research group, a catalytic hydroxylation and alkoxylation of fluoroarenes was also demonstrated (figure 1.43A). Initial studies explored the use of the previously mentioned Ru(II) catalysts bearing a hemilabile phosphine ligand, although these proved ineffective due to formation of an η^5-phenoxo complex **1.94** under the basic conditions (figure 1.43B), which could not undergo arene exchange.[83] Instead, Rh(III)Cp* was investigated as the activating fragment due to the higher oxidation state of the metal, and was shown to be capable of catalysing the S_NAr alkoxylation under non-basic conditions at 150 °C in yields of up to 65%, *via* an η^5-phenoxo complex **1.93**. Exploration of the arene scope revealed that the reaction conditions worked with *ortho*, *meta*, *para* and multi-substituted fluoroarenes, while reactive

functionalities such as carbonyl, carboxyl and alkenyl were also tolerated. The reaction was also chemoselective for fluoroarenes over chloro- or bromoarenes, though heterocycles with coordinating groups (such as pyridine) were not active due to their interference with arene exchange. Also noteworthy was the selectivity of the hydroxylation towards more electron-rich C-F sites on rings with more than one fluorine, which contradicts traditional S_NAr reactions.

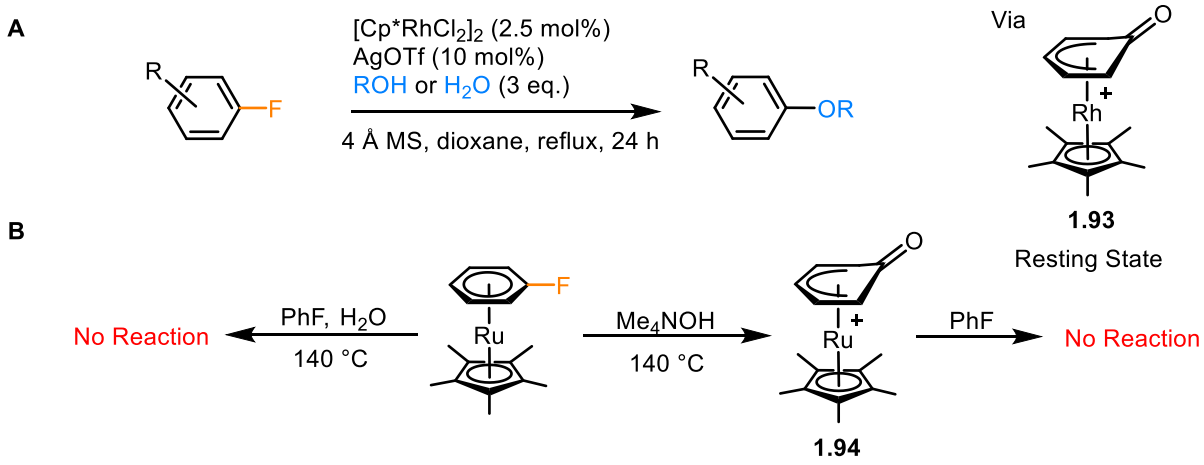

Figure 1.43. *A) Rh-catalysed hydroxylation/alkoxylation of fluoroarenes and B) Attempts at Ru-catalysed hydroxylation of fluorobenzene*

Until now, all examples of catalytic S_NAr discussed have been limited to aryl fluorides, with no reactivity shown by aryl-chlorides or aryl-bromides. Recently, two examples of catalytic processes where aryl chloride are undergoing S_NAr have been published. The first, by Walton and Williams, used the precatalyst $[(\eta^6\text{-}p\text{-cymene})RuCp]^+$ (**1.95**) to couple 4-chlorotoluene with morpholine in 90% yield, though the reaction required 14 days to reach this conversion (figure 1.44).[34] Arene exchange (**1.96B → 1.96A**) was inferred as the rate limiting step here, as the reaction required very high temperatures and only proceeded in coordinating solvents like 1-octanol, cyclohexanone and DMI, demonstrating the catalytic ability of solvent molecules in arene exchange.

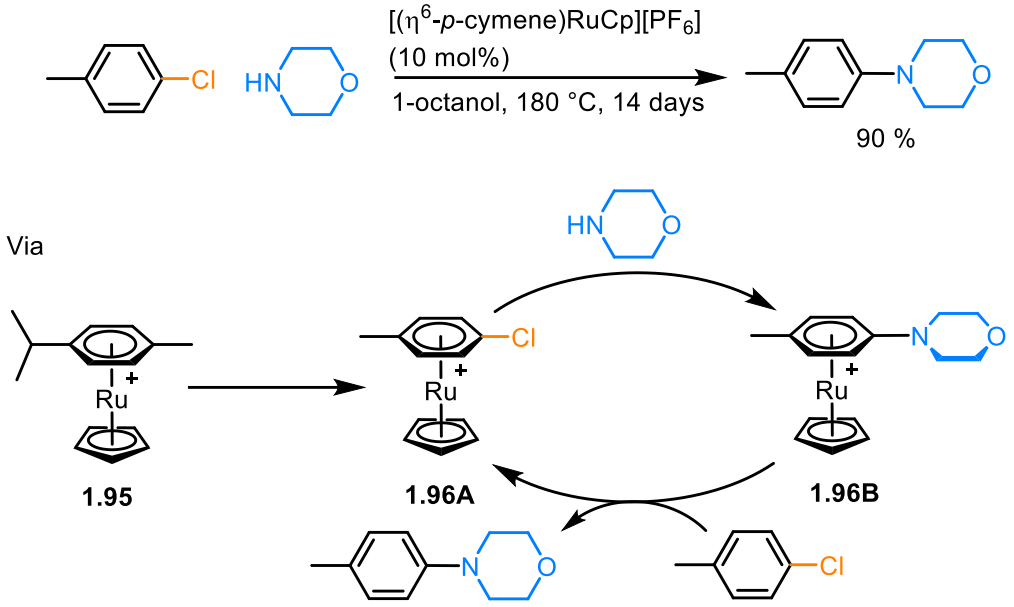

Figure 1.44. *Ru-catalysed amination of unactivated aryl chlorides by Walton and Williams*

In another study, Grushin used a very similar catalytic system to convert aryl chlorides to aryl fluorides, using [(η^{6}naphthalene)RuCp*][BF_4] (**1.97**) as a pre-catalyst and CsF as a source of nucleophilic fluoride (figure 1.45A).[84] This catalytic fluorination proceeded *via* arene exchange to the active catalytic species **1.98A** at 140 °C in anhydrous DMF, giving a catalyst turnover number (TON) of 4.2 after 24 hours. Compared with the previous example, this reaction occurs at a significantly lower temperature, which is likely due to the highly electron-rich Cp* promoting arene exchange more than Cp. Furthermore, when chlorobenzene was used as the reaction solvent, the TON increased to 8.5. This catalytic fluorination procedure also works with aryl bromides and aryl iodides, though unsurprisingly neither perform as well as chlorobenzene. Also noteworthy was the deactivation of the catalysis in the presence of moisture; this is due to formation of a π-phenol complex under basic conditions, which leads to the η5-phenoxide Ru species (**1.94**) (figure 1.45B) which cannot undergo arene exchange.

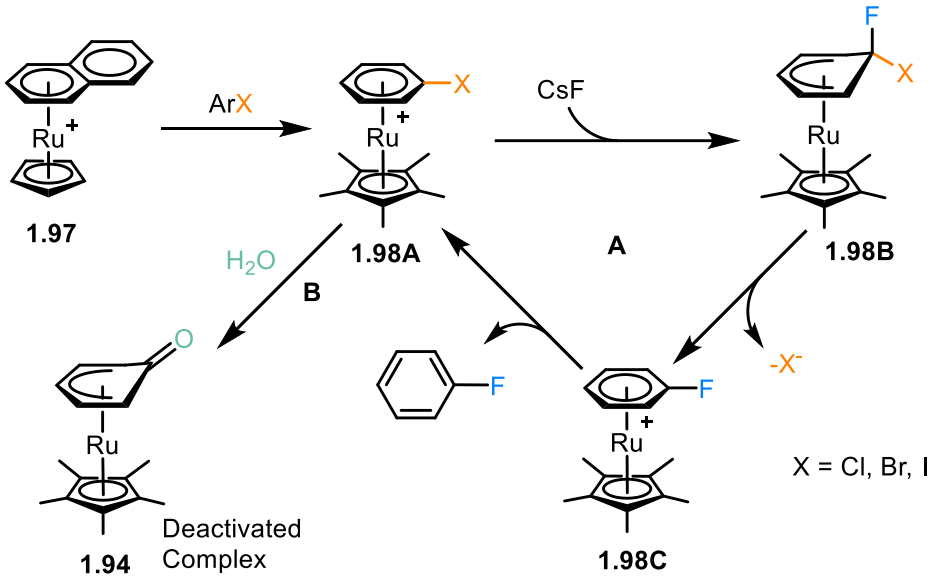

Figure 1.45. *Ru-catalysed fluorination of halobenzenes (pathway A) and catalyst deactivation by hydroxylation (pathway B).*

1.5.2. Catalytic Reactions at Benzylic or More Distal Positions

As well as the ring itself, π-coordination to a metal centre also enhances the reactivity of more distal positions. It is well known that benzylic protons become more acidic on coordination to a metal,[85] and Matsuzaka and Takemoto exploited this in their Ru-catalysed condensation of toluene and aromatic aldehydes to form stilbene derivatives in high yields (figure 1.46).[86] Starting from the catalytically active species, $[(\eta^6\text{-toluene})RuCp^*]^+$ (**1.99A**), initial deprotonation of the benzylic position of the η^6-bound toluene leads to formation of Ru anion **1.99B**, which is stabilised by the electron-withdrawing $RuCp^{*+}$ fragment. Nucleophilic attack on the aldehyde, activated by the $[NHTs]^-$ anion leads to alkyl-substituted complex **199C**, then elimination of $[NHTs]^-$ gives the η^6-coordinated stilbene derivative **1.99D**. Finally, arene exchange with toluene completes the catalytic cycle. Although there was no mention of the rate-limiting step here, it is likely to be arene exchange due to the similarity of this system as some of those mentioned in section 1.5.1, making species **1.99D** the resting state. Some indirect evidence for rate limiting arene exchange was the reduced catalytic activity of the Cp analogue, as well as the high dependence of the reaction yield with temperature and reaction time (50% at 130 °C and 4 h, 98% at 150 °C and 24 h). Also, the important activating role of the $[NHTs]^-$ counter-anion was highlighted by the absence of reactivity when Cl^- or OTs^- counter anions were used. The system was also active towards multiple successive condensation reactions on the same ring, as xylenes were used to make distyrylbenzene derivatives.

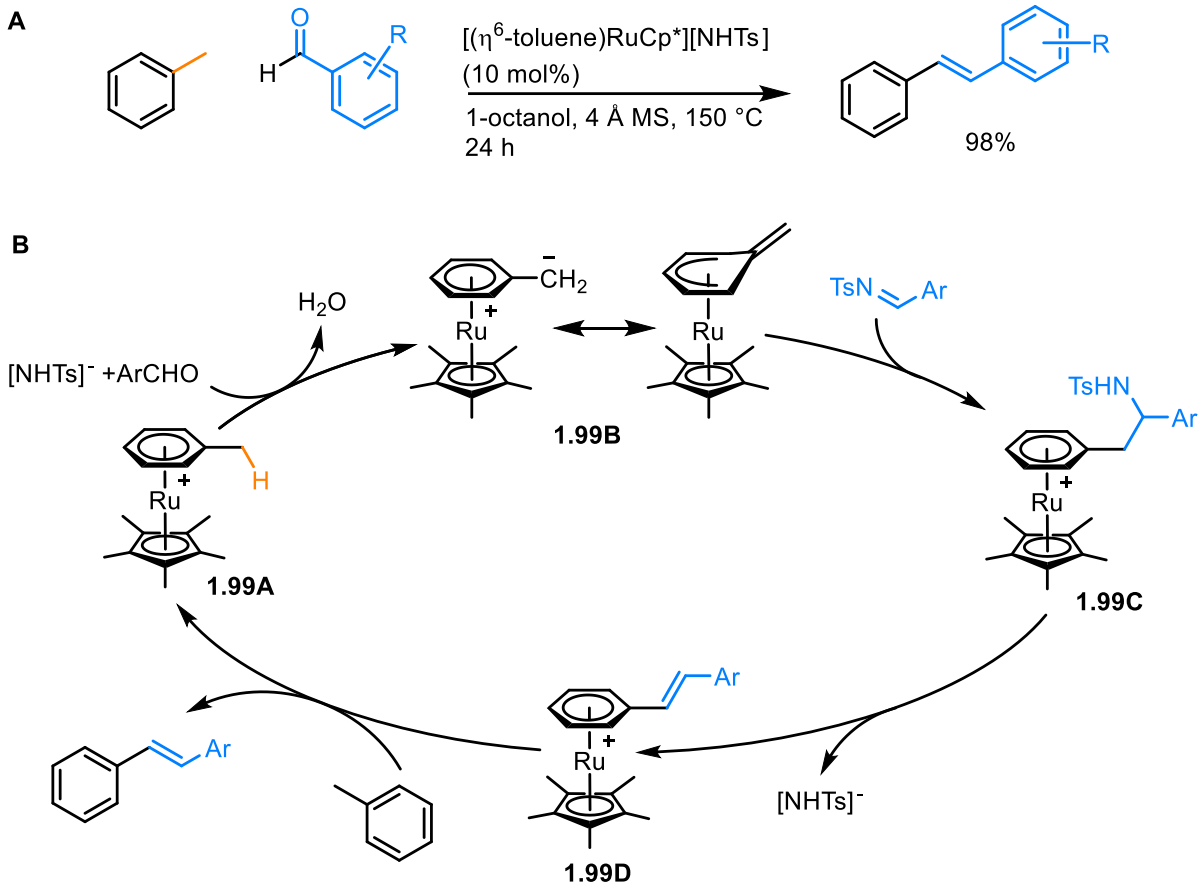

Figure 1.46. *Ru-catalysed condensation between toluene and aromatic aldehydes*

The enhanced electrophilicity of π-coordination applies not only to the ring itself but is extended to vinyl groups conjugated to the arene ring. In 2004, Hartwig first demonstrated a Ru-catalysed anti-Markovnikov hydroamination of the vinyl group in styrene derivatives with secondary amines, such as morpholine (figure 1.47A).[87] This amination was regioselective towards the β-position of styrene, owing to the additional stabilisation of a negative charge in the α-position on π-coordination to a metal. After optimisation of the reaction conditions (5 mol% [Ru(COD)(methylallyl)$_2$], 7 mol% DPPPent, 10 mol% TfOH), the hydroamination occurred with 96% yield and >99% selectivity for the terminal position of the alkene. In a further study, the mechanism of the reaction was found to occur via nucleophilic addition of the amine to the alkenyl group in **1.100A**, leading to formation of the π-bound product **1.100B**, which then underwent arene exchange to regenerate the catalytic Ru species and the free coupled arene (figure 1.47B).[88] Stoichiometric amination of the complex, [(η^6-styrene)Ru(DPPPent)]$^+$, with morpholine at 100 °C was performed to calculate a rate constant,

k_{obs}, of 5.6 x 10^{-3} s^{-1}, while separate arene exchange experiments of the bound product were done to calculate a rate constant, k_{obs}, of 6.2 x 10^{-3} s^{-1}. The comparability of these rate constants demonstrates the fine balance achieved in this study for the bound reactivity and competence with arene exchange. In a later study, Shibata investigated the feasibility of an enantioselective hydroamination reaction by using chiral ligands. Using the ligand (S)-xylylBINAP, an ee of 76% was observed for the reaction, although the overall yield was reduced.[89]

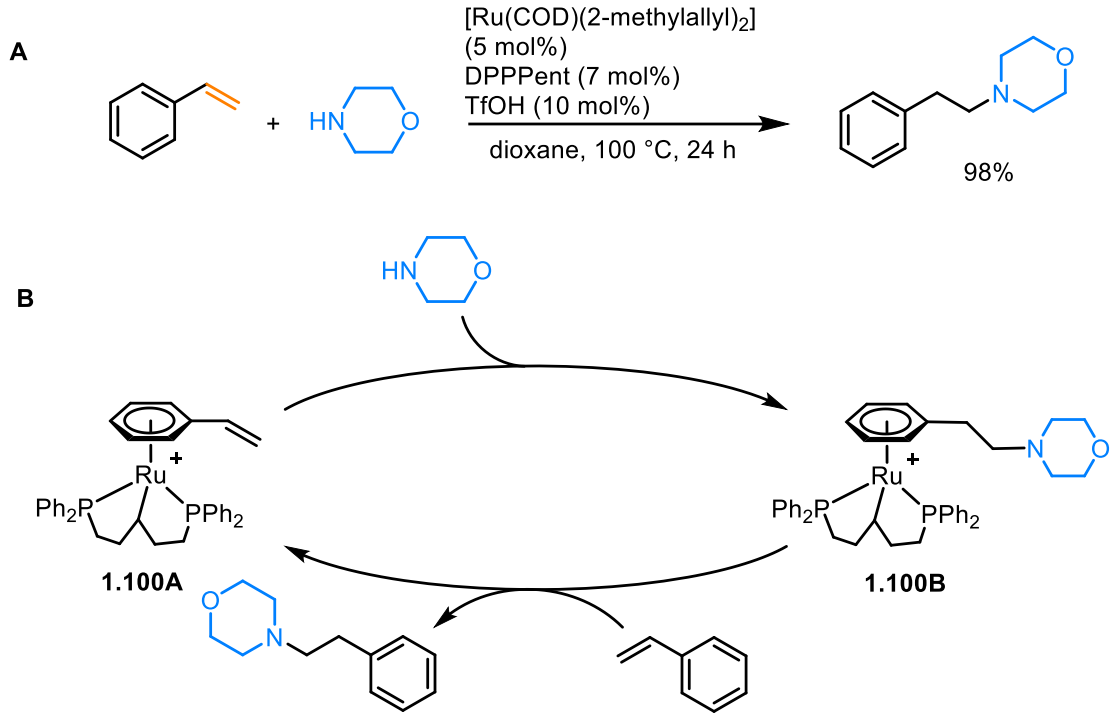

Figure 1.47. *Ru-catalysed hydroamination of styrene*

1.5.3. π-Arene Intermediates Which Undergo Oxidative Addition

Another class of catalytic reactions involves subsequent oxidative addition of an arene ring to a metal centre shortly after η^6-coordination. The first example of this was published in Hartwig's Ni-catalysed hydrogenolysis of aryl ethers (figure 1.48A).[90] While hydrogenolysis usually requires forcing conditions (e.g. 250 °C or 30 bar H_2), this work showed a Ni(0)-catalysed C-O bond activation under just 1 bar of H_2. Also, the reaction conditions were found to be active towards both electron-rich and electron-poor arene rings, while there was no evidence to suggest arene hydrogenation was occurring.

The Ni(0) hydrogenolysis mechanism was not known until several years later when a thorough investigation had been conducted. The mechanism was proposed to go via formation of the

complex [(η^6-ArOR)Ni^0(SIPr)] (**1.101A**) through arene exchange of the η^6-toluene complex. [91] π-coordination activates the aryl ether towards an oxidative addition of the Ni(0) centre into the aryl C-O bond, giving the Ni(II) aryl complex **1.101B** (figure 1.48B). A computational study on this oxidative addition step indicated that it is likely that an η^6- to η^2- ring slip occurs prior to the C-O bond cleavage,[92] although there is no direct experimental evidence for such an intermediate. After oxidative addition, reaction of **1.101B** with H_2 releases an alcohol, ROH, and generates the complex [(η^6-Arene)Ni^0(SIPr)] (**1.101C**), which undergoes arene exchange with the aryl ether to complete the cycle.

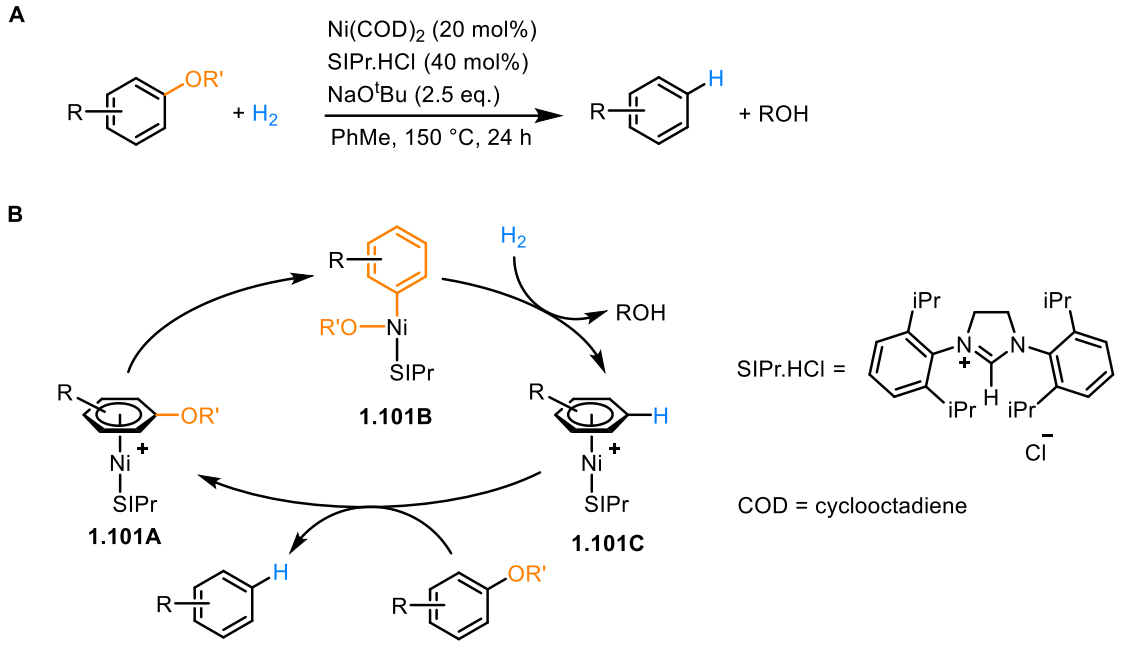

Figure 1.48. *Ni-catalysed hydrogenolysis of aryl ethers.*[91]

Under very similar catalytic conditions, a Ni catalyst was also used to couple fluoroarenes with both primary and secondary amines, giving a series of substituted aniline derivatives in good-excellent yields (figure 1.49A and B).[93] The mechanism of this reaction was only briefly discussed in the report, though an oxidative addition of the C-F bond to the Ni centre in **1.102A** was proposed (figure 1.49C). Based on the similarity between this catalysis and Hartwig's hydrogenolysis conditions, it is likely that the oxidative addition here is also preceded by η^6-coordination of the fluoroarene. While the scope for this coupling initially only included secondary amines, a later report by Iwai and Sawamura showed an extension of the scope to include primary amines, where the Ni catalyst contained bulky phosphine ligands instead of the NHC, improving the selectivity for formation of secondary amines over tertiary amines.[94]

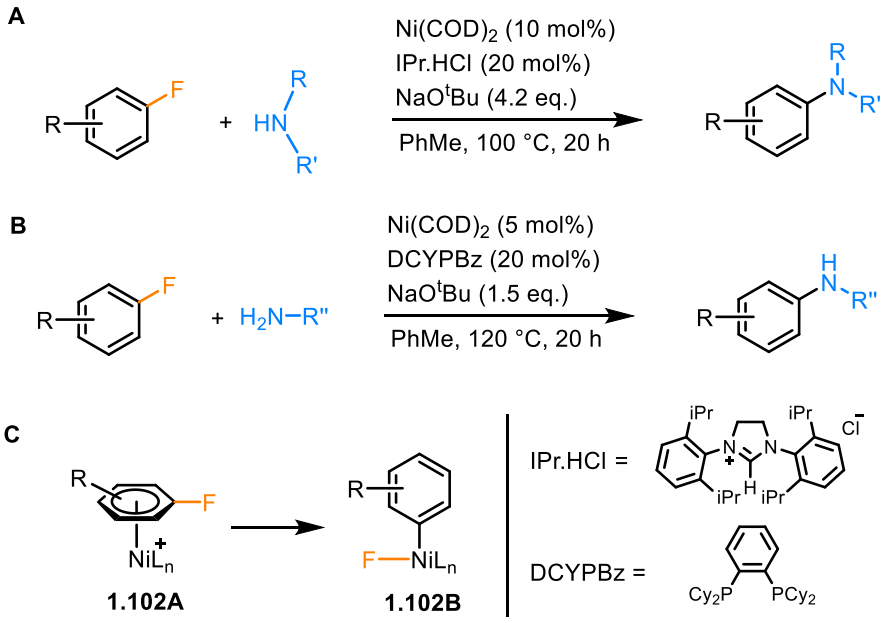

Figure 1.49. *Ni-catalysed amination of aryl fluorides*

The only known example of Nb π-arene complexes existing as key reaction intermediates was reported by Bergman and Arnold, where a Nb(III) catalyst was used for the hydrodefluorination of a small selection of fluoroarenes.[95] The proposed mechanism for the reaction (figure 1.50) included formation of an η^6-arene intermediate, [(η^6-ArF)$Nb^{III}L_n$] (**1.103A**). Unlike the previous examples, there was direct experimental evidence that formation of this π-ArF intermediate precedes oxidative addition of the C-F bond to the Nb centre, resulting in Nb(V) complex **1.103B**. Following oxidative addition, reductive elimination in the presence of $PhSiH_3$ gave Nb(III) complex the η^6-defluorinated arene Nb(III) complex **1.103C**, which can undergo arene exchange with the fluoroarene to complete the catalytic cycle. A detailed computational study indicated that the oxidative addition step occurred via formation of a bimetallic π-arene-bridged complex **1.104** (figure 1.50B), in a pathway calculated to have lower activation energy than a monometallic oxidative addition pathway.[96]

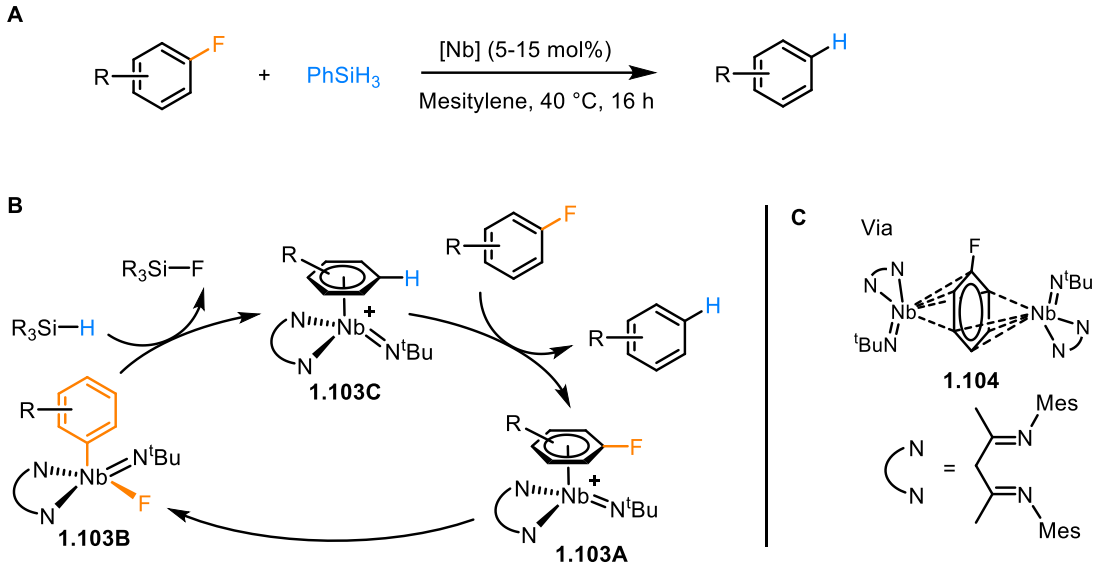

Figure 1.50. *Nb-catalysed hydrodefluorination of aryl fluorides*

1.5.4. Photoactivated Catalysis

In the last few years, significant advances in both theoretical understanding and available practical instrumentation have allowed the field of photocatalysis to grow rapidly. Furthermore, as was discussed in section 1.4.4, certain π-arene metal complexes are susceptible to photo-assisted destabilisation of the metal-arene bond, and therefore photocatalytic arene exchange should be feasible. Despite this, there only currently exists one example of a photocatalytic reaction which proceeds via a transient η^6-arene intermediate. In this example, stoichiometric amounts of the complex $[(MeCN)_3MCp^*]^+$ (**1.105A**, where M = Fe or Ru) were initially used in the Bergman cycloaromatisation of an enediyne, with γ-terpinene as a source of hydrogen (figure 1.51).[97] This results in the formation of the complex $[(\eta^6\text{-}C_6H_4(iPr)_2)MCp^*]^+$ (**1.105B**), which could be irradiated (medium pressure 500 W Hanovia lamp) in MeCN solvent to liberate the free arene and regenerate the preceding tris(acetonitrile) complex. Following this, it was found that the Bergman cycloaromatisation[98] could occur with only a catalytic quantity of the metal fragment, provided the reaction was done under constant irradiation. The catalytic mechanism is simple, the cycloaromatisation occurs to give **1.105B** and is followed by *in-situ* photolytic liberation of the product, and formation of the active metal complex **1.105A**, restarting the catalytic cycle. It is noteworthy that Fe catalysts were found to be slightly more catalytically active than their Ru counterparts, which coincides with Fe complexes having more facile photocatalytic arene exchange.

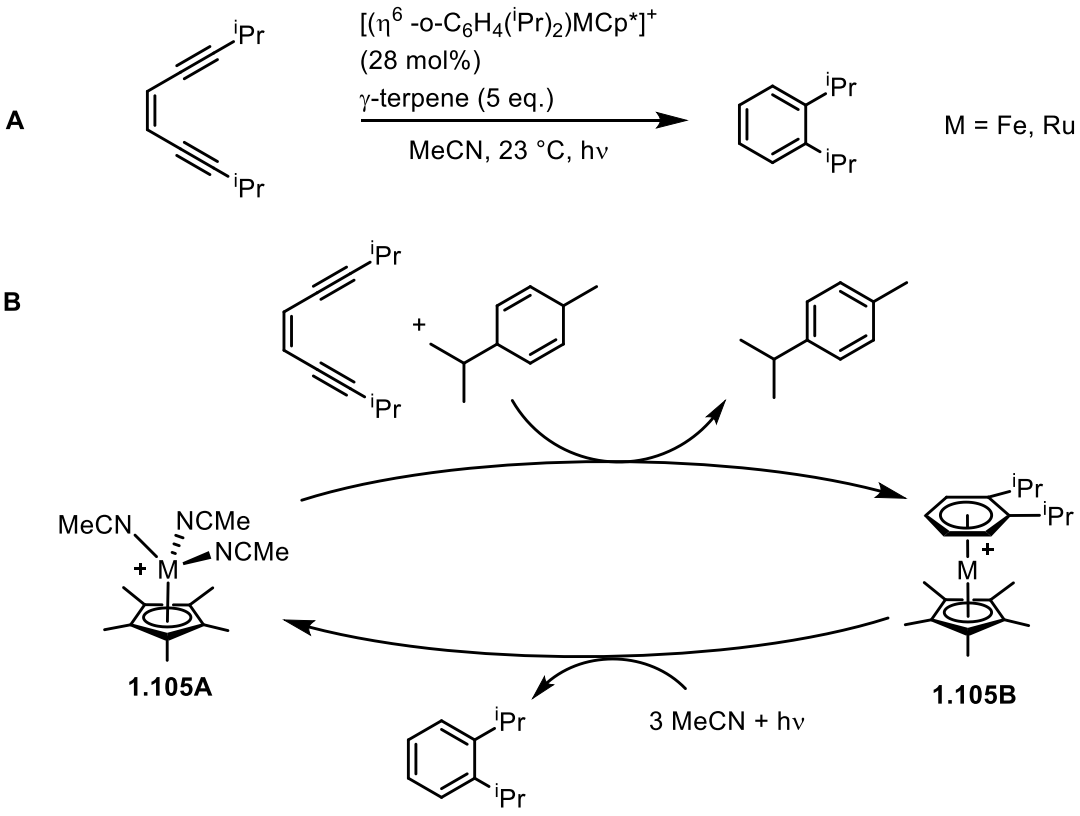

Figure 1.51. *Photocatalysed cycloaromatisation via π-arene metal intermediates (M = Ru(II) or Fe(II)).*

1.6. Summary

As highlighted throughout this chapter, coordination of arene rings to metal centres can have a dramatic effect upon their reactivity. Many research groups have exploited this change in reactivity to develop novel synthetic transformations. Most of these reactions are stoichiometric with respect to the activating metal. Subsequent liberation of the arene require photolysis or oxidation and rarely is the metal recycled. More recently, there has been a drive to develop reactions that are catalytic in the activating metal. A general scheme proposed by Semmelhack forms the foundation of such reactions, where the metal–arene complex reacts and must then undergo an arene exchange process. The rate of each step in the process must be balanced to allow for a catalytic process. To facilitate catalytic reactions several in depth studies have been carried to understand the factors that affect arene exchange (typically rate limiting in such catalytic reactions). With this knowledge in hand, a small library of catalytic reactions has been developed over the past 15 years.

Despite the examples of successful reaction of these pi-arene organometallic complexes, there are no doubt, many more reactions that could be discovered, with likely benefit to industrial synthesis. Furthermore, many of the reactions that remain stoichiometric in the activating metal could potentially be converted to catalytic processes by manipulating the catalytic metal and the reaction conditions. Overall, this field of organometallic arene reaction chemistry seems to have much room for further development and this PhD Thesis has been dedicated to finding new developments in this area.

1.7. Project Aims

The activation of arene rings through π-coordination to a metal fragment has been a highly useful technique for synthetic chemists for decades, since their initial discovery. Over the past two decades, such transformations have seen a resurgence in use with the development of protocols catalytic in the activating metal. The main aims of this project are to establish and develop new stoichiometric transformations and convert both those and already existing reactions into catalytic protocols. Specific aims include:

1. **Develop nucleophilic aromatic fluorination and difluoromethylation procedures for complexes of the form [(η^6-arene)RuCp]$^+$**

The initial aim of this work is to synthesise the sandwich complexes [(η^6-benzene)RuCp(*)][PF_6] from appropriate Ru(II) sources, and then to screen their reactivity towards different nucleophilic sources of fluoride and difluoromethyl. Following optimisation of conditions for fluorination and difluoromethylation, complexes containing different η^6-bound arene rings could be subjected to the optimal conditions to investigate the versatility and functional group tolerance of such aromatic transformations. Finally, translation of the fluorination and difluoromethylation protocols to be catalytic in the activating Ru(II) fragment is a key step to making these reactions viable for common use in organic synthesis.

2. Development of the enolate S_NAr synthesis of 2-aryl-1,3-diones *via* ruthenium η^6-arene intermediates

The first aim here is to prepare the sandwich complex $[(\eta^6\text{-}C_6H_5X][PF_6]$ (where X is F, Cl, or NO_2) and test its reactivity towards the enolate formed via deprotonation of 1,3-cyclohexanedione. Extension and optimisation of the reaction towards bound arenes containing one or two *ortho* methyl substituents indicates the propensity for the enolate S_NAr towards more hindered aromatic rings, while the chemoselectivity of the reaction can be established by performing competition experiments on η^6-bound rings containing multiple different leaving groups. Following S_NAr, photolytic liberation of the bound 2-aryl-1,3-dione from the activating $RuCp^+$ centre, using a coordinating solvent to displace the ring was investigated. The next necessary aim is to elucidate the tolerance of the enolate S_NAr towards a series of different cyclic and acyclic 1,3-diones, then apply the optimised photolysis conditions to each product. In the long-term, the aim of this project is to make the enolate S_NAr catalytic with respect to Ru(II), which can be done by applying already known catalytic protocols to our system. This step is key to making such transformations feasible for use in industrial labs, where scalability of the synthesis is of significant importance.

3. Investigations into increasing the rate of arene exchange

To probe the reaction kinetics of arene exchange, a model system involving the thermodynamically-favoured exchange of benzene in the complex $[(\eta^6\text{-}C_6H_6)RuCp]^+$ by a large excess of hexamethylbenzene will be tested. Monitoring the reaction by *in-situ* mass spectrometry gives the relative ratios of each complex at a given time point, under the assumption that both species behave identically in the mass spectrometer. There are many modifications to the experiment which can be tested to increase the rate of arene exchange, such as the use of light or increasing the temperature. An alternative way to increase the rate of arene exchange is to stabilise the η^4-intermediate formed in the rate-determining step. This can be accomplished by using a coordinating solvent, such as octanol, which can temporarily bind to the free coordination site around the Ru centre. Alternatively, coordinating groups can be tethered to the spectating Cp ligand, giving an intramolecular mode of stabilisation for the intermediate complex. A library of such tether complexes bearing different coordinating groups are synthesised and tested for their influence on the rate of arene exchange in our model system.

4. Ru-catalysed aromatic transformations

The first aim for this work is to further optimise the conditions of a Ru-catalysed S_NAr amination of 4-chlorotoluene (previous work: 90% conversion, 14 days) by further catalyst screening, including the coordinating-tether complexes discussed in chapter 4. The next aim is to synthesise the suspected resting state of the catalysis, $[(\eta^6\text{-N-(4-tolyl)morpholine})RuCp]^+$, to confirm its existence and characteristics.

The other key aim of this chapter is to further optimise a Ru-catalysed hydrodeiodination of 4-iodotoluene, while further extending the iodoarene scope to include more functionalities and iodopyridines. The mechanism for this process is likely to be a radical process, and analysis of the relative performances of functionalised iodoarenes, as well as arenes containing multiple halogen substituents potentially gives further clarity to the nature of the transition state of the mechanism.

Chapter 2

Fluorination and Difluoromethylation of Arenes Activated by η^6-Coordination to Ru(II)

2.1. Introduction

2.1.1. Aromatic Fluorides and Their Role in Chemistry and Society

C-F bonds have been intensively researched for their widespread applications in pharmeceuticals,[99] agrochemicals,[100] and materials chemistry.[101] Due to the small radius and high electronegativity of the fluorine atom, C-F bonds are so highly polarised that they become more electrostatic than covalent.[102] As a result of its properties, incorporation of a C-F bond to organic drug compounds increases the bioavailability and lipophilicity,[99,103] while the inertness of the bond leads to a higher metabolic stability. An estimated 25% of all pharmaceuticals, and 30% of applied agrochemicals contain a fluorine atom or trifluoromethyl group, which is unsurprising given its beneficial influence on properties. A few examples of highly successful pharmaceutical compounds, each containing one or more fluorine atoms are illustrated in figure 2.1.

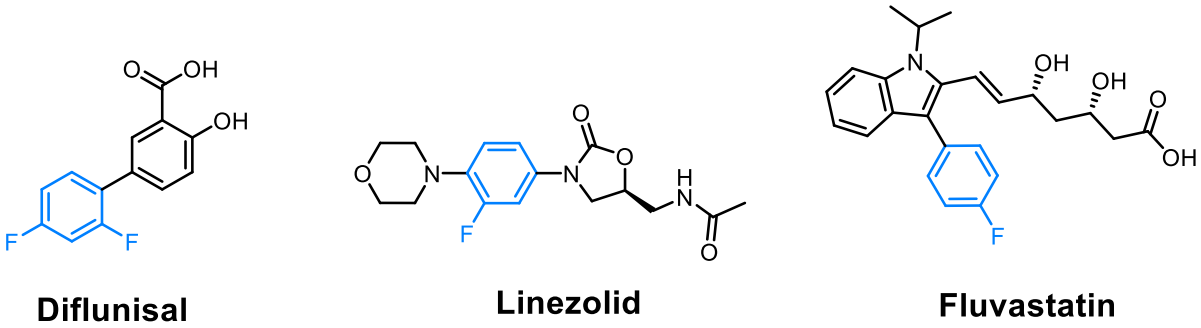

Figure 2.1. *Structures of the pharmaceuticals Diflunisal (anti-inflammatory), Linezolid (antibiotic) and Fluvastatin (lowers cholesterol), with fluorine-substituted aromatic rings highlighted.*

2.1.2. Current Fluorination Technologies

The simplest fluorination reagent known is elemental fluorine, F_2, which exists as a pale yellow gas at room temperature and pressure. Due to its low bond dissociation energy of 36.9 kJ / mol,[104] combined with the strength of C-F bond (BDE up to 544 kJ / mol),[105] fluorine reacts readily with organic compounds, usually in a violent and explosive manner, meaning specialist equipment and expertise are required to use it safely and effectively. Many alternative and milder methods of attaching fluorine atoms to organic frameworks exist, with new procedures, and their mechanisms being explored; these break down into several sub-categories; electrophilic, direct free radical and nucleophilic.

2.1.2.1. Electrophilic Fluorination

Electrophilic fluorination of organic compounds relies on using a source of 'F^+'; given the highly electronegative nature of fluorine, this seems like an unconventional strategy. Despite this, the area is well-studied, and many different electrophilic sources of fluorine are known. The majority of electrophilic fluorine sources have an N-F bond, and are split into two distinct classes: neutral R_2NF agents, and cationic $[R_3N^+F][A^-]$; both work in the same way, to polarise the N-F bond toward the nitrogen atom.[106]

First reported in 1987 by Desmarteau and co-workers,[107] *N*-fluoroperfluoroalkylsulfonamides (**2.1A**) are an extremely strong source of electrophilic fluorine, capable of mono-fluorinating benzene, toluene and many other substituted benzene derivatives. A slightly milder derivative, *N*-fluorobenzenesulfonamide (**2.1B**), was reported in 1990; this compound is weaker than the original version and hence only fluorinated electron-rich aromatics and strong nucleophiles such as Grignard reagents.[108] Other derivatives of these neutral N-F electrophiles, *N*-fluoro-*N*-alkylsulfonamides (**2.1C**) were investigated by W. E. Barnette in 1984.[109] The heterocycle replacing one of the sulfonyl groups significantly weakens the electrophilicity, meaning these 'Barnette reagents' are useful more for fluorinating highly nucleophilic aromatics and carbanions. A study by J Schwartz *et al.*[110] showed stereospecific fluorination of a series of lithiated alkenes with *N*-fluoro-*N*-^{t}butylbenzenesulfonamide, further illustrating their worth in synthetic chemistry.

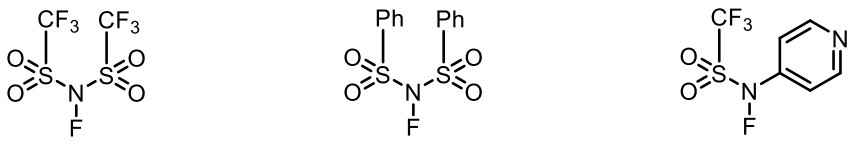

2.1A **2.1B** **2.1C**

Figure 2.2. *Structures of the neutral N-F electrophilic fluorination agents, N-fluoroperfluoromethylsulfonamide (A, left), N-fluorobenzenesulfonamide (B, centre) and N-fluoro-N-pyridinylperfluoromethylsulfonamide (C, right).*

Also of synthetic interest are quaternary $[R_3N^+F][A^-]$ compounds. First isolated and reported by Umemoto and co-workers in 1989 were a library of *N*-fluoropyridinium salts which underwent a rearrangement reaction in which the fluorine atom moves to the 2-position of the pyridine ring on exposure to base.[111] As electrophilic fluorinating agents, *N*-fluoropyridinium

species (**2.2A**) have shown a wide range of tuneable reactivity,[112] with some derivatives capable of fluorinating unactivated benzene rings, with others being milder and reacting only with more nucleophilic substrates. Also reported in the 1980s by Banks and co-workers were a series of *N*-fluoroquinuclidinium salts (**2.2B**),[113,114] which proved effective at fluorinating carbanions. Banks later reported the development of 1-alkyl-4-fluoro-1,4-diazoniadicyclo[2.2.2]dioctane (DABCO) salts,[14] of which selectfluor^{TM} (**2.2C**) is a derivative. This type of fluorinating agent is both strong, oxidising unactivated benzene, and versatile, being able to fluorinate a variety of different alkenes and aromatics.

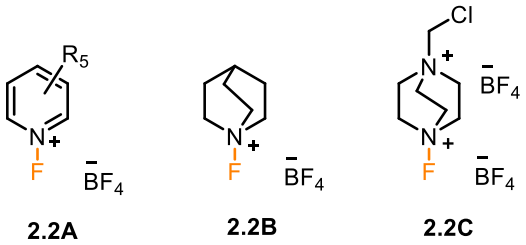

2.2A **2.2B** **2.2C**

Figure 2.3. *Structures of the quarternary N-F electrophilic fluorinating agents; N-fluoropyridinium tetrafluoroborate (left, A), N-fluoroquinuclidinium tetrafluoroborate (centre, B) and Selectfluor^{TM} (right, C).*

2.1.2.2. Nucleophilic Fluorination

Considering the polarity of the C-F bond, the more intuitive way of installing fluoro groups into organic molecules is via nucleophilic sources of fluoride, F^-. Some alkyl and aryl halides can be fluorinated via nucleophilic displacement using many different metal fluorides,[115,116] while a mixture of anhydrous HF in pyridine has been used to fluorinate alcohols in steroids,[117] and an array of alkenes.[118]

On an industrial scale, aniline is converted to fluorobenzene via the Balz-Schiemann reaction (Figure 2.4),[119–121] which involves the formation of diazonium tetrafluoroborate **2.3**, which on exposure to light triggers loss of nitrogen gas, and fluorobenzene is produced. The mechanism by which the decomposition step is likely to occur via S_N1-like displacement of N_2 by nucleophilic attack of one of the BF_4^- fluorides.[121]

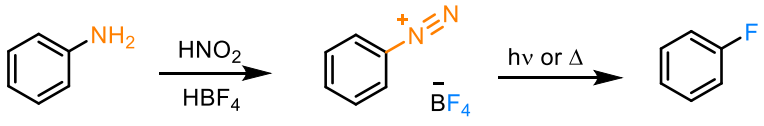

2.3

Figure 2.4. *Balz-Schiemann reaction to form fluorobenzene from aniline via a diazonium intermediate.*

In 2013, Hartwig and co-workers reported a selective fluorination of the pyridine 2-position (Figure 2.5), inspired by the Chichibabin synthesis of 2-aminopyridines.[122] The proposed source of fluoride was commercially available AgF_2, which was able to successfully fluorinate the 6-position of the pyridine ring in 2-phenyl pyridine with an isolated yield of 82%. The scope of the reaction was also established by varying the substituents on the ring, while extensive mechanistic studies led to the proposed mechanism involving coordination of Ag to form the pyridine-coordinated silver complex **2.4**, followed by addition of an Ag-F bond across the π-system, breaking the aromaticity of the ring. **2.5** then reacts with another AgF_2 in a radical hydride abstraction to finally give 2-fluoro-6-phenylpyridine **2.6**, as well as 2 equivalents of AgF and one HF. Another study by the same research group reported overall nucleophilic substitution (S_NAr) of hydride in pyridine rings, via a 2-fluoropyridine species formed *in-situ*.[123]

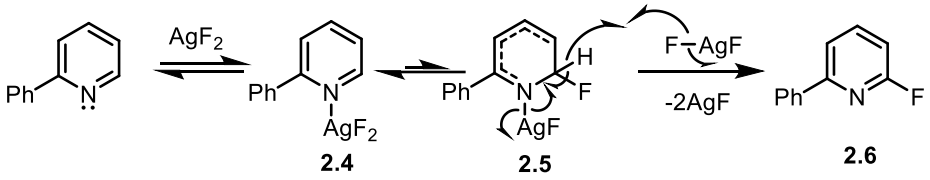

Figure 2.5. *Mechanism of AgF_2-mediated fluorination of pyridine, reported by Hartwig et al.*

2.1.2.3. Fluorination *via* Free-Radicals and Other Approaches

Radical fluorination reactions involve transfer of atomic fluorine, F·, to the substrate. Only a few radical sources of fluoride are currently known; one of these is xenon difluoride, XeF_2. In 1993, Ramsden and co-workers demonstrated an XeF_2-mediated radical fluorination of aryltrimethylsilanes (Figure 2.6),[124] while also optimising solvent for the reaction. In $CHCl_3$ and $CFCl_3$, side products with H or CCl_3 added to the arene instead of F were observed, suggesting aryl radical **2.7** is formed as an intermediate. In CH_3CN, no side-products were observed but the fluorinated yield was below 2%; the other solvent tested, C_6F_6, however gave an improved yield of 87% of the desired fluoroarene and no by-products so was selected as the optimal solvent for the radical fluorination by XeF_2. One major drawback of using XeF_2, however, is the generally high cost of xenon-based reagents, so they are not economically feasible to fluorinate on a large scale.

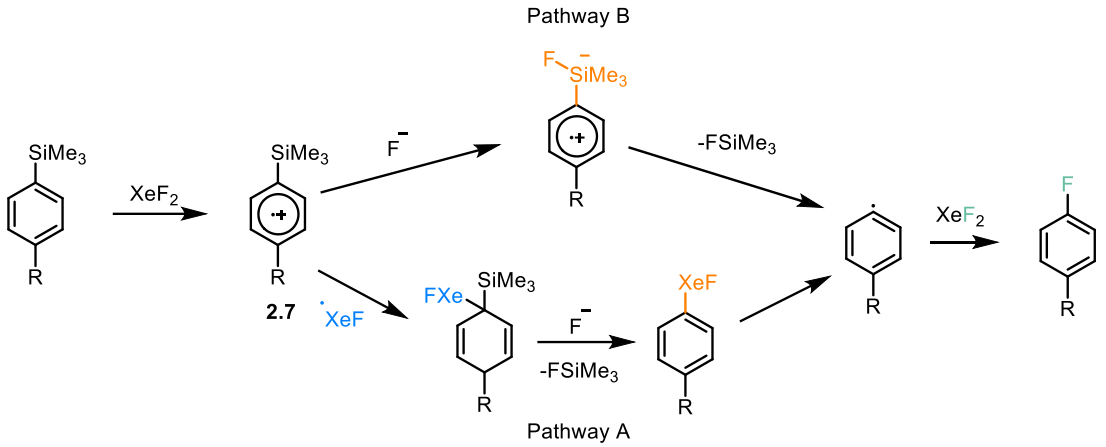

Figure 2.6. *Radical fluorination of aryltrimethylsilanes with XeF_2. Pathway A occurs via addition of fluoride to the Si atom, while pathway B occurs via formation of an allyl cation with a new Xe-C bond.*

At the same time as the pyridine fluorination was reported, Hartwig also demonstrated a Cu(I)-mediated fluorination of aryl iodides (Figure 2.7).[125] The fluoride source used was AgF, and the Cu(I)/Ag(I) system was able to successfully fluorinate a series of substituted aromatics with yields ranging from poor (<40%) to excellent (>95%) over the course of 22 hours in refluxing DMF. Initially, the reaction was predicted to occur via a radical mechanism, however performing the experiment with 1-iodo-2-*n*-butenyl benzene did not form an appreciable quantity of cyclised product so the proposed aryl radical intermediate was ruled out. Instead, the final proposed mechanism involves oxidative addition of the aryl-Iodine bond to Cu(I) to form Cu(III) complex **2.8A**, and following transmetalation of fluoride the fluoroarene is formed *via* reductive elimination of **2.8B**, meaning no 1-electron transfers are likely to happen. In a similar process, fluorination of arenes may be fluorinated by a Pd(0) catalyst in the presence of base and a metal fluoride (M = K, Cs, Ag), as reported by Buchwald in 2014.[126]

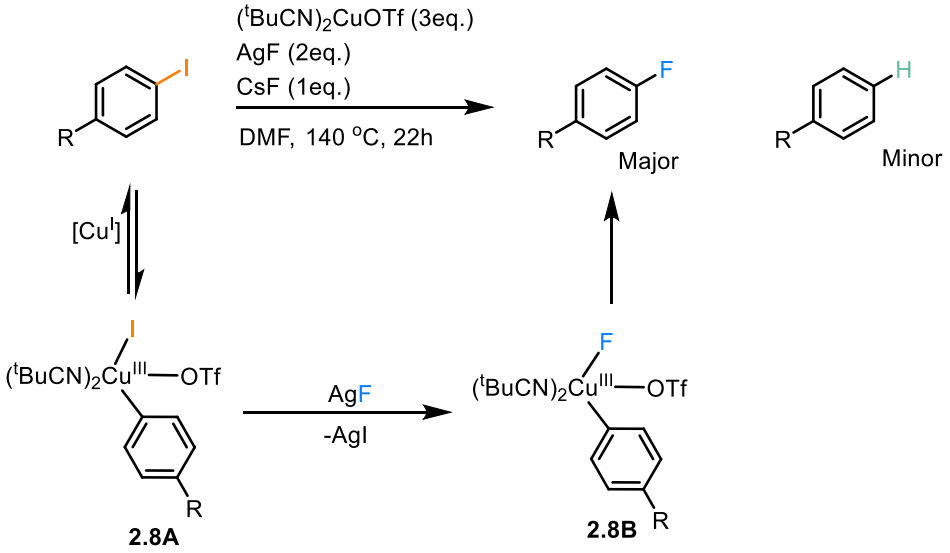

Figure 2.7. *Conditions and proposed mechanism of Cu(I) mediated fluorination of aryl iodides, reported by Hartwig et al.*

Overall, there are many different options for fluorinating organic species, in particular aromatics, with electrophilic agents more useful for electron-rich species such as carbanions and highly nucleophilic arenes, whereas nucleophilic agents are likely a better choice for fluorinating electron-poor species such as alkyl-halides or electron-poor aromatics. Despite being severely limited, free-radical sources of fluorine still have niche uses.

2.1.3. Project Aims

Previously, Grushin reported the Ru-catalysed fluorination of chloroarenes by a nucleophilic source of fluoride, which was proposed to occur via transient π-coordination of the ring to the Ru centre (figure 2.8A).[84] In this section, the nucleophilic aromatic fluorination of η^6-benzene ruthenium complex **2.9**. The proposed pathway by which benzene can be fluorinated is via the formation of a η^5-Meisenheimer complex **2.10**, which can then be oxidised to form either the complex [(η^6-fluorobenzene)RuCp]$^+$, or free fluorobenzene (figure 2.8B).

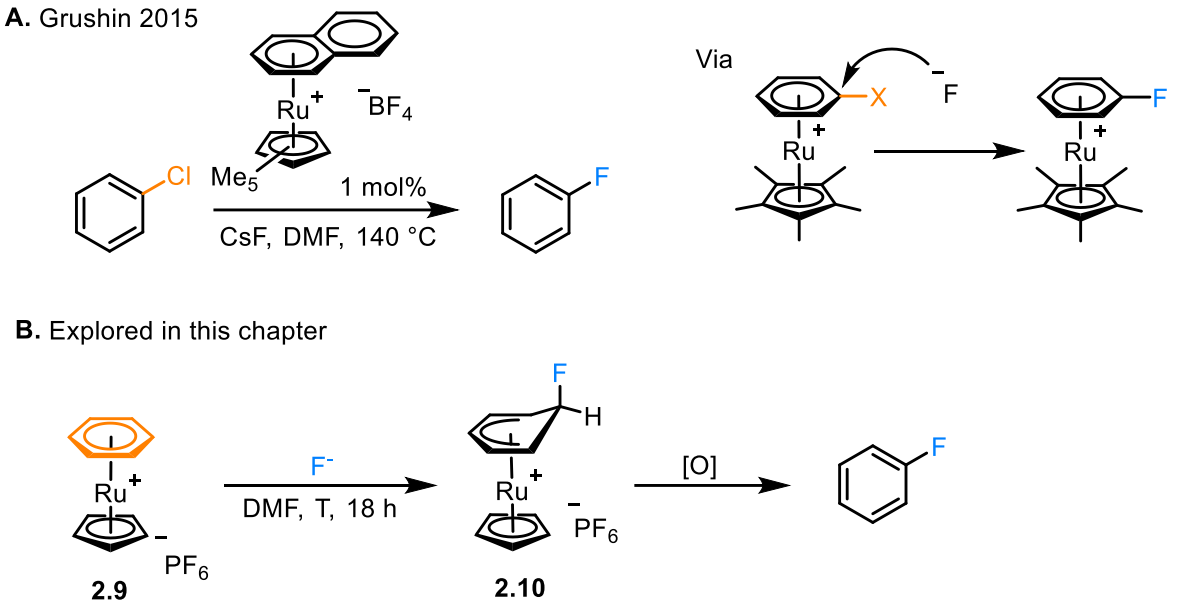

Figure 2.8. *Grushin's Ru-catalysed fluorination of aryl chlorides and the Ru-mediated fluorination of benzene explored in this chapter.*

2.2. Results and Discussion

2.2.1. Synthesis of initial Sandwich complexes [(η^6-benzene)RuCp(*)][PF_6]

First, the sandwich complex, [(η^6-benzene)RuCp][PF_6] (**2.9**) was synthesised via pathway A (figure 2.9). To achieve this the dimeric complex, [(η^6-C_6H_6)$RuCl_2$]$_2$ (**1.45**), freshly cracked cyclopentadiene and base were reacted in ethanol at reflux. Following an anion exchange with [NH_4]PF_6, the pure complex **2.9** was obtained via precipitation from acetonitrile/ether in a high yield (>90%), as an off-white crystalline solid. Due to the high cost of the dimeric ruthenium precursor complex, attempts were made to synthesise complex **2.9** from the cheaper precursor, $RuCl_3$, based on a procedure reported by Loughrey and co-workers.[127] This synthetic approach involved heating $RuCl_3.xH_2O$, cyclopentadiene and benzene in the presence of base, in ethanol solvent, before an *in-situ* anion exchange to incorporate the PF_6 anion. Due to issues with solubility, the isolation and purification of the complex **2.9** proved problematic, so only pathway A was used to synthesise this complex. However, the Cp* analogue, [(η^6-benzene)RuCp*][PF_6] (**2.11**), was successfully prepared *via* pathway B and isolated via trituration of the anion exchange mixture, followed by precipitation from MeCN/Et_2O.

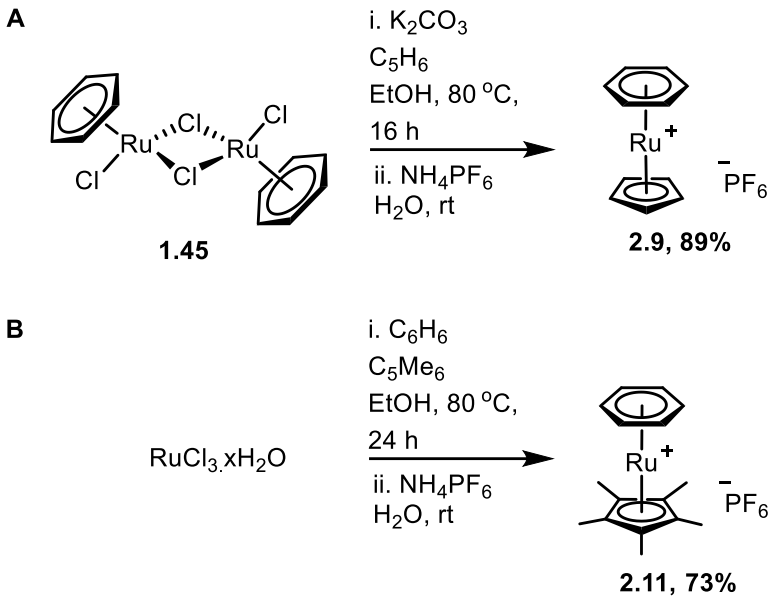

Figure 2.9. *Synthesis of the complexes [(η^6-benzene)RuCp][PF_6] (**2.9**) and [(η^6-benzene)RuCp*][PF_6] (**2.11**)*

Analysis of the ^{1}H NMR spectrum of **2.9** showed decreased chemical shifts for the arene (figure 2.10A), characteristic of the η^6- bond to a metal centre. Further evidence of arene binding was given by mass spectrometry, with the corresponding peaks having distinctive isotope pattern of ruthenium (figure 2.10B).

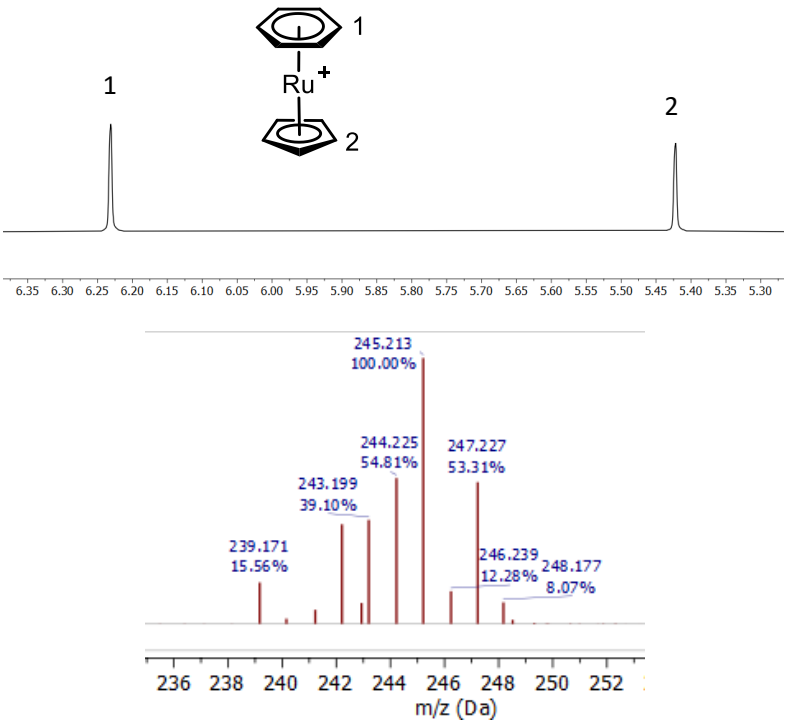

Figure 2.10. *^{1}H NMR and mass spectra of the complex [(η^6-benzene)RuCp]$^+$(**2.9**)*

2.2.2. Attempted Nucleophilic Fluorination of π-Coordinated Aromatic Rings

2.2.2.1. Attempted Fluorination of the Complexes [(η^6-benzene)RuCp(*)]$^+$, and Screening of Fluoride Sources

Initial studies of the reactivity of complex **2.9** towards nucleophilic fluoride were based on the Ru-catalysed fluorination of chloroarenes by Grushin *et al.*, where CsF was selected as the fluoride source in DMF solvent. Under these conditions, no reaction appeared to occur, as the ^{1}H NMR and ESI-mass spectra both matched that of the starting complex. The reaction was attempted with the corresponding Cp* complex, which was also unreactive to these conditions. Other fluoride salts of group 1 metals, including NaF and KF were screened but showed no reactivity here. Following this, two ammonium salts of fluorides were used, with TBAF (table 2.1 entry 5) being the only fluoride source to show any reactivity towards the η^6-benzene ring.

Table 2.1 *Reaction conditions screened for the attempted fluorination of [CpRu(η^6-C_6H_6)]$^+$.*

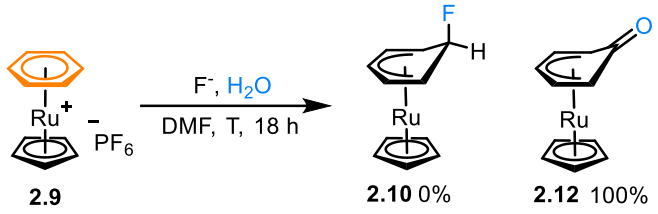

Entry	Fluoride Source	Additive	Temperature (°C)	Equivalents of Fluoride	NMR-Conversion /% (Isolated)
1	CsF	None	140	50	0
2	CsF	None	60	50	0
3	NaF	15-Crown-5	140	50	0
4	KF	18-Crown-6	140	50	0
5	TBAF	None	40	4	90* (70)
6	TMAF	None	40	50	0
7	AgF	None	140	50	0

*Hydroxylation product observed only

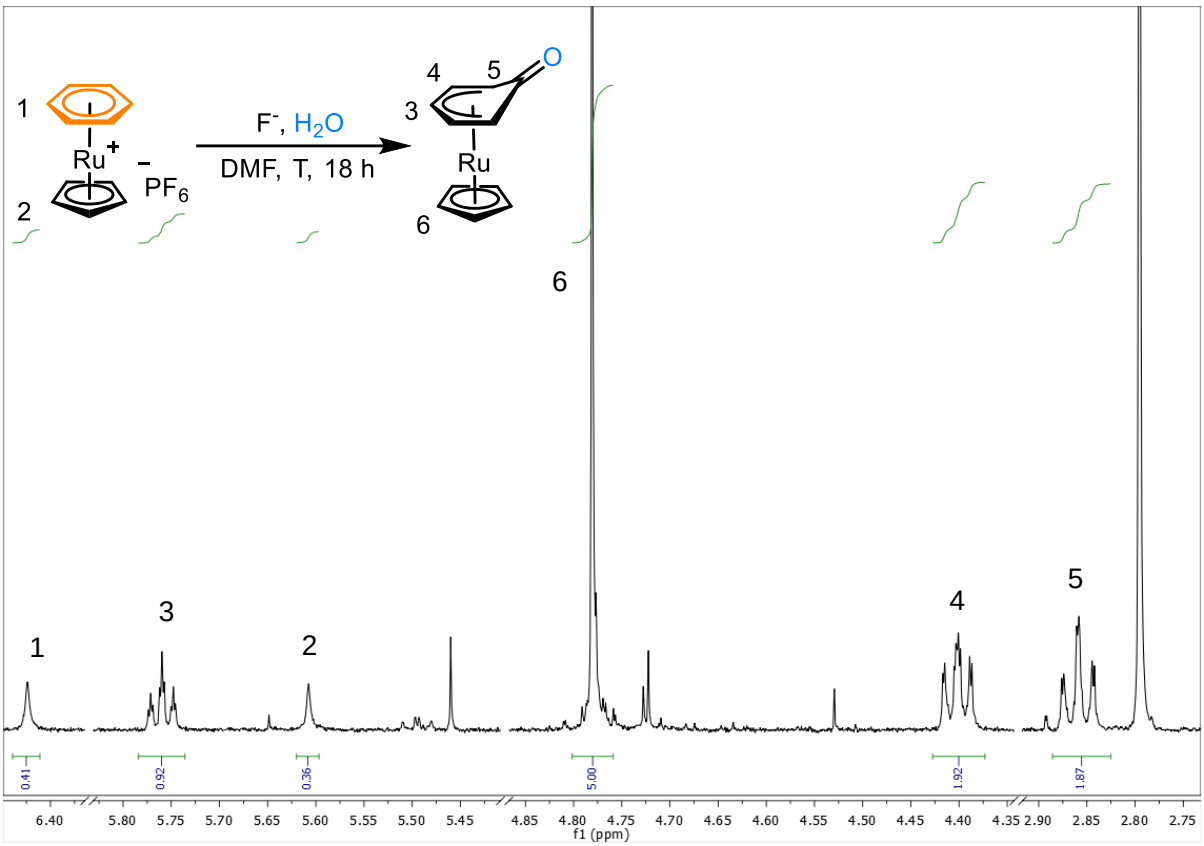

Figure 2.11. *^{1}H NMR Spectrum (Acetone-D_6, 400 MHz, 298 K) of the reaction between complex **2.9** and TBAF, with protons 1-6 assigned*

In the reaction with TBAF, the first indication of a reaction occurring was from appearance of new peaks in the ^{1}H NMR spectrum (figure 2.11), implying a loss of symmetry on the benzene ring. Three peaks with relative integrals of 1:2:2, appearing at 5.8, 4.4 and 2.8 ppm, respectively, each having complicated splitting patterns, suggest addition to the benzene ring, which is likely to be either a fluoride or hydroxy group. Further evidence for a reaction occurring on the benzene ring is given by the appearance of a new cyclopentadienyl peak at 4.8 ppm, with an integral of 5, relative to the other new peaks, while the peaks at 6.4 and 5.6 ppm indicate the presence of leftover starting material. The relative integrals indicate a conversion of around 92%, which did not change as the amount of TBAF was reduced from 50 to 4 equivalents. Analysis of the ^{19}F NMR spectrum proved inconclusive; the peaks at -72 ppm (PF_6) and -150 ppm (TBAF) are very intense, with additional peaks present, but only minor.

Analysis of the reaction by mass spectroscopy showed two different ruthenium peaks: the more intense appearing at 245 (m/z) corresponding to the starting complex, $[CpRu(\eta^6\text{-}C_6H_6)]^+$, and the other around 261, likely corresponding to either the reaction product, or another species formed during the ESI experiment (figure 2.12). Addition of 16 Da to the starting complex is inconsistent with addition of ^{19}F, meaning formation of the desired Meisenheimer complex is unlikely. Instead, the mass to charge ratio matches with that of the complex $[(\eta^6\text{-phenol})RuCp]^+$. This complex is unlikely to be the reaction product, however, as there is an absence of a leaving group on the ring, as well as a ^1H NMR spectrum indicative of a η^5-Meisenheimer complex. It is feasible that the ring had rearomatized during the ionization process on the mass spectrometer.

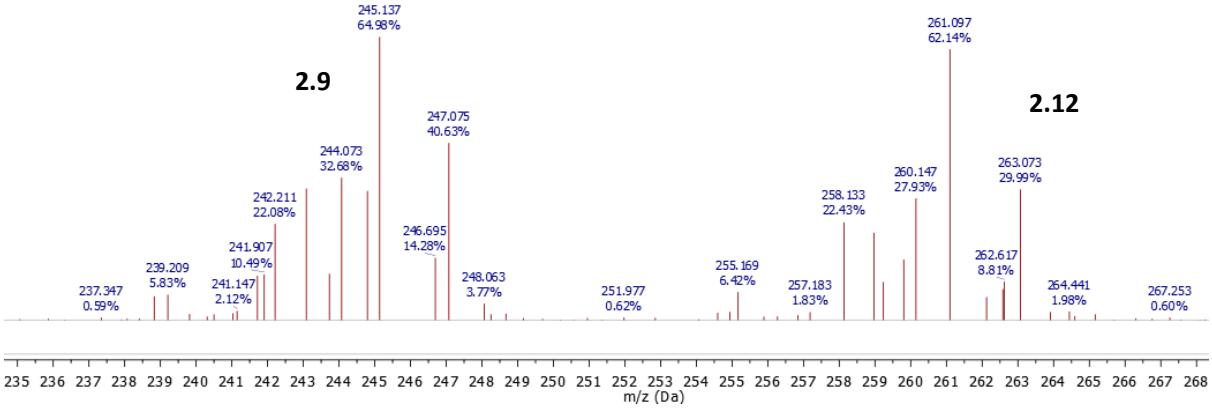

Figure 2.12. *ESI- mass spectrum of the reaction mixture containing the complex $[(\eta^6\text{-benzene})RuCp]^+$ (**2.9**) and TBAF, after removal of the solvents. Peaks corresponding to the TBA^+ cation have been omitted for clarity.*

The addition of a hydroxyl group here is likely a result of water being present in the reaction mixture. Given the synthetic procedure for the complexes employs dry solvents, and the DMF solvent in which this reaction occurred is anhydrous, the source of the water is most probably from the TBAF solution in THF. This is unsurprising; given the hygroscopic nature of TBAF a significant amount of water could have been present.

2.2.2.2. Attempted Isolation of a η^5-Meisenheimer Complex

Due to the presence of multiple (5-50) equivalents of TBAF, NMR spectra were difficult to analyse, making a conclusive determination of the structure of **2.12** problematic. The first attempt at purifying the crude reaction mixture was a small silica column, using 5% MeOH in DCM as the eluent. TLC analysis of the fractions displayed two distinct species, which had been separated during the column. However, analysis of all isolated fractions by ^{1}H NMR spectroscopy and mass spectrometry appeared to indicate the absence of the previously observed Meisenheimer complex, implying it had either stuck to or decomposed on the column.

The next method for removal of the excess TBAF attempted was ion exchange chromatography, using a DOWEX® proton exchange column. The rationale for using this technique was to trap all cationic species (TBA^+ and $[CpRu(\eta^6C_6H_6)]^+$) while allowing neutral compounds, such as the expected Meisenheimer complex, to pass through. The column was prepared by washing the resin with boiling methanol, then 2M HCl, water and finally cold methanol. A solution of freshly made crude Meisenheimer complex in DCM was used and appeared to travel through the column. Analysis by ^{1}H NMR spectroscopy showed that all TBA^+ and the starting complex, $[(\eta^6$-benzene)RuCp$]^+$, had been removed from the sample, however the multiplets from the suspected product were also not present.

The final attempt at removing TBAF was by simply washing a freshly made sample of crude material with THF. This experiment successfully removed all the brown oily material (TBAF), leaving behind an off-white solid. Both the residue and washings were analysed by ^{1}H NMR spectroscopy, though neither spectrum appeared to contain any of the product peaks, despite them being present on analysis of the crude sample before the washing. This finding suggests that the species formed in the reaction of benzene sandwich complex and TBAF is unstable when in solution in the presence of air. To test this hypothesis, a sample of the crude material was dissolved in d^6-acetone and ^{1}H/^{19}F spectra were recorded at different time points over the course of several days (figure 2.13). During the experiment, integrals of the peaks at 5.8, 4.4 and 2.8 ppm (product) were all decreasing uniformly over time, while integrals of the peaks at 6.4 and 5.6 ppm (starting material) were growing over time, giving evidence for decomposition of the product species, likely reversion back into the starting material.

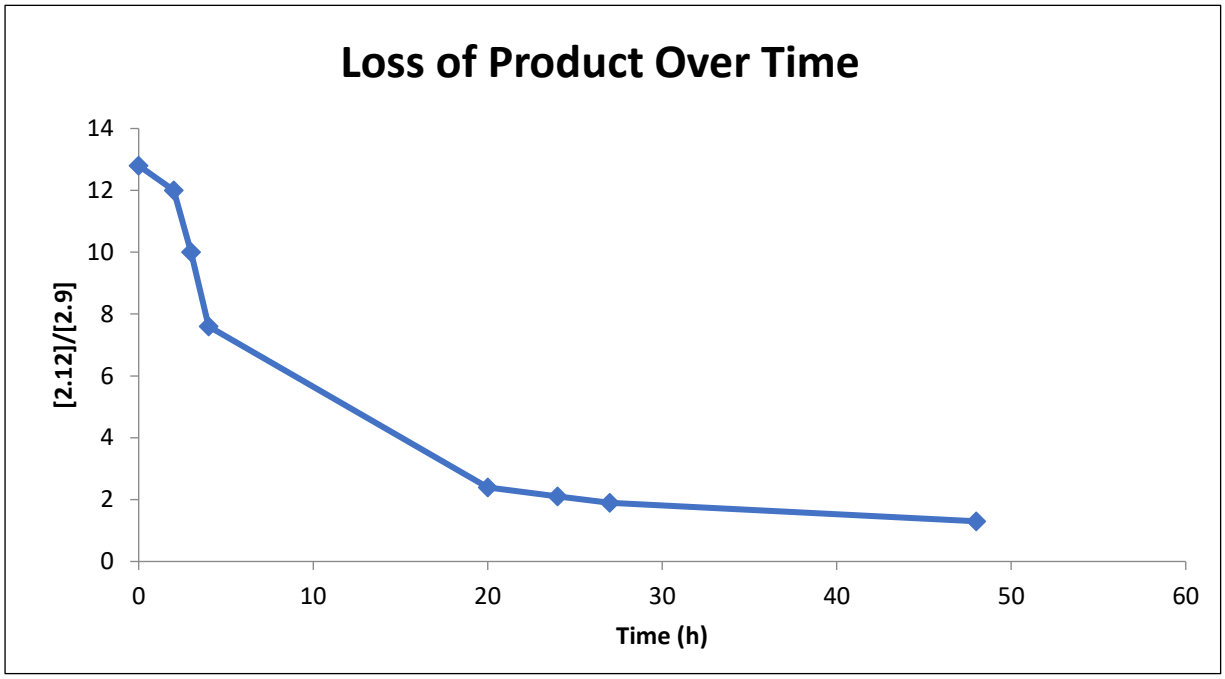

Figure 2.13. *Ratio of the apparent product of the attempted fluorination of complex [(η^5-hydroxycyclohexandienyl)RuCp]$^+$(**2.12**) to the starting complex, [(η^6-C_6H_6)RuCp]$^+$(**2.9**). Relative amounts of each species is derived from comparison of cyclopentadienyl peaks in ^{1}H NMR over the course of two days.*

2.2.2.3. Attempted In-Situ Oxidation of η^5-Meisenheimer Complex

As an alternative to purification of the product, a series of oxidants were screened to perform an *in-situ* hydride abstraction from the Meisenheimer complex **2.12**, re-aromatizing the ring (figure 2.14) to give the η^6-phenol complex **2.13**. Once the top ring is re-aromatized the species should become much more stable in solution, simplifying the purification process.

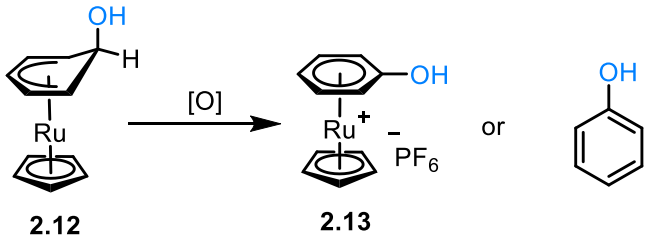

Figure 2.14. *Proposed oxidation of the Meisenheimer ruthenium complex discussed in section 2.2.1*

The initial oxidising agent used was 2,3-dichloro-5,6-dicyano-1,4-benzoquinone (DDQ) as it had successfully oxidised the Meisenheimer complex formed during the nucleophilic trifluoromethylation of η^6-bound nitrobenzene,[46] forming free 1-nitro-2-trifluoromethyl benzene. However, NMR spectroscopy and ESI-MS analysis of this reaction both showed presence of only starting material and TBAF. Instead, a weaker oxidising agent was used, trityl chloride, which can react as a hydride acceptor to form triphenylmethane.[64] Spectroscopic

analysis revealed that the trityl chloride had not reacted, as the ^{1}H NMR spectrum was unchanged after the reaction. The next oxidising agent used was elemental iodine, I_2, as it has previously been used to oxidise Meisenheimer species bound η^5- to $Cr(CO)_3$ centres.[37, 65] However, like with DDQ, iodine appeared to destroy the product complex, leaving behind just starting material and TBAF. Following this, a series of other oxidants were screened for possible conversion of a Meisenheimer complex to a π-arene. These compounds were 1,4-benzoquinone, $NOBF_4$, PCl_5 and MnO_2; each oxidant appeared to either destroy the product or showed no reaction at all.

2.2.3. Reactivity of Different π-Arene Complexes Towards Nucleophilic Fluoride

To further increase the reactivity of an η^6-arene towards nucleophilic attack, an EWG can be added to the ring. Synthesis of such π-arene complexes was achieved by refluxing the precursor complex, $[(CpRu(NCMe)_3][PF_6]$ (**1.45**) with the desired arene in anhydrous 1,2-DCE (figure 2.15). Purification of the η^6-chlorobenzene and nitrobenzene complexes (**2.14** and **2.15**, respectively) *via* precipitation from $MeCN/Et_2O$ give the sandwich complexes in good to excellent yields.

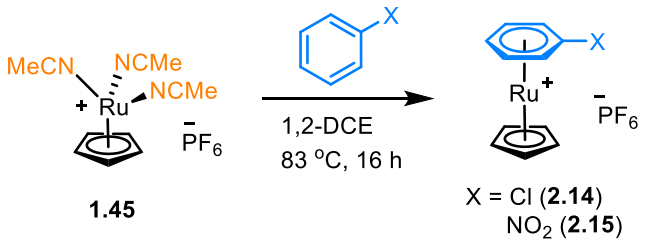

Figure 2.15. *Synthesis of the complexes [(η^6-C_6H_5X)RuCp][PF_6], where X = Cl, NO_2*

As Walton showed previously, it is possible to get either S_NAr displacement of the EWG or formation of a Meisenheimer complex via attack on the carbon *ortho* to the functional group.[128] In this published example, the ratio of substitution to addition products varied, though in most cases they formed in a 1:1 mixture. Starting with either sandwich complex **2.14** or **2.15**, exposure to a fluoride source (CsF or TBAF) appeared to yield exclusively a product of S_NAr displacement on the ring, while ^{1}H and ^{19}F NMR spectroscopic analysis indicated that hydroxylated complex **2.13** had formed (figure 2.16). Another experiment was performed

where the CsF had been dried under vacuum at 200 °C, but still the η^6-phenol complex had formed.

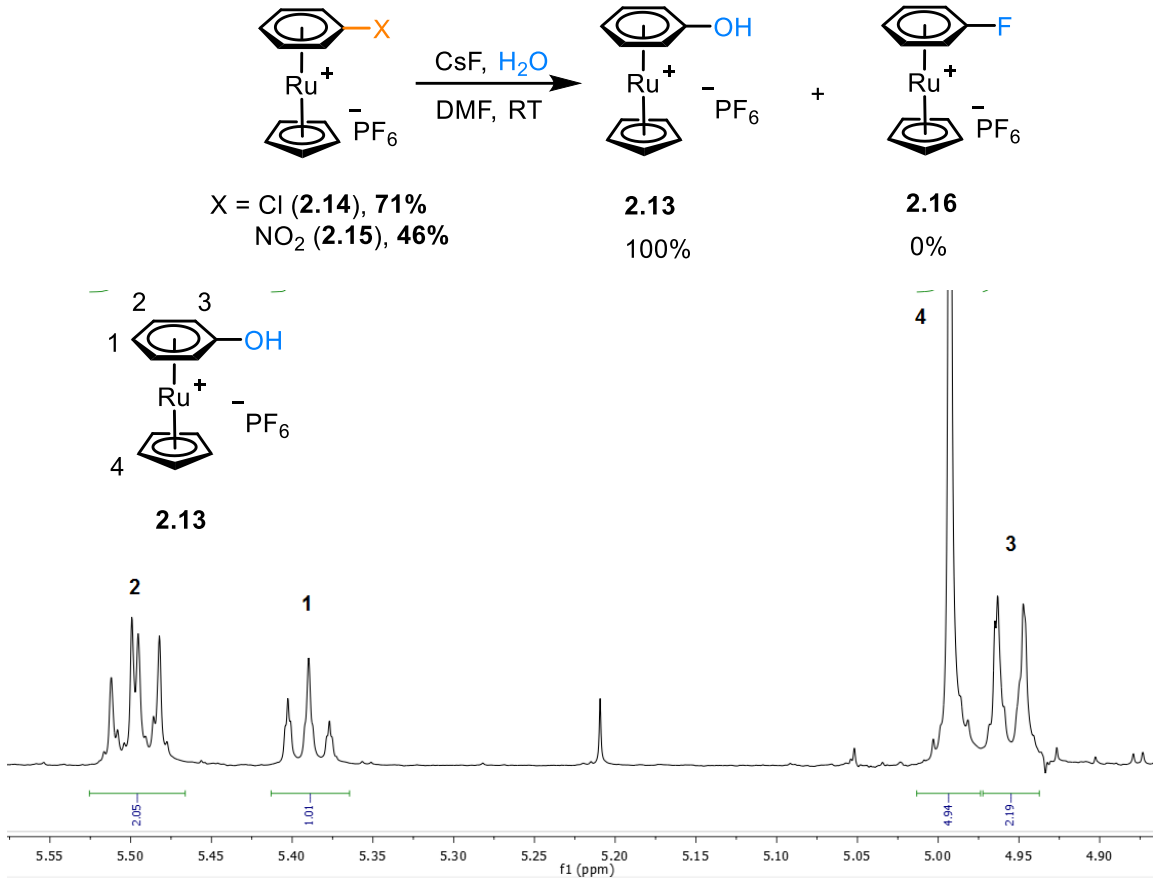

Figure 2.16. *Hydroxylation of complexes* ***2.14*** *and* ***2.15****, formed from an attempted fluorination*

To establish the origin of the water in the reaction, an experiment was performed in the absence of fluoride, and no reaction occurred. This suggests that the CsF was likely the source of water even despite the drying procedure. Alternatively the water was from elsewhere and fluoride is required to deprotonate it, forming nucleophilic hydroxide. While S_NAr of η^6-aryl chlorides is already established,[129] similar processes using η^6-nitroarenes are relatively unexplored, making it a potentially useful alternative for future study.

2.2.4. Trifluoromethylation and Attempted Difluoromethylation of π-Coordinated Aromatic Rings

Based on the previous trifluoromethylation procedure by Walton, in which treatment of the complex $[CpRu(\eta^6\text{-}C_6H_5NO_2)][PF_6]$ (**2.15**) yielded a 1:1 mixture of an S_NAr product **2.17** Meisenheimer complex **2.18**, a similar difluoromethylation was attempted (figure 2.17). An advantage which difluoromethylation has over trifluoromethylation is that the CF_2H proton can

be removed, meaning more functional groups may be added. Furthermore, CF_2H groups provide alternative lipophilicity to CF_3 groups, which may alter the behaviour of pharmaceuticals in biological assays.

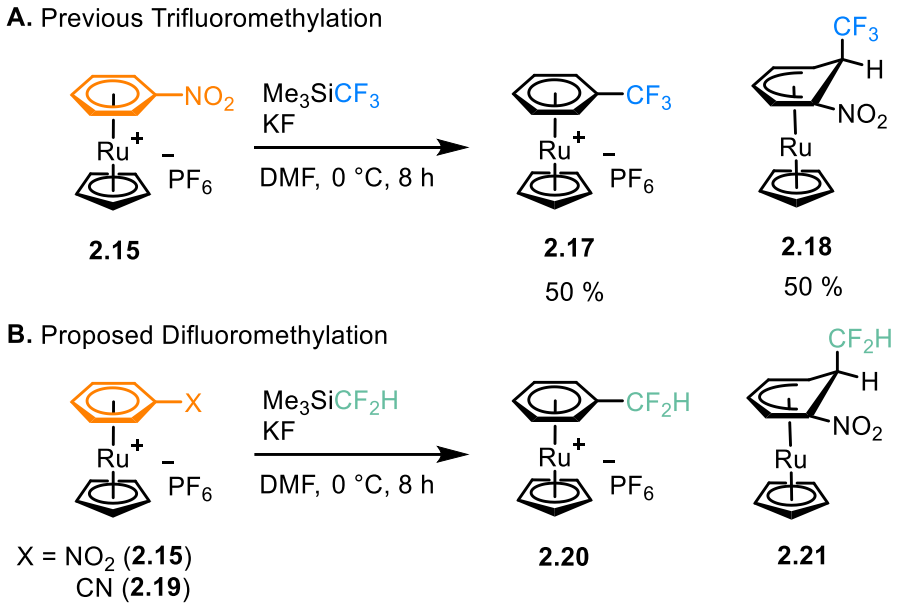

Figure 2.17. *Previous nucleophilic trifluoromethylation of unactivated arenes by Pike and Walton, and proposed difluoromethylation procedure*

Initially, complex **2.15** was exposed to the difluoromethyl source, CF_2HSiMe_3, which did not appear to show any reactivity on analysis of the ^1H NMR spectrum of the crude reaction mixture. As a reference, the equivalent trifluoromethylation was performed, with formation of the Meisenheimer complex **2.18** observed by ^1H and ^{19}F NMR spectroscopy. These data imply that the difluoromethyl source is much less reactive, perhaps due to the lower stability of $[CF_2H]^-$ compared to $[CF_3]^-$. To promote formation of nucleophilic difluoromethyl, KF was replaced as the additive with KOtBu, which has been used previously in similar reactions.[130]

When the reaction was attempted in the presence of KOtBu, a neutral Meisenheimer complex of ruthenium (figure 2.18) was observed, suggesting the reaction had been successful. Purification was achieved by triturating the crude product with diethyl ether, and then filtration of the mixture followed by vacuum removal of solvent from the filtrate gave the product as a brown oil. This strategy successfully removed all remaining salts as well as any leftover starting complex and gave a pure product in a moderate (52%) yield. Analysis of multinuclear NMR spectra indicated the formation of Meisenheimer complex **2.22** (figure 2.18), as well as loss

of the PF_6 anion. Finally, ESI-MS analysis suggested the group which had added onto the ring to be OH, rather than the desired CF_2H, which was confirmed when the same spectrum was observed from a reaction where the difluoromethylating agent was absent. Following successful isolation of a pure Meisenheimer complex, reactivity towards many different oxidising agents was tested.

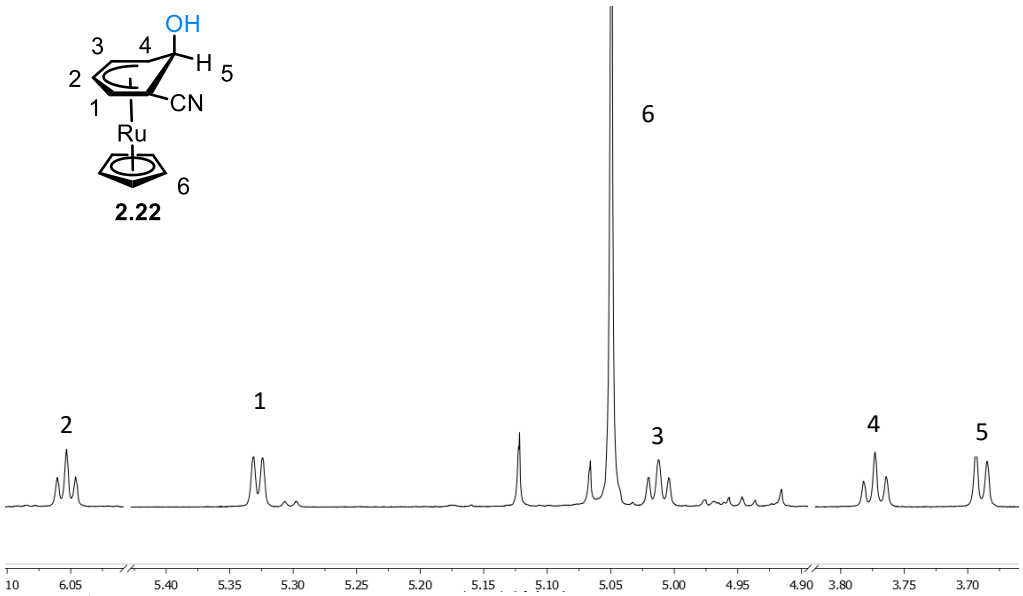

Figure 2.18. *^{1}H NMR Spectrum of proposed Ru Meisenheimer complex,* ***2.22****, with all peaks assigned (599 MHz, acetone-D_6, 298 K).*

Oxidation of this complex could result in one of two products, either a rearomatized arene still coordinated to the Ru centre, or a free arene ring. As was shown in the previous trifluoromethylation paper, oxidation of the CF_3 Meisenheimer with DDQ resulted in free 1-nitro-2-trifluoromethylbenzene. Reacting complex **2.22** with DDQ gave a similar result, a free arene as shown by the ^{1}H NMR spectrum (figure 2.19). Other oxidising agents, such as Ph_3CCl, $NOBF_4$, 1,4-benzoquinone and I_2 were also screened, but all either resulted in formation of a free arene species or did not react at all. The identity of the free arene produced by the DDQ oxidation was initially investigated by comparing the 1H NMR spectrum (figure 2.19) to multiple different arenes, including 2-cyanophenol and salicylic acid but neither matched. However, analysis of the reaction mixture by ESI-MS suggested 2- cyanophenol had formed, as a small peak at m/z = 120 was observed.

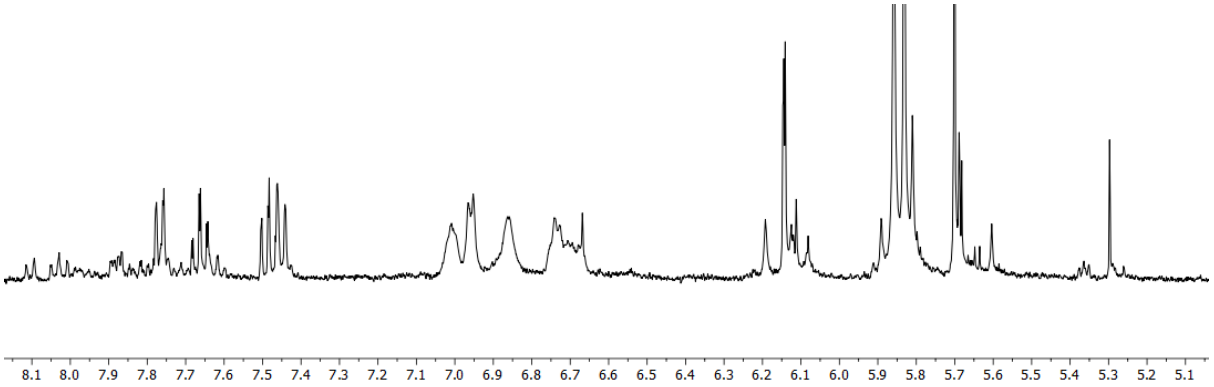

Figure 2.19. *^{1}H NMR spectrum of the crude product after oxidation of* ***2.22*** *by DDQ*

2.3. Conclusions and Outlook

To summarise, this chapter presents the attempted fluorination and difluoromethylation reactions of unactivated arenes bound η^6- to Ru. First, a fluorination of η^6-bound benzene was attempted, although presence of residual moisture led to the formation of a suspected hydroxylated η^5-Meisenheimer ruthenium complex, although attempts to isolate or further react the complex *in-situ* were unsuccessful. A difluoromethylation procedure, based on a previous nucleophilic trifluoromethylation done in the group, was also attempted on η^6-coordinated nitrobenzene and benzonitrile. Again, the presence of moisture led to an undesired hydroxylation reaction. However, the neutral Meisenheimer complex, [(η^5-1-hydroxy-2-cyanocyclohexadienyl)RuCp], was successfully isolated and characterized. Oxidation of this complex with DDQ led to the formation of a free aromatic compound, which is likely to be 2-cyanophenol. Further insight gained from this chapter was the observation of the different relative stabilities of η^5- bound Meisenheimer intermediates were observed, with more electron-deficient rings proving more stable with regards to both isolation and subsequent oxidation.

Chapter 3

Enolate S_NAr of Unactivated Arenes *via* $[(\eta^6\text{-arene})RuCp]^+$ Intermediates

3.1. Introduction

3.1.1. C-C Bond-Forming S_NAr Reactions

As discussed previously, nucleophilic aromatic substitution (S_NAr) of free arenes is mostly limited to those with one or more electron-withdrawing substituents, or electron-poor heterocycles such as pyridine. Most commonly, the nucleophiles used here tend to be amines or phenoxides,[131] though some carbon-based nucleophiles are reactive enough to be arylated, such as 1,3-dicarbonyls.[132–134] For example, dimethylmalonate in the presence of base was able to attack the C-X (X = F, Cl) bond in 4-halogeno-nitrobenzene derivatives, resulting in formation of new alkyl-substituted arenes (figure 3.1A).[132] In another study, a series of carbon based nucleophiles were found to be active in the vicarious nucleophilic substitution reaction with nitrobenzene (figure 3.1B).[134] Following this step, the newly substituted nitrobenzene ring can partake in a more typical S_NAr reaction with a halo-nitroarene, resulting in formation of a series of diaryl methane derivatives, in a good overall yield of 70-90%, making it not only an efficient process, but combines two different modes of nucleophilic aromatic substitution sequentially.

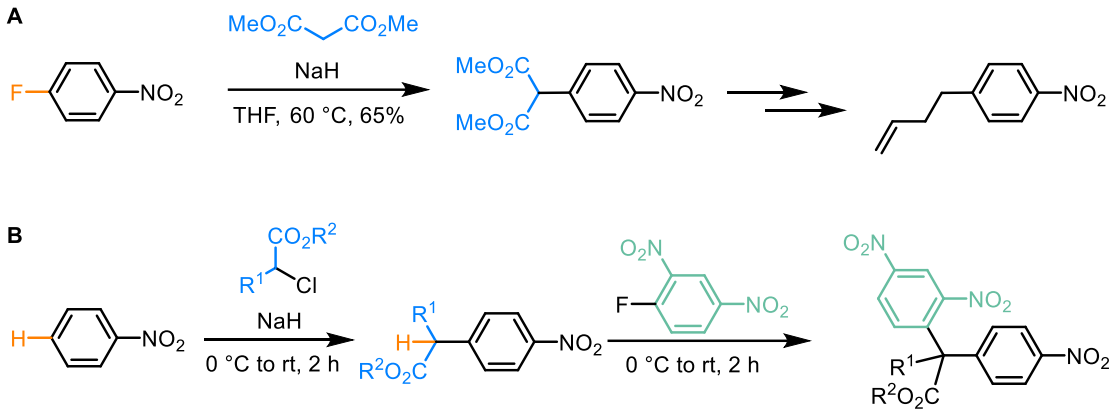

Figure 3.1. *Nucleophilic aromatic substitution (S_NAr) reactions of carbon nucleophiles with electron-poor arenes.*

When asymmetric 1,3-diones are used in the S_NAr reaction with an arene, a new chiral centre is formed. Until recently, control of this stereochemistry was rarely explored, and limited to oxygen nucleophiles in intramolecular reactions.[135–137] In 2005, Jørgensen and co-workers reported the first example of an intermolecular process, in which an enantiopure organocatalyst was used to catalyse the S_NAr reaction of an asymmetric 1,3-dione and 1-fluoro-2,5-nitrobenzene (figure 3.2).[138] After optimisation of the reaction conditions, the reaction

proceeded enantioselectively, giving an ee of 87%. The generality of this process was also tested with a series of different fluoro-nitro arenes and 1,3-diones. The enantioselectivity of the reaction was mostly unaffected by different functional groups, although the ee was significantly lower for lactams with an unprotected nitrogen.[138] Also noteworthy was that aryl rings, which were less activated towards nucleophilic aromatic substitution (i.e. fewer EWGs) unsurprisingly, were only able to generate trace amounts of the desired products. Nevertheless, this work has paved the way for an enantioselective intermolecular S_NAr process.

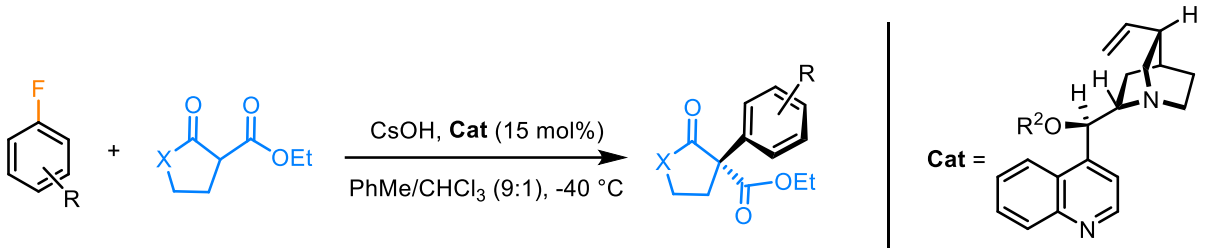

Figure 3.2. *Asymmetric S_NAr reaction mediated by an enantiopure organocatalyst, denoted Cat.*

3.1.2. Metal-Mediated Coupling of Enolates to Aromatic Rings

Recently, 2-aryl-1,3-diones have emerged as a promising new class of herbicidal acetyl-CoA carboxylase (ACCase) inhibitors, making efficient synthesis of such compounds highly sought after by agricultural companies.[139] One method of synthesis of these compounds involved a Pd(II)-catalysed cross-coupling of a cyclic 1,3-dione with an aryl bromide (figure 3.3A), based on previous work by Buchwald *et al.*[140] This coupling reaction was moderately successful, with the steric hindrance of the bulky dione and *ortho*-substituted aryl bromide coupling partners proved problematic.[139] More recently, various Pd cross-coupling reactions have been successfully applied to bulky aryl halides,[141] although another major issue has emerged, the cost of palladium. Due to this, the scalability of such coupling reactions is very limited, making them no longer feasible for industrial synthesis. In a more successful alternative pathway, aryl lead compounds were used in the presence of a large excess of DMAP in a solvent mixture of 4:1 chloroform/toluene (figure 3.3)[142], based on previous work by Morgan and Pinhey.[143] While the pathway involving lead-based coupling was highly efficient for small scale synthesis (<1 g scale), multiple steps were found to be incompatible with a large scale reaction, so a novel approach was pursued.

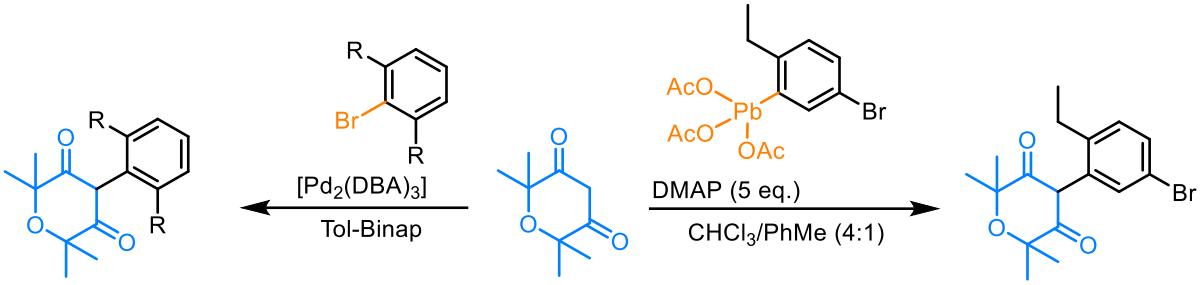

Figure 3.3. *Pd and Pb-mediated coupling reactions of a 1,3-dione with an aromatic ring*

Because of the unactivated nature of the arenes used in the example above, a simple S_NAr process such as one discussed in section 3.1.1 is unsuitable for the synthesis of 2-aryl-1,3-diones. While it is theoretically possible to add and subsequently remove nitro groups from the unsubstituted positions in the aromatic rings, this would significantly reduce the overall efficiency of the synthesis due to the additional steps, which themselves could prove difficult due to the presence of other functional groups. Instead, the reaction of an unactivated aromatic ring should be feasible with an arene coordinated η^6- to a metal, due to the strongly electron-withdrawing nature of ML_n fragments (see section 1.2). Such S_NAr processes of π-coordinated arenes are rare, with the only examples being intramolecular cyclisation reactions (figure 3.4A),[144] though an intermolecular reaction should also be feasible.

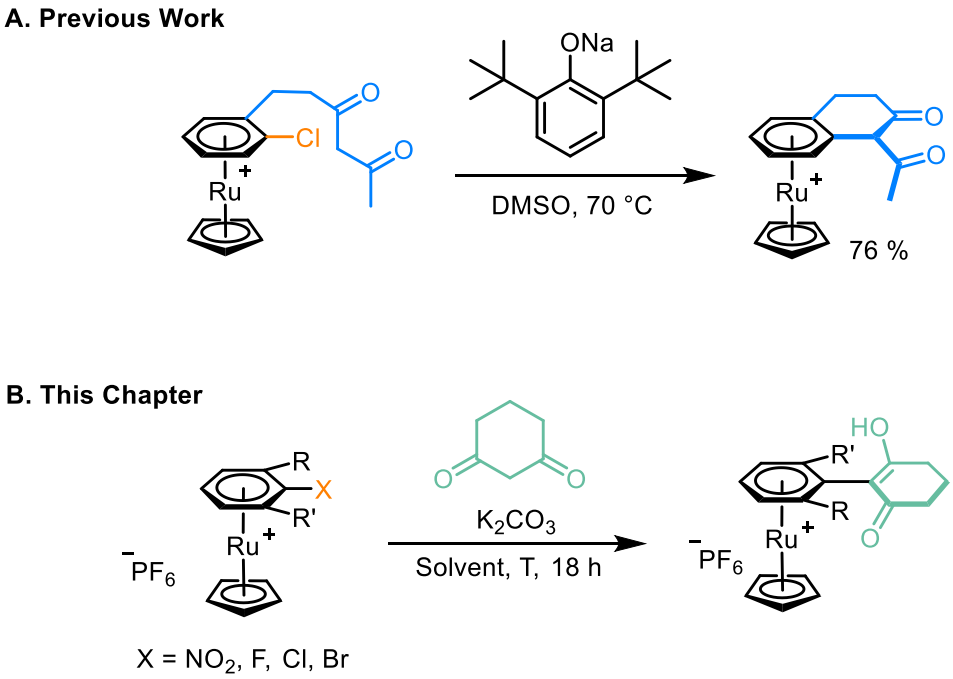

Figure 3.4. *Previous intramolecular cyclisation via S_NAr by Pigge et al., and an intermolecular enolate S_NAr reaction discussed in this chapter*

3.2. Results and Discussion

3.2.1. Synthesis of Sandwich Complexes [CpRu(η^6-Arene)][PF$_6$]

Before investigating the proposed C-C bond forming S_NAr reaction, a small library of ruthenium sandwich complexes of the general formula [(η^6-Arene-X)RuCp][PF$_6$], where X is a leaving group, were synthesised by refluxing the precursor complex, [(NCMe)$_3$RuCp][PF$_6$], with the selected arene in either 1,2-DCE or EtOH solvent (figure 3.5, table 3.1).

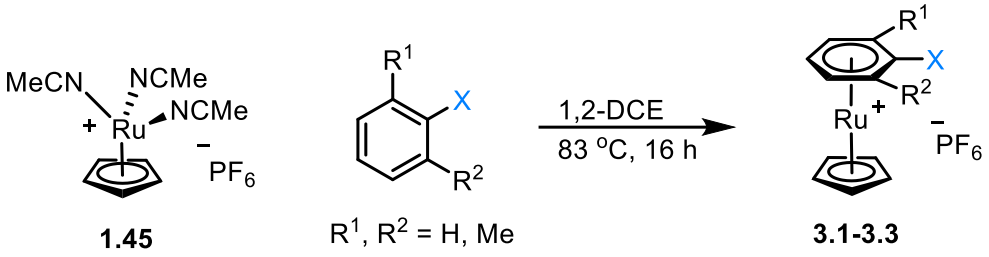

Figure 3.5. *Synthesis of ruthenium sandwich complexes* ***3.1-3.3*** *used in this work*

Table 3.1. *Complexes of the general formula [(η^6-arene)RuCp]$^+$* ***(3.1-3.3)*** *used for enolate S_NAr*

Arene	Yield (%)	Complex Number
Fluorobenzene	92	**3.1A**
Chlorobenzene	96	**3.1B**
Nitrobenzene	87	**3.1C**
2-Fluorotoluene	94	**3.2A**
2-Chlorotoluene	97	**3.2B**
2-Nitrotoluene	89	**3.2C**
2-Fluoro-*m*-xylene	94	**3.3A**
2-Chloro-*m*-xylene	95	**3.3B**
2-Nitro-*m*-xylene	88	**3.3C**
2-mesyl-*m*-xylene	96	**3.3D**

Confirmation of successful arene π-complexation was obtained through analysis of heteronuclear NMR spectra, mass spectrometry and elemental analysis. Also, single crystals of several of these complexes were obtained through either vapour diffusion of diethyl ether into a concentrated acetone solution or via a slow evaporation method. All crystal structures of these

complexes (figure 3.6) show the expected pseudo-linear geometry, with the Ru-C_6(plane) distances all in agreement with similar complexes.[84]

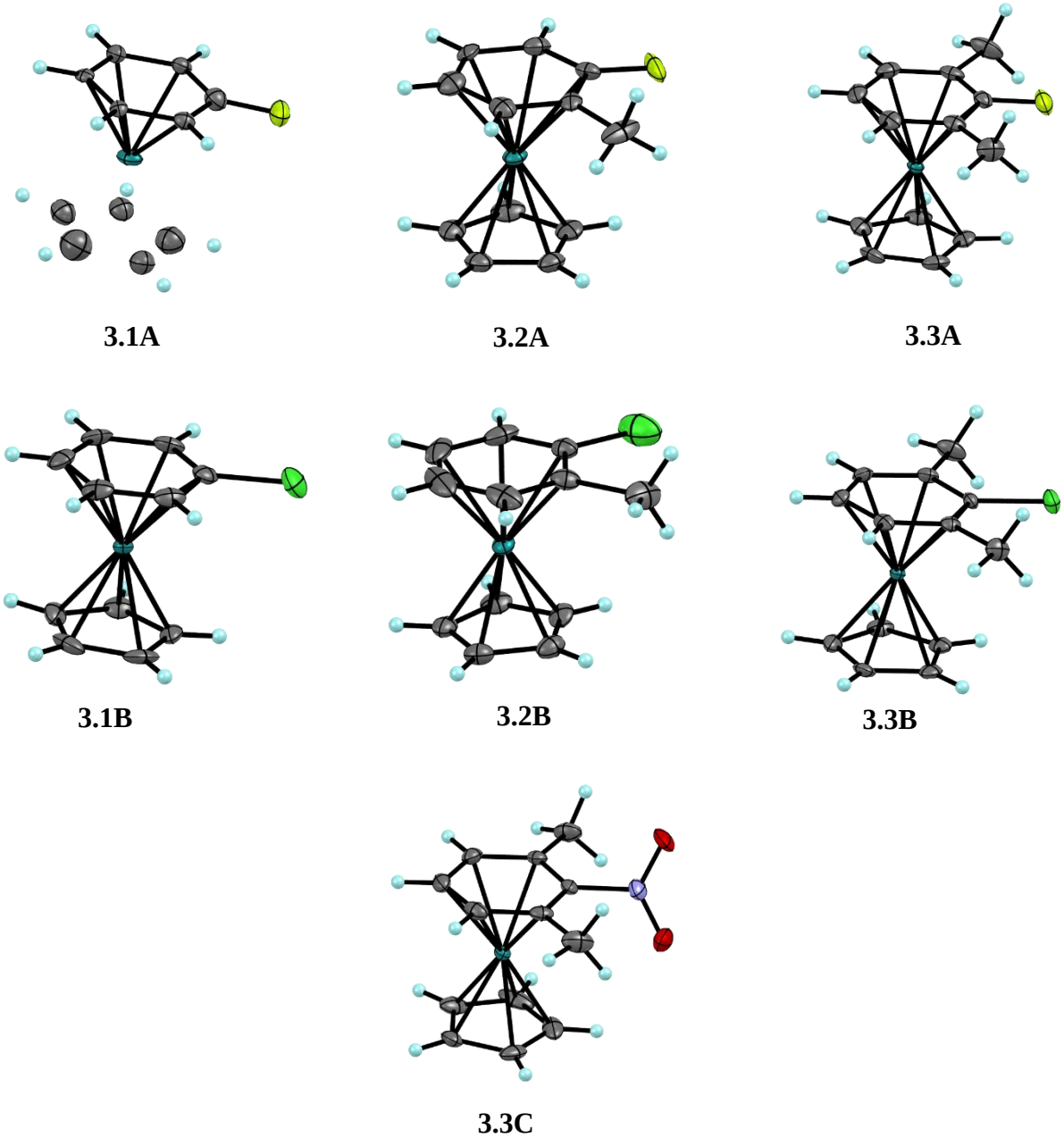

Figure 3.6. *ORTEP plots of the molecular structures of cationic Ru sandwich complexes* ***3.1A, B, 3.2A, B*** *and* ***3.3A-C****, with thermal ellipsoids at a 50% probability level. In the case of* ***3.1A****, an additional PhF ring due to disorder is omitted for clarity. In all cases,* $[PF_6]^-$ *counter anions are omitted for clarity. Atom colours: carbon, grey; hydrogen, light blue; fluorine, yellow; chlorine, green; nitrogen, blue; oxygen, red and ruthenium, teal.*

3.2.2. A New Intermolecular S_NAr Reaction Using Enolates as Nucleophiles

Initial S_NAr studies were performed by reacting the complex $[(\eta^6\text{-}C_6H_5F)RuCp][PF_6]$ (**3.1A**) with 1,3-cyclohexanedione and K_2CO_3 in anhydrous DMF at 40 °C (figure 3.7A). The product compound was purified by triturating the crude residue with DCM, followed by filtration, and finally precipitation by adding diethyl ether to a concentrated acetone solution of the complex. Analysis by ^1H NMR spectroscopy (figure 3.7B), in combination with mass spectrometry, indicated the formation of complex **3.4** as expected.

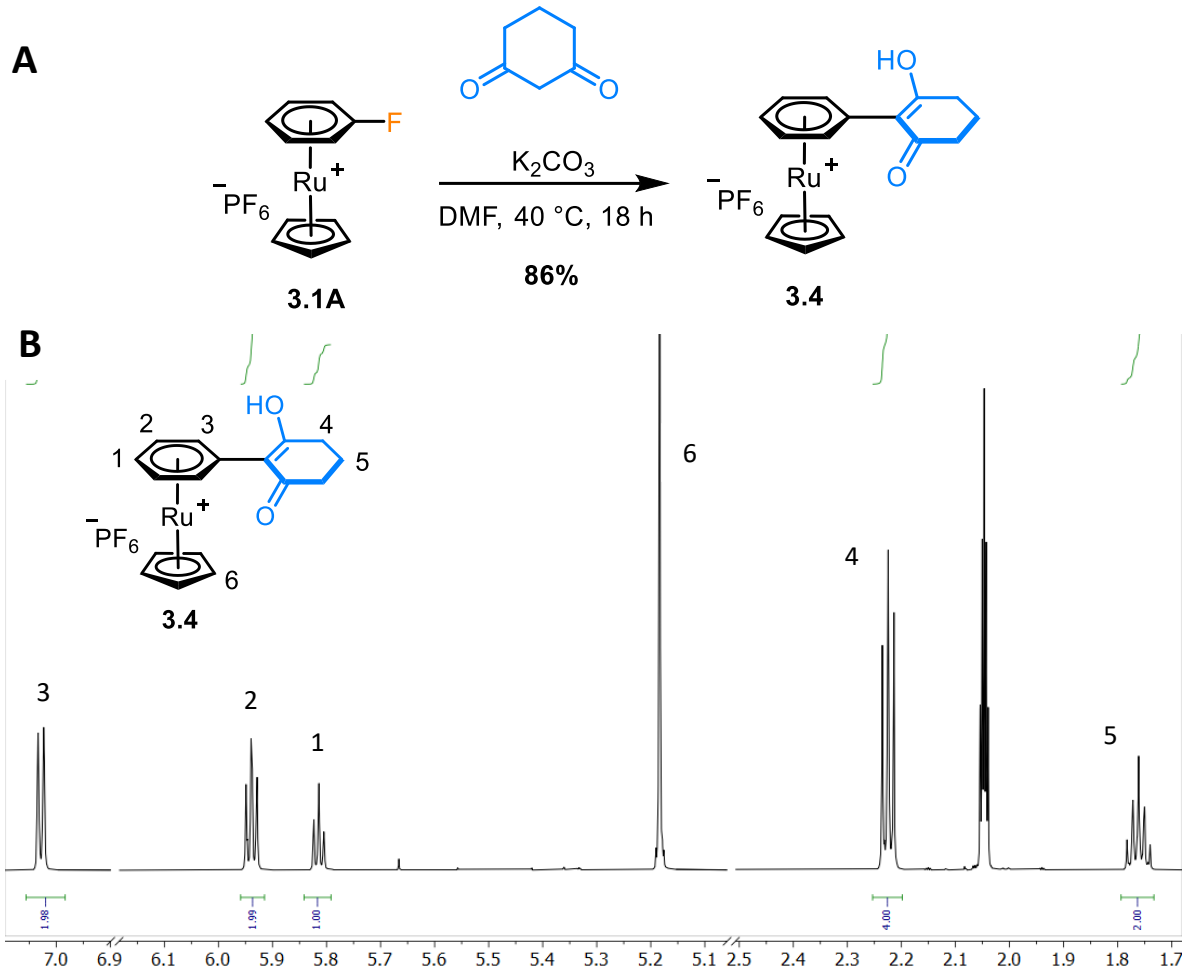

Figure 3.7. A. *Nucleophilic aromatic substitution of an enolate on the complex* $[(\eta^6\text{-}C_6H_5F)RuCp]^+$ ***(3.1A). B.*** *Assigned* ^1H *NMR Spectrum of the product complex* ***3.4*** *(599 MHz, Acetone-*D_6*, 298 K).*

An interesting feature in the ^1H NMR spectrum of the coupled complex **3.4** (figure 3.7B) was the absence of a peak corresponding to the proton in the 2-position of the dione ring; this implies that after substitution this ring exists in the enol form, likely stabilised by conjugation

of the enol C=C double bond with the arene ring. When the bound arene was changed to chlorobenzene or nitrobenzene, no difference in reactivity was observed, as both complexes appeared to undergo the same substitution reaction as smoothly as the fluorobenzene complex. As an aside, the reaction using the η^6-nitrobenzene complex **3.1C** was repeated at 0 °C to determine the possibility of attack at the position *ortho-* to the nitro group (figure 3.8), as has been demonstrated before in the group using trifluoromethyl nucleophiles.[46] Analysis of the reaction mixture here by ^{1}H NMR spectroscopy indicated that the only product formed, even at a cooler temperature, was the S_NAr product **3.4**, with no sign of the η^5-Meisenheimer complex **3.5** forming.

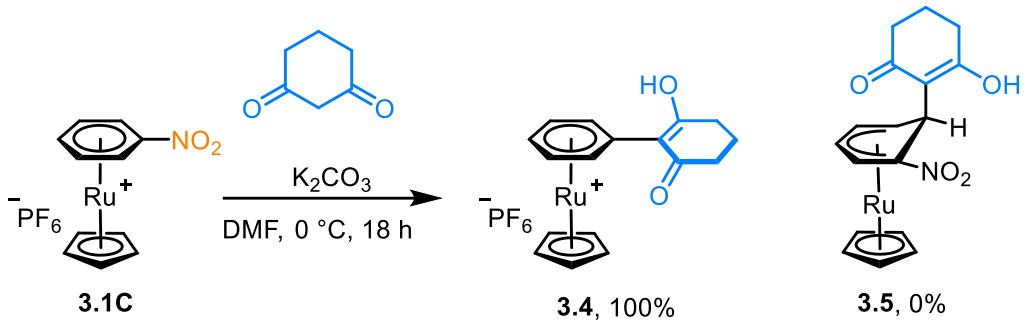

Figure 3.8. *Reaction of an enolate with the complex [(η^6-$C_6H_5NO_2$)RuCp]$^+$(**3.1C**) at 0 °C.*

3.2.3. Optimisation of C-C Bond-Forming S_NAr and Leaving Group Competition Experiments

The S_NAr reaction of complexes **3.1A-C** with enolates occurs efficiently under mild conditions although the choice of solvent remained an issue, as removing DMF by evaporation was time consuming due to its high boiling point. To improve the efficiency in this process, a series of solvents with lower boiling points were screened (table 3.2). Of these solvents, only THF (entry 5), CH_2Cl_2 (entries 3 and 11) and MeCN (entry 8) facilitated full consumption of the starting complex. Of these three solvents, the latter two appeared to give rise to side reactions, indicated by additional aromatic peaks in the crude ^{1}H NMR spectrum, while only the desired product was formed in THF, making this the optimal choice of solvent.

Table 3.2. *Solvent and temperature screen for the S_NAr reaction used to form complex* ***3.4.*** *Conversions were measured by comparing starting material peaks with product in the ^1H NMR spectrum (400 MHz, Acetone-D_6, 298 K). Isolated yield taken from scaled-up reaction only.*

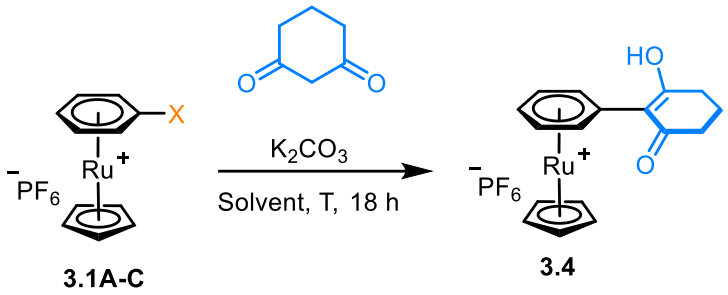

3.1A-C **3.4**

Entry	Starting Complex	X	Solvent	Temperature (°C)	Conversion (Isolated yield) /%
1	**3.1A**	F	DMF	40	100
2	**3.1B**	Cl	DMF	40	100
3	**3.1B**	Cl	DMF	0	100
4	**3.1B**	Cl	CH_2Cl_2	RT	100
5	**3.1B**	Cl	THF	RT	100 (**81**)
6	**3.1B**	Cl	1,4-dioxane	RT	25
7	**3.1B**	Cl	EtOH	RT	0
8	**3.1B**	Cl	MeCN	RT	100
9	**3.1B**	Cl	2-methyl THF	RT	50
10	**3.1C**	NO_2	DMF	40	100
11	**3.1C**	NO_2	CH_2Cl_2	RT	100

With optimised conditions for the enolate-based S_NAr of complexes with the general formulae $[(\eta^6\text{-}C_6H_5X)RuCp][PF_6]$ (where X = F, Cl, NO_2) in hand, the effects of methyl groups *ortho* to the leaving group were investigated. When one methyl group is added *ortho* to the leaving group, the reaction requires an elevated temperature of around 70 °C to occur (table 3.3). While the reaction proceeded to complete conversion at these temperatures in anhydrous DMF with 2-chloro and 2-nitrotoluene complexes **3.2B** (entry 2) and **3.2C** (entry 4), 2-fluorotoluene complex **3.2A** appeared undergo an undesired hydroxylation reaction, highlighting the susceptibility of aryl fluorides to hydrolysis.

Table 3.3. *Solvent and temperature screen for the S_NAr reaction used to form the complex* ***3.6****. Conversions were measured by comparing starting material peaks with product in the ^1H NMR spectrum (400 MHz, CD_3OD, 298 K). Isolated yield taken from scaled-up reaction only.*

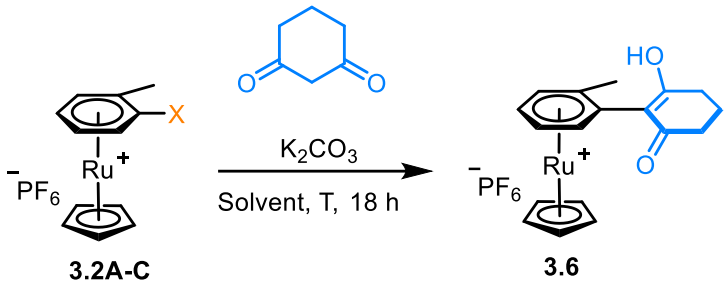

3.2A-C **3.6**

Entry	Starting Complex	X	Solvent	Temperature (°C)	Conversion (Isolated yield) /%
1	**3.2A**	F	DMF	70	83[a]
2	**3.2B**	Cl	DMF	70	100 (**69**)
3	**3.2B**	Cl	THF	65	76
4	**3.2C**	NO_2	DMF	70	100

[a] *Remaining 17% of starting material converted to hydroxylation product*

Incorporation of a second methyl group was found to hinder the S_NAr further, with even higher temperatures of 90 °C required to perform the S_NAr reaction on complexes **3.3A-C**. Of the three, the 2-chloro-*m*-xylene complex (**3.3B**) performed the best under the initial conditions in DMF, achieving a conversion of 90% (table 3.4), which was measured by comparing starting material and product peaks in the ^1H NMR spectrum. Nitro-*m*-xylene complex **3.3C** was able to undergo the reaction to 80% conversion (table 3.4, entry 12), whereas the fluorinated complex (**3.3A**) again partially hydroxylated (table 3.4, entry 1). These data suggest chloride to be the optimal leaving group in our system, so attempts to further optimise the reaction were performed on complex **3.3B** only. First, a solvent screen was performed (table 3.4, entries 3-10), although the initial solvent, DMF, was found to be optimal (entry 3), with only NMP (entry 4) giving a comparable conversion.

Table 3.4. *Solvent and temperature screen for the S_NAr reaction used to form the complex* ***3.7****. Conversions were measured by comparing starting material peaks with product in the ^1H NMR spectrum (400 MHz, CD_3OD, 298 K). Isolated yield taken from the scaled-up reaction only.*

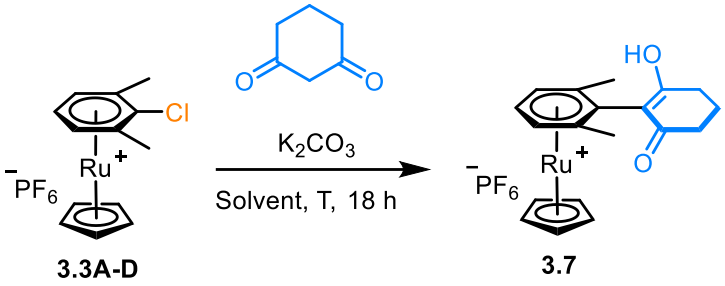

3.3A-D **3.7**

Entry	Starting Complex	X	Solvent	Temperature (°C)	Conversion (Isolated yield) /%
1	**3.3A**	F	DMF	80	61[a]
2	**3.3B**	Cl	DMF	80	76
3	**3.3B**	Cl	DMF	90	87 (**66**)
4	**3.3B**	Cl	NMP	90	85
5	**3.3B**	Cl	DMF	120	67
6	**3.3B**	Cl	1,2-DCE	83	0
7	**3.3B**	Cl	1,4-Dioxane	90	0
8	**3.3B**	Cl	EtOH	78	0
9	**3.3B**	Cl	MeCN	82	17
10	**3.3B**	Cl	2-methyl THF	80	Trace
11	**3.3C**	NO_2	DMF	80	67
12	**3.3C**	NO_2	DMF	90	80
13	**3.3D**	OMs	DMF	90	0[b]

[a] *Hydroxylation also occurred*

[b] *Only hydroxylation occurred*

A base screen was also performed (table 3.5), though no improvement was made on the initial base, K_2CO_3. A noteworthy observation here, is that inorganic salts appeared to generally work better in the reaction than organic amine bases. Overall, the optimised conditions for the enolate-based S_NAr reaction of η^6-arene complexes bearing 0-2 *ortho* methyl groups are described by entries 7, 13 and 17, respectively, of table 3.1.

Table 3.5. *Base screen for the S_NAr reaction used to form the complex [(η^6-2-(2,6-dimethylphenyl)cyclohexanedione)RuCp]$^+$(**3.7**). Conversions were measured by comparing starting material peaks with product in the ^{1}H NMR spectrum (400 MHz, Acetone-D_6, 298 K).*

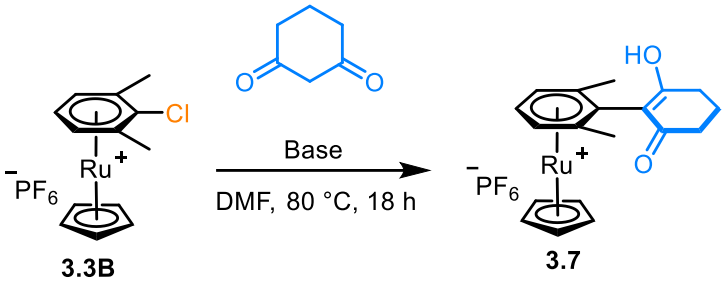

3.3B 3.7

Entry	Base	Conversion (%)
1	K_2CO_3	67
2	DBU	30
3	NEt_3	Trace
4	Pyridine	Trace
5	DIPEA	Trace
6	NaH	Trace
7	KO^{t}Bu	12
8	NaOH	40
9	$NaHCO_3$	36
10	$(NH_4)_2CO_3$	Trace
11	NaOMe	Trace
12	Na(2,4-di-tert-butylphenoxide)	Trace

Following optimisation, a series of competition experiments were studied to establish which leaving groups performed the best in the S_NAr reaction (figure 3.9). Unsurprisingly, fluoride proved to be the best leaving group (figure 3.9A, B) due to the higher polarisation of the C-F bond promoting nucleophilic attack, leading to complexes **3.9** and **3.11**, respectively. The reaction showed a strong preference for substituting NO_2 over chloride (**f**igure 3.9C), giving a 1:9 ratio of complexes **3.11** and **3.9**, respectively. A milder preference for chloride over bromide was observed (figure 3.9D), as a 2:1 ratio of complexes **3.14** and **3.9** formed. Next, the impact of having sterically hindering *ortho* methyl groups was highlighted as the reaction preferred to substitute the less hindered chloride (figure 3.9E), even at a higher temperature. This reaction was not completely selective, however, as a 5.3:1 ratio of complexes **3.16** and **3.17** formed. Finally, an η^6-bound arene with a fluoride, the best leaving group, hindered by two *ortho* methyls, as well as the worst performing leaving group, bromide, which was unhindered (**3.18)**. After exposure to the S_NAr conditions at 90 °C, the ^1H NMR and mass spectra implied that the substitution had occurred exclusively at the bromide, giving exclusively the fluorinated complex **3.19**. These data all indicate a rate-determining nucleophilic attack on the ring, while steric hindrance appears to have a more significant effect on the reaction than the degree of C-X bond polarisation.

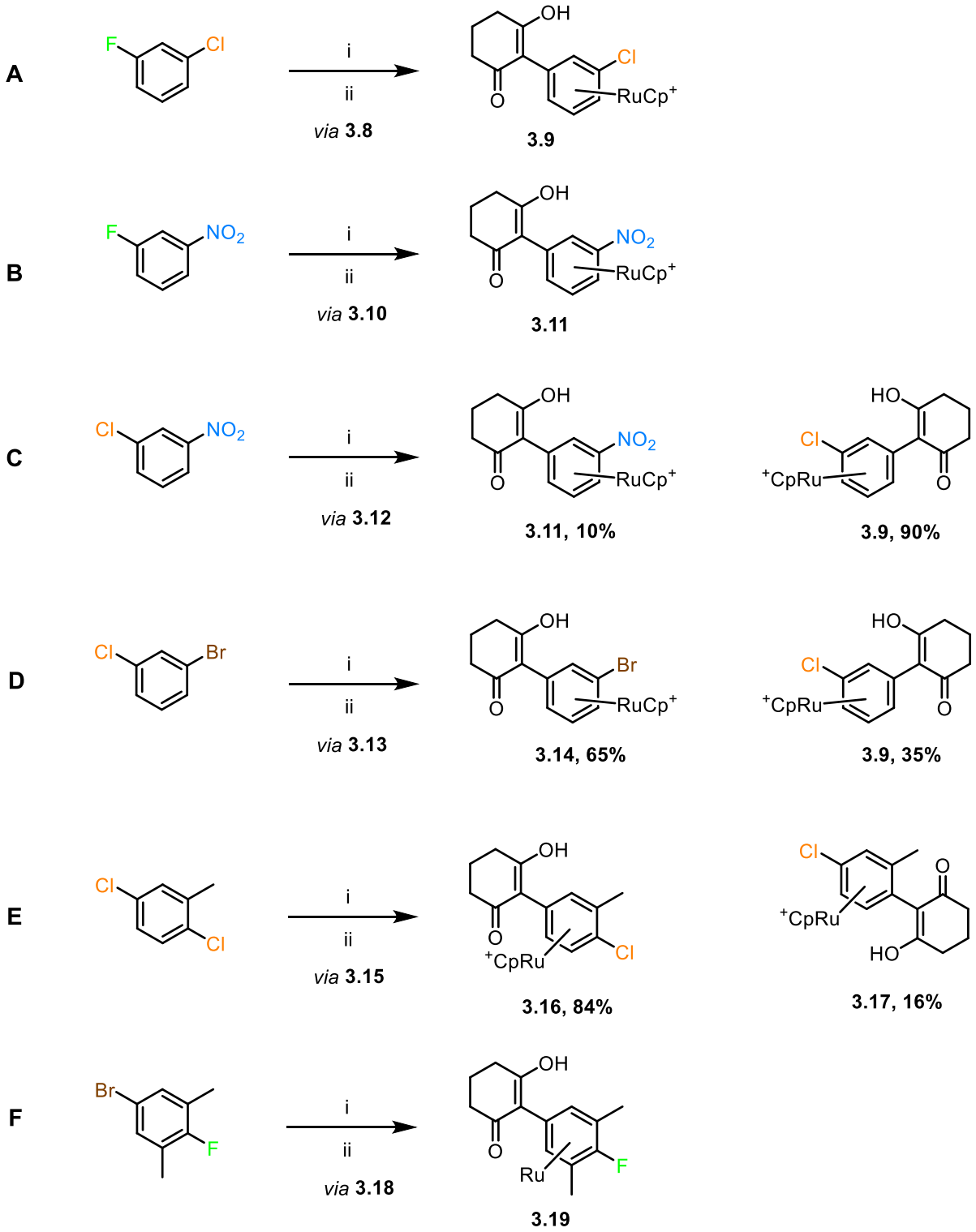

Figure 3.9. *Leaving group competition experiments via their respective sandwich complexes, [(η^6-arene)RuCp]$^+$ (**3.8**, 89%; **3.10**, 75%; **3.12**, 83%; **3.13**, 90%; **3.15,** 88%; and **3.18**, 90%). Relative quantities of each product were measured by comparing peaks in the ^{1}H NMR spectrum (400 MHz, Acetone-D_6, 298 K), and where appropriate mass spectrometry analysis (LCMS, ESI, MeCN) was used to determine which product was in excess. Conditions: i. [CpRu(NCMe)$_3$][PF$_6$], 1,2-DCE, 83 ˚C, 18 h; and ii. Cyclohexanedione (1 eq.), K_2CO_3, DMF, RT ˚C (A-D and F) or 70 ˚C (E) or 90 ˚C (F).*

3.2.4. Dione Scope in C-C Bond-Forming S_NAr

To determine the versatility of the S_NAr reaction with respect to the nucleophile, a series of 1,3-diones bearing different functional groups were tested under the optimised reaction conditions for the synthesis of complex **3.6** (table 3.6). Generally, the reaction conditions are tolerant of many different functionalities, including esters and amides, cyclic ethers and amines, and spirocycles of varying sizes. Of the poorer performing diones, cyclopentanedione surprisingly only reacted to a conversion of around 89% (table 3.6, entry 10), despite its structural similarity to cyclohexanedione. This result can be rationalised by the lower pK_a of 1,3-cyclopentanedione (4.3)[145] compared with cyclohexanedione (5.2)[146], meaning the enolate form of cyclopentanedione is more stabilised and consequently, less nucleophilic. 2,2',6,6'-tetramethyl tetrahydropyran-3,5-dione (entry 9) reacted with a final conversion of 65%; it is likely that this nucleophile was sterically hindered by the presence of four methyl groups within close proximity to the nucleophilic α-carbon. Interestingly, the only aliphatic dione tested, acetylacetone, reached only a 72% conversion, despite its higher reactivity as a nucleophile than a cyclic dione.[145]

Table 3.6. *Dione scope for nucleophilic S_NAr with complex* ***3.2B****. Conversions were measured by comparing starting material peaks with product in the ^1H NMR spectrum (400 MHz, Acetone-D_6, 298 K).*

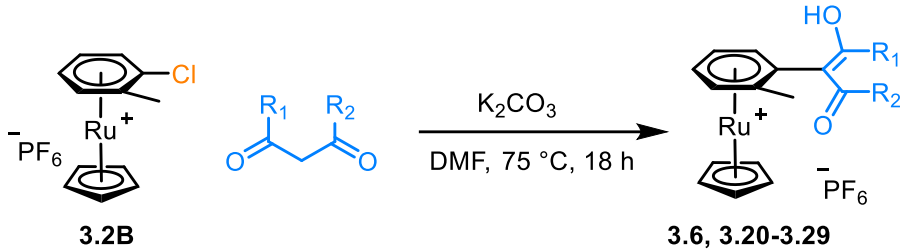

3.2B **3.6, 3.20-3.29**

Entry	Dione	Product Complex	Conversion (Isolated yield) /%
1	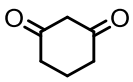	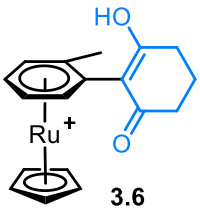 **3.6**	100 (**69**)
2	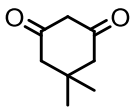	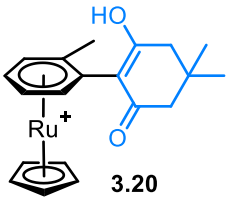 **3.20**	100 (**61**)
3	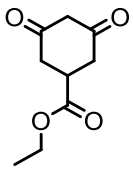	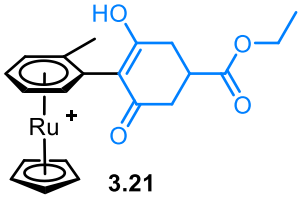 **3.21**	100 (**63**)
4	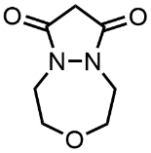	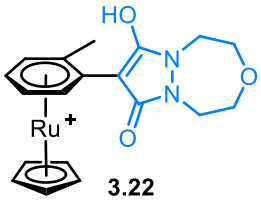 **3.22**	100 (**68**)
5	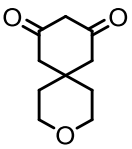	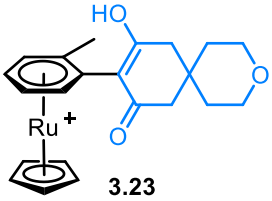 **3.23**	100 (**70**)

6	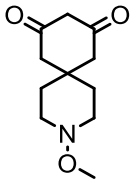	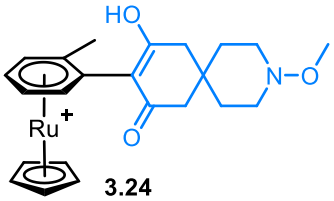 **3.24**	100 (**63**)
7	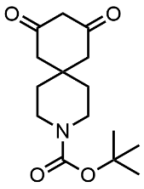	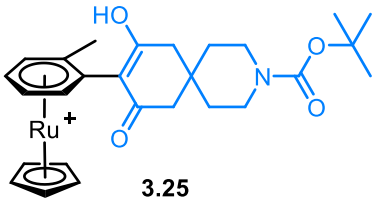 **3.25**	100 (**61**)
8	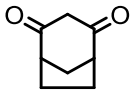	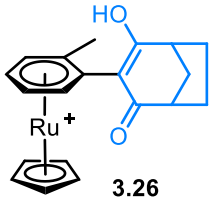 **3.26**	100[a]
9	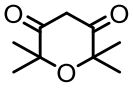	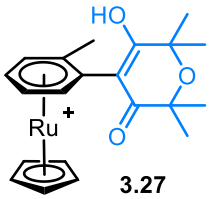 **3.27**	65[a]
10	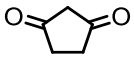	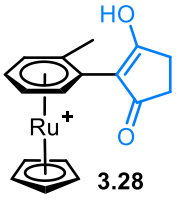 **3.28**	89 (**62**)
11	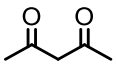	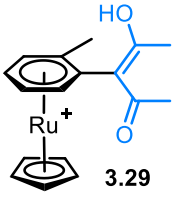 **3.29**	72[a,b]

[a] *No yield presented as impurities still present in ^{1}H NMR spectrum of isolated compound*

[b] *Significant amount of free arene also observed*

An interesting feature of the ^{1}H NMR spectrum of the crude product from the reaction with acetylacetone (**3.29**), is the presence of free arene peaks (figure 3.10), likely to be either unreacted 2-chlorotoluene or the free coupled aromatic. This implies that [Acac]$^{-}$ could be

reacting directly with the ruthenium centre, and displacing the η^6-arene. Further evidence for such a ligand substitution is discussed in section 3.2.5.

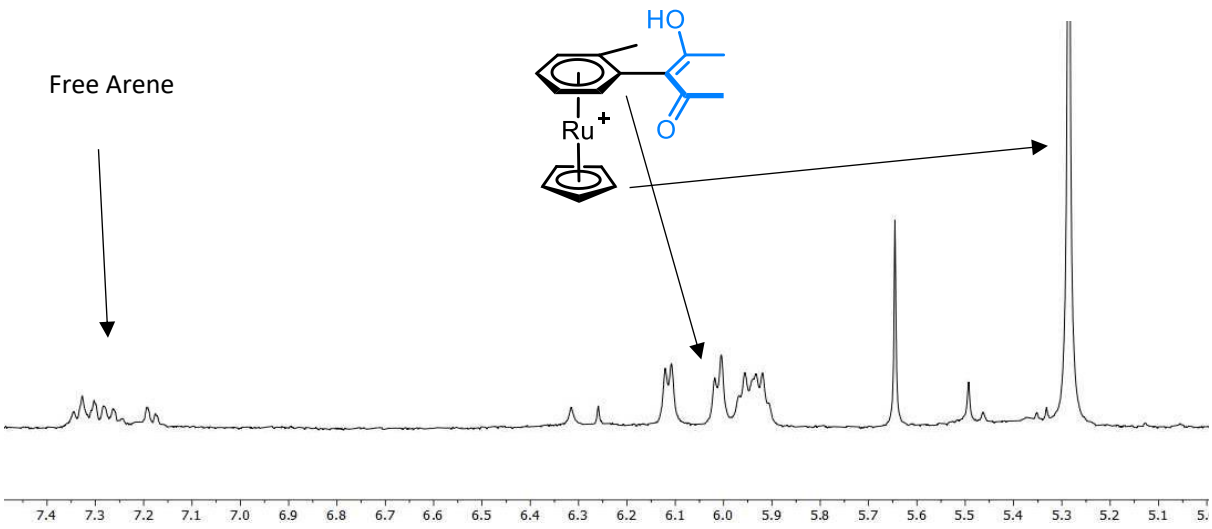

Figure 3.10. *NMR spectrum of crude product from the reaction of [(η^6-2-chlorotoluene)RuCp][PF_6] with acetylacetone in the presence of base.*

Overall, a number of diones were found to be reactive towards our S_NAr reaction with the complex [(η^6-2-chlorotoluene)RuCp][PF_6], with many being of interest for agrochemical applications.[139,142] A future aim for this part of the project is to translate the same reactions to the η^6-bound 2-chloro-m-xylene, as well as arenes with larger alkyl groups *ortho* to the leaving group.

3.2.5. Photolytic Liberation of Arene and Regeneration of Ru Fragment

As discussed in chapter 1,[36,46,47] an arene ring bound η^6- to ruthenium can be liberated via photolysis by UV irradiation in the presence of either a coordinating solvent, or an excess of other ligands. Following the S_NAr reaction of η^6-arene complexes of ruthenium with enolates discussed in sections 3.2.2-3.2.4 of this chapter, the coupled arene was quantitatively liberated via a simple photolysis procedure in which a solution of complex **3.6** in CD_3CN is irradiated with UV light (365 nm). Initial reactions were performed using a commercial UV nail salon lamp (36 W), where the photolysis of complex **3.6** went to complete conversion in 24 hours (365 nm) or 48 hours (254 nm). The reaction time was decreased to within 15 minutes using a Penn photoreactor M2 (365 nm, 100-240 V), shown in figure 3.11. *In-situ* NMR spectra of the photolysis of complex **3.6** show the gradual disappearance of peaks of bound arene (figure 3.11, 6.0-5.7 ppm) and the corresponding cyclopentadienyl ring. Simultaneously, the peaks corresponding to the free arene (7.2-7.0 ppm) grow in, as well as the singlet at 4.3 ppm, which

aligns with the cyclopentadienyl ring in the deuterated complex $[(CD_3CN)_3RuCp][PF_6]$, until the reaction is complete at 10 minutes. This procedure not only shows the rapid quantitative formation of the free arene, but also formation of the MeCN-d_3 analogue of the complex initially used to synthesise complexes of the formula $[(\eta^6\text{-arene})RuCp][PF_6]$ (section 3.2.1), highlighting the recyclability of the ruthenium fragment. One limitation, however, is the air sensitivity of this complex in solution, rendering it problematic to isolate and purify for further use. One interesting feature of these *in-situ* NMR spectra is the singlet at ca. 4.5 ppm, which appears to grow in alongside the Cp peak at 4.3 ppm. It is unclear what this peak corresponds to, although analysis of the integrals in the NMR spectra indicate that the Cp peak at 4.3 ppm under-integrates slightly compared with the free arene. Furthermore integral of the peak at 4.5 closely matches this difference, meaning it is likely that this peak is also related to the complex $[(CD_3CN)_3RuCp]^+$.

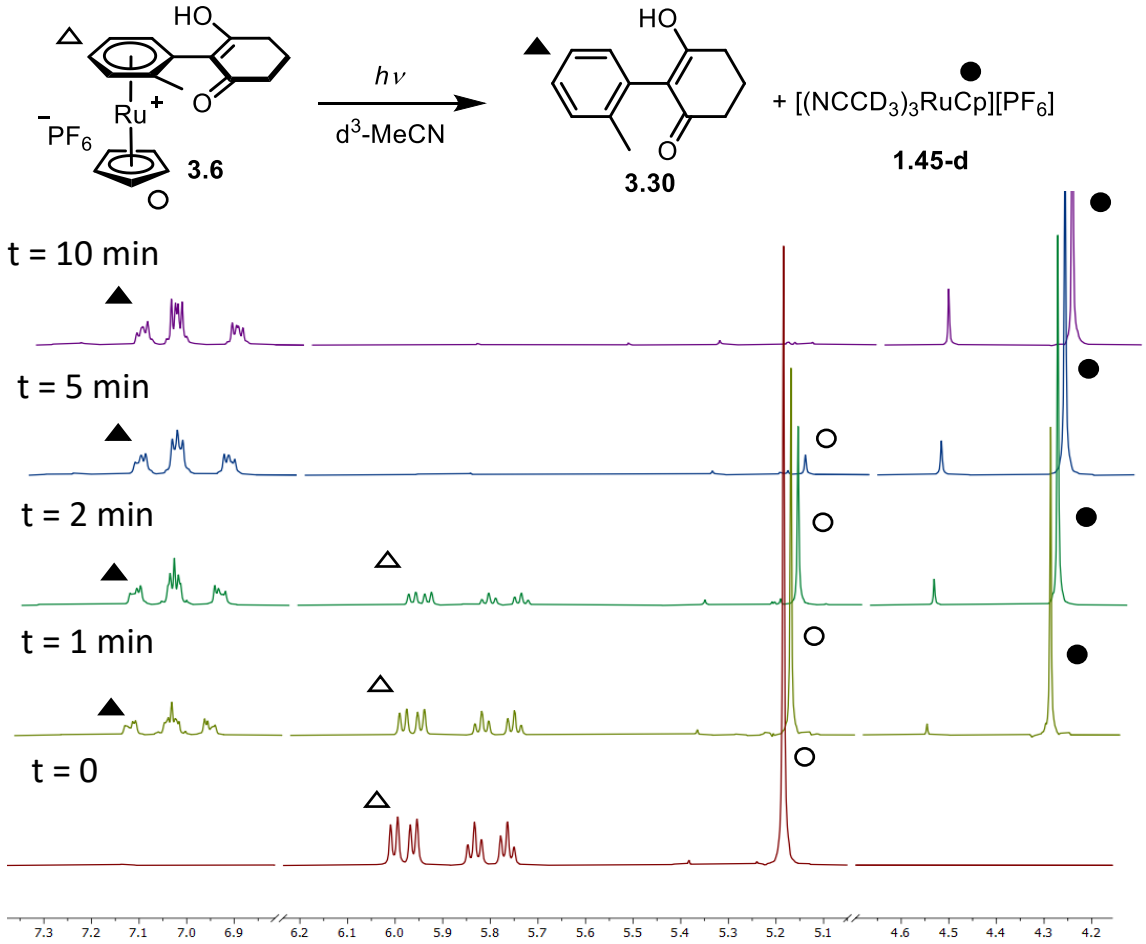

Figure 3.11 *Stacked ^1H NMR spectra for the aromatic region of the ^1H NMR spectra taken at different time-points of the photolysis of complex* ***3.11***.

In the case of complexes **3.4** and **3.6**, the photolysis procedure was scaled up such that the free arenes could be isolated via an acidic work up of the reaction mixture (figure 3.12). Following purification via column chromatography, free arenes were characterised by ^{1}H NMR and mass spectroscopy. In this procedure, the Ru complex by-product was not isolated as the reactions had been performed in the presence of air.

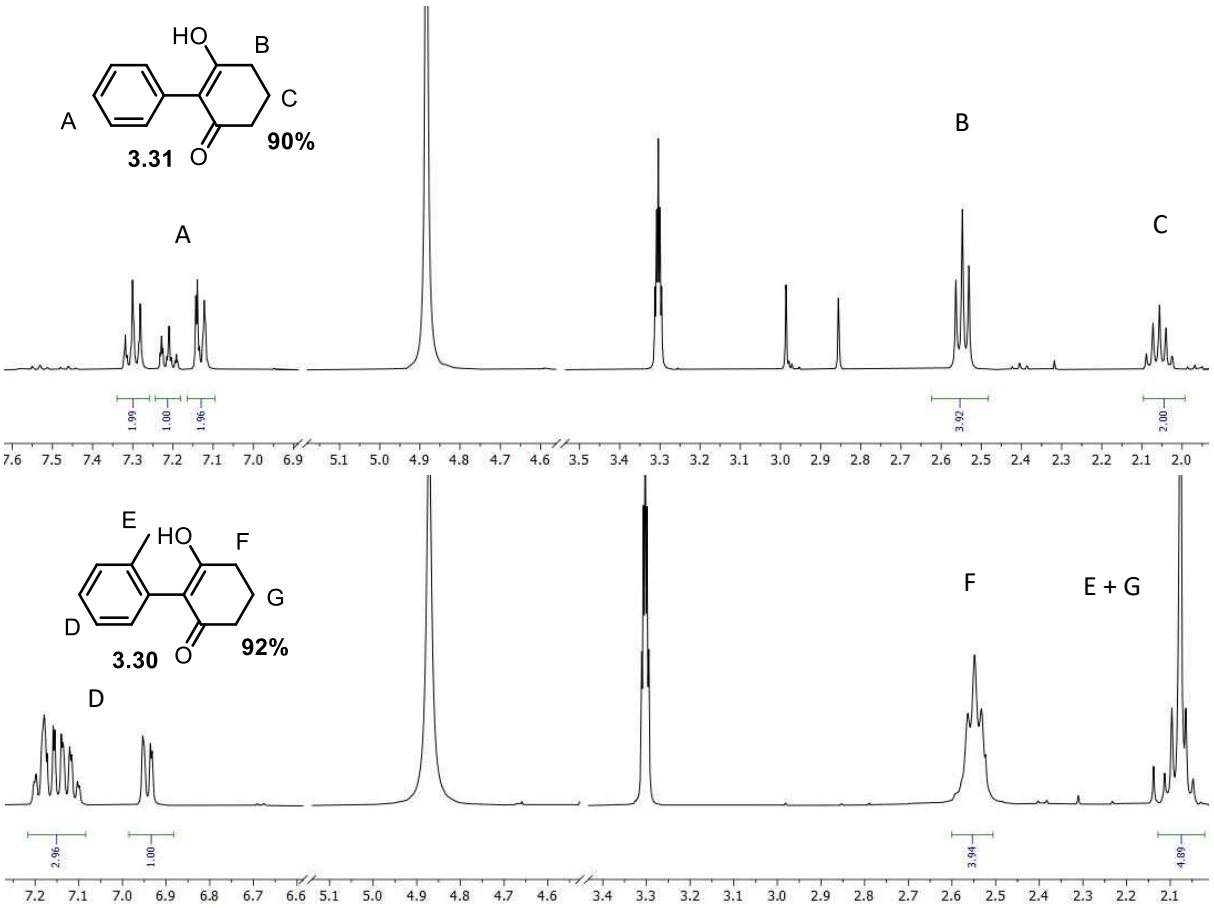

Figure 3.12. *^{1}H NMR spectra (400 MHz, 298 K, CD_3OD) of free arenes and isolated from photolysis of complexes **3.4** and **3.6** respectively*

The photolysis procedure was then applied to each complex formed from the dione scope (see section 3.2.4), and their reaction times were compared (table 3.7). All different arenes appeared to fully undergo the photolysis within 20 minutes, with only small variations in the rates. A noteworthy observation with complex **3.12** (table 3.7, entry 13) was that the coupled arene appeared to undergo photolysis fully within 10 minutes, whereas the residual amount of unreacted 2-chloro-m-xylene complex **3.3B** did not undergo photolysis in this time, and only begun to react after 15-20 minutes of irradiation. *In-situ* ^{1}H NMR analysis of the photolysis reaction with complex **3.35** (table 3.7, entry 12) indicated the presence of bound arene even

after 40 minutes of irradiation as there was a large Cp singlet at 5.2 ppm and some multiplets between 6 and 7 ppm, characteristic of an η^6-arene. Interestingly, there was also a Cp singlet at 5.5 ppm, which remained even after 2 hours of irradiation. The mass spectrum of this mixture suggested the presence of a ruthenium complex with an m/z of 315 Da (^{102}Ru isotope), which matches neither of the tri(acetonitrile) species **1.45**, or the sandwich complex **3.35**. The identity of this Ru species is not clear, although this m/z matches the expected molecular weight of a ruthenium complex with the formula [(η^2-acac)(HCO_2)RuCp] (315 Da, ^{102}Ru isotope), likely to have formed *via* formate-mediated substitution of an acetonitrile ligand during the ionization process. This gives some more evidence that anionic acetylacetonate may have displaced some bound arene in the S_NAr step.

Table 3.7. *Photolysis of ruthenium complexes, resulting in formation of aryl-1,3-diones.*

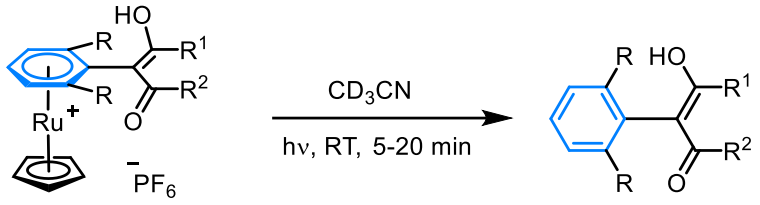

Entry	Free Arene	Time for Quantitative Photolysis
1	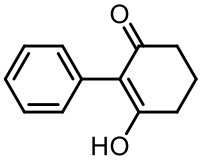	5
2	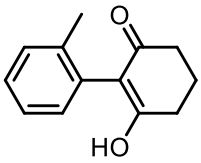	10
3	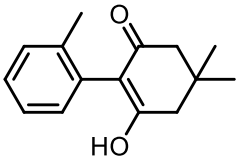	10
4	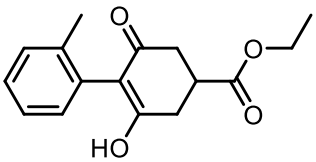	5

5	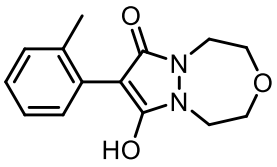	15
6	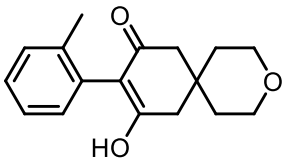	5
7	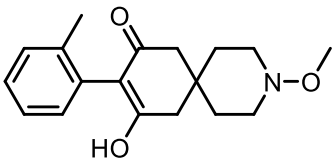	5
8	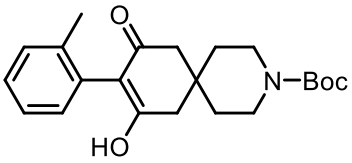	10
9	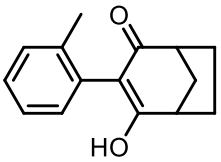	5
10	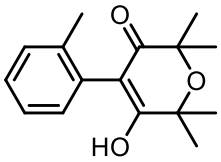	15
11	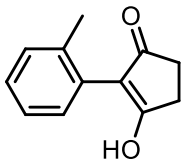	15
12	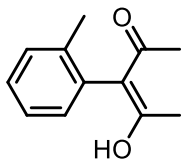	>120[a]
13	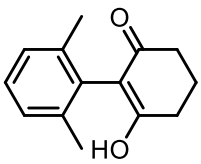	15

[a] *[RuCp]⁺ species present which was not reactive towards irradiation*

3.2.6. Attempts at Ru-Catalysed S_NAr and Pseudo-Catalysis Study

Due to the high cost of the ruthenium precursor complexes used in this chapter, it is highly important that the S_NAr procedure is translated into one where a catalytic quantity of ruthenium is required. A proposed catalytic cycle is shown in figure 3.13 below, where the η^6-coordinated arene undergoes S_NAr with the enolate, then arene exchange generates the initial complex and the free product arene. Of the two steps in this catalytic cycle, arene exchange is rate determining, and remains a difficult challenge to overcome.

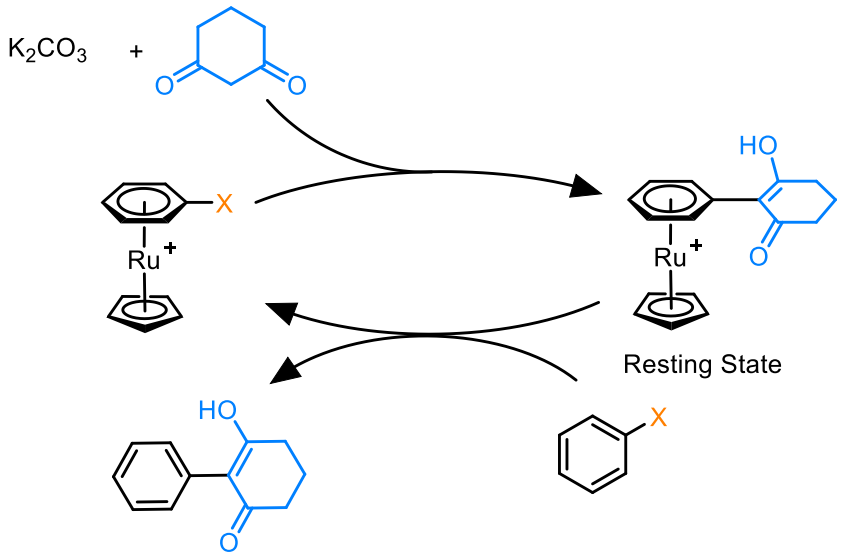

Figure 3.13. *Proposed mechanism for the Ru-catalysed coupling of unactivated arenes with 1,3-diones*

In an attempt to make the enolate S_NAr catalytic in ruthenium, a protocol based on the previous work by Walton and Williams,[34] was tested on both halobenzene and halotoluene (X = F, Cl). Analysis of ^1H NMR spectra of the catalytic mixtures indicate that only the starting arene is present, as well as a small amount of a ruthenium complex. Mass spectra indicate the presence of the ruthenium complex, $[(\eta^6$-2-phenyl-1,3-cyclohexanedione)RuCp$]^+$, meaning the starting arene successfully binds to the Ru centre, then undergoes S_NAr but gets stuck at the arene exchange step. While it is expected that arene exchange is limiting the catalysis, it is surprising that no arene exchange appears to occur at all, given this catalytic protocol is very similar to the one reported by Walton and Williams in 2015.[34]

In a separate study undertaken, a one-pot conversion of 2-chlorotoluene to 2-tolylcyclohexane-1,3-dione was achieved with an overall conversion of 22% (figure 3.14). In this process, the activating Ru fragment is regenerated at the end, therefore completing a stepwise-catalytic

cycle. In this experiment a deuterated coordinating solvent, CD_3CN, was used so that each intermediate could be observed via *in-situ* ^{1}H and ^{19}F NMR and conversions at each step were calculated by comparison of the cyclopentadienyl peaks of each complex formed. While further optimisation is necessary to improve the efficiency of the pseudo-catalysis, this result serves as a useful proof-of-concept for protocols like this, where the catalytic ruthenium fragment can be recycled *in-situ*, without the need of isolation and purification.

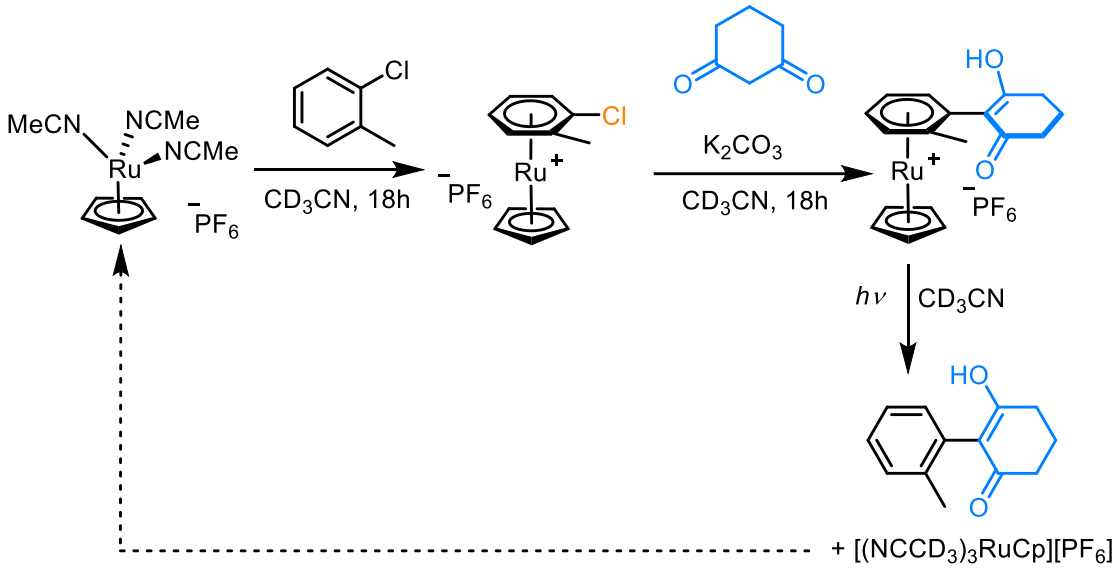

Figure 3.14. *One-pot ruthenium facilitated coupling of 2-chlorotoluene with 1,3-cyclohexanedione*

3.3. Conclusions and Outlook

In this chapter, synthesis of a series of 2-arylcyclohexane-1,3-dione derivatives, which have proven a useful class of agricultural compounds as herbicides, was discussed. The synthetic pathway was via a new intermolecular S_NAr reaction of arenes bound η^6 to an activating $[RuCp]^+$ fragment, based on a previous intramolecular protocol.[144] First, the S_NAr was optimised for unhindered arenes, followed by subsequent optimisation for rings bearing one and two *ortho* methyl groups. Next, a series of competition experiments revealed that leaving group ability for the S_NAr went in the order: $F^- >> NO_2^- > Cl^- > Br^-$, while other reactions indicated that steric hindrance has a larger effect on relative substitution rates than differences in the degree of bond-polarisation for aromatics with different leaving groups. A series of diones of interest to Syngenta were also screened, and it was found that many different functionalities, such as esters, amides, cyclic ethers and amines, as well as different spirocycles were all tolerated by the S_NAr reaction conditions, though linear diones did not work as well.

Finally, a protocol for the rapid photolytic liberation of the coupled arene was developed, with the reaction also regenerating a useful precursor ruthenium complex, $[(CD_3CN)_3RuCp]^+$, which can theoretically be isolated and reused to make further sandwich complexes.

The key future development for this work is the development of a S_NAr procedure which is catalytic in ruthenium. While attempts at this were made in this study, none were successful due to the inability of the suspected intermediate complex, [(η^6-2-benzylcyclohexane-1,3-dione)RuCp]$^+$ to undergo arene exchange under the conditions used here. A one-pot protocol for the conversion of 2-chlorotoluene to 2-tolylcyclohexane-1,3-dione, pseudo-catalytic in ruthenium was demonstrated, and although the overall conversion was a modest 22%; this serves as a good proof-of-concept for the *in-situ* recyclability of the activating $[RuCp]^+$ fragment.

Chapter 4

Accelerating the Rate of Arene Exchange of Ru(II) Sandwich Complexes

4.1. Introduction

As discussed in section 1.4 of this thesis, arene exchange remains a challenging process, often limiting the capability of certain metals in catalysis. Due to the high stability of the η^6-arene metal bond, sophisticated chemistry is often necessary to reduce the high energy barrier for exchanging bound arenes. Early methods of promoting arene exchange included the use of coordinating solvents to temporarily bind to and stabilise the metal centre following the η^6- to η^4- ring slip of the outgoing arene. Use of coordinating solvents was found to significantly enhance the rate of arene exchange. [34,54]

To improve the reliability of the stabilising coordination, metal complexes were designed to incorporate intramolecular coordinating groups tethered to one of the spectating ligands. The first example of such a complex was reported by Kundig in 1998, which was a chromium arene complex bearing a methacrylate ligand which could change its hapticity during the arene exchange process (figure 4.1). The enhancing effect of the multidentate methacrylate ligand was so large that the complex could undergo arene exchange at room temperature at a comparable rate as the analogous complex, [(η^6-arene)$Cr(CO)_3$], would undergo exchange at 170 °C.

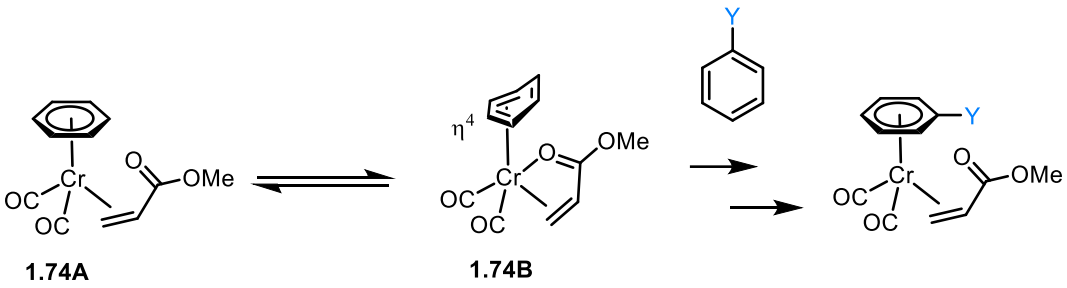

Figure 4.1. *Arene exchange catalysed by an intramolecular methacrylate tether*

A series of complexes of the form [(η^6-arene)RuCp-L]$^+$, where Cp-L is a cyclopentadienyl ring tethered to a coordinating group, have recently been developed by Walton and Williams, and their conversions at a set time points were compared with those containing Cp ligands. A library of different tether complexes were synthesised (figure 4.2) and their rates of arene exchange were tabulated over 3 and 16 hours in both cyclohexanone and octanol solvent (table 4.1). All complexes with tethered coordinating groups installed appeared to perform better in arene exchange than the non-functionalised Cp complex **1.95**, though a large variance in performance for each tether was observed. The best performing complex contained a pyridine tether (**4.5**), and this achieved full arene exchange after 16 hours at 150 °C.

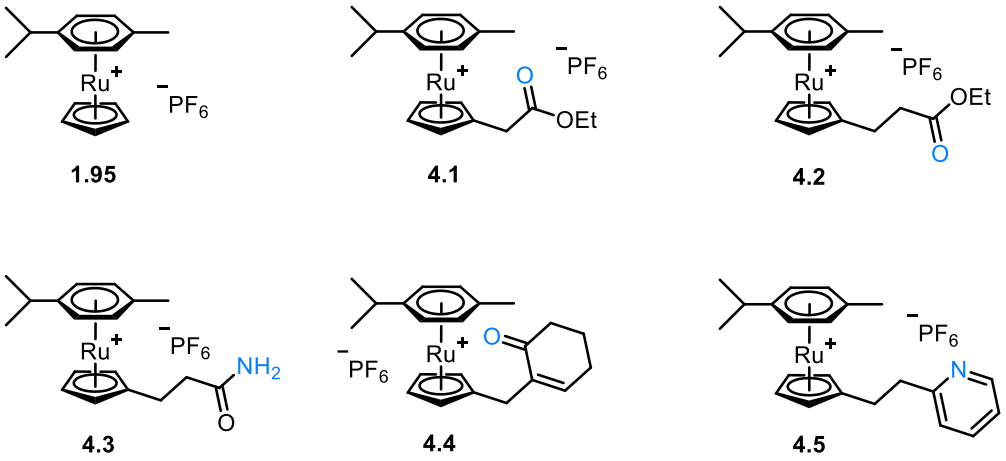

Figure 4.2. *Ruthenium complexes with tethered coordinating groups for improved rates of arene exchange*

Table 4.1. *Percentages for arene exchange, after 3 and 16 hours, of tethered ruthenium complexes, using either cyclohexanone or 1-octanol as solvent.*

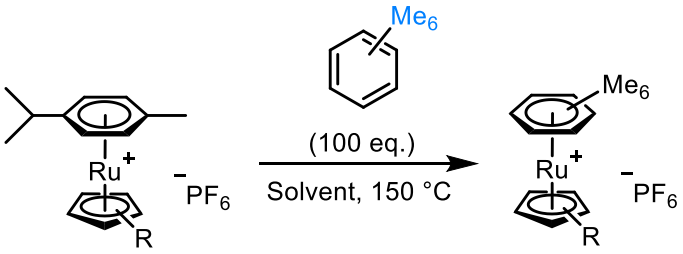

	Arene Exchange Conversion (%)			
Solvent	**Cyclohexanone**		**1-Octanol**	
Complex	**3 h**	**16 h**	**3 h**	**16 h**
4.1	6	38	17	92
4.2	(6)[a]	(50)[a]	(15)[a]	(84)[a]
4.3	9	51	13 (18)[b]	90 (88)[b]
4.4	--[c]	--[c]	(17)[d]	(85)[d]
4.5	12	50	12	65
4.6	44	100	36	100

[a] Values for decarboxylated **4.2** ([(MeCp)Ru(*p*-cymene)]$^+$), which forms under exchange conditions. [b] Values for the octyl ester of **4.3**, which forms in 1-octanol. [c] Complex **4.4** reacts with cyclohexanone, leading to invalid results. [d] Values for the octyl ester of **4.4**, which forms under the exchange conditions.

In this chapter, arene exchange reactions of an updated library of ruthenium tether complexes will be studied, as well as the effect that irradiation has on the rate of arene exchange. The aim of expanding the library of tether complexes is to discover new groups which can further enhance the rate of arene exchange, and therefore improve the catalytic ability of such complexes.

4.2. Results and Discussion

4.2.1. Temperature Dependence of the Rate of Arene Exchange

Initial arene exchange studies were performed using a model system (figure 4.3), where 50 equivalents of hexamethylbenzene were used to displace benzene in the complex $[(\eta^6\text{-}C_6H_6)RuCp]^+$ (**2.9**). In the model system, arene exchange is inherently thermodynamically favourable due to the incoming arene being more electron-rich, which gives the more thermodynamically stable η^6-hexamethylbenzene complex **4.6**.

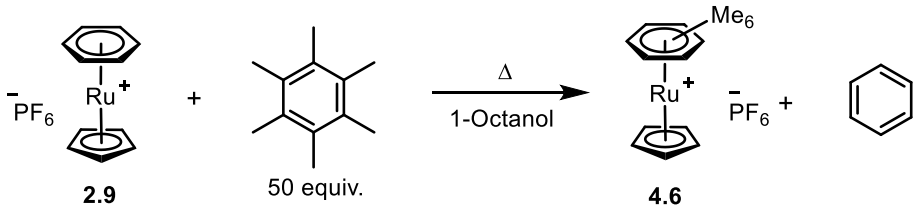

Figure 4.3. *Model system used to study the rate of arene exchange at different temperatures*

The mechanism by which this system undergoes arene exchange is likely identical to the one mentioned in section 1.4, where the outgoing arene 'unzips' by reducing its hapticity, while the incoming arene displaces it (figure 4.4). The key intermediate here is formed from a ring-slip of the outgoing arene from η^6- to η^4-, forming a much less stable 16 VE complex of ruthenium. One way of increasing the rate of this step, and by extension the overall rate of arene exchange, is by increasing the temperature of the reaction.

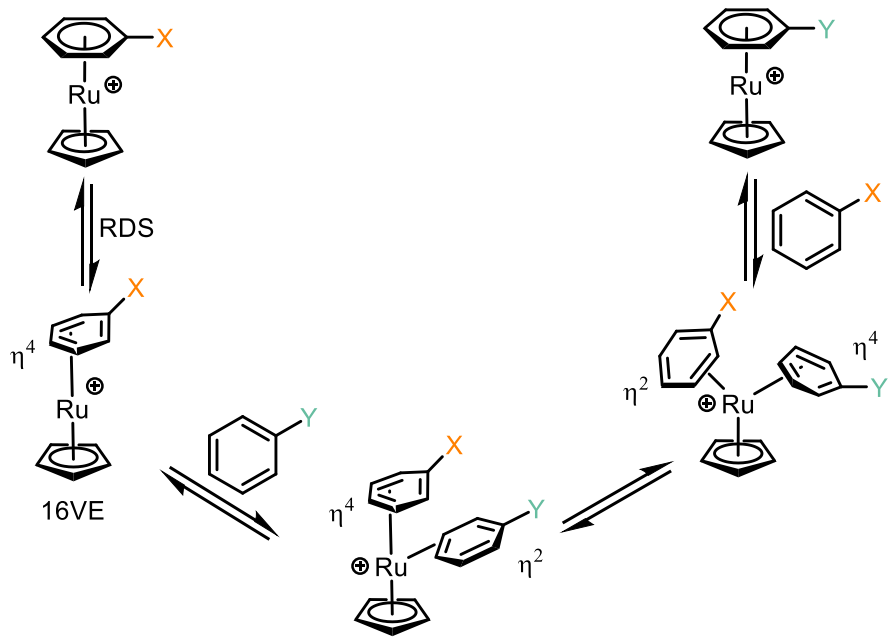

Figure 4.4. *Proposed 'unzipping' mechanism of arene exchange for [(η⁶-arene)RuCp] complexes.*

The arene exchange experiment was performed at three different temperatures, 120, 150 and 180 ºC, and the progress was monitored by analysis of relative peak integrals in QTOF mass spectrometry. This method assumes that both Ru complexes in figure 4.3 behave identically in the spectrometer, and therefore their relative peak integrals reflects their relative abundances in the reaction mixture. The rate graphs (figure 4.5) appear to coalesce with the expected trend, with arene exchange fastest at 180 °C, going to completion within two hours. Reducing the temperature to 150 °C reduces the rate significantly, and the reaction reaches a final conversion of around 95% after 6 hours, while lowering the temperature to 120 °C reduces the rate so much that only 50% of the starting material had been consumed after 48 hours. Interestingly, for the reactions at 120 and 150 °C, the reaction appears to plateau after a certain time, and stops before 100% conversion. This occurrence is difficult to explain given the thermodynamic drive for replacing benzene with the more strongly binding hexafluorobenzene, as well as the fact that free benzene should quickly vaporize at these temperatures, which would make any equilibrium between the complex species heavily weighted towards the product.

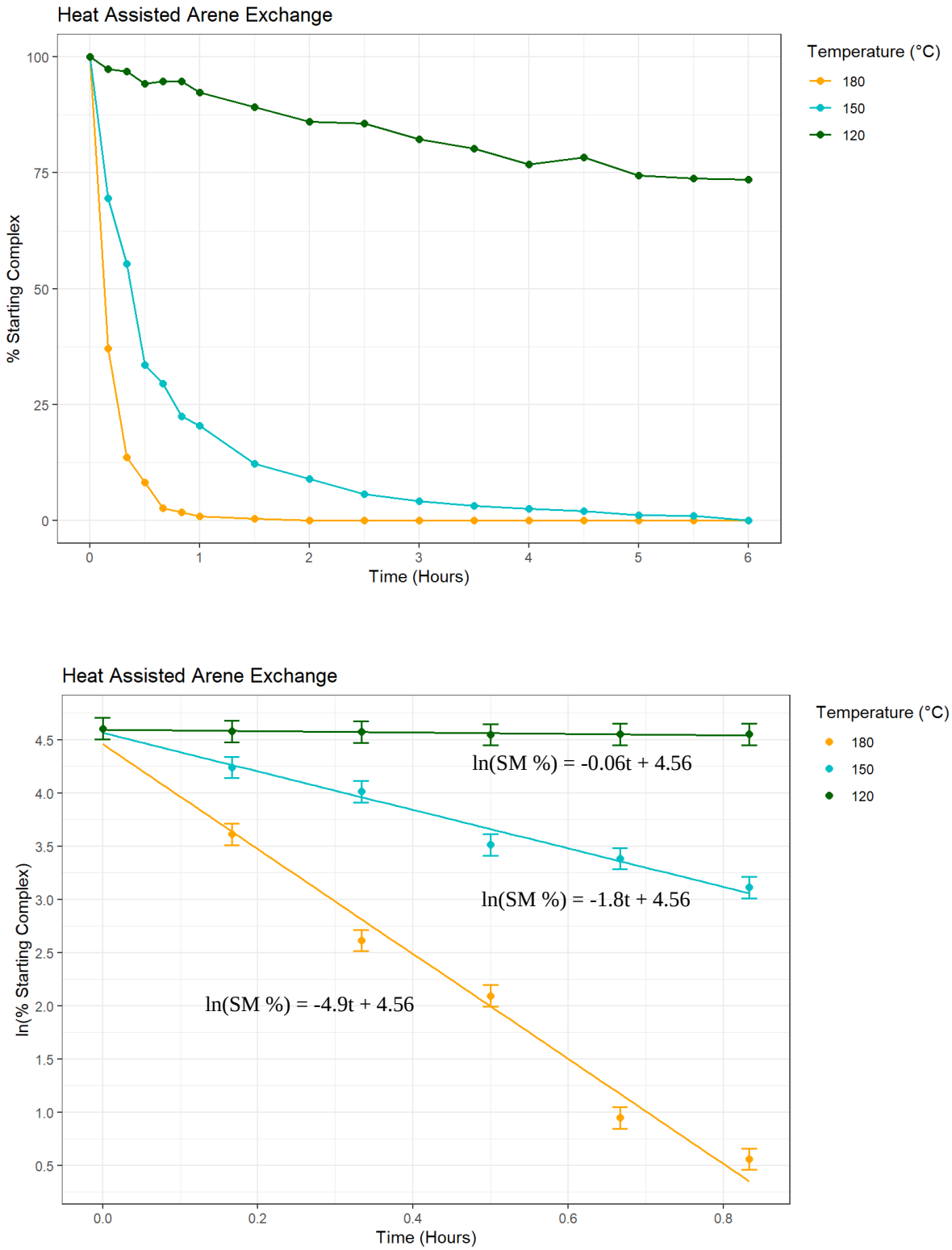

Figure 4.5. *Arene exchange of complex* ***2.9*** *at 180, 150 and 120 °C, illustrated by the consumption of the starting complex in the model system shown in figure 4.3 (top), and a linear plot of Ln(% starting complex) over time used to calculate the rate constant,* k_{obs}*, of the reaction at each temperature.*

Based on the mechanism where the rate-determining step is the haptotropic shift of the outgoing arene from η^6 to η^4, the arene exchange reaction should follow first order kinetics and the rate law described by equation 1. The apparent rate constant, k_{obs} can be calculated from equation 2. Values for k_{obs} in tables 4.1-4.4 were calculated using least squares regression in MS Excel.

$$[A] = [A]_0 e^{-kt} \quad (1)$$

$$k_{obs} = -\left[\frac{Ln(\frac{A}{A_0})}{t}\right] \quad (2)$$

Where k_{obs} is the observed rate constant, A is the amount of starting material at time, t, A_0 is the original amount of starting material, and t is time.

From this, a half-life for the reaction, $t_{1/2}$, was calculated using the equation:

$$t_{1/2} = \frac{Ln(2)}{k_{obs}} \quad (3)$$

A table containing the calculated values of k_{obs} and $t_{1/2}$ is below (Table 4.1), as a quantitative representation on how significantly the arene exchange is affected by reducing the temperature.

Table 4.2. *Kinetic data obtained from the arene exchange experiments assisted solely by conventional heating.*

Temperature (ºC)	k_{Obs} **(h^{-1})**	$t_{1/2}$ **(hours)[a]**	**Final Conversion (experimental) (%)**
180	4.9±0.1	0.14	>99
150	1.8±0.1	0.39	92
120	0.1±0.1	6.9	38

[a] Values for $t_{1/2}$ calculated using equation 3.

4.2.2. Light-Assisted Arene Exchange

Irradiation with UV (365 nm) light can be used to liberate an arene bound η^6- to $[RuCp]^+$, in the presence of a coordinating solvent, such as acetonitrile. Based on this observation, it is not unfeasible that light can be used to promote arene exchange, as the rate-determining step of arene exchange is expected to be the dissociative first step. To establish the effect that light has on arene exchange, our model arene exchange system was irradiated with 365 nm light (figure 4.6, table 4.3). This experiment was done by suspending the reaction tube, in an oil bath at 150 °C, surrounded by LED strips emitting the selected wavelength of light. The selected temperature for this reaction was 150 °C as this meant the reaction was slow enough to be able to observe a significant change in the rate, while the reaction was able to go close to completion. After monitoring the reaction at various time points by QTOF mass spectrometry, the resultant plot of % conversion against time (table 4.3) indicates a small but noticeable increase in the rate of arene exchange when the system is irradiated with 365 nm light. In the presence of light, the reaction proceeds to >99% completion within 2 hours, whereas in the absence of light, the reaction reaches its final conversion at around 4 hours. When the wavelength was changed to 385 nm, a smaller change in the rate was observed, while when 420 nm light was used, there was barely any difference between the irradiated arene exchange system and the initial one in the absence of any light. This observation is unsurprising, as increasing the wavelength reduces the amount of additional energy entering the system.

Table 4.3. *Calculated rate constants, k_{obs}, and half lives, $t_{1/2}$ for the arene exchange of complex* ***2.9*** *described in figure 4.6.*

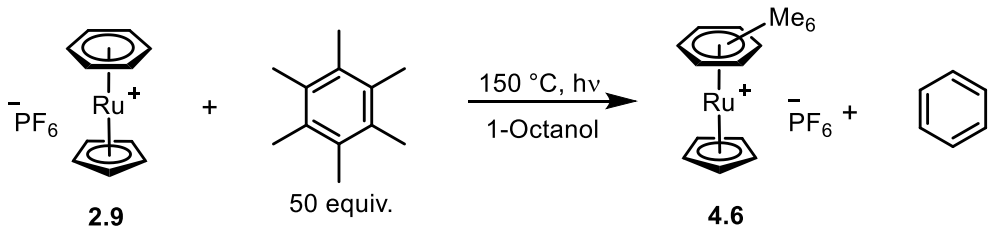

Irradiation	k_{obs} / h^{-1}	$t_{1/2}$ /hours
365 nm	2.7±0.1	0.26
Dark	1.8±0.1	0.39

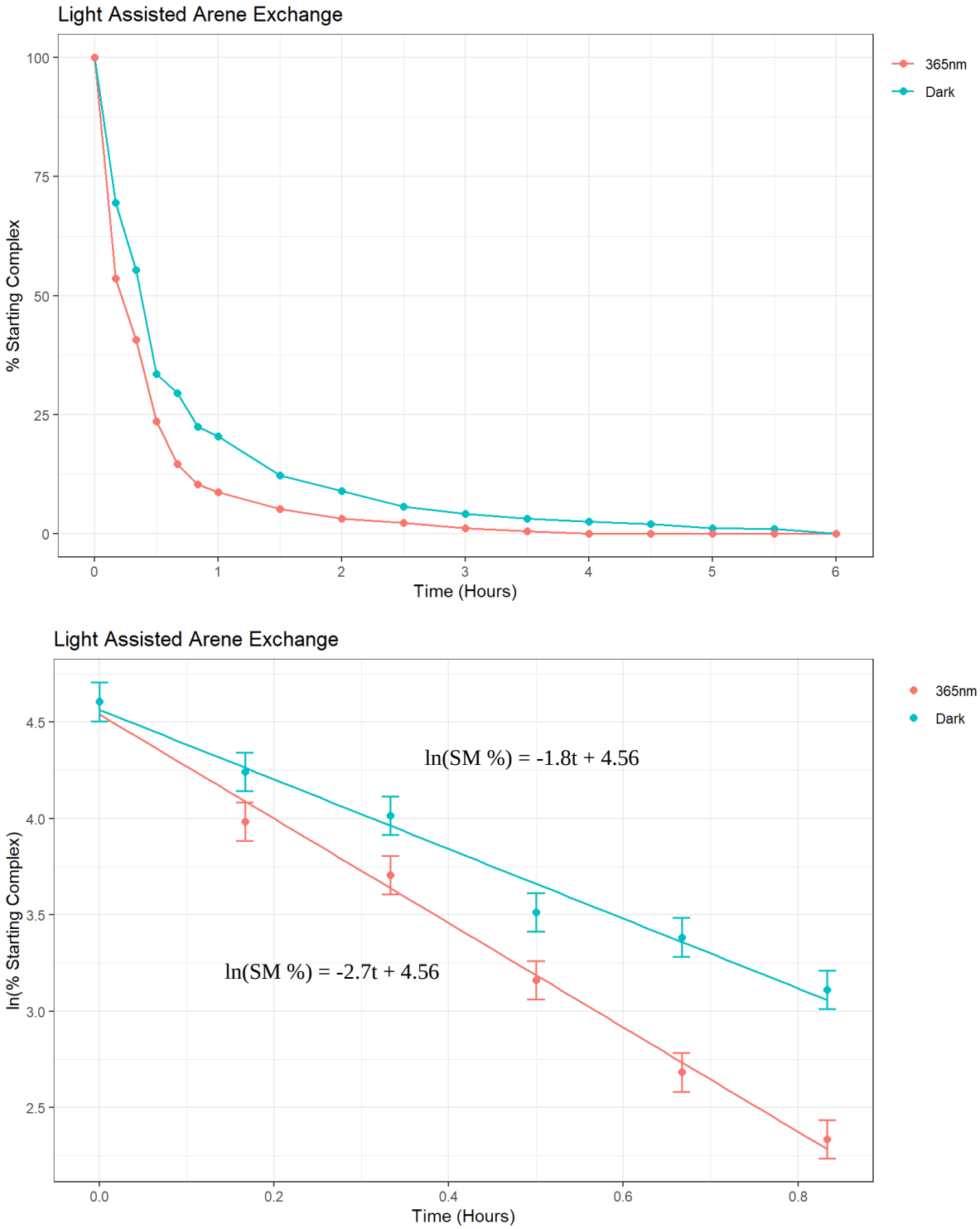

Figure 4.6. *Arene exchange of complex* ***2.9*** *under irradiation conditions (365 nm), illustrated by the consumption of the starting complex in the model system shown in figure 4.3 (top), and a linear plot of Ln(% starting complex) over time (bottom), used to calculate the rate constant, k_{obs}, of the reaction at each temperature.*

The rate constant, k_{obs}, and half lives, $t_{1/2}$ for each wavelength were calculated using the equations described in section 4.2.1, and are presented alongside the values from the initial arene exchange experiments in table 4.3 below. The values calculated here show quantitatively, the magnitude by which irradiation promotes arene exchange at 150 °C (table 4.3, entries 1-4). However, the increase in rate observed here is much less significant than increasing the temperature from 150 to 180 °C (table 4.2 entry 5). A potential reason for only a small observed effect of irradiation could be the nature of the setup for this experiment. To achieve simultaneous heating and irradiation, the vial containing the reaction mixture was suspended in an oil bath at 150 °C, surrounded by LED strips emitting the desired wavelength which were lining the inside of a plastic tube. Due to this, very little of the reaction mixture was exposed to the light, and therefore with a more optimised setup with more efficient irradiation it is likely that a larger effect will be observed from irradiating the arene exchange system.

4.2.3. Arene Exchange Accelerated by Tethered Coordinating Groups

4.2.3.1. Synthesis of a Library of Tethered Cyclopentadienyl Ruthenium Complexes

Investigations began with the synthesis of a library of ruthenium complexes bearing coordinating groups tethered to the cyclopentadienyl ring. Figure 4.7 below shows the 12 complexes targeted to explore the effects of different functional groups on the rate of arene exchange in the $[(\eta^6\text{-arene})RuCp]^+$ system. In previous work, [34] the ester and pyridine tethers showed good enhancement of arene exchange so were synthesised as a comparison to others. Complexes with OH, OMe and thiophene tethers were also synthesised and can be used to form a comparison between hard and soft donating groups, with an OMe tethered to a phosphine proving to be the optimal donating group for aiding arene exchange in a previous ruthenium catalysed amination of aryl chlorides.[82] Furthermore, each tether complex was synthesised with both a benzene and p-cymene capping group to investigate the effects of the arene on exchange as well.

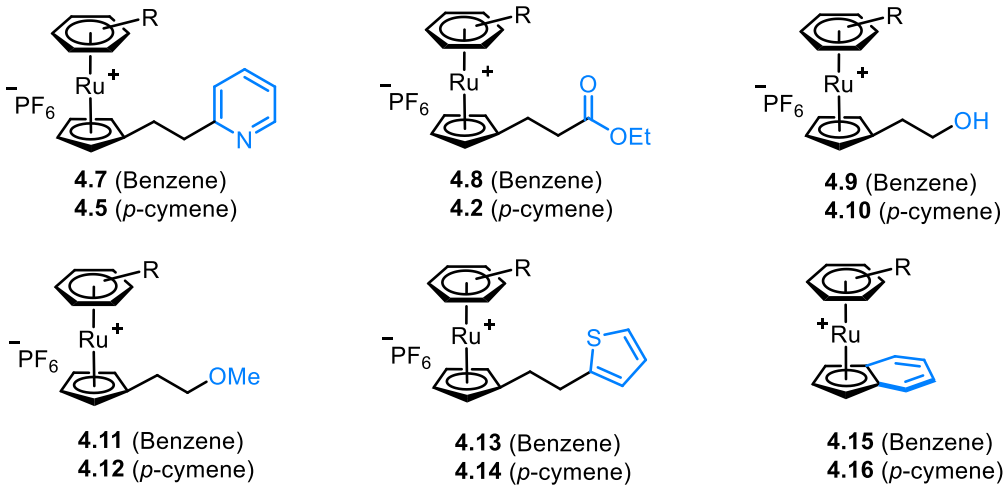

Figure 4.7. *Targeted tether complexes of the formula [(η^6-arene)Ru(Cp-L)]PF_6 (where arene = p-cymene or, benzene and L is a coordinating group) for enhanced rate of arene exchange.*

Ester tether complexes **4.8** and **4.2** were synthesised by the route described in figure 4.8. The first step was a simple nucleophilic substitution of the bromide in methyl 3-bromopropionate (**4.17**) by NaCp to form a 1:1 mixture of the two isomer compounds **4.18A** and **4.18B**. This mixture of isomers was then reacted crude with the ruthenium precursor complex [(η^6-arene)$RuCl_2$]$_2$ (where arene = benzene or p-cymene) in the presence of base to give the ester-tethered sandwich complex in a moderate yield. A noteworthy occurrence here is the change from a methyl to an ethyl ester in the complexation step due to transesterification with the ethanol solvent. Both the benzene (**4.8**) and *p*-cymene (**4.2**) complexes here were fully characterised using multinuclear NMR spectroscopy and high-resolution mass spectrometry.

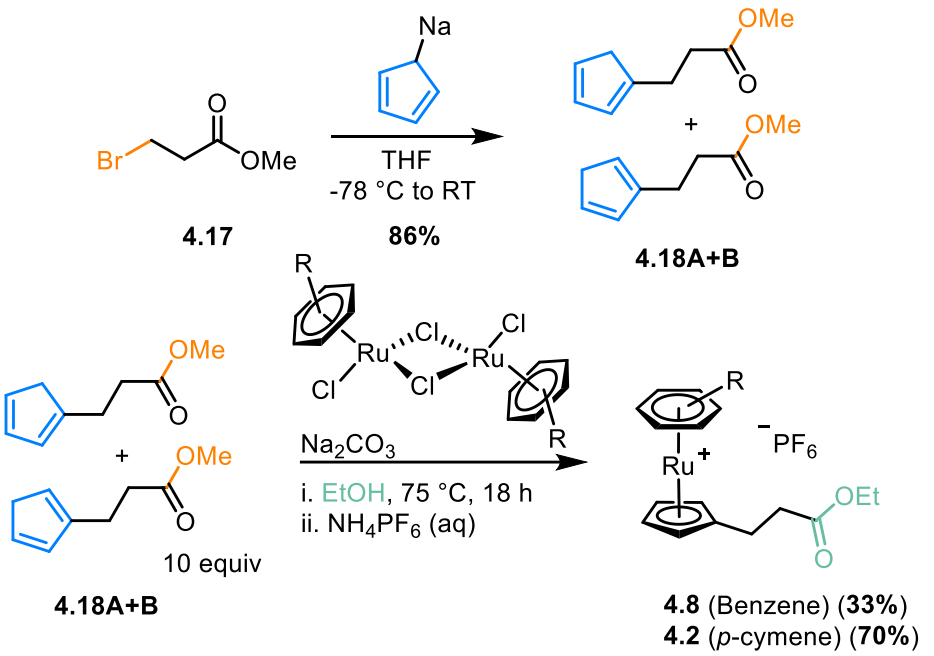

Figure 4.8. *Synthesis of the complex [(η^6-arene)Ru(Cp-es)][PF_6] (where arene = benzene, p-cymene and Cp-es = cyclopentadienyl-ester tether)*

The synthesis of the pyridine tether complexes (**4.5** and **4.7**) was more problematic. The initial synthetic route (figure 4.9) began with the bromination of 2-pyridineethanol (**4.19**) via the Appel reaction. The product of this reaction, 2-pyridyl bromide (**4.20**) was not characterised, due to its high susceptibility to a rapid degradation via the elimination of HBr to form the pyridyl alkene. Instead, NaCp (2M in THF) was added *in-situ* to the crude solution of 2-bromoethyl pyridine in THF, to form the 1:1 mixture of cyclopentadienes **4.21A** and **4.21B**. Although more stable than the precursor bromide, these Cp isomers are also susceptible to degradation, so the crude product was reacted with the Ru precursor complex, [(η^6-p-cymene)$RuCl_2$]$_2$ to form the pyridine-tethered sandwich complex **4.5**. At this stage, the main impurity was the triphenylphosphine oxide formed in the initial bromination step. This side product was removed *via* column chromatography to give the purified ruthenium complex in a low yield of around 10%.

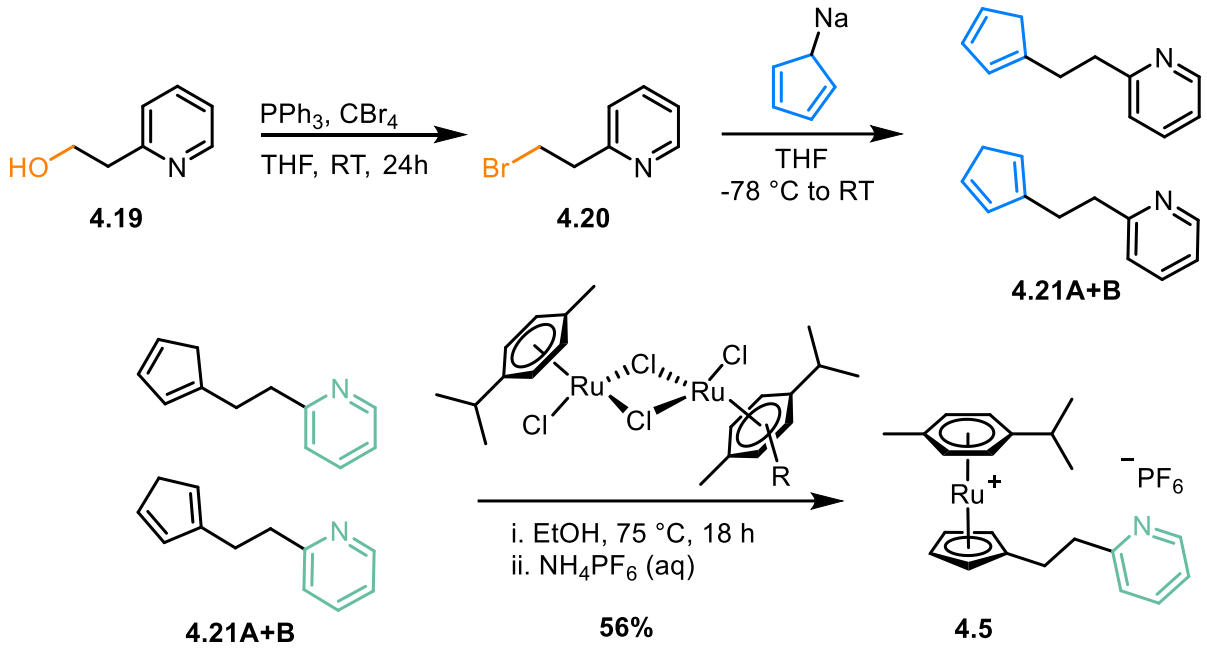

Figure 4.9. *Synthesis of the complex [(η^6-arene)Ru(Cp-Pyr)][PF_6] (where arene = benzene, p-cymene and Cp-Pyr = cyclopentadienyl-pyridine tether)*

In the initial synthesis of the pyridine-tethered ruthenium sandwich complex, the main issue was the inefficiency of the reaction, mainly due to the formation of triphenylphosphine oxide and its removal by column chromatography. To avoid formation of this side-product, the first step was changed to a mesylation reaction of 2-pyridineethanol (**4.22**, figure 4.10). The resulting mesylate was isolated after an aqueous work-up and reacted with NaCp as expected to form the mixture of Cp isomers in a higher purity than before, which could then be reacted with either Ru precursor complex to form the pyridine tethered sandwich complexes **4.5** (arene = *p*-cymene) and **4.7** (arene = benzene). The purification of both complexes was much simpler, as the only necessary step was a precipitation of each respective complex from the precipitation of a concentrated acetone solution in diethyl ether. Both complexes were then fully characterised by multinuclear NMR spectroscopy and high-resolution mass spectrometry to confirm their identity.

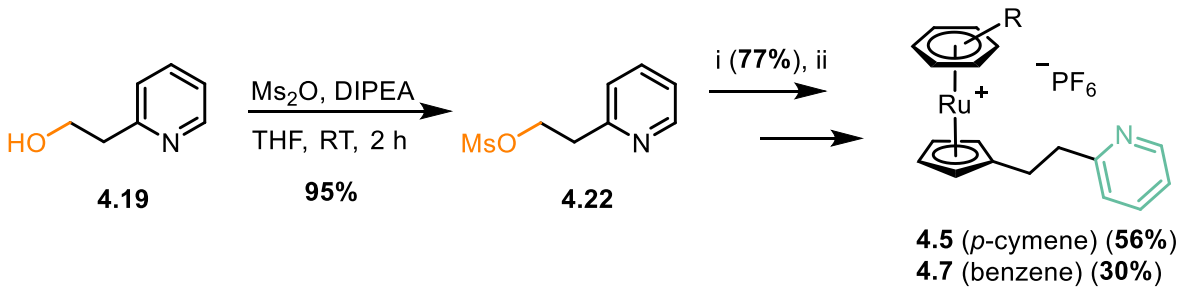

Figure 4.10. *Synthesis of pyridine tether complexes* ***4.5*** *and* ***4.7*** *via mesylation of 2-pyridineethanol, where the capping arene is benzene or p-cymene. Conditions: i. NaCp (2.4 M in THF), THF, -78 °C to RT, 18 h and ii. [(η^6-arene)Ru(Cp-Pyr)][PF_6] (where arene = benzene or p-cymene), K_2CO_3, EtOH, 80 °C, 18 h, then NH_4PF_6, H_2O, RT, 5 min.*

Synthesis of the complex with a hydroxyl tether was less problematic. Starting with 2-bromoethyl acetate (**4.23**), the cyclopentadienyl ring was installed via nucleophilic substitution of bromide with NaCp to form a 1:1 mixture of the cyclopentadiene isomers **4.24A** and **4.24B**. The hydroxy-tethered sandwich complexes **4.9** (arene = benzene) and **4.10** (arene = *p*-cymene) were generated in relatively good yields via reaction with their respective Ru precursor, with the hydroxyl moiety forming from the reaction of the ester group with ethanol, giving ethyl acetate as a side product. Initially, these complexes were synthesised as alternative precursors to the pyridine-tethered complexes **4.5** and **4.7**. Activation of the hydroxyl group via reaction with tosyl chloride gave the corresponding tosylate in a high yield (**4.25**, figure 4.11). Following this, the Grignard reagent, 2-pyridyl magnesium bromide was prepared from 2-pyridyl bromide and added *in-situ* to the tosylated ruthenium complex. Analysis of the crude product by ^{1}H NMR spectroscopy indicated that the tosylate group had mostly remained intact, while ESI-MS suggested that a small amount of the desired complex (**4.5**) had formed, but the sample consisted of mostly the starting material. While functionalisation of the OH group was unsuccessful, both of the hydroxy-tethered complexes here were kept for arene exchange experiments.

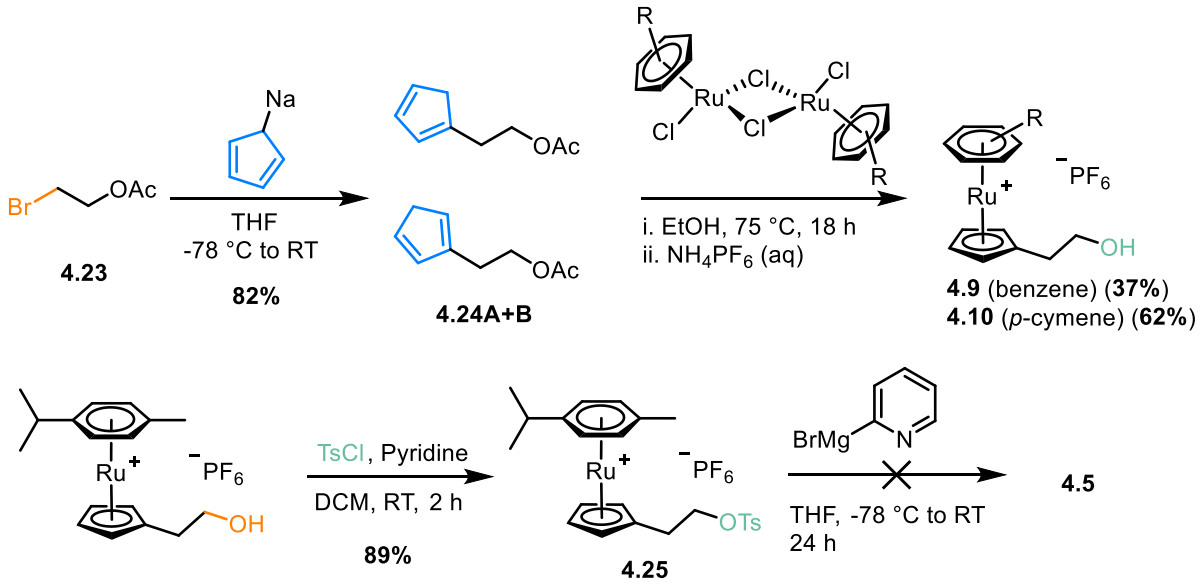

Figure 4.11. *Synthesis of the complex [(η^6-arene)Ru(Cp-OH)][PF_6] (**4.9** and **4.10**, where arene = benzene, p-cymenerespectively, and Cp-Pyr = cyclopentadienyl-hydroxy tether), and subsequent tosylation followed by attempted addition of a 2-pyridyl group.*

Methoxy (**4.11** and **4.12**) and thiophene (**4.13** and **4.12**) tether complexes were synthesised in modest yields from their respective alcohols (**4.27**, figure 4.12A and **4.29**, figure 4.12B, respectively). Each route started with formation of the cyclopentadiene isomers **4.28A+B** and **4.30A+B**, followed by their complexation to ruthenium. Again, multinuclear NMR spectroscopy and accurate mass analysis were used to confirm formation of each complex.

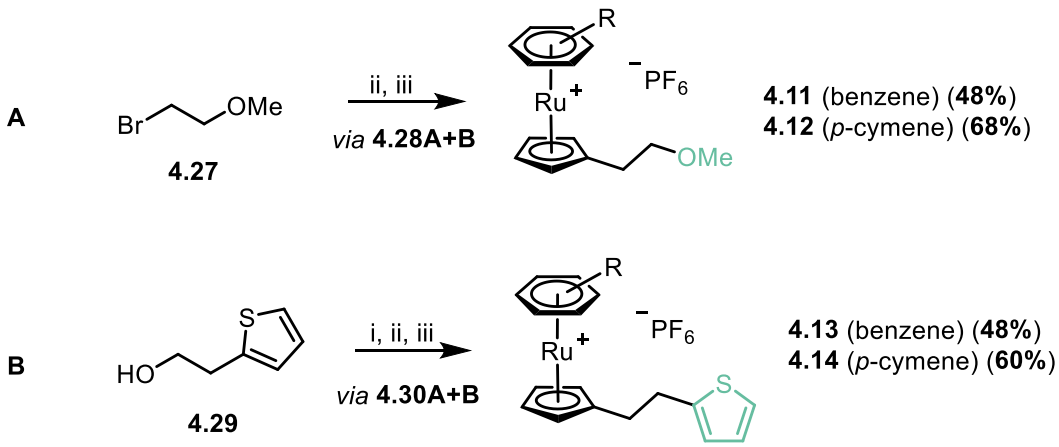

Figure 4.12. *Synthesis of thiophene and methoxy tether complexes. Conditions: i. Ms_2O, DIPEA, THF, RT, 2 h, ii. NaCp (2M in THF, 1 eq.), THF, -78 °C to RT, 16 h and iii. Either [(η^6-benzene)$RuCl_2]_2$ or [(η^6-p-cymene)$RuCl_2]_2$ (0.1 eq.), Na_2CO_3 (1 eq.), EtOH, 75 °C, 24 h.*

Finally, a pair of complexes were synthesised where an indenyl ring was bound η^5-to ruthenium (figure 4.13). This ligand is well-known to readily undergo a η^5 to η^3- ring-slip, temporarily vacating a coordination site around the Ru centre. It is feasible that this free coordination site is occupied by the incoming arene, beginning the arene exchange process. Indenyl sandwich complexes **4.15** and **4.16** were prepared via reaction with indene in the presence of base.

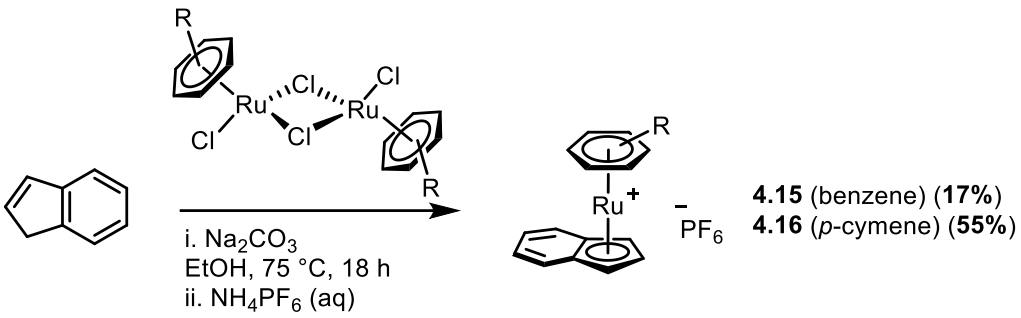

Figure 4.13. *Synthesis of the complexes [(η^6-arene)Ru(η^5-indene)][PF_6] (**4.15** and **4.16** where arene = benzene or p-cymene, respectively)*

4.2.3.2. Arene Exchange of Tethered Cyclopentadienyl Ruthenium Complexes

With the ten coordinating group-tethered Ru complexes in hand, the rate of arene exchange was explored for each complex in the model system described by figure 4.14. Each complex was reacted with 50 equivalents of hexamethylbenzene in 1-octanol solvent and aliquots of the reaction mixture were taken and analysed by QTOF mass spectrometry at selected time points over the course of 6 hours, with the resulting graphs described by figure 4.14 and table 4.4.

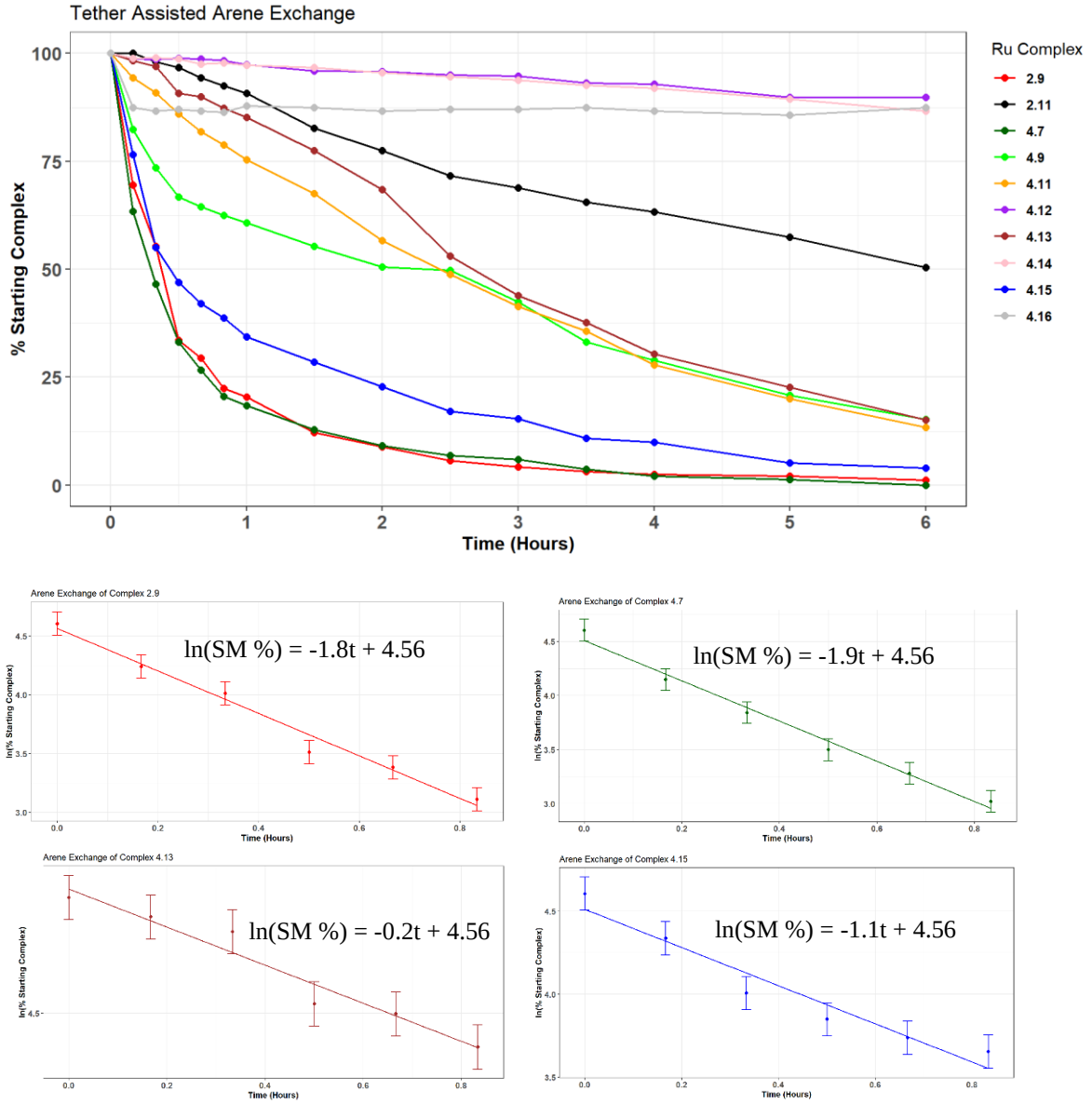

Figure 4.14. *Progress of arene exchange of [(η^6-arene)Ru(Cp-L)]PF_6 (where arene = benzene or p-cymene and Cp-L is a cyclopentadienyl ring functionalised with a coordinating group, L), with hexamethylbenzene (top middle), and linear plots of Ln(% conversion) against time for selected benzene-capped complexes,* ***2.9*** *(Cp, top left),* ***4.7*** *(pyridyl tether, top right),* ***4.13*** *(thiophenyl tether, bottom left) and* ***4.15*** *(indenyl, bottom right).*

Clearly, the data in figure 4.14 demonstrate the significant effects of the coordinating tether groups on both the rate and extent of arene exchange. It can be observed that benzene complexes containing the 2-pyridyl tether (**4.7**) and indenyl ligand (**4.16**) reach >99% and 95% conversion, respectively. This performance is comparable the standard complex with just a Cp ligand (**2.9**), which reached around 98% conversion after 6 hours. Their initial rate constants, k_{obs} However, the benzene complexes with hydroxy (**4.9**), methoxy (**4.11**) and thiophene (**4.13**) tethers performed far worse than to the standard complex (**2.9**). Each of these tether complexes reached around 83-86% conversion after 6 hours, compared to almost quantitative conversion in **2.9**. The arene exchange graphs of the methoxy and thiophene tether complexes look more sigmoidal in shape compared with the 'best' performing complexes which show an exponential decay in rate characteristic of 1st order kinetics. A potential explanation of this is that the product of arene exchange can help to further catalyse the reaction. This means the process is slow initially, until there is a significant enough build-up of the product complex to catalyse the arene exchange, then eventually slows down once most of the starting material is used up. A mechanistic description of this self-catalysis process involving $Cr(CO)_3$ systems, initially mentioned in section 1.4, is shown below in figure 4.15.

A general trend of these arene exchange reactions is that the complexes with benzene as the initial capping arene vastly outperform those with *p*-cymene. For example, the benzene pyridyl tether complex (**4.7**) reached 95% conversion in 6 hours, whereas the *p*-cymene complex (**4.5**) did not undergo arene exchange at all, while the other *p*-cymene tether complexes showed a very low rate of arene exchange. This trend is unsurprising given the relation between the electron density of benzene and *p*-cymene, and their relative strength of the η^6 interaction, as well as the fact that *p*-cymene is a bulkier capping ligand, making approach of the incoming arene sterically hindered. Using equations 1-3, the observed rate constant, k_{obs} and half-life, $t_{1/2}$ for the arene exchange of each complex were calculated and are shown in table 4.4 below.

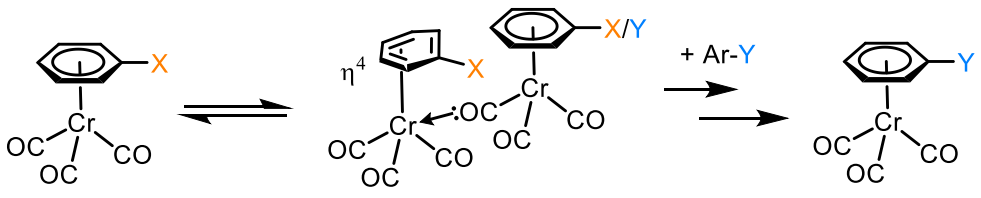

Figure 4.15. *Arene exchange catalysed by a second [(η^6-arene)$Cr(CO)_3$] complex.*

Table 4.4. *Values of k_{obs} and $t_{1/2}$ for the arene exchange complexes **2.9**, **4.7**, **4.13** and **4.15**, calculated from the linear best fit lines in figure 4.14. In all cases here, first order kinetics are assumed.*

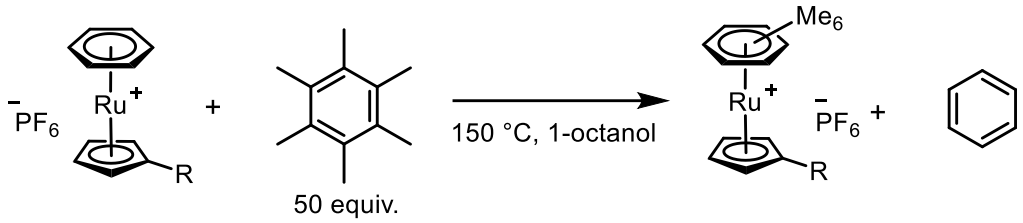

Entry	Complex	$t_{1/2}$ (hours)	k_{obs} (h^{-1})	Final Conversion (%)
1	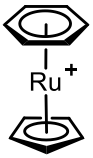	0.40	1.8±0.1	>99
2	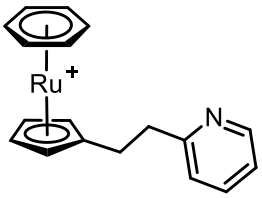	0.48	1.9±0.1	>99
3	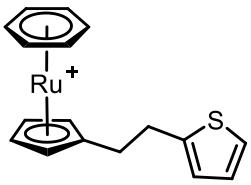	34.2	0.2±0.1	85
4	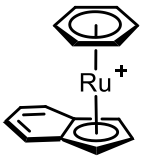	0.94	1.1±0.1	96

Not discussed here are the ethyl ester tether complexes **4.2** and **4.8**. The arene exchange of such complexes are challenging to monitor because the product of the trans-esterification reaction (i.e the complex with an octyl ester and benzene as the capping group) has an identical molecular weight to the arene exchange product containing the ethyl ester (figure 4.16). Due to the increased steric bulk of the octyl ester group compared to the ethyl ester, the arene exchange rate is expected to slow down after trans-esterification as the approach of the incoming arene is more restricted. Due to these reasons, any kinetic data related to the arene exchange of complexes **4.2** and **4.8** would not necessarily reflect the true exchange capability of an ester-functionalised Cp complex.

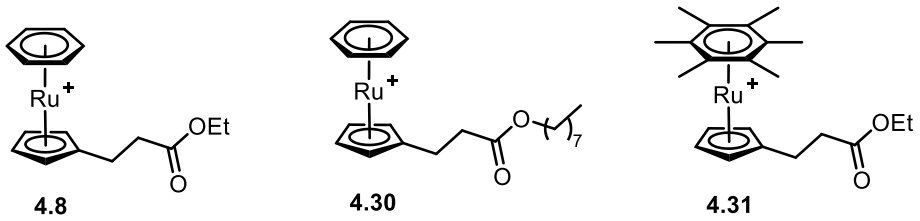

Figure 4.16. *Structures of cationic complexes* ***4.8****,* ***4.30*** *and* ***4.31,*** *which have exact weights (most abundant isotope) of 345.043, 429.137 and 429.137 Da, respectively.*

4.3. Conclusions

To summarise, insight has been found that temperature has a major effect on the rate of arene exchange, and while less significant, irradiation with UV light also enhances the rate of reaction, with the highest energy wavelength tested, 365 nm, having the largest effect, albeit hindered by the inefficient nature of the experimental setup. Furthermore, the data in this chapter suggests that there is potential for the improvement in the rate of arene exchange of ruthenium complexes with the installation of coordinating groups tethered to the cyclopentadienyl ligand, with the pyridine tether complex **4.7** producing the most promising results. Further enhancements to the rate of arene exchange can be made by optimising this pyridyl-tethered complex, such as making the pyridine more electron-rich or by having other alkyl groups along the alkyl tether to force the pyridine ring closer to the ruthenium centre. It is hypothesised that optimisation of arene exchange in such complexes will translate to more efficient catalytic processes in which arene exchange is the rate-determining step. Furthermore, the nature of the outgoing capping arene has a significant effect on its rate of arene exchange, with both electronic and steric factors contributing to this. To measure the relative effects of electronics and sterics, the exchange of an arene containing bulky electron-withdrawing groups can be investigated; if the rate here is faster than the exchange of benzene, then electronics are more important, whereas if the rate is lower then steric hindrance is more important.

Chapter 5

Ruthenium-Catalysed Aromatic Transformations *via* Transient η^6-Arene Intermediates

5.1. Introduction

Catalytic transformations of arenes *via* transient η^6-coordination to the activating metal fragment can be achieved when the on-ring reaction can be followed up by spontaneous exchange between the transformed arene and the starting compound. To reiterate, achieving this requires a fine balance of the magnitude by which the metal fragment is activating the arene ring, i.e. how strongly electron-withdrawing it is, and the ability of the metal π-arene complex to undergo spontaneous arene exchange, which depends on the strength of the η^6-bond. Naturally, a more electron-withdrawing metal fragment will lead to stronger donation from the aromatic ring, and therefore a complex more inert towards arene exchange, whereas a less electron-withdrawing metal fragment will lead to an η^6-bound ring which is more inert to the desired transformation, such as S_NAr or C-H activation. While such on-ring reactions have been known for many decades now, a resurgence in the field since the turn of the millennium has seen many examples where the fine balance between complex stability and ring-reactivity has been found and tuned. As a result, most aromatic transformations catalytic in the activating metal have been reported in the last decade. There are many different such catalytic protocols, differing by both the reaction occurring and the catalyst, but most examples follow a common core mechanism, shown in figure 5.1 below. In this chapter, aromatic transformations catalysed by a $[RuCp]^+$ fragment are discussed, with their mechanisms both suspected to occur via transient η^6-coordination.

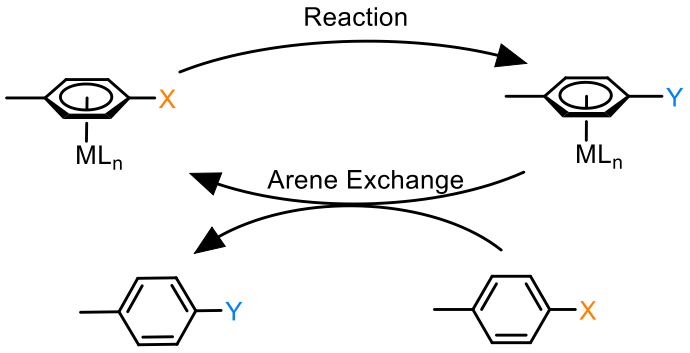

Figure 5.1. *Currently accepted mechanism by which an aromatic transformation is catalysed by an activating metal fragment, denoted ML_n*

5.2. Amination of Aromatic Rings

5.2.1. Metal-Catalysed Aromatic Amination

Aromatic amines, such as aniline, are used extensively as precursors to dyes, pharmaceuticals and pesticides,[147,148] making their synthesis highly useful in society, and therefore there exist many different methods of making aromatic C-N bonds. One of the most well-known aromatic amination methods is the Buchwald-Hartwig reaction,[149] which requires the use of a Pd catalyst. While Pd-catalysed aminations of aromatic rings were first demonstrated more than 10 years before Hartwig's initial study,[150,151] they were inefficient and had limited reaction scope. Furthermore, early reports included the use of organo-tin reagents,[152,153] which were later removed from the procedure and replaced by a strong base instead.[154,155] In the Buchwald-Hartwig amination reaction mechanism (figure 5.2), the Pd(II) pre-catalyst **5.1** undergoes reduction to **5.2**, then ligand dissociation to form the active Pd(0) catalyst **5.3A**. Oxidative insertion into an aryl C-X (where X = halide) bond [154,155] forms a dimeric palladium species **5.3B**. Following this step, the amine coordinates to the Pd(II) centre (**5.3C**), and in the presence of base is deprotonated to form complex **5.3D**, which can reductively eliminate to give the aryl amine and regenerate the catalytically active Pd(0) complex. Further developments to the catalytic procedure involved improvement of the ligands to bulky phosphines (DPPF, DBA or BINAP),[156–158] which facilitated coupling with primary amines, extension of the arene scope to include *ortho*-substituted rings, and allowed for the use of weaker bases in the reaction.[159,160]

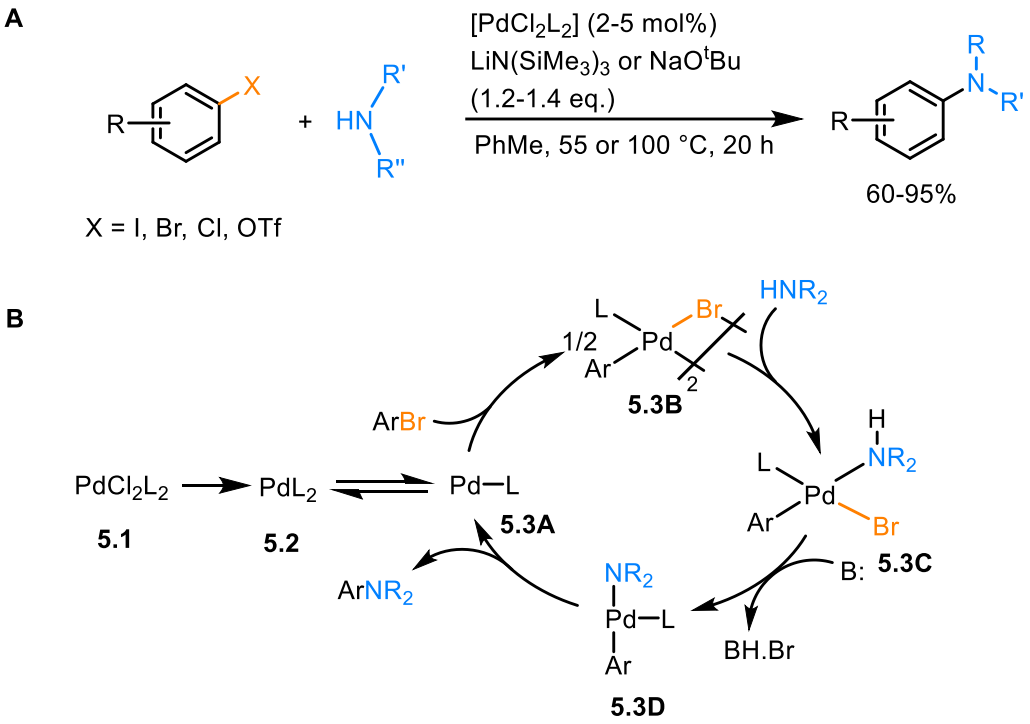

Figure 5.2. *Buchwald-Hartwig amination of aryl halides*

In a more recent development, the Pd-mediated cross-coupling of hindered, electron-deficient anilines with sterically hindered aryl halides was demonstrated (figure 5.3A).[141] Coupling reactions of such hindered substrates are not common due to the low nucleophilicity of electron-poor anilines, while *ortho*-substituted aryl halides are also difficult to couple. To achieve such a transformation, biarylphosphorinane ligands, AlisonPhos and AliPhos, were used to make a highly reactive active Pd(0) catalyst. Although the Buchwald-Hartwig, and other Pd-catalysed aromatic aminations are useful, palladium remains an extremely expensive metal to work with, making these coupling reactions difficult to scale up. As a result, interest in cheaper Cu(I)-mediated aromatic aminations has seen a resurgence recently. One of the most well-known Cu(I)-mediated amination reactions is the Ulmann coupling, which, despite its inherent usefulness in synthetic organic chemistry, has many limitations such as the requirement of a stoichiometric amount of copper, as well as generally low reaction yields. In a recent study, Mei *et al.* demonstrated the electrochemical C-H amination of arenes with secondary amines (figure 5.3B).[161]

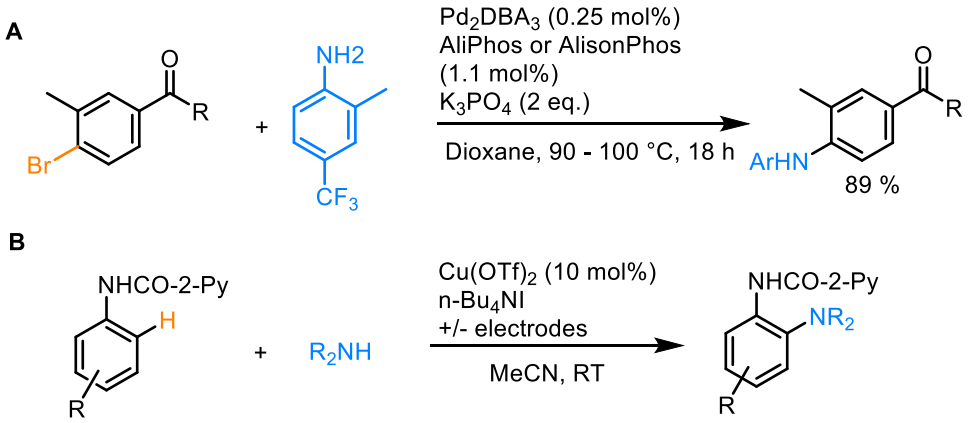

Figure 5.3. *Recent examples of Pd-catalysed aryl amination and Cu-catalysed electrochemical aromatic C-H amination*

Aromatic aminations without the need of a metal catalyst are possible through alternative methods such as nucleophilic aromatic substitution. In fact, an analysis of reactions used in medicinal chemistry by Brown *et al.*, revealed nucleophilic aromatic substitution to be the most frequent transformation behind amide bond formation.[162] S_NAr is unsurprisingly a popular method by which aromatic amines are formed, although these processes are inherently limited in scope due to the necessity of electron-withdrawing groups on the arene (see section 1, figure 1.3). Previously, Walton and Williams demonstrated the amination of 'unactivated' (i.e. no covalent EWGs) arenes, catalysed by transient η^6-coordination to an activating $[RuCp]^+$ fragment (figure 5.4).[34] In this study, amination proceeded to 90% conversion over the course of 14 days at 180 °C, with the reaction limited by the slow arene exchange of complex **5.4**. In sections 5.2.1 and 5.2.2, a series of studies are discussed where more catalysts are investigated, including the 'tether' catalysts to improve the amination conversion over shorter reaction times.

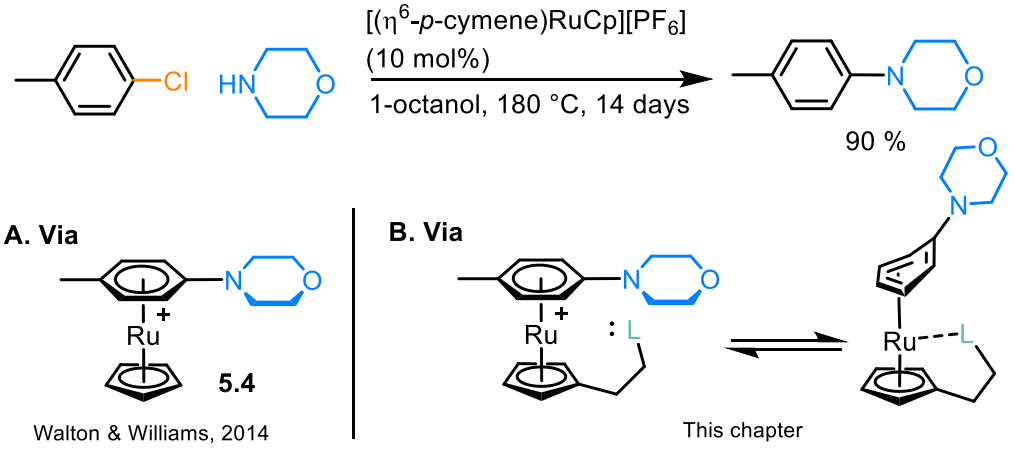

Figure 5.4. *Ru-catalysed amination of unactivated aryl chlorides*

5.2.2. Mechanistic Studies of Ru-Catalysed Amination

Initial studies were performed to obtain information on the mechanism of catalytic S_NAr amination, particularly which of the two steps (figure 5.5) are rate determining, the S_NAr step (**5.5** → **5.4**) or arene exchange (**5.4** → **5.5**).

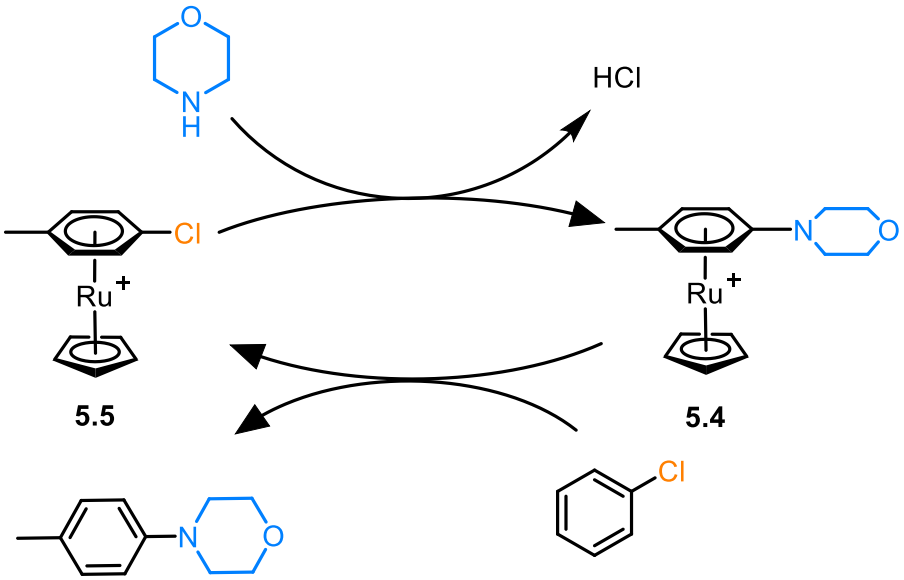

Figure 5.5. *Mechanism of ruthenium-catalysed amination of 4-chlorotoluene by Walton and Williams*

To elucidate information on the catalytic mechanism, the complex [(η^6-4-chlorotoluene)RuCp][PF_6] (**5.5**) was synthesised from the reaction of precursor tris(acetonitrile) ruthenium complex (**1.45**) with *p*-chlorotoluene (figure 5.6A). Following this, the expected intermediate of the catalytic S_NAr, the N-(*p*-tolyl)morpholine complex **5.4** was synthesised by reacting complex **5.5** with morpholine in the presence of base (figure 5.5). This reaction proceeded smoothly at 40 °C, and following purification, the product was fully characterised by 2D NMR spectroscopy and accurate mass analysis.

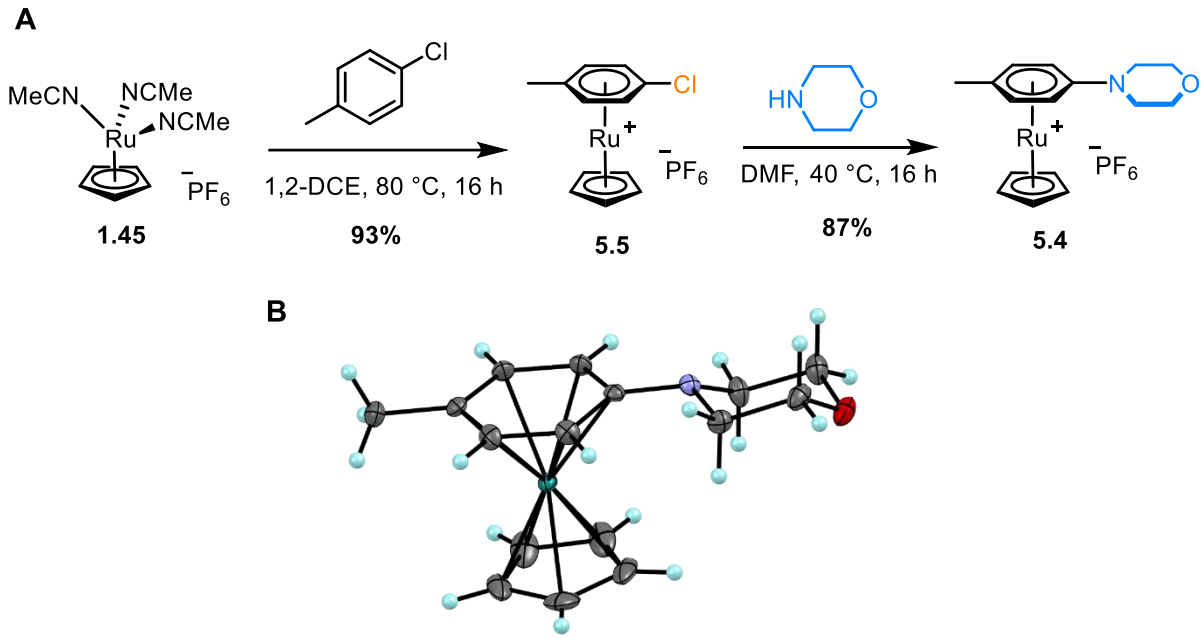

Figure 5.6. *A) Two-step synthesis of the complex [(η^6-4-(p-tolyl)morpholine)RuCp][PF_6] (**5.4**), and B). ORTEP plot of the molecular structure of cationic Ru sandwich complex **5.4**, with thermal ellipsoids at a 50% probability level. The [PF_6]$^-$ counter anion is omitted for clarity. Atom colours: carbon, grey; hydrogen, light blue; nitrogen, blue; oxygen, red and ruthenium, teal.*

A single crystal of complex **5.4** was obtained via the vapour diffusion of diethyl ether into a concentrated acetone solution of the complex. Analysis via single crystal X-ray diffraction confirmed the structure of the sandwich complex (figure 5.6B). Formation of this intermediate at temperatures as low as 40 °C strongly implies that, in the catalytic cycle, this S_NAr step is fast, while the arene exchange process is rate-determining, as the reaction takes up to 14 days at 180 °C. Furthermore, when monitoring catalytic reactions, ^{1}H-NMR spectroscopic analysis revealed the product bound intermediates as the catalyst resting state.

5.2.2. Ruthenium-Catalysed Amination of Aryl Chlorides

Following on from the previous study by Walton and Williams,[34] the key aim was to reduce the reaction time from 14 days to <1 day. To accomplish this, efforts were made to use conditions which could favour the rate-determining arene exchange step of the catalysis, including use of UV irradiation and changing the spectator ligand design with the aim of improving the rate of the arene exchange step. Our initial catalyst screening is shown in table 5.1.

Table 5.1. *Conditions screened for the ruthenium-catalysed amination of 4-chlorotoluene and 4-fluorotoluene*

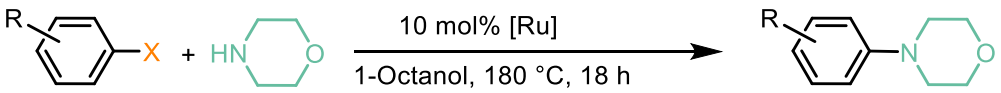

Entry	Catalyst	Irradiation (nm)	X group	Conversion /% after 18 h and (24 h)
1	None	Dark	Cl	0
2	$[CpRu(NCMe)_3]^+$ (**1.45**)	Dark	Cl	20
3	$[CpRu(NCMe)_3]^+$ (**1.45**)	365[a]	Cl	88
4	$[CpRu(NCMe)_3]^+$ (**1.45**)	254[a]	Cl	50
5	$[(\eta^6\text{-}C_6H_6)RuCp]^+$ (**2.9**)	Dark	Cl	20
6	$[(\eta^6\text{-}p\text{-cymene})RuCp]^+$ (**1.95**)	Dark	Cl	23
7	$[(\eta^6\text{-}4\text{-chlorotoluene})RuCp]^+$ (**5.5**)	Dark	Cl	11
8	$[Cp^*Ru(NCMe)_3]^+$ (**5.6**)	Dark	Cl	36
9	$[Cp^*Ru(NCMe)_3]^+$ (**5.6**)	Dark	F	41 (43)
10	$[(\eta^6\text{-}C_6H_6)RuCp^*]^+$ (**2.11**)	Dark	Cl	36
11	$[(\eta^6\text{-}C_6H_6)RuCp^*]^+$ (**2.11**)	Dark	F	44
12	$[(\eta^6\text{-}4\text{-chlorotoluene})RuCp^*]^+$ (**5.7**)	Dark	Cl	34 (45)
13	$[(\eta^6\text{-}4\text{-chlorotoluene})RuCp^*]^+$ (**5.7**)	Dark	F	48 (51)

[a.] Reactions performed with UV lamp (365 nm) suspended above (ca. 5 cm) the reaction submerged in heated oil bath.

The data in table 5.1 imply that irradiation has a significant enhancing effect on the catalysis when the complex $[(CpRu(NCMe)_3]^+$ (**1.45**) is used, (entries 2-4) as the conversion increases from 20 to 88% on irradiation with 365 nm light, although it drops to 50% with higher energy light. This irradiation setup was only used for these experiments, as the setup did not withstand the high temperatures of the catalytic process and began to fall apart after few uses. For this reason, the remainder of the catalyst screening was done in the absence of light, although these few results show the potential for light to drastically enhance the catalytic rate. A general trend observed here is that catalysts with a Cp* ligand fair better than those with Cp. For example, using the catalyst $[(NCMe)_3RuCp]^+$ (**1.45**, table 5.1, entry 2) leads to a conversion of 20%,

whereas the Cp* derivative gives a 36% conversion (**5.7**, entry 8). The same trend applies to all sandwich complex catalysts as well, when the spectator ligand is Cp, the conversions range from 11-23% (entries 5-7), which each increase to 34-36% when Cp* is used (entries 10 and 12). This trend could be because a Cp* ring has more electron density than its unsubstituted counterpart, leading to a higher amount of electron density being pushed towards the ruthenium centre. Consequently, the η^6- interaction between the capping arene and Ru centre is weakened, making Cp* complexes more prone to arene exchange, the rate determining step in this catalytic process. It is worth noting that the increased size of the Cp* ring could also feasibly slow arene exchange due to steric effects, but the results in table 5.1 suggest that electronic effects are more significant in this case.

Another general trend observed here is the small increase in conversion when the leaving group is changed from Cl to F. While aromatic fluorides are already known to be better at S_NAr than chlorides, it is surprising that the S_NAr step appears to have an, albeit small, effect on the catalysis, given that arene exchange is the proposed rate-determining step. An alternative explanation for this observation is that the slightly increased electron density in the aromatic ring of fluorotoluene compared to chlorotoluene makes the former better at displacing the product arene in the arene exchange step, and this small difference is reflected in the relative conversions.

Further to this work, the tether complexes first discussed in chapter 4 were applied to the S_NAr amination reaction. The motivation for using such catalysts is their ability to stabilise the initial η^4-intermediate formed in the proposed arene exchange mechanism (figure 5.7), increasing the rate of arene exchange, and therefore the catalytic efficiency of the reaction. The performances of such tethered catalysts are shown in table 5.2.

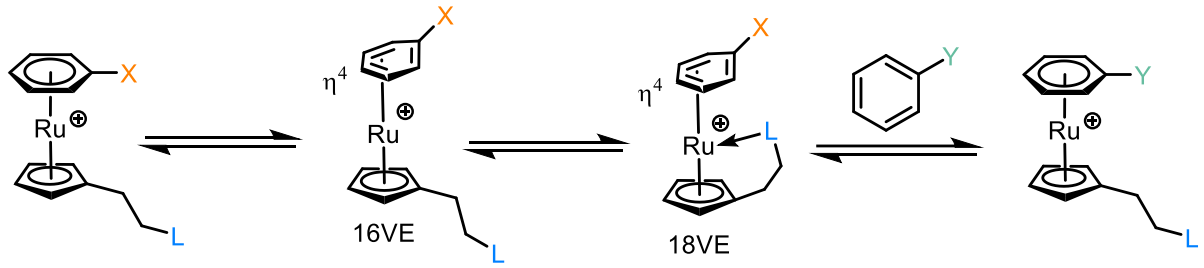

Figure 5.7. *Proposed stabilisation of the η^4-intermediate formed during arene exchange by coordination of a built-in coordinating group to the Ru centre.*

Table 5.2. *Conditions screened for the ruthenium-catalysed amination of 4-chlorotoluene and 4-fluorotoluene. Tether groups, R, are coloured blue in the table for clarity.*

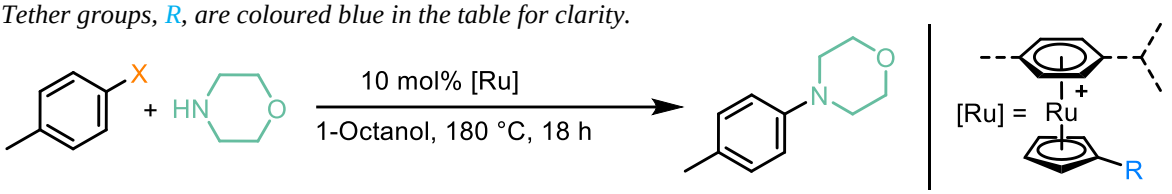

Entry	Catalyst	X group	Conversion /% after 18 h and (24 h)
1	$[(\eta^6\text{-}C_6H_6)Ru(Cp\text{-}Es)]^+$ (**4.8**)	Cl	39
2	$[(\eta^6\text{-}C_6H_6)Ru(Cp\text{-}Es)]^+$ (**4.8**)	F	59
3	$[(\eta^6\text{-}p\text{-cymene})Ru(Cp\text{-}Es)]^+$ (**4.2**)	Cl	23
4	$[(\eta^6\text{-}C_6H_6)Ru(Cp\text{-}Pyr)]^+$ (**4.7**)	Cl	22
5	$[(\eta^6\text{-}C_6H_6)Ru(Cp\text{-}Pyr)]^+$ (**4.7**)	F	32 (41)
6	$[(\eta^6\text{-}p\text{-cymene})Ru(Cp\text{-}Pyr)]^+$ (**4.5**)	Cl	32 (32)
7	$[(\eta^6\text{-}p\text{-cymene})Ru(Cp\text{-}Pyr)]^+$ (**4.5**)	F	32(32)
8	$[(\eta^6\text{-}C_6H_6)Ru(Cp\text{-}OH)]^+$ (**4.9**)	Cl	18 (18)
9	$[(\eta^6\text{-}p\text{-cymene})Ru(Cp\text{-}OH)]^+$ (**4.10**)	Cl	20 (20)
10	$[(\eta^6\text{-}C_6H_6)Ru(Cp\text{-}OMe)]^+$ (**4.11**)	Cl	2 (2)
11	$[(\eta^6\text{-}p\text{-cymene})Ru(Cp\text{-}OMe)]^+$ (**4.12**)	Cl	16 (16)
12	$[(\eta^6\text{-}C_6H_6)Ru(Cp\text{-thiophene})]^+$ (**4.13**)	Cl	Trace
13	$[(\eta^6\text{-}p\text{-cymene})Ru(Cp\text{-thiophene})]^+$ (**4.14**)	Cl	Trace
14	$[(\eta^6\text{-}C_6H_6)Ru(\eta^5\text{-indenyl})]^+$ (**4.15**)	Cl	0
15	$[(\eta^6\text{-}p\text{-cymene})Ru(\eta^5\text{-indenyl})]^+$ (**4.16**)	Cl	0

Surprisingly, the general performance of the modified Cp complexes is poor compared to the Cp* complexes. While the benzene-capped Ru Cp-ester (**4.8**, table 5.2, entries 1 and 2) and Cp-Pyridine (**4.7**, table 5.2 entries 4 and 5) complexes produce comparable results to Cp*, while the rest produce conversions more alike the Cp complexes. In other cases (thiophene, **4.13** and **4.14**, and indenyl tethers **4.15** and **4.16**) the catalysts do not produce any significant quantity of product at all. A reason for this could be that the tether complexes are generally less stable; more evidence for this is the unchanged conversions for several of these catalysts from

18 to 24 hours (table 5.2, entries 5-11), suggesting that they are decomposing more quickly than in the Cp or Cp* variants. It is feasible to suggest that some of the tethered complexes *are* producing the free product at a higher rate than either Cp or Cp* complexes but are limited by low stability; a useful future experiment to test this hypothesis would be to monitor the conversions at shorter time points, e.g., within the first 3-5 hours of the reaction to establish this.

5.3. Ruthenium-Catalysed Aromatic Hydrodeiodination

5.3.1. Introduction to Metal-Mediated Dehalogenation

Organic halides have widespread uses in both chemistry as reagents, solvents and intermediates in many synthetic processes.[163] They also can have a significant impact on society, in both manufactured materials such as PVC or PTFE, and naturally occurring chemicals such as thyroxin which is one of very few organic halides synthesised in the human body.[164] However, despite their use, the vast majority of halogenated chemicals are listed as pollutants, with many toxic to human or aquatic life. For these reasons, dehalogenation of organic matter has become a highly important field of study. One of the most common methods of removing halogens from organic materials is via hydrogenolysis, or hydrodehalogenation.

There are many dehalogenation processes known which are mediated by group 1 metals; lithium,[165,166] sodium,[167,168] and potassium,[169,170] and group 2 metals, magnesium[171,172] and calcium.[173,174] There are also a broad range of transition metals that have been reported to facilitate hydrodehalogenation reactions, with palladium being the most commonly used metal for this process.[163] One of the first examples of this was reported by Heck in 1977 in the palladium-catalysed reduction of nitro- and haloaromatic compounds,[175] and the process was found to be tolerant towards a number of different functional groups and the conditions were found to remove chloride, bromide and iodide from arenes. More recently, a particularly interesting study by Jimenez and co-workers outlined the use of a temporary halogen substituent to act as a blocker for the *para* position of a mono-substituted aromatic ring, enabling a regioselective substitution at the *ortho* position (figure 5.8).[176] The final step of the synthesis was a hydrodehalogenation using 10 wt% Pd-on-carbon and atmospheric pressure of hydrogen to give the final 1,2-substituted arene.

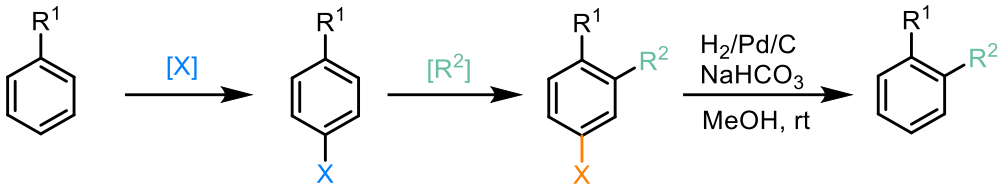

Figure 5.8. *Use of a halogen as a temporary blocker for the para position of an aromatic ring*

5.2.2. Radical Hydrodehalogenation Reactions

In 2016, Studer reported a metal-free radical hydrodehalogenation (figure 5.9), which is highly relevant to the studies discussed in section 5.2.3 of this chapter. Using electron-based catalysis, and an alcoholate as the organic chain reductant, hydrodeiodination of aryl, alkyl, alkenyl and alkynyl iodides was achieved.[177] Discussed in this paper is the activation of alcohols towards hydrogen donation through deprotonation. This was done using sodium hydride to deprotonate 2-(2-methoxyethoxy)ethanol, which is an excellent H-donor and therefore a useful electron-transfer agent for the reduction of organo-iodides. Overall, deiodinated organic substrates were formed in good to quantitative yields, although only electron-rich substrates could be deiodinated, and required large excess of both the base and hydrogen donor.

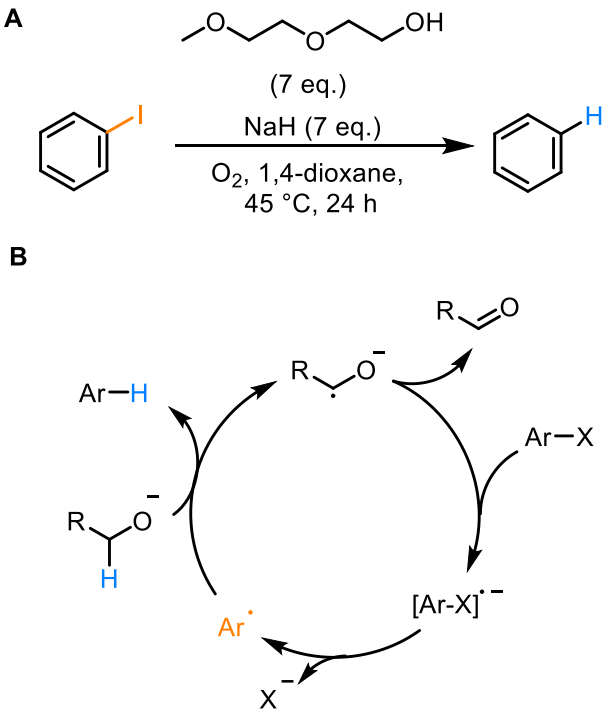

Figure 5.9. *Radical hydrodeiodination of aryl iodides using alcoholate as an organic chain reductant*

In another study by the same group, a similar radical hydrodehalogenation of aryl bromides and chlorides was accomplished using similar conditions to the radical deiodination above, through a very similar radical mechanism.[178] In this example, the solvent, 1,4-dioxane, was also used as a proton donor for the radical process, and 1,10-phenanthroline as the radical initiator. Generally, the reaction conditions were versatile towards many different aromatic substrates bearing different functional groups, with yields varying between 30 and >90%. The reaction also extended to defluorination, though yields were slightly lower for fluorinated substrates.

During the early stages of optimisation for the ruthenium-catalysed amination of aryl chlorides (see sections 5.2.2 and 5.2.3), *p*-halotoluenes were screened for their reactivity towards S_NAr by a previous MChem student, Archie McNeillis. While fluoro, chloro and bromo derivatives all appeared to undergo S_NAr in modest to high yields, iodotoluene showed no S_NAr reactivity here. Instead, analysis of the ^1H NMR spectra of the reaction with *p*-iodotoluene indicated the formation of toluene (figure 5.10), formed via a hydrodeiodination process. The mechanism by which this occurs is currently unknown, but is likely to go via a radical pathway, and is discussed further in section 5.2.3.

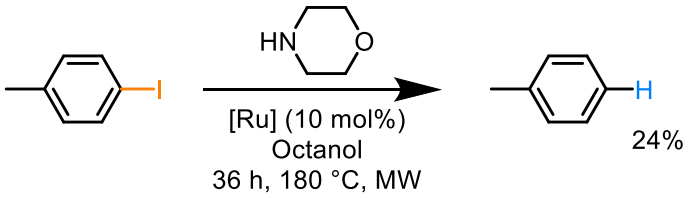

Figure 5.10. *Ru-catalysed hydrodeiodination of unactivated aryl iodides*

Further optimisation (table 5.3) led to use of DBU as the base instead of morpholine, while the Ru catalyst loading could be reduced to 1%, albeit longer reaction times were necessary for comparable conversions (table 5.1, entries 3 and 4). Solvent screening indicated that octanol was the optimal solvent for the reaction, and the conversion unsurprisingly dropped when the temperature was lowered to 150 or 120 °C (table 5.2, entries 6 and 7), while microwave heating gave higher conversions than conventional, likely due to uneven heating on the inside compared to the outside of the microwave vial.

Table 5.3. *Previous optimisation for the Ru-catalysed hydrodeiodination of 4-iodotoluene*

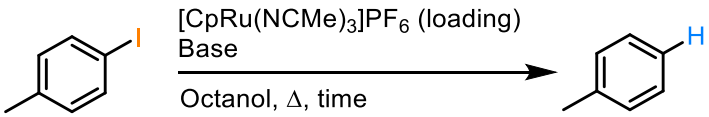

Entry	Base	Catalyst Loading (mol%)	Time (h)	Temperature (°C)	Heating method	Conversion (%)
1	Morpholine	10	18	180	MW	24
2	DBU	10	6	180	MW	100
3	DBU	10	3	180	MW	97
4	DBU	1	18	180	MW	98
5	DBU	10	18	180	Conventional	84
6	DBU	10	3	150	MW	79
7	DBU	10	3	120	MW	0

5.2.3. Ru-Catalysed Hydrodeiodination

Based on the previous work outlined in section 5.2.2, further investigations were made into shortening the reaction time of the microwave-assisted hydrodeiodination reaction, entries 1-4) further (table 5.4, entries 1-4). Reducing the reaction time to 1 hour, then 30 minutes did not appear to significantly affect the reaction conversion, while the conversion decreased to 79% with a 10-minute reaction time. Furthermore, it was previously established that in haloarenes containing both an iodine as well as an additional halogen (F, Cl or Br), only hydrodeiodination is observed, with the other C-X bond remaining intact. This does not necessarily mean the other positions are not prone to hydrodehalogenation, so a series of 4-halotoluenes were tested (table 5.3, entries 5-7) for their activity. Unsurprisingly, 4-fluoro and 4-chlorotoluene (entries 5 and 6, respectively) did not undergo any dehalogenation, although 4-bromotoluene did appear to undergo hydrodebromination to a small extent. This finding is strong evidence that the deiodination reaction is *not* an S_NAr process, and instead reaffirms the idea of a radical mechanism, where weaker C-X bonds are more prone to breaking.

Table 5.4. *Optimisation of reaction time for the ruthenium-catalysed hydrodeiodination of 4-iodotoluene, and investigations into the activity of other 4-halotoluenes. Conversions were calculated by comparing the integrals of the starting material and product in a ^{1}H NMR spectrum of the crude reaction mixture ($CDCl_3$, 400 MHz, 298 K).*

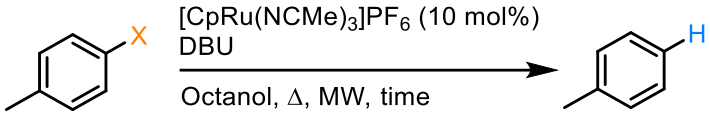

Entry	X Group	Reaction Time (mins)	Conversion (%)
1	I	180	100
2	I	60	98
3	I	30	94
4	I	10	79
5	F	180	0
6	Cl	180	0
7	Br	180	24

With an optimised set of conditions for the ruthenium-catalysed hydrodeiodination of aryl iodides in hand, investigations were conducted to obtain more mechanistic insight into the process. Here, *para*-substituted iodoarenes bearing both EDGs and EWGs were explored to examine their relative performances (5**.8**-**5.16**, table 5.5), as well as some iodopyridines (**5.17**-**5.19**), to gain insight into the nature of the transition state of the reaction and whether there was positive or negative charge build-up in such a species. To best highlight the relative performance of each arene, these experiments were run using reduced catalyst loading and each was monitored after 10 minutes.

Table 5.5. *Catalytic hydrodeiodination of a series of iodoarenes and iodopyridines.* [a] *Trace amount of debromination observed*

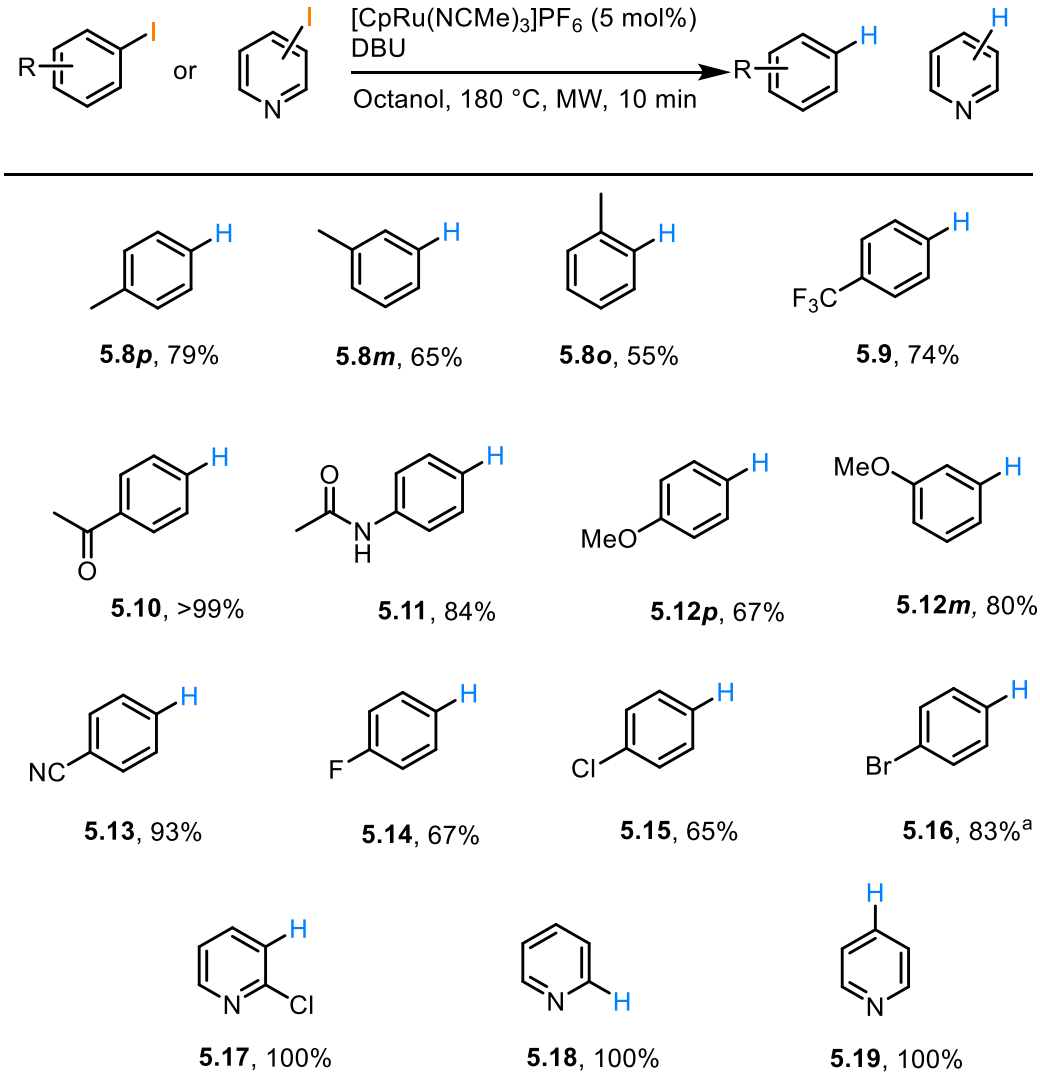

In these experiments, moving the methyl group of the base substrate iodotoluene to *meta*- and *ortho*- positions appeared to have a negative effect on the conversion, with *ortho* performing the worst (**5.8**). A possible explanation for this is that having a substituent close to the reacting centre could sterically hinder the reaction. However, in the case of the methoxy-substituted iodoarene (**5.12**), the performance improved on moving the substituent to a *meta* position over *para*-, suggesting that electrons are also important in the reaction. When the methoxy group is in the *meta*-position, less electron density is placed on the reacting C-I position, hence these results imply build-up of negative charge during the deiodination. A general trend observed with the hydrodeiodination of *para*-functionalised iodoarenes is that the ones bearing EWGs, such as trifluoromethyl (**5.9**), keto (**5.10**) and nitrile (**5.13**) groups, performed better than those with EDGs. There are a few exceptions here, although this observation suggests that the

transition state of the deiodination process includes some degree of negative charge build-up. Furthermore, the electron-poor iodopyridines all quantitatively underwent the hydrodeiodination, further suggesting negative charge build-up. A plot of the conversions against the Hammett parameter for each *para* substituent is shown in figure 5.10. The data in the graph do not appear to show any correlation between the Hammett parameter for a substituent and the corresponding deiodination conversion. Therefore, it is reasonable to conclude that there is little/no significant charge build-up in the transition state, implying a radical process. The Ru-catalysed hydrodeiodination is proposed to follow the mechanism shown in Figure 5.12.

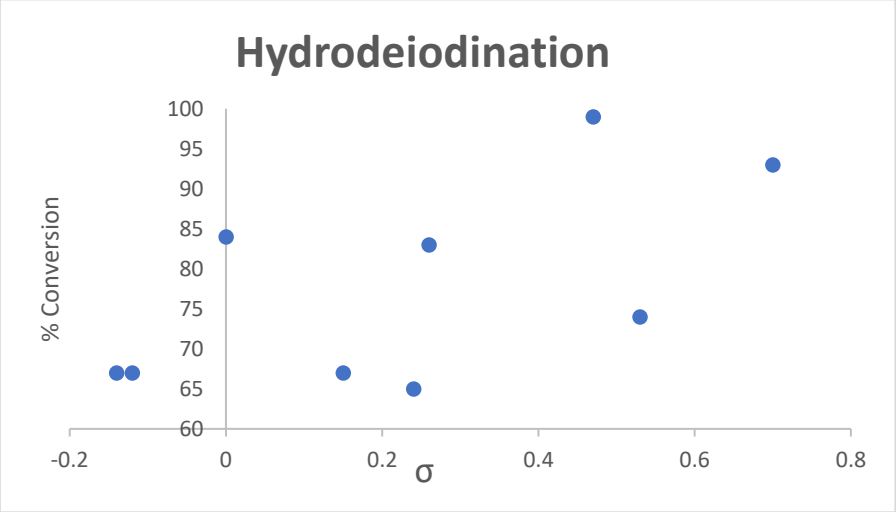

Figure 5.11. *Plot of conversion against relative Hammett parameters for each of the para-functionalised iodoarenes described in table 5.4.*

Based on previous work in the Walton group, a reaction mechanism has been proposed for the ruthenium-catalysed aromatic hydrodeiodination (figure 5.12A). The radical mechanism here initiates with the complex [(η^6-4-iodotoluene)RuCp]$^+$ (**5.20A**) undergoing a single electron transfer (SET) with DBU, which is known to facilitate such radical initiations. [179,180] Loss of iodide results in the formation of a η^6-bound 4-tolyl radical **5.20B**. This species then abstracts a hydrogen from the deprotonated 1-octanol, resulting in the formation of the η^6-bound toluene complex **5.20C**, which can arene exchange with the excess 4-iodotoluene present to restart the cycle. The resting state of this process is the bound toluene complex **5.20D**, meaning arene exchange is the rate-determining step. It is worth noting that the deprotonated alcohol solvent **5.21B** is a better H-transfer reagent than its protonated form (**5.21A**), meaning a stoichiometric

amount of the base, DBU, is required. The resulting radical anion **5.21C** undergoes a SET reaction with the $[DBU]^{+\cdot}$ radical cation to form an aldehyde. This process is consistent with the observed formation of octanal (**5.21D**) at the same rate as the toluene product. Such a mechanism highlights the dual functionality of the DBU present as both a base and single electron transfer agent. In fact, this single electron transfer process which triggers deiodination can only occur when the aromatic ring is bound η^6- to ruthenium, because of the additional stabilisation that π-coordination gives to the arene radical. This was demonstrated previously by Houk *et al*. when the radical addition to the chromium complex $[(\eta^6\text{-}C_6H_6)Cr(CO)_3]$ was 10^5 fold faster than with free C_6H_6, due to the C_6H_6 LUMO stabilisation from π-coordination.[181] To further help confirm this radical process, in a previous study in the research group, iodobenzene (**5.22**) was converted to bromobenzene (**5.24**) via reaction of an η^6-bound radical with N-bromosuccinamide (NBS) in a yield of 31% using the catalyst $[Cp^*Ru(NCMe)_3][PF_6]$ (figure 5.12B). Such a reaction also indicates the potential for further applications of a radical deiodination process beyond just hydrodeiodination.

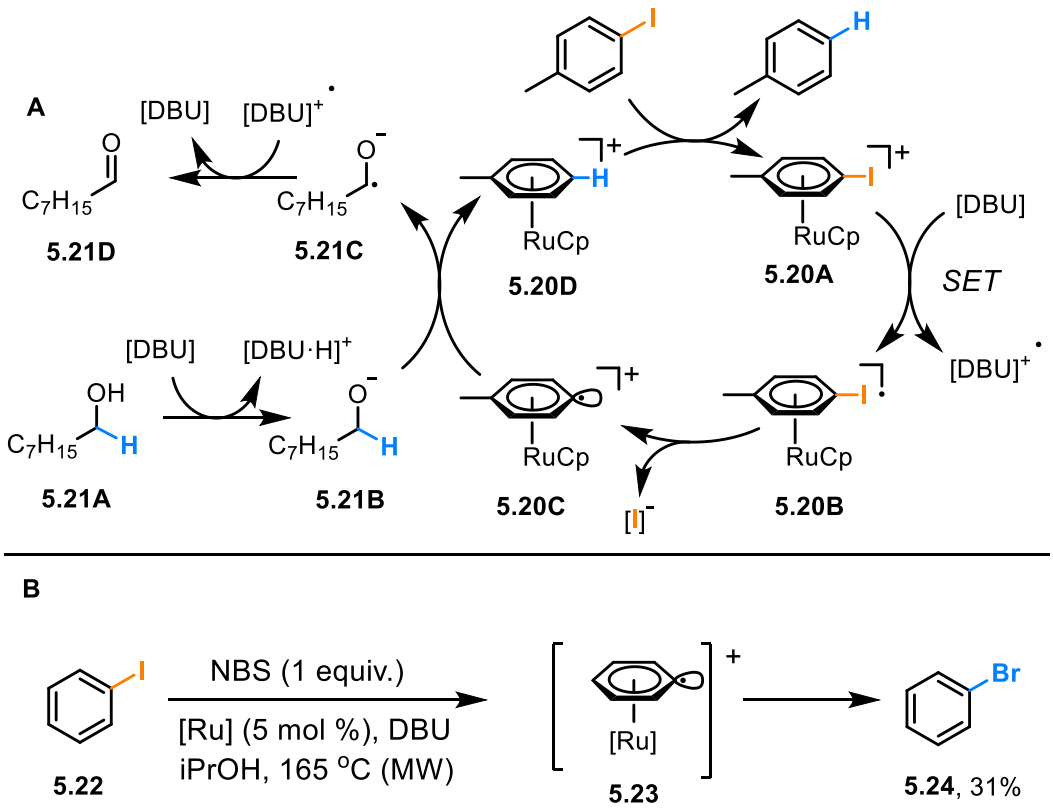

Figure 5.12. *A) Currently proposed radical mechanism for the ruthenium-catalysed hydrodeiodination of 4-iodotoluene via π-arene intermediates. B) Conversion of iodobenzene to bromobezene via the reaction of a η^6-bound arene radical with N-bromosuccinamide.*

5.3. Conclusions and Outlook

Overall, a known aryl amination via ruthenium catalysed S_NAr has been further developed with more catalysts tested for their activity. This includes the complexes bearing coordinating groups tethered to the cyclopentadienyl ligand which have previously demonstrated slightly enhanced rates of arene exchange. In the catalyst screening, the best performing Ru complexes were those with Cp* ligands, most likely due to the electronic effect of a more electron-rich spectator ligand pushing additional electron density towards the Ru centre, weakening the η^6-bond and increasing the arene exchange step of the catalysis, which is likely rate-determining. Despite their slightly enhanced rates of arene exchange, the tether complexes mostly did not perform as well, with the best being the pyridinyl tethered complex. This could be due to the observed catalyst decomposition which was evidenced by the lack of increase in the conversion between 18 and 24 hours of the reaction beginning. Future work in this S_NAr includes investigation of catalyst deactivation by analysing the catalytic mixture at different time points within the first few hours of the reaction. Also, recent work by Shi and coworkers has indicated that use of hemilabile phosphine ligands enhance the rate of arene exchange significantly,[82] acting in a similar way to the cyclopentadienyl tethers discussed in this chapter, with catalysis achieved at temperatures as low as 120 °C.

Also discussed in this section was a previously well established and highly optimised ruthenium-catalysed hydrodeiodination of 4-iodotoluene. In this section, further improvements were made to the catalytic conditions, namely a near quantitative conversion was achieved in just 30 minutes under microwave conditions at 180 °C, where the previous reaction time was 3 hours. Also, other haloarenes were found to be completely inactive towards the dehalogenation conditions, with only 4-bromotoluene exhibiting a small amount of debromination. This finding is strong evidence that the mechanism of the deiodination is not an S_NAr, but more likely a radical process, as only the weaker C-X bonds were broken under these conditions. Further investigations into the scope of the hydrodeiodination indicated that having EWGs *para* to the C-I bond enhanced the performance of the substrate, while having EDGs made them slightly less active compared with the base 4-iodotoluene substrate. A Hammett plot also indicated a fairlyweak correlation between increasing the Hammett parameter for the substituent in the 4-position and the relative % conversion. This evidence indicates that the transition state of the reaction mechanism has at least some degree of negative charge build-up, aligning with a radical mechanism. Future work in this area includes finding

out the exact mechanism of the deiodination reaction, as it is still not certain that the process occurs via a ruthenium π-arene complex.

Chapter 6

Conclusions and Future Work

6.1. Project Conclusions

The overarching aim of this project was to discover and optimise new aromatic transformations facilitated by η^6-coordination to Ru(II) and develop both new and already existing stoichiometric reactions into processes which operate, with catalytic quantities of ruthenium, through transient η^6-intermediates. While such transition metal complexes and their reactivities have long been established, a renaissance in this field has occurred in the last 20 years, with most studies highlighting the potential for catalytic arene transformations. Discussed in chapters 2 through 5 of this thesis were four separate projects conducted over the last three-and-a-half years. A brief summary of the progress made throughout this project are discussed herein.

At the beginning of the project, a method of fluorinating a benzene ring, based on the previous work of Grushin and coworkers,[84] was envisioned to occur via the η^5-Meisenheimer complex (figure 6.1A). While a complex of this nature was likely formed, it was unstable and all attempts to purify or oxidise it *in-situ* were unsuccessful. Another issue encountered was the high sensitivity of the system to any moisture present, as only hydroxylation was observed, rather than a desired fluorination. Another synthetic target, based on a trifluoromethylation procedure developed previously in the group,[46] was a difluoromethylation of the sandwich complex $[(\eta^6\text{-}C_6H_5X)RuCp]^+$ (where X = CN, NO_2). Again, the moisture sensitivity proved a barrier to the desired process, as only the Meisenheimer complex, $[(\eta^5\text{-}C_6H_5CNO)RuCp]^+$ was formed, though on this occasion the compound was stable enough to be isolated and purified. The Meisenheimer complex was also subjected to oxidising conditions, which resulted in the formation of a free arene ring, though its identity was not conclusively identified (figure 6.1B). Although largely unsuccessful, this project gave new insight into the nature and stability of η^5-Meisenheimer complexes of ruthenium.

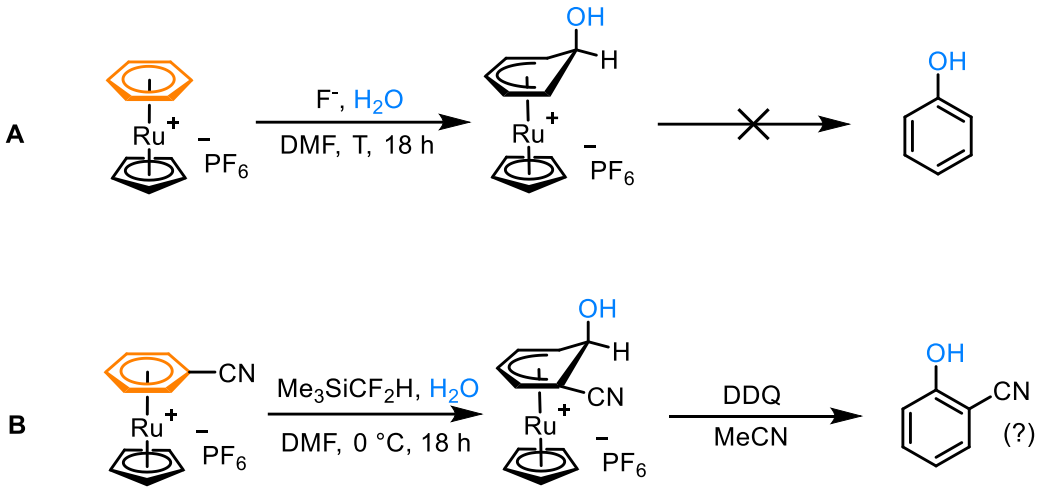

Figure 6.1. *Attempted fluorination and difluoromethylation procedures, which both resulted in hydroxylation due to trace amounts of water present*

Following the previous work, a new S_NAr process was investigated, using enolates as potential nucleophiles to generate 2-aryl-1,3-cyclohexanedione derivatives, which have emerged recently as a new class of herbicides.[139,142] Starting with the sandwich complexes of the form $[(\eta^6\text{-}C_6H_5X)RuCp]^+$ (where X = F, Cl, NO_2), the reaction with 1,3-cyclohexane in the presence of base yielded the desired bound 2-aryl-1,3-cyclohexanedione complex in a high yield (figure 6.2, step 1). Next, the equivalent process was optimised for bound arenes bearing methyl group(s) *ortho* to the S_NAr site, while competition reactions indicated that, while certain leaving groups preferentially substitute, the reaction prefers to occur on the less sterically hindered site, irrespective of which leaving groups are present. The enolate S_NAr also displayed high tolerance for many diones containing several different functionalities, except for the only aliphatic dione tested, which resulted in the formation of free arene, likely by displacement of the η^6 arene by $[acac]^-$ ligands. A promising result observed during this project is the ability to rapidly liberate the transformed arene, as well as a recoverable ruthenium complex, via a simple photolysis reaction (figure 6.2, step 2). The quantitative formation of the free arene and the complex $[(MeCN)_3RuCp]^+$ drastically improves the overall efficiency of the process, as the ruthenium species can be recycled to form new sandwich complexes. Furthermore, a one-pot stepwise synthesis of 2-*o*-tolyl-1,3-cyclohexanedione, pseudo-catalytic in ruthenium was achieved, further highlighting the potential of this process to be catalytic in Ru. However, all attempts at a catalytic system proved unsuccessful, with mass spectrometry analysis suggesting the lack of arene exchange of the bound S_NAr product.

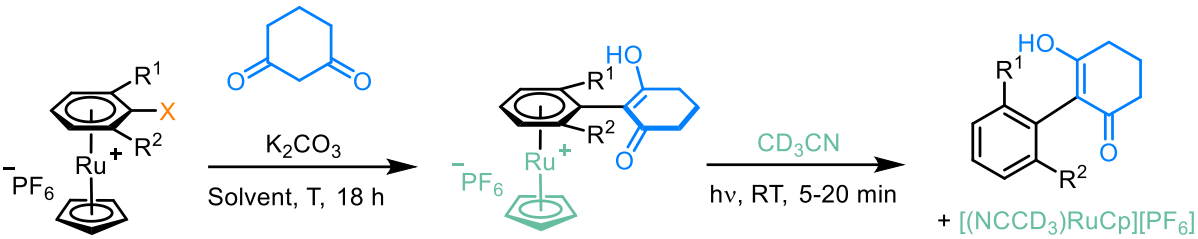

Figure 6.2. *Enolate S_NAr of unactivated arenes facilitated by η^6-coordination to Ru, followed by quantitative photolytic liberation of the arene. R^1, R^2 = H or Me*

To create a more efficient catalysis, it is important to fully understand arene exchange, particularly for $[RuCp]^+$-based systems, and how to accelerate the rate of this process. During initial experiments using our model arene exchange system (figure 6.3A), a strong temperature dependence was observed, while a less significant enhancement on the rate was made by irradiating the arene exchange system with UV light (360 nm). Then, a library of complexes with built-in coordinating groups tethered to the Cp ligand were prepared and tested under arene exchange conditions. While some of these tether complexes gave an improved rate of arene exchange at 150 °C, while many others appeared to hinder the reaction.

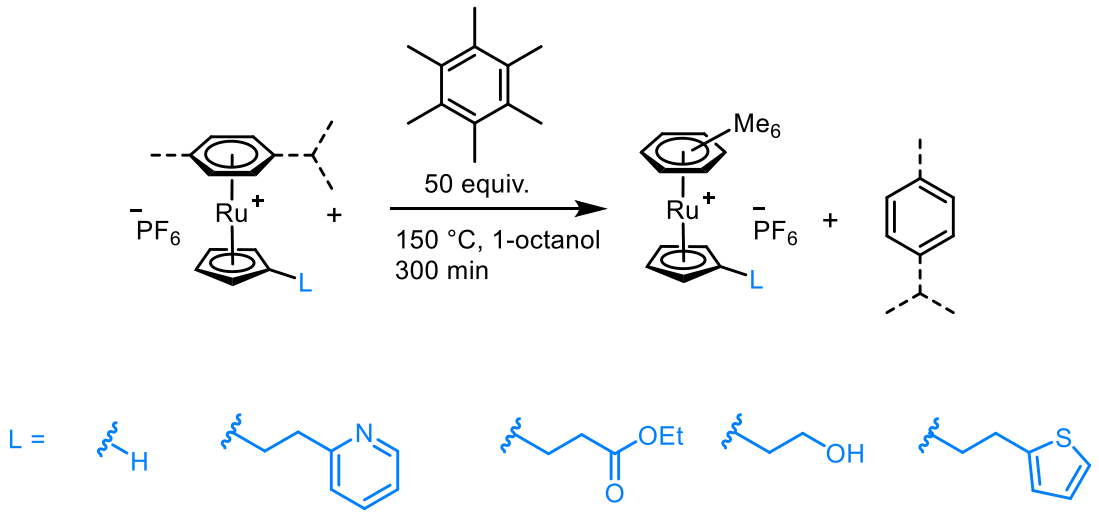

Figure 6.3. *Arene exchange of the complexes $[(\eta^6$-arene)RuCp$][PF_6]$ (where arene = benzene, p-cymene and L = functional group) with hexamethylbenzene*

In parallel with the arene exchange studies, the tether catalysts were tested for their performance in a ruthenium-catalysed S_NAr amination of aryl chlorides/fluorides. The performance of these catalysts mostly reflected their performance in the arene exchange studies, with a few exceptions. A key issue that was observed here is the instability of these

tether complexes under the catalytic conditions, where decomposition leads to cease in turnover.

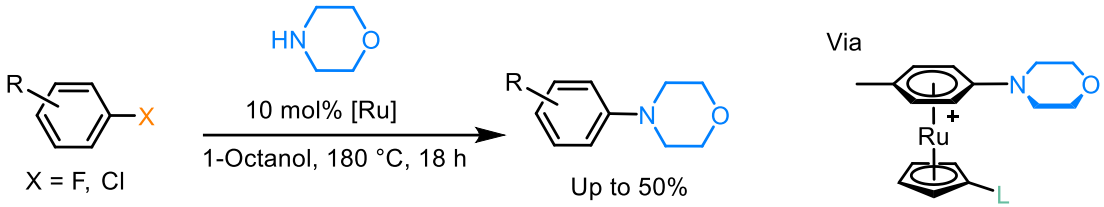

Figure 6.4. *Ruthenium-catalysed amination via S_NAr of unactivated haloarenes*

Finally, a ruthenium-catalysed hydrodiodination was further optimised, and the reaction time shortened to less than an hour under microwave heating (figure 6.5). Arenes with EWGs *para* to the deiodination site were found to perform better than those with EDGs, indicating a negative charge build-up in the transition state. The reaction is also selective for deiodination over other dehalogenation reactions, with only trace amounts of debromination also observed. Future work here will be to gather further information based on which a full hydrodeiodination mechanism can be proposed.

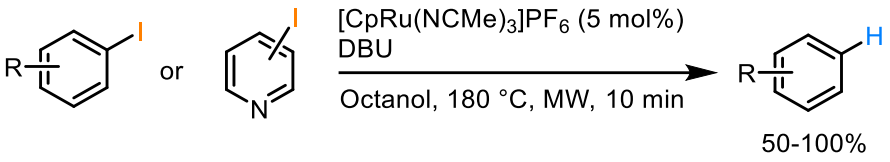

Figure 6.5. *Ruthenium catalysed hydrodeiodination of a series of iodoarenes*

6.2. Future Work

In addition to the points made in section 6.1, there are many different areas which are useful to explore, some as a direct continuation of the work discussed above or moving towards new areas of research. A key area which must be addressed is the translation of the procedure for enolate S_NAr of unactivated arenes to a protocol which is catalytic in ruthenium. It is not currently clear how this can be done, as attempts for catalysis using current $[RuCp]^+$-based frameworks failed due to the lack of arene exchange ability of the bound product. In recent years, a number of papers have demonstrated alternative ruthenium frameworks, which have performed well in catalytic protocols such as S_NAr amination (figure 6.6A),[80,82] whereas similar Rh(I-III) catalysts were used for aromatic hydroxylation/alkoxylation,[83] due to their additional resistance to catalyst deactivation. In these studies, phosphine ligands containing

hemi-labile tethers were found to significantly increase the rate of arene exchange at lower temperatures. It is feasible that such catalysts can be applied to our enolate S_NAr as well as other systems such as S_NAr amination of unactivated chloroarenes and Ru-catalysed hydrodeiodination/halogen exchange. Further changes to our existing catalytic system using coordinating group-functionalised Cp ligands can be made based on investigation into catalyst decomposition. A useful way to gain this insight is to first establish the timescale which catalytic turnover occurs, by monitoring product formation at the early stages (1-3 hours) of the catalysis, and also deciphering the possible catalyst deactivation pathways.

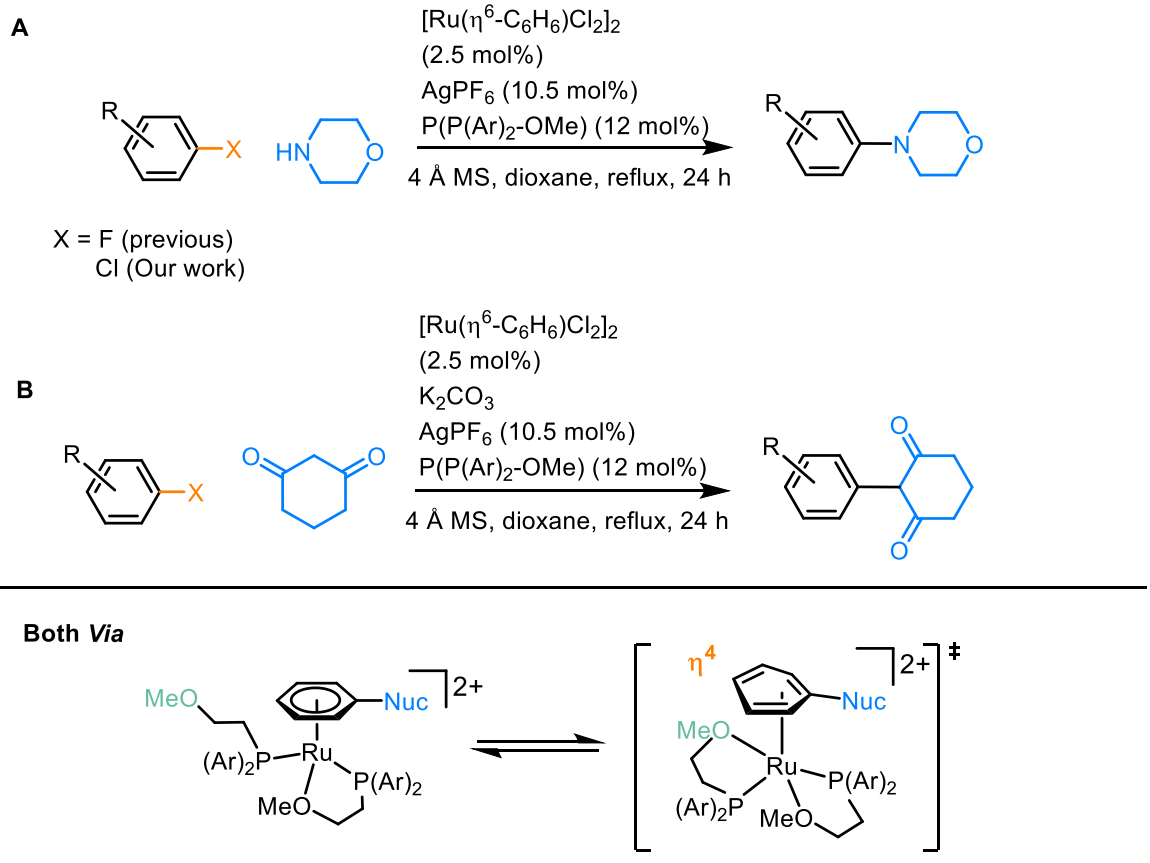

Figure 6.6. *Previous and proposed ruthenium-catalysed aromatic transformations. Both processes are proposed to occur via temporary coordination of a hemilabile group attached to the phosphine ligand of the active catalyst.*

Another potential area of exploration is the extension of the enolate S_NAr to linear 1,3-diones, which did not perform as well as cyclic diones. A likely reason for this is likely the partial displacement of the η^6-coordinated arene, as implied by the presence of free arene peaks in the crude enolate S_NAr reaction mixture in the reaction with $[acac]^-$. One possible solution to this problem is to hinder the approach to the Ru centre, by adding a functional group *para* to the leaving group, which should not affect approach to the C-X bond itself.

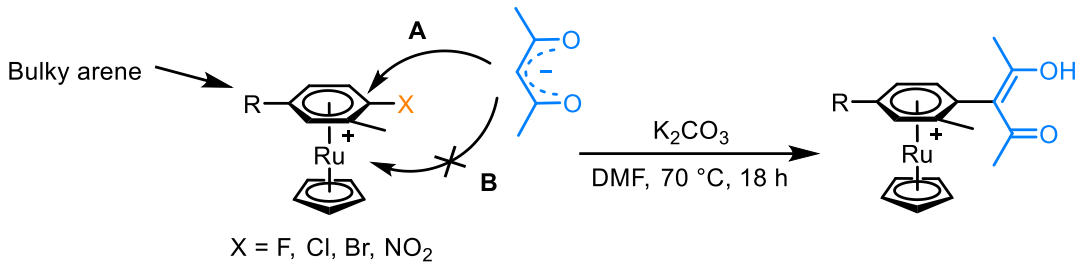

Figure 6.7. *Potential use of a bulky arene to block ligand substitution and hence promote on-ring S_NAr.*

A further extension of this procedure to other carbon-based nucleophiles, such as grignards or other carbanion sources such as NaCp. It has been established previously that some stronger nucleophiles tend to attack an η^6-coordinated ring *ortho* to the C-X (where X is a leaving group) bond resulting in the formation of a η^5-coordinated Meisenheimer intermediate as the 'kinetic' product.[2] In some instances, where the metal is ruthenium, a mixture of the Meisenheimer complex and S_NAr product form (figure 6.8A).[128] In thesis cases, it would be useful to be able to exert some degree of control on which of the two products forms (figure 6.8B), which could be done by adding or subtracting functional groups from the η^6-bound ring.

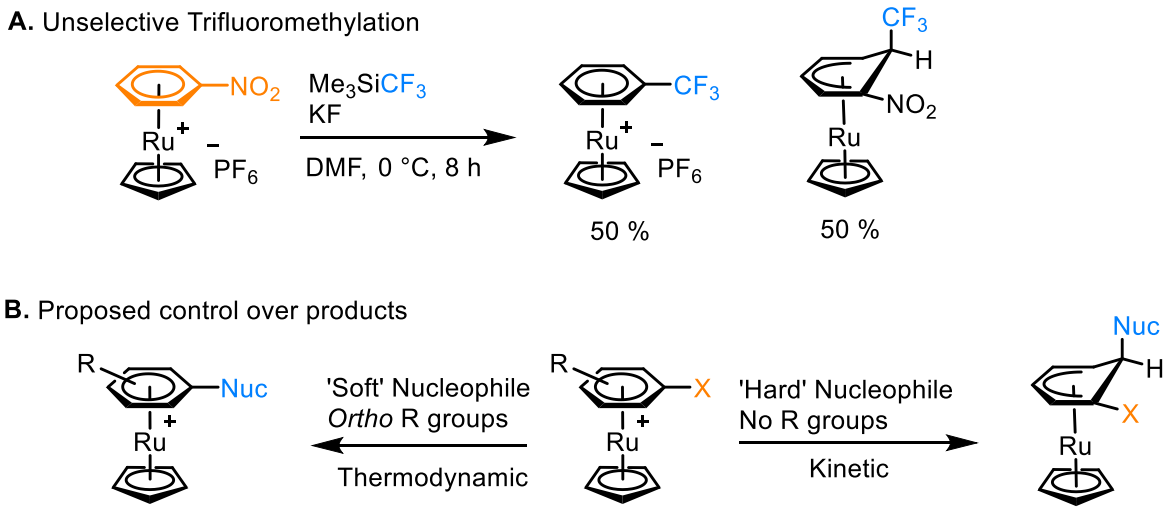

Figure 6.8. *Previous S_NAr trifluoromethylation, resulting in both S_NAr and Meisenheimer products, and a proposed method of controlling formation of such complexes*

Optimising the catalytic transformations of π-arene ruthenium complexes is an important target, as their potential applications and impact on synthetic methodology is clear. Achieving the fine balance between arene reactivity and ability to undergo rapid arene exchange is key to the progression of this field and its everyday applicability. A possible route forward is through

the development of photocatalytic protocols as, despite the experimental evidence that irradiation can be used to facilitate cleavage of the ruthenium η^6-arene bond, such chemistry is still at an early stage and is largely unexplored. It is feasible that such developments can be made as the fields of both theoretical and practical photochemistry advance over the next few years. Overall, the outlook of this field of organometallic chemistry is bright and several significant developments are anticipated over the next decade or two.

Chapter 7

Experimental Methodology

7.1. Experimental Methods

7.1.1. General Experimental Considerations

All chemicals were purchased from Sigma Aldrich and used without further purification unless stated otherwise. Solvents were degassed by purging with inert gas (Ar or N_2) and using freeze-pump-thaw techniques, and then dried over activated molecular sieves if necessary. Commercial reagents were used with no further purification. All air sensitive reactions were carried out using Schlenk apparatus.

NMR spectra (1H, 13C, 19F, 31P) were recorded on a Varian VXR-400 spectrometer (1H at 399.97 Hz, 13C at 100.57 MHz, 19F at 76.50 MHz), a Varian VNMRS-600 spectrometer (1H at 599.69 MHz, 13C at 150.34 MHz, 150.50 MHz). or a Varian VNMRS-700 spectrometer (1H at 699.73 MHz, 13C at 175.95 MHz, 31P at 150.50 MHz). Spectra were recorded at 295 K in commercially available deuterated solvents and referenced internally to the residual solvent proton resonances. The number of protons (n) for a given resonance signal is indicated by nH. The multiplicity of each signal is indicated by s (singlet); d (doublet); t (triplet); q (quartet); quin (quintet) or sept (septet). Coupling constants (*J*) are quoted in Hz and are recorded to the nearest 0.5 Hz. Identical proton coupling constants (*J*) are averaged in each spectrum and reported to the nearest 0.5 Hz. The coupling constants are determined by analysis using MestReNova software. Spectra were assigned using COSY, HSQC, HMBC and NOESY experiments as necessary. Accurate mass data (ESI-MS) were generated using a Waters QTOF spectrometer.

7.1.2. X-Ray Studies

The X-ray single crystal data have been collected by Dr. Dmitrii S. Yufit using λMoKα radiation (λ =0.71073 Å) on a Bruker D8Venture diffractometer (Photon100 CMOS detector, IμS-microsource, focusing mirrors, 1° ω-scan) equipped with a Cryostream (Oxford Cryosystems) open-flow nitrogen cryostats at the temperature 120.0(2)K. The structures were solved by direct method and refined by full-matrix least squares on F2 for all data using SHELXTL [G.M. Sheldrick, Acta Cryst. (2008), A64, 112-122] and OLEX2 [O. V. Dolomanov, L. J. Bourhis, R. J. Gildea, J. A. K. Howard, H. Puschmann, J. Appl. Cryst. (2009),

42, 339- 341.] software. All non-hydrogen atoms were refined anisotropically, the hydrogen atoms were placed in the calculated positions and refined in riding mode.

7.2. Synthetic Procedures

7.2.1. Chapter 2 – Fluorination and Difluoromethylation of π-Arene Ruthenium(II) Complexes

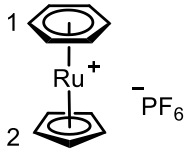

[Ru(η^6-benzene)(η^5-cyclopentadienyl)]PF_6 ***(2.9)***

Using a procedure adapted from literature,[52] to a flame-dried Schlenk flask charged with potassium carbonate (0.86 g, 6.0 mmol, 6 equiv.) and EtOH (30 mL) was added freshly cracked cyclopentadiene (1.5 mL, 18 mmol, 18 equiv.) and [(η^6-benzene)$RuCl_2$]$_2$ (0.5 g, 1 mmol, 1 equiv.). The mixture was stirred under an inert atmosphere at 80 °C for 24 h. The resulting suspension was filtered, and the filtrate concentrated *in vacuo* to ~10 mL. Next, a solution of NH_4PF_6 (0.68 g, 4.2 mmol, 4.2 equiv.) in H_2O (10 mL) was added dropwise to the EtOH solution, resulting in formation of a brown precipitate, which was isolated by filtration and washed with EtOH (5 mL). The crude brown solid was then dissolved in a minimum of MeCN (~0.5 mL), and the solution added dropwise to Et_2O (~5 mL). The resulting brown precipitate was filtered and washed with Et_2O (2 × 5 mL) to give the title compound as an off-white solid (0.35 g, 0.89 mmol, 89 %). Product identity and purity were verified by comparison to literature NMR/ESI-MS spectra.

^{1}H NMR (699 MHz, CD_3CN) δ 6.11 (6H, **s**, H^1), 5.37 (5H, **s**, H^2), $^{13}C\{^1H\}$ NMR (176 MHz, CD_3CN) δ 86.6 (s, C^1), 80.9 (s, C^2), ^{19}F NMR (Acetone-D_6) -72.5 (d, *J* 708 Hz, $F^{Counter\text{-}ion}$), ^{31}P (acetone-D6) δ -144.3 (sept., $J_{P\text{-}F}$ 707 Hz, $P^{Counter\text{-}ion}$), *m/z* (HRMS$^+$) 238.9956 $[M - PF_6]^+$ ($C_{11}H_{11}{}^{96}Ru$ requires 238.9937).

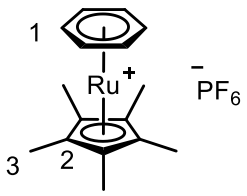

[Ru(η^6-benzene)(η^5-pentamethylcyclopentadienyl)]PF_6 ***(2.11)***

A solution of $RuCl_3 \cdot 3H_2O$ (110 mg, 0.42 mmol, 1 equiv.) in EtOH (5 mL) was heated to reflux at 80 °C for 45 mins. To the resulting dark brown solution was added benzene (65 mg, 75 µL, 0.77 mmol, 2 equiv.) and freshly cracked pentamethyl cyclopentadiene (0.1 g, 0.12 mL, 0.77 mmol, 2 equiv.) and the solution was further heated to reflux at 80 °C for 16 h, then allowed to cool to rt. Solvent was removed in *vacuo* to give a crude brown solid, then dichloromethane (5 mL) and H_2O (5 mL) were added and the layers separated. The organic layer was further extracted using H_2O (3 × 3 mL), and the aqueous layers were combined. A solution of NH_4PF_6 in H_2O (0.3 M) was added dropwise until a brown precipitate stopped forming. The dark brown solid was filtered then analysed by ^{1}H NMR and ESI-MS, but did not contain any peaks from the title compound. The yellow aqueous filtrate was concentrated to dryness in *vacuo*, and the resulting crude residue was washed with 1,2-DCE (3 × 5 mL) and the resulting suspension filtered to give a white solid and a pale yellow filtrate. The 1,2-DCE was removed from the filtrate in *vacuo*, then the resulting dark brown solid was dissolved in a minimum of MeCN (1 mL). The MeCN solution was added dropwise to Et_2O (5 mL) and the brown precipitate was filtered then washed with Et_2O (2 × 2 mL) and dried under vacuum to give the title compound as a dark brown solid (0.12 g, 0.31 mmol, 73 %). Product identity and purity were verified by comparison to literature NMR/ESI-MS spectra.

^{1}H NMR (700 MHz, CD_3CN) δ 5.79 (6H, s, H^1), 2.00 (15H, s, H^3), $^{13}C\{^1H\}$ NMR (176 MHz, CD_3CN) δ 97.3 (s, C^2), 87.7 (s, C^1), 10.5 (s, C^3), ^{19}F NMR (Acetone-D_6) -72.5 (d, *J* 708 Hz, $F^{Counter\text{-}ion}$), ^{31}P (acetone-D6) δ -144.3 (sept., $J_{P\text{-}F}$ 707 Hz, $P^{Counter\text{-}ion}$), *m/z* (ESI-HRMS$^+$) 309.0736 $[M - PF_6]^+$ ($C_{16}H_{21}{}^{96}Ru$ requires 309.0719).

Attempted Fluorination of Complex 2.9 – General Experimental

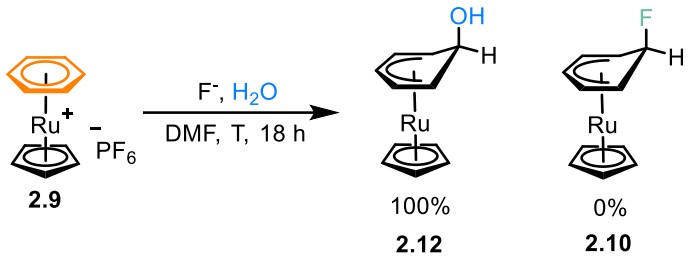

To a flame-dried Schlenk flask was added the fluoride source (5-50 equiv.) and either $[(\eta^6\text{-}C_6H_6)RuCp(*)][PF_6]$, then anhydrous DMF (1 mL). The flask was then sealed under inert atmosphere and mixture was stirred at 40-140 °C for 24 h. Aliquots were taken from the resulting suspension and analysed by ^1H, ^{19}F NMR (in acetone-D_6) and ESI-MS (in MeCN). If necessary, DMF was removed in *vacuo* and the resulting brown residue was analysed by ^1H, ^{19}F NMR (in acetone-D_6) and ESI-MS (in MeCN), then purification methods were attempted.

Attempted Fluorination of 2.9 with CsF

Experiment performed according to the general procedure, using CsF (200 mg, 1.3 mmol, 51 equiv.) dried overnight at 260 °C under vacuum, $[(\eta^6\text{-}C_6H_6)RuCp][PF_6]$ (10 mg, 0.026 mmol, 1 equiv.) or $[(\eta^6\text{-}C_6M_6)RuCp^*][PF_6]$ (10 mg, 0.025 mmol, 1 equiv.) and DMF (1 mL). Analysis of the reaction mixtures by NMR (^1H, ^{19}F) and ESI-MS showed no reaction had occurred.

Attempted Fluorination of 2.9 with NaF

Experiment performed according to the general procedure, using oven-dried NaF (60 mg, 1.25 mmol, 51 equiv.), $[(\eta^6\text{-}C_6H_6)RuCp][PF_6]$ **(**10 mg, 0.026 mmol, 1 equiv.) or complex **2.BF$_4$** (10 mg, 0.025 mmol, 1 equiv.), 15-crown-5 (27.5 mg, 25 µL, 0.125 mmol, 5 equiv.) and DMF (1 mL). Analysis of the reaction mixtures by NMR (^1H, ^{19}F) and ESI-MS showed no reaction had occurred.

Attempted Fluorination of 2.9 with KF

Experiment performed according to the general procedure, using oven-dried KF (73 mg, 1.25 mmol, 50 equiv.), [(η^6-C_6H_6)RuCp][PF_6] **(**10 mg, 0.026 mmol, 1 equiv.) or complex or [(η^6-C_6M_6)RuCp*][PF_6] (10 mg, 0.025 mmol, 1 equiv.), 18-crown-6 (27.5 mg, 25 μL, 0.125 mmol, 5 equiv.) and DMF (1 mL). Analysis of the reaction mixtures by NMR (^{1}H, ^{19}F) and ESI-MS showed no reaction had occurred.

Attempted Fluorination of 2.9 with TMAF

Experiment performed according to the general procedure, using TMAF (14 mg, 0.15 mmol, 5 equiv.), [(η^6-C_6H_6)RuCp][PF_6] **(**20 mg, 0.050 mmol, 1 equiv.) and anhydrous DMF (1 mL). Analysis of the reaction mixtures by NMR (^{1}H, ^{19}F) and ESI-MS showed no reaction had occurred.

Attempted Fluorination of 2.9 with AgF

Experiment performed according to the general procedure, using AgF (19 mg, 0.15 mmol, 5 equiv.), [(η^6-C_6H_6)RuCp][PF_6] **(**20 mg, 0.050 mmol, 1 equiv.), and DMF (1 mL). Analysis of the reaction mixtures by NMR (^{1}H, ^{19}F) and ESI-MS showed no reaction had occurred.

Attempted Fluorination of 2.9 with TBAF

Experiment performed according to the general procedure, using TBAF (0.5 mL 1M solution in THF, 0.5 mmol, 4 equiv.), [(η^6-C_6H_6)RuCp][PF_6] **(**50 mg, 0.125 mmol, 1 equiv.) and DMF (1 mL). Analysis of the reaction mixtures by NMR (^{1}H, ^{19}F) indicated a reaction, so solvent was removed in *vacuo* and re-analysed by NMR (^{1}H, ^{19}F) and ESI-MS.

Purification of the reaction product was also attempted using column chromatography (5 % MeOH in DCM), (10 % MeOH in DCM), (5 % EtOAc in Pet. Ether); analysis of each fraction by NMR (^{1}H, ^{19}F) and ESI-MS suggested decomposition of the product.

Negative (Cl^-) ion exchange chromatography was attempted. The resin was prepared by washing with boiling MeOH, 2M HCl, and distilled water. The crude material was eluted

through the ion-exchange resin using MeOH; analysis of each fraction by NMR (^{1}H, ^{19}F) and ESI-MS suggested decomposition of the product.

Attempted Oxidation of Meisenheimer Complex 2.11

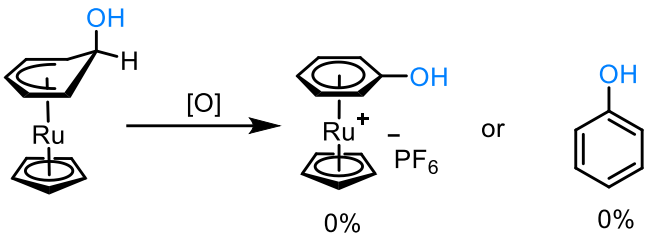

To a crude reaction mixture formed an experiment outlined in section 7.2.3.1., an oxidant (5 equiv.) was added and the resulting mixture was stirred at rt for 16 h. The resulting dark brown suspension was analysed by NMR (^{1}H and ^{19}F), and ESI-MS.

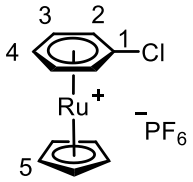

[Ru(η^{6}-chlorobenzene)(η^{5}-cyclopentadienyl)]PF_6 ***(2.14 & 3.1B)***

Tris(acetonitrile)cyclopentadienylruthenium(II) hexafluorophosphate (150 mg, 0.357 mmol, 1 eq.) was dissolved in anhydrous 1,2-DCE (8 mL). Chlorobenzene (45 µL, 0.40 mmol, 1.1 eq.) was added and the reaction was stirred at reflux under inert atmosphere overnight. The reaction mixture was cooled to room temperature, filtered and the filtrate dried in *vacuo* to give a brown solid. The crude product was dissolved in a minimum of acetonitrile, then added dropwise to diethyl ether (10 mL). The liquid phase was decanted off and the resulting solid dried to give the title compound as an off-white solid (146 mg, 344 mmol, 96%).

^{1}H NMR (599 MHz, acetone) δ 6.83 – 6.80 (2H, m, H^{2}), 6.49 (2H, dd, J = 6.4, 5.6 Hz, H^{3}), 6.37 (1H, td, J = 5.7, 0.7 Hz, H^{4}), 5.65 (5H, s, H^{5}), $^{13}C\{^{1}H\}$ NMR (151 MHz, acetone) δ 106.6 (s, C^{1}), 88.7 (s, C^{3}), 87.0 (s, C^{2}), 86.5 (s, C^{4}), 83.4 (s, C^{5}), ^{19}F NMR (376 MHz, Acetone) δ -72.4 (d, J = 707.8 Hz, $F^{Counter\text{-}ion}$), ^{31}P (acetone-D6) δ -144.3 (sept., $J_{P\text{-}F}$ 707 Hz, $P^{Counter\text{-}ion}$); *m/z* (ESI-HRMS, ESI-MS)$^{+}$ 272.9547 ($C_{10}H_{11}{}^{35}Cl^{96}Ru^{+}$ requires 272.9510).

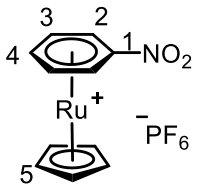

[Ru(η^6-nitrobenzene)(η^5-cyclopentadienyl)]PF_6 ***(2.15 & 3.1C)***

Tris(acetonitrile)cyclopentadienylruthenium(II) hexafluorophosphate (150 mg, 0.357 mmol, 1 eq.) was dissolved in anhydrous 1,2-DCE (8 mL). Nitrobenzene (41 µL, 0.40 mmol, 1.1 eq.) was added and the reaction was stirred at reflux under inert atmosphere overnight. The reaction mixture was cooled to room temperature, filtered and the filtrate dried in *vacuo* to give a brown solid. The crude product was dissolved in a minimum of acetonitrile, then added dropwise to diethyl ether (10 mL). The liquid phase was decanted off and the resulting solid dried to give the title compound as an off-white solid (135 mg, 0.310 mmol, 87%).

^{1}H NMR (599 MHz, acetone) δ 7.46 – 7.44 (2H, m, H^2), 6.79 (2H, dd, J = 6.7, 5.7 Hz, H^3), 6.71 (1H, t, J = 5.8 Hz, H^4), 5.77 (5H, s, H^5), ^{13}C{^{1}H} NMR (151 MHz, acetone) δ 111.4 (s, C^1), 88.5 (s, C^4), 86.4 (s, C^3), 83.7 (s, C^5), 82.9 (s, C^2), ^{19}F NMR (376 MHz, Acetone) δ -72.4 (d, J = 707.8 Hz, $F^{Counter\text{-}ion}$), ^{31}P (acetone-D6) δ -144.3 (sept., $J_{P\text{-}F}$ 707 Hz, $P^{Counter\text{-}ion}$); *m/z* (ESI-HRMS, ESI-MS)$^+$ 283.9788 ($C_{10}H_{11}NO_2{}^{96}Ru^+$ requires 283.9750).

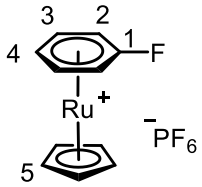

[Ru(η^6-fluorobenzene)(η^5-cyclopentadienyl)]PF_6 ***(2.16 & 3.1A)***

Tris(acetonitrile)cyclopentadienylruthenium(II) hexafluorophosphate (150 mg, 0.357 mmol, 1 eq.) was dissolved in anhydrous 1,2-DCE (8 mL). Fluorobenzene (38 µL, 0.41 mmol, 1.1 eq.) was added and the reaction was stirred at reflux under inert atmosphere overnight. The reaction mixture was cooled to room temperature, filtered and the filtrate dried in *vacuo* to give a brown solid. The crude product was dissolved in a minimum of acetonitrile, then added dropwise to diethyl ether (10 mL). The liquid phase was decanted and the resulting solid dried to give the title compound as an off-white solid (133 mg, 0.328 mmol, 92%).

^{1}H (599 MHz, acetone) δ 6.84 – 6.79 (2H, m, H^{2}), 6.46 (2H, tdd, *J* = 5.5, 2.8, 1.3 Hz, H^{3}), 6.26 (1H, td, *J* = 5.7, 3.7 Hz, H^{4}), 5.64 (5H, s, H^{5}) $^{13}C\{^{1}H\}$ (151 MHz, acetone) δ 137.8 (d, *J* = 275.3 Hz, C^{1}), 86.1 (s, C^{4}), 85.8 (d, *J* = 6.4 Hz, C^{3}), 82.5 (s, C^{5}), 78.4 (d, *J* = 21.2 Hz, C^{2}), ^{19}F NMR (376 MHz, Acetone) δ -72.4 (d, *J* = 707.9 Hz, $F^{Counter\text{-}ion}$), -137.60, ^{31}P (acetone-D6) δ -144.3 (sept., $J_{P\text{-}F}$ 707 Hz, $P^{Counter\text{-}ion}$); *m/z* (ESI-HRMS, ESI-MS)$^{+}$ 256.9843 ($C_{10}H_{11}F^{96}Ru^{+}$ requires 256.9842).

Attempted Fluorination of the Complexes [(η^{6}-C_6H_5X)RuCp][PF_6] (X = Cl, NO_2)

To a flame-dried Schlenk flask was added CsF (15-20 Equiv., dried at 260 ^{o}C under vacuum for 16 h), [(η^{6}-C_6H_5X)RuCp][PF_6] (1 equiv.) and anhydrous DMF (1 mL), then the resulting suspension was stirred at 60 ^{o}C for 24 h. The mixture was allowed to cool to room temperature, and the solvent was removed in *vacuo* leaving a solid brown residue. MeCN (2 mL) was added to the residue and the resulting suspension was filtered. The filtrate was concentrated to dryness in *vacuo* and the brown solid was dissolved in a minimum of MeCN (0.5 mL), and then added dropwise to Et_2O (3 mL). The resulting brown precipitate was filtered and washed with Et_2O (3 × 1 mL) to give a light brown solid, which was analysed by NMR and ESI-MS.

Attempted Fluorination of [(η^6-C_6H_5Cl)RuCp]PF_6 (2.14)

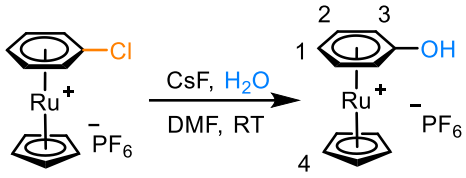

*[Ru(η^6-Phenol)(η^5-cyclopentadienyl)]PF_6 (**2.13**)*

Experiment performed following the general procedure using CsF (100 mg, 0.66 mmol, 20 equiv. dried at 260 °C under vacuum for 16 hours) and [(η^6-C_6H_5Cl)RuCp][PF_6] (15 mg, 0.031 mmol, 1 equiv.). The product complex was isolated as a light brown solid (9.0 mg, 0.022 mmol, 71 %).

^{1}H NMR (Acetone-D_6) δ 5.50 (2H, dd, $^3J_{H\text{-}H}$ 6.8 Hz, $^3J_{H\text{-}H}$ 5.2 Hz, H^2), 5.40 (H, t, $^3J_{H\text{-}H}$ 5.1 Hz, H^1), 4.99 (5H, s, H^4), 4.96 (2H, d, $^3J_{H\text{-}H}$ 6.2 Hz, H^3); ^{19}F NMR (Acetone-D_6) δ -72.5 (6F, d, *J* 707.8 Hz, PF_6); *m/z* (LRMS$^+$) 261.211 [M – PF_6]$^+$ ($C_{11}H_{10}NO_2{}^{96}Ru$ requires 260.985).

Attempted Fluorination of [(η^6-$C_6H_5NO_2$)RuCp]PF_6 (2.15)

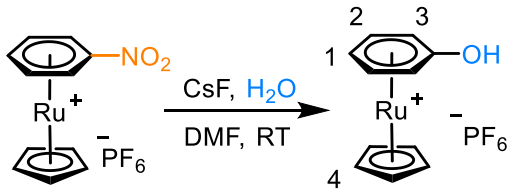

*[Ru(η^6-Phenol)(η^5-cyclopentadienyl)]PF_6 (**2.13**)*

Experiment performed following the general procedure using CsF (100 mg, 0.66 mmol, 20 equiv. dried at 260 °C under vacuum for 16 hours) and [(η^6-C_6H_5Cl)RuCp][PF_6] (15 mg, 0.031 mmol, 1 equiv.). The product complex was isolated as a dark brown solid (5.8 mg, 0.014 mmol, 46 %).

^{1}H NMR (Acetone-D_6) δ 5.50 (2H, dd, $^3J_{H\text{-}H}$ 6.8 Hz, $^3J_{H\text{-}H}$ 5.2 Hz, H^2), 5.39 (1H, m, H^1), 4.99 (5H, s, H^4), 4.96 (2H, m, H^3); ^{19}F NMR (Acetone-D_6) δ -72.5 (6F, d, *J* 707.8 Hz, PF_6); *m/z* (LRMS, ESI-MS$^+$) 261.211 [M – PF_6]$^+$ ($C_{11}H_{10}NO_2{}^{96}Ru$ requires 260.985).

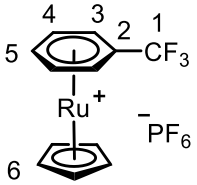

[Ru(η^6-α,α,α-trifluorotoluene)(η^5-cyclopentadienyl)]PF_6 ***(2.17)***

Tris(acetonitrile)cyclopentadienylruthenium(II) hexafluorophosphate (60 mg, 0.138 mmol) was dissolved in anhydrous 1,2-DCE (8 mL). α,α,α-trifluorotoluene (22 mg, 30 µL, 0.152 mmol) was added and the reaction was stirred at reflux under inert atmosphere overnight. The reaction mixture was cooled to room temperature, filtered and the filtrate dried in *vacuo* to give a brown solid. The crude product was dissolved in a minimum of acetonitrile, then added dropwise to diethyl ether (10 mL). The liquid phase was decanted off and the resulting solid dried to give the title compound as an off-white solid off-white solid (56 mg, 89%).

^{1}H NMR (599 MHz, acetone-D_6) δ 6.91 – 6.85 (2H, m, H^3), 6.67 (3H, dd, *J* = 3.8, 1.6 Hz, $H^{4\text{ and }5}$), 5.74 (5H, s, H^6), ^{13}C{^{1}H} NMR (151 MHz, acetone-D_6) δ 123.2 (q, $^1J_{C\text{-}F}$ 274 Hz, C^1), 91.8 (q, $^2J_{C\text{-}F}$ 38 Hz, C^2), 87.8 (s, C^5), 86.2 (s, C^4), 83.6 (q, *J* = 2.8 Hz, C^3), 82.6 (s, C^6), ^{19}F NMR (376 MHz, Acetone-D_6) δ -62.32 (s, CF_3) -72.5 (d, *J* = 707.7 Hz, $F^{Counter\text{-}ion}$), ^{31}P{^{1}H} NMR (acetone-D_6) δ -144.3 (sept., $J_{P\text{-}F}$ 707 Hz, $P^{Counter\text{-}ion}$); *m/z* (HRMS, ESI-MS)$^+$ $[M\text{-}PF_6]^+$ 306.9836 ($C_{12}H_{10}F_3{}^{96}Ru^+$ requires 306.9811).

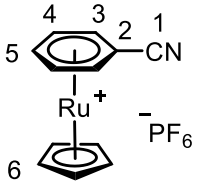

[Ru(η^6-benzonitrile)(η^5-cyclopentadienyl)]PF_6 ***(2.19)***

Tris(acetonitrile)cyclopentadienylruthenium(II) hexafluorophosphate (100 mg, 0.236 mmol, 1 eq.) was dissolved in anhydrous 1,2-DCE (8 mL). Benzonitrile (28 µL, 0.260 mmol, 1.1 eq.) was added and the reaction was stirred at reflux under inert atmosphere overnight. The reaction mixture was cooled to room temperature, filtered and the filtrate dried in *vacuo* to give a brown solid. The crude product was dissolved in a minimum of acetonitrile, then added dropwise to diethyl ether (10 mL). The liquid phase was decanted

off and the resulting solid dried to give the title compound as an off-white solid (84 mg, 0.201 mmol, 85 %).

^{1}H NMR (599 MHz, acetone-D_6) δ 6.93 – 6.90 (2H, m, H^3), 6.70 – 6.67 (2H, m, H^4), 6.66 – 6.60 (1H, m, H^5), 5.79 (5H, s, H^6), ^{13}C{^{1}H} NMR (151 MHz, acetone-D_6) δ 115.31 (s, C^1), 88.67 (s, C^3), 87.57 (s, C^5), 86.71 (s, C^4), 83.28 (s, C^6), 72.97 (s, C^2), ^{19}F NMR (376 MHz, Acetone-D_6) δ -72.54 (d, *J* = 707.7 Hz, $F^{Counter\text{-}ion}$), ^{31}P{^{1}H} NMR (acetone-D_6) δ -144.3 (sept., $J_{P\text{-}F}$ 707 Hz, $P^{Counter\text{-}ion}$); *m/z* (HRMS, ESI-MS)$^+$ $[M\text{-}PF_6]^+$ 263.9900 ($C_{12}H_{10}N^{96}Ru^+$ requires 263.9889).

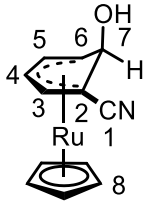

[Ru(η^5-1-hydroxy-2-cyanocyclohexadienyl)(η^5-cyclopentadienyl)] ***(2.22)***

To a Schlenk flask was added KO^{t}Bu (15 mg, 0.14 mmol, 3 eq.) and the solid was dried by heating under vacuum. Then, [CpRu(η^6-benzonitrile)][PF_6] (20 mg, 0.046 mmol, 1 eq.) and degassed N,N-DMF (2 mL) and the mixture was stirred for 24 hours at RT. The solvent was removed and the resulting brown residue washed with Et_2O (3 x 1 mL). The filtrate was dried in *vacuo* to give the title compound as a pale-yellow oil (10 mg, 76%).

^{1}H NMR (700 MHz, Acetone-D^6) δ 6.05 (1H, t, J 5.0 Hz, H^4), 5.33 (1H, d, J 5.1 Hz, H^4), 5.10 (5H, s, H^8), 5.01 (1H, t, J 6.3 Hz, H^5), 3.76 (1H, t, J 6.4 Hz, H^6), 3.69 (1H, d, J 6.2 Hz, H^7); ^{13}C{^{1}H} NMR (175 MHz, Acetone-D^6) δ 124.0 (s, C^1), 82.1 (s, C^4), 79.9 (s, C^5), 79.4 (s, C^3), 79.14 (s, C^2), 78.9 (s, C^8), 58.9 (s, C^7), 32.3 (s, C^6); *m/z* (HRMS, ESI-MS)$^+$ $[M+H]^+$ 286.9985 ($C_{12}H_{11}NO^{96}Ru$ requires 286.9995).

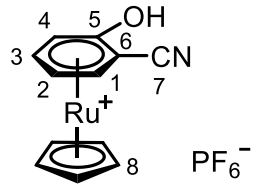

[Ru(η^6-2-hydroxybenzonitrile)(η^5-cyclopentadienyl)][PF_6]

Tris(acetonitrile)cyclopentadienylruthenium(II) hexafluorophosphate (20 mg, 0.046 mmol) was dissolved in anhydrous 1,2-DCE (3 mL). 2-hydroxybenzonitrile (6.0 mg, 0.051 mmol) was added and the reaction was stirred at reflux under inert atmosphere overnight. The reaction mixture was cooled to room temperature, filtered and the filtrate dried in *vacuo* to give a brown solid. The crude product was dissolved in a minimum of acetonitrile, then added dropwise to diethyl ether (10 mL). The liquid phase was decanted off and the resulting solid dried to give the title compound as a brown solid (19 mg, 0.044 mmol, 96 %).

^{1}H NMR (599 MHz, Acetone-D_6) δ 6.66 (1H, d, J = 5.0 Hz, H^1), 6.53 (1H, d, J = 6.3 Hz, H^4), 6.38 (1H, t, J = 6.1 Hz, H^3), 6.21 (1H, t, J = 5.2 Hz, H^2), 5.59 (5H, s, H^8); ^{13}C{^{1}H} NMR (101 MHz, Acetone-D_6) δ 119. (s, C^7), 116.2 (s, C^{Arene}), 115.5 (s, C^{Arene}), 86. (s, C^{Arene}), 86.1 (s, C^{Arene}), 80.9 (s, C^8), 80.8 (s, C^{Arene}), 73.8 (s, C^{Arene}).

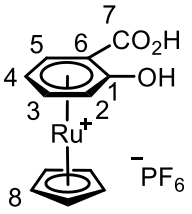

[Ru(η^6-salicylic acid)(η^5-cyclopentadienyl)][PF_6]

Tris(acetonitrile)cyclopentadienylruthenium(II) hexafluorophosphate (20 mg, 0.046 mmol) was dissolved in anhydrous 1,2-DCE (3 mL). Salicylic acid (7.0 mg, 0.051 mmol) was added and the reaction was stirred at reflux under inert atmosphere overnight. The reaction mixture was cooled to room temperature, filtered and the filtrate dried in *vacuo* to give a brown solid. The crude product was dissolved in a minimum of acetonitrile, then

added dropwise to diethyl ether (10 mL). The liquid phase was decanted off and the resulting solid dried to give the title compound as a brown solid (18 mg, 0.039 mmol, 88 %).

^{1}H NMR (599 MHz, acetone-D_6) δ 6.61 (1H, dd, *J* = 5.6, 1.1 Hz, H^5), 6.27 – 6.24 (1H, m, H^3), 6.20 (1H, d, *J* = 6.3 Hz, H^2), 6.06 (1H, t, *J* = 5.6 Hz, H^4), 5.38 (5H, s, H^8), ^{13}C{^{1}H} NMR (151 MHz, acetone-D_6) δ 170.6 (s, C^7), 141.2 (s, C^1), 86.3 (s, C^3), 83.8 (s, C^5), 81.6 (s, C^4), 80.2 (s, C^8), 75.2 (s, C^2), 74.8 (s, C^6), ^{19}F NMR δ -72.5 (d, *J* = 707.7 Hz, $F^{Counter-ion}$), ^{31}P{^{1}H} NMR (acetone-D6) δ -144.3 (sept., J_{P-F} 707 Hz, $P^{Counter-ion}$); *m/z* (HRMS, ESI-MS)$^{+}$ 299.1830 ($C_{12}H_{11}O_2{}^{96}Ru^{+}$ requires 299.1848).

7.2.2. Chapter 3 – Enolate S_NAr of Unactivated Arenes *via* π-Arene Ruthenium Complexes

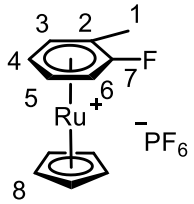

[Ru(η^6-2-fluorotoluene)(η^5-cyclopentadienyl)]PF_6 ***(3.2A)***

Tris(acetonitrile)cyclopentadienylruthenium(II) hexafluorophosphate (100 mg, 0.236 mmol, 1 eq.) was dissolved in anhydrous 1,2-DCE (8 mL). 2-Fluorotoluene (30 µL, 0.260 mmol, 1.1 eq.) was added and the reaction was stirred at reflux under inert atmosphere overnight. The reaction mixture was cooled to room temperature, filtered and the filtrate dried in *vacuo* to give a brown solid. The crude product was dissolved in a minimum of acetonitrile, then added dropwise to diethyl ether (10 mL). The liquid phase was decanted off and the resulting solid dried to give the title compound as an off-white solid (93.5 mg, 0.222 mmol, 94 %).

^{1}H NMR (599 MHz, acetone-D_6) δ 6.78 (1H, dd, *J* = 6.1, 4.2 Hz, H^6), 6.52 (1H, td, *J* = 4.4, 2.2 Hz, H^3), 6.34 (1H, tdd, *J* = 6.0, 2.5, 1.1 Hz, H^5), 6.19 (1H, td, *J* = 5.7, 3.1 Hz, H^4), 5.60 (5H, s, H^8), 2.50 (3H, d, *J* = 1.6 Hz, H^1), ^{13}C{^{1}H} NMR (151 MHz, acetone-D_6) δ 136.2 (d, *J* = 273.3 Hz, C^7), 93.8 (d, *J* = 17.3 Hz, C^2), 86.8 (d, *J* = 4.0 Hz, C^3), 84.5 (s, C^4), 84.0 (d,

J = 6.5 Hz, C^5), 81.7 (s, C^8), 76.6 (d, *J* = 22.6 Hz, C^6), 13.9 (d, *J* = 1.1 Hz, C^1), ^{19}F NMR (376 MHz, Acetone-D_6) δ -72.5 (d, *J* = 707.8 Hz, $F^{Counter\text{-}ion}$), -142.1 (F^{Arene}),), ^{31}P (acetone-D_6) δ -144.3 (sept., $J_{P\text{-}F}$ 707 Hz, $P^{Counter\text{-}ion}$); *m/z* (HRMS, ESI-MS)$^+$ 270.9995 ($C_{12}H_{12}F^{96}Ru^+$ requires 270.9962).

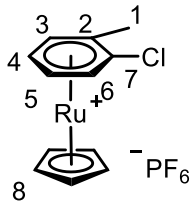

[Ru(η^6-2-chlorotoluene)(η^5-cyclopentadienyl)]PF_6 ***(3.2B)***

Tris(acetonitrile)cyclopentadienylruthenium(II) hexafluorophosphate (200 mg, 0.472 mmol, 1 eq.) was dissolved in anhydrous 1,2-DCE (8 mL). 2-chlorotoluene (62 µL, 0.524 mmol, 1.1 eq.) was added and the reaction was stirred at reflux under inert atmosphere overnight. The reaction mixture was cooled to room temperature, filtered and the filtrate dried in *vacuo* to give a brown solid. The crude product was dissolved in a minimum of acetonitrile, then added dropwise to diethyl ether (10 mL). The liquid phase was decanted off and the resulting solid dried to give the title compound as an off-white solid (200 mg, 0.458 mmol, 97 %).

^{1}H NMR (599 MHz, acetone-D_6) δ 6.84 – 6.74 (1H, m, H^6), 6.59 (1H, dd, *J* = 5.8, 1.0 Hz, H^3), 6.38 (1H, td, *J* = 5.8, 1.0 Hz, H^5), 6.29 (1H, td, *J* = 5.8, 0.7 Hz, H^4), 5.59 (5H, s, H^8), 2.60 (3H, s, H^1), ^{13}C{^{1}H} NMR (151 MHz, acetone) δ 106.7 (s, C^7), 102.2 (s, C^2), 87.5 (s, $C^{3/6}$), 87.3 (s, $C^{3/6}$), 85.3 (s, $C^{4/5}$), 85.2 (s, $C^{4/5}$), 82.5 (s, C^8), 18.5 (s, C^1), ^{19}F NMR (376 MHz, Acetone-D_6) δ -72.5 (d, *J* = 707.7 Hz, $F^{Counter\text{-}ion}$), ^{31}P (acetone-D_6) δ -144.3 (sept., $J_{P\text{-}F}$ 707 Hz, $P^{Counter\text{-}ion}$); *m/z* (HRMS, ESI-MS)$^+$ 286.9703 ($C_{12}H_{12}Cl^{96}Ru^+$ requires 286.9666).

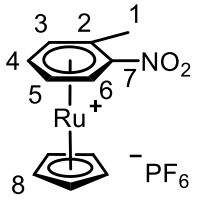

[Ru(η^6-2-nitrotoluene)(η^5-cyclopentadienyl)]PF_6 ***(3.2C)***

Tris(acetonitrile)cyclopentadienylruthenium(II) hexafluorophosphate (100 mg, 0.236 mmol, 1 eq.) was dissolved in anhydrous 1,2-DCE (8 mL). 2-Nitrotoluene (31 µL, 0.263 mmol, 1.1 eq.) was added and the reaction was stirred at reflux under inert atmosphere overnight. The reaction mixture was cooled to room temperature, filtered and the filtrate dried in *vacuo* to give a brown solid. The crude product was dissolved in a minimum of acetonitrile, then added dropwise to diethyl ether (10 mL). The liquid phase was decanted off and the resulting solid dried to give the title compound as an off-white solid (94 mg, 0.210 mmol, 89 %).

^{1}H NMR (599 MHz, acetone-D_6) δ 7.22 (1H, dd, *J* = 6.0, 0.7 Hz, H^6), 6.72 (1H, d, *J* = 5.9 Hz, H^3), 6.65 (1H, td, *J* = 6.0, 0.7 Hz, H^5), 6.56 (1H, td, *J* = 5.9, 0.7 Hz, H^4), 5.74 (5H, s, H^8), 2.70 (3H, s, H^1), ^{13}C{^{1}H} NMR (151 MHz, acetone-D_6) δ 110.5 (s, C^1), 99.3 (s, C^2), 89.2 (s, C^3), 88.6 (s, C^4), 86.2 (s, C^5), 85.0 (s, C^8), 84.2 (s, C^6), 18.8 (s, C^1), ^{19}F NMR (376 MHz, Acetone-D_6) δ -72.45 (d, *J* = 707.7 Hz, $F^{Counter\text{-}ion}$), ^{31}P (acetone-D_6) δ -144.3 (sept., $J_{P\text{-}F}$ 707 Hz, $P^{Counter\text{-}ion}$); *m/z* (HRMS, ESI-MS)$^+$ 297.9944 ($C_{12}H_{12}NO_2{}^{96}Ru^+$ requires 297.9907).

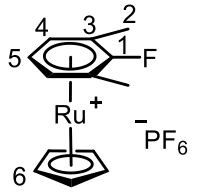

[Ru(η^6-2-fluoro-m-xylene)(η^5-cyclopentadienyl)]PF_6 ***(3.3A)***

Tris(acetonitrile)cyclopentadienylruthenium(II) hexafluorophosphate (100 mg, 0.236 mmol, 1 eq.) was dissolved in anhydrous 1,2-DCE (8 mL). 2-Fluoro-*m*-xylene (33 µL, 0.261 mmol, 1.1 eq.) was added and the reaction was stirred at reflux under inert atmosphere overnight. The reaction mixture was cooled to room temperature, filtered and the filtrate dried in *vacuo* to give a brown solid. The crude product was dissolved in a minimum of acetonitrile, then added dropwise to diethyl ether (10 mL). The liquid phase

was decanted off and the resulting solid dried to give the title compound as an off-white solid (95.6 mg, 0.219 mmol, 94 %)

^{1}H NMR (599 MHz, acetone-D_6) δ 6.37 (2H, dd, *J* = 5.6, 3.7 Hz, H^4), 6.09 (1H, td, *J* = 5.7, 2.5 Hz, H^5), 5.54 (5H, s, H^6), 2.49 (6H, d, *J* = 1.7 Hz, 6H, H^2), ^{13}C{^{1}H} NMR (151 MHz, acetone) δ 136.6 (d, *J* = 271.5 Hz, C^1), 93.8 (d, *J* = 18.6 Hz, C^3), 86.9 (d, *J* = 4.0 Hz, C^4), 84.5 (d, *J* = 4.0 Hz, C^5), 82.7 (s, C^6), 14.9 (d, *J* = 1.4 Hz, C^2), ^{19}F NMR (376 MHz, Acetone-D_6) δ -72.4 (d, *J* = 707.8 Hz, $F^{Counter\text{-}ion}$), -146.7 (1F, s, F^{Arene}), ^{31}P (acetone-D6) δ -144.3 (sept., $J_{P\text{-}F}$ 707 Hz, $P^{Counter\text{-}ion}$); *m/z* (HRMS, ESI-MS)$^+$ 285.0150 ($C_{13}H_{14}F^{96}Ru^+$ requires 285.0156).

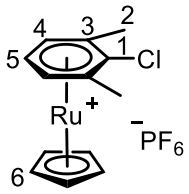

[Ru(η^6-2-chloro-m-xylene)(η^5-cyclopentadienyl)]PF_6 ***(3.3B)***

Tris(acetonitrile)cyclopentadienylruthenium(II) hexafluorophosphate (200 mg, 0.472 mmol, 1 eq.) was dissolved in anhydrous 1,2-DCE (8 mL). 2-Chloro-*m*-xylene (69 µL, 0.522 mmol, 1.1 eq.) was added and the reaction was stirred at reflux under inert atmosphere overnight. The reaction mixture was cooled to room temperature, filtered and the filtrate dried in *vacuo* to give a brown solid. The crude product was dissolved in a minimum of acetonitrile, then added dropwise to diethyl ether (10 mL). The liquid phase was decanted off and the resulting solid dried to give the title compound as an off-white solid (201 mg, 0.448 mmol, 95 %).

^{1}H NMR (599 MHz, acetone-D_6) δ 6.49 (2H, d, *J* = 5.7 Hz, H^4), 6.22 (1H, t, *J* = 5.8 Hz, H^5), 5.53 (5H, s, H^6), 2.61 (6H, s, H^2), ^{13}C{^{1}H} NMR (151 MHz, acetone-D_6) δ 109.3 (s, C^1), 102.6 (s, C^3), 87.8 (s, C^4), 85.3 (s, C^5), 83.6 (s, C^6), 20.3 (s, C^2), ^{19}F NMR (76 MHz, Acetone-D_6) δ -72.46 (d, *J* = 707.8 Hz, $F^{Counter\text{-}ion}$), ^{31}P (acetone-D_6) δ -144.3 (sept., $J_{P\text{-}F}$ 707 Hz, $P^{Counter\text{-}ion}$); *m/z* (HRMS, ESI-MS)$^+$ 300.9880 ($C_{13}H_{14}{}^{35}Cl^{96}Ru^+$ requires 300.9860).

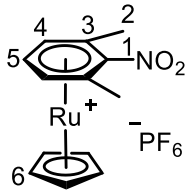

[Ru(η^6-2-nitro-m-xylene)(η^5-cyclopentadienyl)]PF_6 ***(3.3C)***

Tris(acetonitrile)cyclopentadienylruthenium(II) hexafluorophosphate (100 mg, 0.236 mmol, 1 eq.) was dissolved in anhydrous 1,2-DCE (8 mL). 2-Nitro-*m*-xylene (35 µL, 0.260 mmol, 1.1 eq.) was added and the reaction was stirred at reflux under inert atmosphere overnight. The reaction mixture was cooled to room temperature, filtered and the filtrate dried in *vacuo* to give a brown solid. The crude product was dissolved in a minimum of acetonitrile, then added dropwise to diethyl ether (10 mL). The liquid phase was decanted off and the resulting solid dried to give the title compound as an off-white solid (96 mg, 0.208 mmol, 88 %).

^{1}H NMR (599 MHz, acetone-D_6) δ 6.60 (2H, d, *J* = 5.9 Hz, H^4), 6.44 (1H, t, *J* = 5.9 Hz, H^5), 5.73 (5H, s, H^6), 2.53 (6H, s, H^2), ^{13}C{^{1}H} NMR (151 MHz, acetone) δ 111.4 (s, C^1) 96.1 (s, C^3), 86.2 (s, C^5), 85.9 (s, C^4), 84.1 (s, C^6), 16.0 (s, C^2), ^{19}F NMR (acetone-D_6) δ -71.4 (d, *J* = 707.8 Hz, $F^{Counter\text{-}ion}$), ^{31}P{^{1}H} NMR (acetone-D_6) δ -144.3 (sept., $J_{P\text{-}F}$ 707 Hz, $P^{Counter\text{-}ion}$); *m/z* (HRMS, ESI-MS)$^+$ 312.0126 $[M\text{-}PF_6]^+$ ($C_{13}H_{14}{}^{35}Cl^{96}Ru^+$ requires 312.0100).

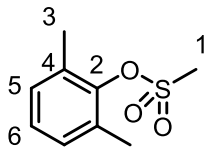

2,6-dimethylphenyl methanesulfonate

To an oven-dried, 2-neck round-bottom flask were added 2,6-dimethylphenol (200 mg, 1.64 mmol, 1 eq.), pyridine (329 µL, 4.09 mmol, 2.5 eq.) and anhydrous THF (5 mL), then the resulting solution was cooled to 0 °C and stirred for 5 minutes. Methanesulfonic anhydride (571 mg, 3.28 mmol, 2 eq.) was added, then the reaction was stirred for two hours, allowing it to warm to room temperature. Then, the mixture was evaporated to dryness under reduced pressure, and the resulting orange residue was dissolved in CH_2Cl_2 (30 mL), and washed with water (3 x 30 mL) before drying over $MgSO_4$. The resulting

suspension was filtered and the filtrate was concentrated to dryness under reduced pressure, giving the title compound as a pale red oil (315 mg, 1.57 mmol, 96%).

^{1}H NMR (400 MHz, $CDCl_3$) δ 7.09 (3H, s, $H^{5, 6}$), 3.28 (3H, s, H^{1}), 2.40 (6H, d, *J* = 0.8 Hz, H^{3}); *m/z* (HRMS, ESI-MS)$^{+}$ 201.0588 $[M+H]^{+}$ ($C_9H_{13}O_3S^{+}$ requires 201.0585).

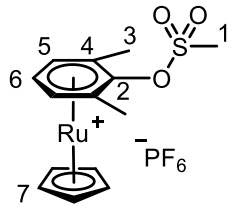

[Ru(η^{6}-2,6-dimethylphenyl methanesulfonate)(η^{5}-cyclopentadienyl)]PF_6 ***(3.3D)***

Tris(acetonitrile)cyclopentadienylruthenium(II) hexafluorophosphate (40 mg, 0.184 mmol, 1 eq.) was dissolved in anhydrous 1,2-DCE (8 mL). 2,6-dimethylphenyl methanesulfonate (41 mg, 202 mmol, 1.1 eq.) was added and the reaction was stirred at reflux under inert atmosphere overnight. The reaction mixture was cooled to room temperature, filtered and the filtrate dried in *vacuo* to give a brown solid. The crude product was dissolved in a minimum of acetonitrile, then added dropwise to diethyl ether (10 mL). The liquid phase was decanted off and the resulting solid dried to give the title compound as an off-white solid (75 mg, 0.146 mmol, 79 %).

^{1}H NMR (599 MHz, acetone-D_6) δ 6.45 (2H, d, *J* = 5.8 Hz, H^{5}), 6.24 (1H, t, *J* = 5.8 Hz, H^{6}), 5.55 (5H, s, H^{7}), 3.66 (3H, s, H^{1}), 2.57 (6H, s, H^{2}), ^{13}C{^{1}H} NMR (151 MHz, acetone-D_6) δ 121.5 (s, C^{2}), 98.8 (s, C^{4}), 86.8 (s, C^{5}), 84.8 (s, C^{6}), 82.4 (s, C^{7}), 39.3 (s, C^{1}), 16.9 (s, C^{3}), ^{19}F NMR δ -72.4 (d, *J* = 707.8 Hz, $F^{Counter\text{-}ion}$), ^{31}P{^{1}H} NMR (acetone-D6) δ -144.3 (sept., $J_{P\text{-}F}$ 707 Hz, $P^{Counter\text{-}ion}$); *m/z* (HRMS, ESI-MS)$^{+}$ 360.9986 $[M\text{-}PF_6]^{+}$ ($C_{14}H_{17}O_3S^{96}Ru^{+}$ requires 360.9974).

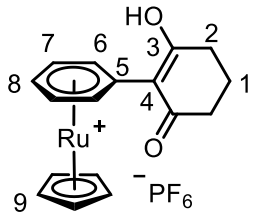

[Ru(η^6-6-hydroxy-4,5-dihydro-[1,1'-biphenyl]-2(3H)-one)(η^5-cyclopentadienyl)]PF_6 ***(3.4)***

Potassium carbonate (65.2 mg, 0.472 mmol, 2 eq.), 1,3-cyclohexanedione (29 mg, 0.260 mmol, 1.1 eq.), [CpRu(η^6-chlorobenzene)]PF_6 (**1b**, 100 mg, 0.235 mmol, 1 eq.) and anhydrous DMF were combined in an oven-dried Schlenk flask and stirred at 40 °C for 18 h. The reaction mixture was evaporated to dryness in *vacuo*, then the resulting brown residue was triturated with dichloromethane (3x5 mL) and filtered. The filtrate was dried under reduced pressure, then the brown solid was dissolved in a minimum of dichloromethane and the solution added dropwise to diethyl ether (5 mL). The solvents were decanted and the residue dried to give the title compound as a brown solid (95 mg, 0.191 mmol, 81%).

^{1}H NMR (599 MHz, Acetone-D_6) δ 7.03 (2H, dd, J = 7.0, 0.9 Hz, H^6), 6.04 – 5.87 (2H, m, H^7), 5.82 (1H, td, J = 5.5, 0.8 Hz, H^8), 5.19 (5H, s, H^9), 2.32 – 2.14 (4H, m, H^2), 1.88 – 1.63 (2H, m, H^1), ^{13}C{^{1}H} NMR (151 MHz, acetone-D_6) δ 190.7 (s, C^3), 109.0 (s, C^5), 102.1 (s, C^4), 85.5 (s, C^6), 83.7 (s, C^7), 81.0 (s, C^8), 78.5 (s, C^9), 38.3 (s, C^2), 20.9 (s, C^1), ^{19}F NMR δ -72.95 (d, J = 707 Hz, $F^{Counter\text{-}ion}$), ^{31}P (acetone-D6) δ -145.74 (sept., $J_{P\text{-}F}$ 707 Hz, $P^{Counter\text{-}ion}$); *m/z* (HRMS, ESI-MS)$^+$ 349.0302 [M-PF6] ($C_{17}H_{17}O_2{}^{96}Ru^+$ requires 349.0305).

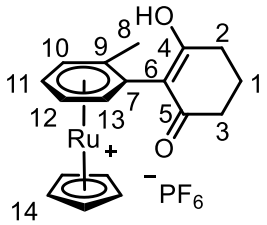

[Ru(η^6-2-(2-tolyl)cyclohexane-1,3-dione)(η^5-cyclopentadienyl)]PF_6 ***(3.6)***

Potassium carbonate (63.0 mg, 0.456 mmol, 2 eq.), 1,3-cyclohexanedione (29 mg, 0.260 mmol, 1.1 eq.), [CpRu(η^6-2-chlorotoluene)]PF_6 (**2b**, 100 mg, 0.228 mmol, 1 eq.) and anhydrous DMF were combined in an oven-dried Schlenk flask and stirred at 75 °C for 18

h. The reaction mixture was evaporated to dryness in *vacuo*, then the resulting brown residue was triturated with dichloromethane (3x5 mL) and filtered. The filtrate was dried under reduced pressure, then the brown solid was dissolved in a minimum of dichloromethane and the solution added dropwise to diethyl ether (5 mL). The solvents were decanted and the residue dried to give the title compound as a brown solid (80 mg, 0.156 mmol, 69%).

^{1}H NMR (599 MHz, CD_3OD) δ 6.10 (1H, d, *J* = 5.7 Hz, H^{10}), 6.00 – 5.94 (2H. m, $H^{12, 13}$), 5.92 (1H, td, *J* = 5.5, 1.2 Hz, H^{11}), 5.27 (5H, s, H^{14}), 2.49 – 2.33 (4H, m, $H^{2/3}$), 2.16 (3H, s, H^{8}), 1.97 (2H, p, *J* = 6.5 Hz, H^{1}), ^{13}C{^{1}H} NMR (151 MHz, CD_3OD) δ 193.2 (s, $C^{4/5}$), 191.8 (s, $C^{4/5}$), 105.9 (s, C^{6}), 105.5 (s, C^{7}), 102.5 (s, C^{9}), 88.8 (s, C^{13}), 86.1 (s, C^{10}), 82.9 (s, C^{12}), 82.3 (s, C^{11}), 79.7 (s, C^{14}), 36.4 (s, $C^{2/3}$), 35.8 (s, $C^{2/3}$), 20.8 (s, C^{1}), 18.9 (s, C^{8}), ^{19}F NMR δ -72.69 (d, *J* = 707 Hz, $F^{Counter\text{-}ion}$); *m/z* (HRMS, ESI-MS)$^{+}$ 363.0447 [M-PF6] ($C_{18}H_{19}O_2{}^{96}Ru^{+}$ requires 363.0461).

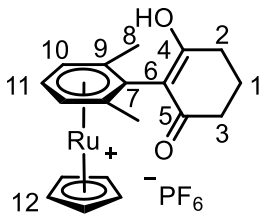

[Ru(η^{6}-2-(2-m-xylene)cyclohexane-1,3-dione)(η^{5}-cyclopentadienyl)]PF_6 ***(3.7)***

Potassium carbonate (63.0 mg, 0.456 mmol, 2 eq.), 1,3-cyclohexanedione (29 mg, 0.260 mmol, 1.1 eq.), [CpRu(η^{6}-2-chloro-1,3-dimethylbenzene)]PF_6 (**3b**, 100 mg, 0.220 mmol, 1 eq.) and anhydrous DMF were combined in an oven-dried Schlenk flask and stirred at 75 °C for 18 h. The reaction mixture was evaporated to dryness in *vacuo*, then the resulting brown residue was triturated with dichloromethane (3x5 mL) and filtered. The filtrate was dried under reduced pressure, then the brown solid was dissolved in a minimum of dichloromethane and the solution added dropwise to diethyl ether (5 mL). The solvents were decanted and the residue dried to give the title compound as an impure brown solid (77 mg).

^{1}H NMR (599 MHz, acetone-D_6) δ 5.93 (2H, d, *J* = 5.6 Hz, H^{10}), 5.81 (1H, t, *J* = 5.7 Hz, H^{11}), 5.23 (5H, s, H^{12}), 2.22 (4H, ddd, *J* = 24.9, 6.8, 5.8 Hz, $H^{2, 3}$), 2.09 (6H, s, H^{8}), 1.89 – 1.82 (2H, m, H^{1}), ^{13}C{^{1}H} NMR (151 MHz, acetone-D_6) δ 189.2 (s, $C^{4/5}$), 186.6 (s, $C^{4/5}$),

110.0 (s, C^{7}), 102.3 (s, C^{6}), 102.1 (s, C^{9}), 84.9 (s, C^{10}), 81.4 (s, C^{11}), 79.8 (s, C^{12}), 37.6 (s, $C^{2/3}$), 37.4 (s, $C^{2/3}$), 21.7 (s, C^{1}), 19.3 (s, C^{8}), ^{19}F NMR δ -72.5 (d, *J* = 707 Hz, $F^{Counter\text{-}ion}$), ^{31}P (acetone-D_6) δ -145.74 (sept., $J_{P\text{-}F}$ 707 Hz, $P^{Counter\text{-}ion}$); *m/z* (HRMS, ESI-MS)$^{+}$ 377.0621 [M-PF6] ($C_{19}H_{21}O_2{}^{96}Ru^{+}$ requires 377.0618).

Solvent, Base and Temperature Screening for the Ru-Mediated Enolate SNAr of Unactivated Arenes - General Experimental

To an oven dried Schlenk tube were added [Ru] (1 eq.), 1,3-cyclohexanedione (2 eq.), base (3 eq.) and anhydrous solvent (2 mL). The reaction mixture was heated to the desired temperature for 18 hours, then dried under reduced pressure to give a crude brown residue which was triturated with acetonitrile (3x5 mL), then filtered. The filtrate was dried in vacuum, and the resulting brown residue dissolved in d_6-acetone and analysed by ^{1}H NMR. Conversions were calculated by ^{1}H NMR spectroscopy. Mass spectrometry analysis was used to confirm the presence of any product(s) and/or starting material(s).

Table 7.1. *Solvent and temperature screening for the Ru-mediated enolate S_NAr of unactivated arenes*

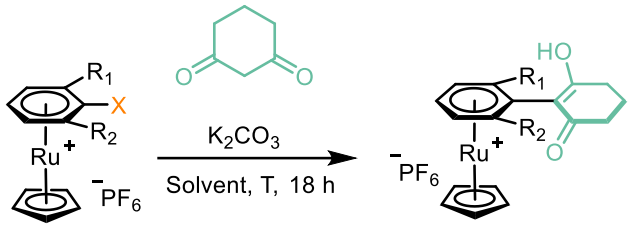

Entry	Starting Complex	Solvent	Temperature (°C)	Conversion (%)
1	**3.1a**	DMF	40	100
2	**3.1b**	DMF	40	100
3	**3.1b**	CH_2Cl_2	RT	100
4	**3.1c**	DMF	40	100
5	**3.1c**	DMF	0	100
6	**3.1c**	CH_2Cl_2	RT	100
7	**3.1c**	**THF**	**RT**	**100**
8	**3.1c**	1,4-dioxane	RT	25
9	**3.1c**	EtOH	RT	0
10	**3.1c**	MeCN	RT	100
11	**3.1c**	2-methyl THF	RT	50
12	**3.2a**	DMF	60	83
13	**3.2b**	**DMF**	**70**	**100**
14	**3.2b**	THF	65	76
15	**3.2c**	DMF	70	100
16	**3.3a**	DMF	80	60
17	**3.3b**	DMF	80	76
18	**3.3b**	**DMF**	**90**	**87**
19	**3.3b**	NMP	90	85
20	**3.3b**	DMF	120	67
21	**3.3b**	1,2-DCE	83	0
22	**3.3b**	1,4-Dioxane	90	0
23	**3.3b**	EtOH	78	0
24	**3.3b**	MeCN	82	17
25	**3.3b**	2-methyl THF	80	Trace
26	**3.3c**	DMF	90	60

General Experimental – Base screen

Base (0.068 mmol, 2 eq.), 1,3-cyclohexanedione (0.040 mmol, 1.1 eq.), [CpRu(η^6-2-chloro-1,3-dimethylbenzene)]PF_6 (10 mg, 0.024 mmol, 1 eq.) and anhydrous DMF were combined in an oven-dried Schlenk flask and stirred at 80 °C for 18 h. The reaction mixture was evaporated to dryness in *vacuo*, then the resulting brown residue was triturated with dichloromethane (3 x 5 mL) and filtered. The filtrate was dried under reduced pressure, then the brown solid was dissolved in a minimum of dichloromethane and the solution added dropwise to diethyl ether (5 mL). The solvents were decanted and the residue dried to give the complex. Values of conversion were calculated by comparison of the cyclopentadienyl peaks for the starting complex and product in ^{1}H NMR spectroscopy.

Table 7.2. *Base screening for the enolate S_NAr of Ru complex* ***3.6***

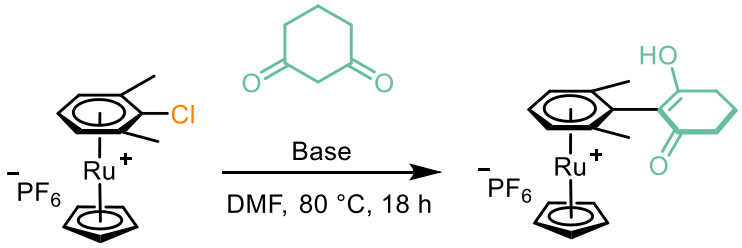

Entry	Base	Conversion
1	DBU	30*
2	Net_3	Trace
3	Pyridine	Trace
4	DIPEA	Trace
5	NaH	Trace
6	KO^{t}Bu	12
7	NaOH	40
8	$NaHCO_3$	36
9	$(NH_4)_2CO_3$	Trace
10	NaOMe	Trace
11	Na(2,4-di-tert-butylphenoxide)	Trace
12	K_2CO_3	67

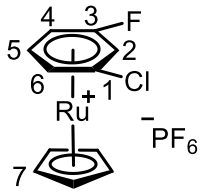

[Ru(η^6-1-Chloro-3-fluorobenzene)(η^5-cyclopentadienyl)]PF_6 ***(3.8)***

Tris(acetonitrile)cyclopentadienylruthenium(II) hexafluorophosphate (40 mg, 0.092 mmol, 1 eq.) was dissolved in anhydrous 1,2-DCE (8 mL). 1-Chloro-3-fluorobenzene (10 µL, 0.101 mmol, 1.1 eq.) was added and the reaction was stirred at reflux under inert atmosphere overnight. The reaction mixture was cooled to room temperature, filtered and the filtrate dried in *vacuo* to give a brown solid. The crude product was dissolved in a minimum of acetonitrile, then added dropwise to diethyl ether (10 mL). The liquid phase was decanted off and the resulting solid dried to give the title compound as a brown solid (40 mg, 0.82 mmol, 89 %).

^{1}H NMR (599 MHz, acetone-D_6) δ 7.47 – 7.36 (1H, m, H^2), 6.86 (1H, ddd, *J* = 6.1, 3.4, 1.5 Hz, H^4), 6.75 (1H, ddd, *J* = 5.9, 3.1, 1.1 Hz, H^6), 6.62 (1H, td, *J* = 6.0, 2.9 Hz, H^5), 5.77 (5H, s, H^7), ^{13}C{^{1}H} NMR (151 MHz, acetone-D_6) δ 137.0 (d, *J* = 279.1 Hz, C^3), 104.8 (d, *J* = 7.0 Hz, C^1), 87.9 (s, C^6), 85.1 (d, *J* = 6.5 Hz, C^5), 84.8 (s, C^7), 80.5 (d, *J* = 23.6 Hz, C^2), 78.2 (d, *J* = 21.4 Hz, C^4), ^{19}F NMR (376 MHz, Acetone-D_6) δ -72.5 (d, *J* = 707.6 Hz, $F^{Counter\text{-}ion}$), -138.07 (1F, s, F^{Arene}), ^{31}P (acetone-D_6) δ -144.3 (sept., $J_{P\text{-}F}$ 707 Hz, $P^{Counter\text{-}ion}$); *m/z* (HRMS, ESI-MS)$^+$ 290.9451 ($C_{11}H_9{}^{35}ClF^{96}Ru^+$ requires 290.9453).

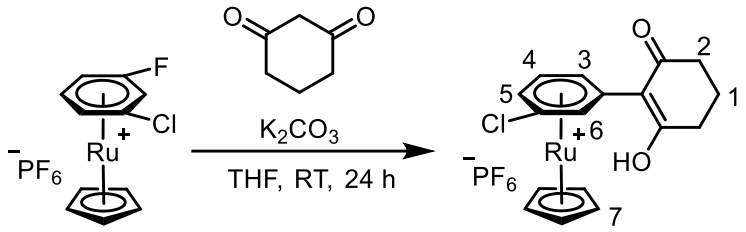

[Ru(η^6-3'-chloro-6-hydroxy-4,5-dihydro-[1,1'-biphenyl]-2(3H)-one)(η^5-cyclopentadienyl)]PF_6 ***(3.9)***

To a flame-dried Schlenk flask, **3.8** (20 mg, 0.045 mmol, 1 eq.), cyclohexanedione (5 mg, 0.045 mmol, 1 eq.) and K_2CO_3 (13 mg, 0.09 mmol, 2 eq.) were combined in anhydrous THF (3 mL). The mixture was stirred at RT for 24 hours, then the solvent was removed under reduced pressure. The crude brown residue was triturated with CH_2Cl_2 (3 x 3 mL) and concentrated to dryness under reduced pressure. Analysis of the brown residue by ^{1}H NMR spectroscopy and mass spectrometry indicated formation of complex **3.9** exclusively.

^{1}H NMR (400 MHz, Acetone-D_6) δ 7.45 (1H, s, H^6), 7.00 – 6.93 (1H, m, H^5), 6.38 (1H, dd, J = 5.8, 1.4 Hz, H^3), 6.17 (1H, t, J = 6.0 Hz, H^3), 5.34 (5H, s, H^7), 2.35 (4H, t, J = 6.0 Hz, H^2), 1.84 (2H, tt, J = 7.0, 5.9 Hz, H^1), ^{19}F NMR (376 MHz, Acetone-D_6) δ -72.51 (d, J = 707.6 Hz, $F^{Counter\text{-}ion}$); *m/z* (HRMS, ESI-MS)$^+$ 382.9924 $[M\text{-}PF_6]^+$ ($C_{17}H_{16}{}^{35}Cl^{96}Ru^+$ requires 382.9915).

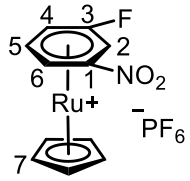

[Ru(η^6-1-fluoro-3-nitrobenzene)(η^5-cyclopentadienyl)]PF_6 ***(3.10)***

Tris(acetonitrile)cyclopentadienylruthenium(II) hexafluorophosphate (40 mg, 0.092 mmol, 1 eq.) was dissolved in anhydrous 1,2-DCE (8 mL). 1-fluoro-3-nitrobenzene (12 µL, 0.101 mmol, 1.1 eq.) was added and the reaction was stirred at reflux under inert atmosphere overnight. The reaction mixture was cooled to room temperature, filtered and the filtrate dried in *vacuo* to give a brown solid. The crude product was dissolved in a minimum of acetonitrile, then added dropwise to diethyl ether (10 mL). The liquid phase was decanted

off and the resulting solid dried to give the title compound as a brown solid (35 mg, 0.069 mmol, 75 %).

^{1}H NMR (599 MHz, acetone) δ 7.97 (1H, dt, *J* = 3.2, 1.3 Hz, H^{2}), 7.38 (1H, ddd, *J* = 6.1, 2.7, 1.2 Hz, H^{6}), 7.18 (1H, ddd, *J* = 6.2, 3.7, 1.5 Hz, H^{4}), 6.90 (1H, td, *J* = 6.2, 2.8 Hz, H^{5}), 5.90 (5H, s, H^{7}), ^{13}C{^{1}H} NMR (151 MHz, acetone) δ 135.8 (d, *J* = 280.5 Hz, C^{3}), 110.2 (s, C^{1}), 85.1 (s, C^{7}), 84.8 (d, *J* = 6.5 Hz, C^{5}), 82.2 (s, C^{6}), 80.1 (d, *J* = 21.5 Hz, C^{4}), 74.2 (d, *J* = 25.6 Hz, C^{2}), ^{19}F NMR (376 MHz, Acetone-D_6) δ -72.4 (d, *J* = 708 Hz, $F^{Counter\text{-}ion}$), -136.0 (1F, s, F^{Arene}), ^{31}P (acetone-D_6) δ -144.3 (sept., $J_{P\text{-}F}$ 708 Hz, $P^{Counter\text{-}ion}$); *m/z* (HRMS, ESI-MS)$^{+}$ 301.9701 ($C_{11}H_9NO_2F^{96}Ru^{+}$ requires 301.9693).

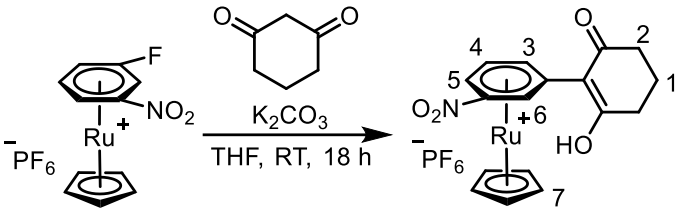

*[Ru(η^{6}-3'-nitro-6-hydroxy-4,5-dihydro-[1,1'-biphenyl]-2(3H)-one)(η^{5}-cyclopentadienyl)]PF_6 (**3.11**)*

To a flame-dried Schlenk flask, **3.10** (20 mg, 0.044 mmol, 1 eq.), cyclohexanedione (5 mg, 0.045 mmol, 1 eq.) and K_2CO_3 (13 mg, 0.09 mmol, 2 eq.) were combined in anhydrous THF (3 mL). The mixture was stirred at RT for 24 hours, then the solvent was removed under reduced pressure. The crude brown residue was triturated with CH_2Cl_2 (3 x 3 mL) and concentrated to dryness under reduced pressure. Analysis of the brown residue by ^{1}H NMR spectroscopy and mass spectrometry indicated formation of complex **3.16** exclusively.

^{1}H NMR (400 MHz, Acetone-D_6) δ 8.43 (1H, d, *J* = 1.2 Hz, H^{6}), 7.51 (1H, d, *J* = 6.4 Hz, H^{5}), 7.00 (1H, dd, *J* = 5.9, 1.6 Hz, H^{3}), 6.37 (1H, t, *J* = 6.2 Hz, H^{4}), 5.38 (5H, s, H^{7}), 2.36 – 2.22 (4H, m, H^{2}), 1.88 – 1.69 (2H, m, H^{1}), ^{19}F NMR (376 MHz, Acetone-D_6) δ -72.51 (d, *J* = 707.6 Hz, $F^{Counter\text{-}ion}$); *m/z* (HRMS, ESI-MS)$^{+}$ 400.0120 [M-PF_6]$^{+}$ ($C_{17}H_{16}{}^{35}NO_4{}^{96}Ru^{+}$ requires 400.0114).

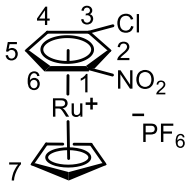

[Ru(η^6-1-chloro-3-nitrobenzene)(η^5-cyclopentadienyl)]PF_6 ***(3.12)***

Tris(acetonitrile)cyclopentadienylruthenium(II) hexafluorophosphate (40 mg, 0.092 mmol, 1 eq.) was dissolved in anhydrous 1,2-DCE (8 mL). 1-Chloro-3-nitrobenzene (12 µL, 0.101 mmol, 1.1 eq.) was added and the reaction was stirred at reflux under inert atmosphere overnight. The reaction mixture was cooled to room temperature, filtered and the filtrate dried in *vacuo* to give a brown solid. The crude product was dissolved in a minimum of acetonitrile, then added dropwise to diethyl ether (10 mL). The liquid phase was decanted off and the resulting solid dried to give the title compound as a brown solid (36 mg, 0.077 mmol, 83 %).

^{1}H NMR (599 MHz, acetone-D_6) δ 7.93 (1H, t, *J* = 1.2 Hz, H^2), 7.46 (1H, dd, *J* = 6.2, 1.3 Hz, H^6), 7.16 (1H, dd, *J* = 6.1, 1.2 Hz, H^4), 6.92 (1H, t, *J* = 6.2 Hz, H^5), 5.90 (5H, d, *J* = 1.0 Hz, H^7), ^{13}C{^{1}H} NMR (151 MHz, acetone-D_6) δ 110.9 (s, C^1), 105.5 (s, C^3), 90.1 (s, C^4), 86.2 (s, C^5), 85.8 (s, C^7), 83.8 (s, C^2), 82.5 (s, C^6), ^{19}F NMR (376 MHz, Acetone) δ -72.5 (d, *J* = 707.8 Hz, $F^{Counter\text{-}ion}$), ^{31}P (acetone-D_6) δ -144.3 (sept., $J_{P\text{-}F}$ 708 Hz, $P^{Counter\text{-}ion}$); *m/z* (HRMS, ESI-MS)$^+$ $[M\text{-}PF_6]^+$ 314.9413 ($C_{11}H_9{}^{35}ClNO_2{}^{96}Ru^+$ requires 317.9398).

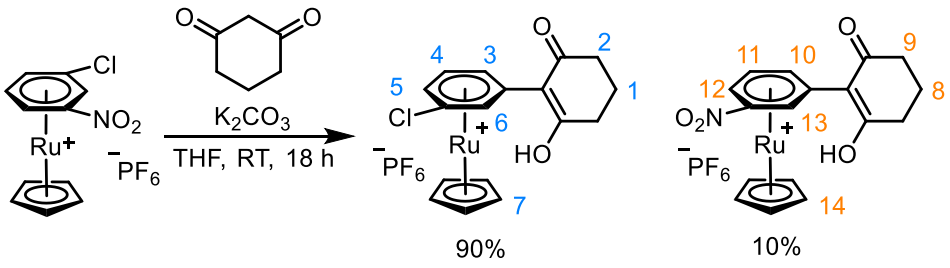

[Ru(η^6-3'-chloro-6-hydroxy-4,5-dihydro-[1,1'-biphenyl]-2(3H)-one)(η^5-cyclopentadienyl)]PF_6 ***(3.9)*** *and [Ru(η^6-3'-nitro-6-hydroxy-4,5-dihydro-[1,1'-biphenyl]-2(3H)-one)(η^5-cyclopentadienyl)]PF_6* ***(3.11)***

To a flame-dried Schlenk flask, **3.12** (20 mg, 0.043 mmol, 1 eq.), cyclohexanedione (5 mg, 0.045 mmol, 1 eq.) and K_2CO_3 (13 mg, 0.09 mmol, 2 eq.) were combined in anhydrous THF (3 mL). The mixture was stirred at RT for 24 hours, then the solvent was removed

under reduced pressure. The crude brown residue was triturated with CH_2Cl_2 (3 x 3 mL) and concentrated to dryness under reduced pressure. Analysis of the brown residue by ^1H NMR spectroscopy and mass spectrometry indicated formation of complexes **3.9** and **3.11** in a 9:1 ratio.

^1H NMR (400 MHz, Acetone-D_6) δ 8.43 (1H, s, H^{13}), 7.66 (1H, t, J = 1.2 Hz, H^6), 7.51 (1H, d, J = 6.4 Hz, H^{12}), 7.14 (1H, d, J = 6.3 Hz, H^5), 6.99 (1H, d, J = 6.1 Hz, H^{10}), 6.37 (1H, t, J = 6.2 Hz, H^{11}), 6.31 (1H, dd, J = 5.8, 1.5 Hz, H^3) 6.09 (1H, t, J = 6.0 Hz, H^4), 5.38 (5H, s, H^{14}), 5.28 (5H, s, H^7), 2.32 – 2.22 (8H, m, $H^{2, 9}$), 1.83 – 1.74 (4H, m, $H^{1, 8}$), ^{19}F NMR (376 MHz, Acetone-D_6) δ -72.51 (d, J = 707.6 Hz, $F^{Counter\text{-}ion}$); *m/z* (LRMS, ESI-MS)$^+$ 382.99 [**3.9**-PF_6]$^+$ ($C_{17}H_{16}{}^{35}Cl^{96}Ru^+$ requires 382.99) and 400.01 [**3.11**-PF_6]$^+$ ($C_{17}H_{16}{}^{35}NO_4{}^{96}Ru^+$ requires 400.01).

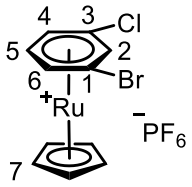

[Ru(η^6-1-bromo-3-chlorobenzene)(η^5-cyclopentadienyl)]PF_6 ***(3.13)***

Tris(acetonitrile)cyclopentadienylruthenium(II) hexafluorophosphate (60 mg, 0.138 mmol, 1 eq.) was dissolved in anhydrous 1,2-DCE (8 mL). 1-bromo-3-chlorobenzene (18 µL, 0.152 mmol, 1.1 eq.) was added and the reaction was stirred at reflux under inert atmosphere overnight. The reaction mixture was cooled to room temperature, filtered and the filtrate dried in *vacuo* to give a brown solid. The crude product was dissolved in a minimum of acetonitrile, then added dropwise to diethyl ether (10 mL). The liquid phase was decanted off and the resulting solid dried to give the title compound as a brown solid (57 mg, 0.124 mmol, 90 %).

^1H NMR (599 MHz, acetone-D_6) δ 7.39 (1H, t, J = 1.1 Hz, H^2), 6.86 (2H, app. ddd, J = 6.0, 2.5, 1.1 Hz, $H^{4, 6}$), 6.58 (1H, t, J = 5.9 Hz, H^5), 5.74 (5H, s, H^7), $^{13}C\{^1H\}$ NMR (151 MHz, acetone-D_6) δ 105.3 (s, C^3), 91.1 (s, C^2), 89.5 (s, $C^{4/6}$), 89.0 (s, C^1), 87.2 (s, $C^{4/6}$), 85.9 (s, C^5), 84.7 (s, C^7), ^{19}F NMR (376 MHz, Acetone-D_6) δ -72.50 (d, J = 707.8 Hz, $F^{Counter\text{-}ion}$), ^{31}P NMR (acetone-D_6) δ -144.3 (sept., $J_{P\text{-}F}$ 708 Hz, $P^{Counter\text{-}ion}$); *m/z* (HRMS, ESI-MS)$^+$ [M-PF_6]$^+$ 350.8658 ($C_{11}H_9{}^{35}Cl^{79}Br^{96}Ru^+$ requires 350.8652)

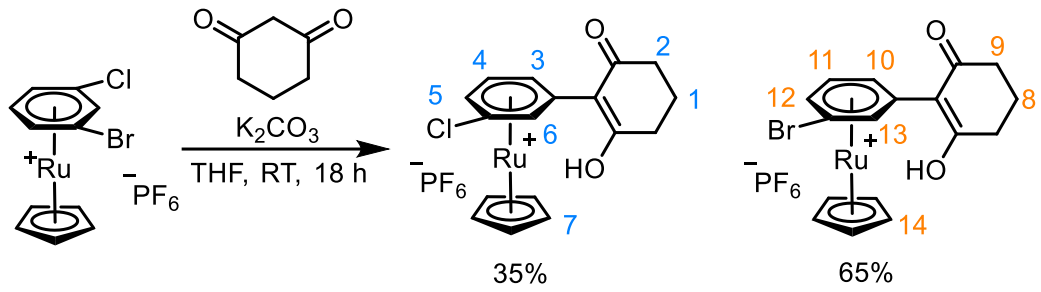

[Ru(η^6-3'-chloro-6-hydroxy-4,5-dihydro-[1,1'-biphenyl]-2(3H)-one)(η^5-cyclopentadienyl)]PF_6 ***(3.9)*** *and [Ru(η^6-3'-bromo-6-hydroxy-4,5-dihydro-[1,1'-biphenyl]-2(3H)-one)(η^5-cyclopentadienyl)]PF_6* ***(3.14)***

To a flame-dried Schlenk flask, **3.13** (20 mg, 0.040 mmol, 1 eq.), cyclohexanedione (4.5 mg, 0.040 mmol, 1 eq.) and K_2CO_3 (12 mg, 0.08 mmol, 2 eq.) were combined in anhydrous THF (3 mL). The mixture was stirred at RT for 24 hours, then the solvent was removed under reduced pressure. The crude brown residue was triturated with CH_2Cl_2 (3 x 3 mL) and concentrated to dryness under reduced pressure. Analysis of the brown residue by ^{1}H NMR spectroscopy and mass spectrometry indicated formation of complexes **3.9** and **3.14** in a 1:2 ratio.

^{1}H NMR (400 MHz, Acetone-D_6) δ 7.75 (1H, s, H^{13}), 7.71 (1H, s, H^6), 7.18 (2H, t, J = 7.0 Hz, $H^{5,\ 12}$), 6.40 – 6.31 (1H, m, H^{10}), 6.31 – 6.27 (1H, m, H^3), 6.10-6.05 (2H, m, $H^{4,\ 11}$), 5.29-5.26 (10H, m, $H^{7,\ 14}$), 2.33 – 2.21 (8H, m, $H^{2,\ 9}$), 1.79 (4H, p, J = 6.5 Hz, $H^{1,\ 8}$), ^{19}F NMR (376 MHz, Acetone-D_6) δ -72.51 (d, J = 707.6 Hz, $F^{Counter\text{-}ion}$); *m/z* (LRMS, ESI-MS)$^+$ 382.99 [**3.9**-PF_6]$^+$ ($C_{17}H_{16}{}^{35}Cl^{96}Ru^+$ requires 382.99) and 429.01 [**3.14**-PF_6]$^+$ ($C_{17}H_{16}{}^{35}O_2{}^{81}Br^{96}Ru^+$ requires 429.02).

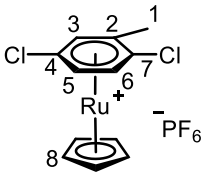

[Ru(η^6-2,5-dichlorotoluene)(η^5-cyclopentadienyl)]PF_6 ***(3.15)***

Tris(acetonitrile)cyclopentadienylruthenium(II) hexafluorophosphate (100 mg, 0.236 mmol, 1 eq.) was dissolved in anhydrous 1,2-DCE (8 mL). 2,5-dichlorotoluene (35 µL, 0.260 mmol, 1.1 eq.) was added and the reaction was stirred at reflux under inert atmosphere overnight. The reaction mixture was cooled to room temperature, filtered and

the filtrate dried in *vacuo* to give a brown solid. The crude product was dissolved in a minimum of acetonitrile, then added dropwise to diethyl ether (10 mL). The liquid phase was decanted off and the resulting solid dried to give the title compound as a brown solid (95 mg, 0.210 mmol, 88 %).

^{1}H NMR (599 MHz, acetone-D_6) δ 7.34 (1H, d, *J* = 1.3 Hz, H^3), 6.77 (1H, dd, *J* = 6.0, 1.3 Hz, H^5), 6.71 (1H, d, *J* = 6.0 Hz, H^6), 5.70 (5H, s, H^8), 2.56 (3H, s, H^1), ^{13}C{^{1}H} NMR (151 MHz, acetone-D_6) δ 106.9 (s, C^7), 105.0 (s, C^4), 103.0 (s, C^2), 89.3 (s, C^3), 87.8 (s, $C^{5/6}$), 87.8 (s, $C^{5/6}$), 85.5 (s, C^8), 18.9 (s, C^1), ^{19}F NMR δ -72.5 (d, *J* = 707.7 Hz, $F^{Counter\text{-}ion}$), ^{31}P (acetone-D_6) δ -144.3 (sept., $J_{P\text{-}F}$ 707 Hz, $P^{Counter\text{-}ion}$); *m/z* (HRMS, ESI-MS)$^+$ 320.9318 ($C_{12}H_{11}{}^{35}Cl_2{}^{96}Ru^+$ requires 320.9314).

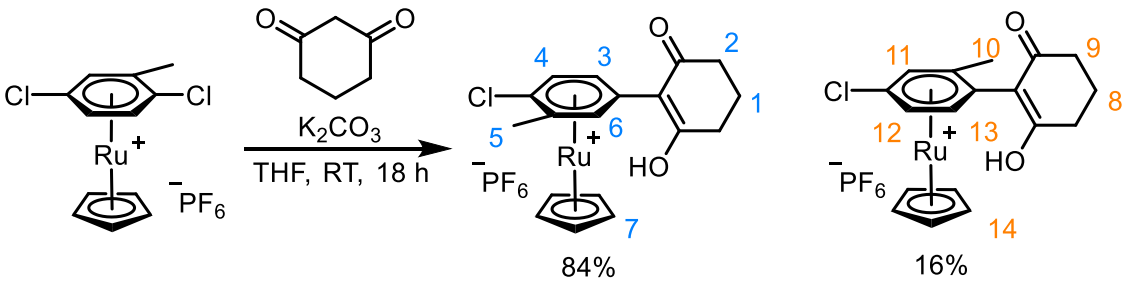

[Ru(η^6-4'-chloro-6-hydroxy-3'-methyl-4,5-dihydro-[1,1'-biphenyl]-2(3H)-one)(η^5-cyclopentadienyl)]PF_6 ***(3.16)*** *and [Ru(η^6-4'-chloro-6-hydroxy-2'-methyl-4,5-dihydro-[1,1'-biphenyl]-2(3H)-one)(η^5-cyclopentadienyl)]PF_6* ***(3.17)***

To a flame-dried Schlenk flask, **3.15** (20 mg, 0.042 mmol, 1 eq.), cyclohexanedione (5 mg, 0.045 mmol, 1 eq.) and K_2CO_3 (13 mg, 0.09 mmol, 2 eq.) were combined in anhydrous DMF (3 mL). The mixture was stirred at 75 °C for 24 hours, then the solvent was removed under reduced pressure. The crude brown residue was triturated with CH_2Cl_2 (3 x 3 mL) and concentrated to dryness under reduced pressure. Analysis of the brown residue by ^{1}H NMR spectroscopy and mass spectrometry indicated formation of complexes **3.16** and **3.17** in a ratio of 5.25:1, respectively.

^{1}H NMR (400 MHz, Acetone-D_6) δ 7.65 (1H, s, *J* = 1.2 Hz, H^6), 7.06 (1H, dt, *J* = 6.3, 0.9 Hz, H^3), 6.52 (1H, d, *J* = 1.5 Hz, H^{11}), 6.35 (1H, dd, *J* = 5.9, 0.6 Hz, H^{12}), 6.19-6.17 (2H, m, $H^{4,\ 13}$), 5.35 (5H, s, H^{14}), 5.21 (5H, s, H^7), 2.44 (3H, s, H^5), 2.25 (4H, t, *J* = 6.4 Hz, H^2), 2.17 (4H, t, *J* = 6.4 Hz, H^9), 2.09 (3H, s, H^{10}), 1.77-1.75 (4H, m, $H^{1,\ 8}$), ^{19}F NMR (376

MHz, Acetone-D_6) δ -72.51 (d, *J* = 707.6 Hz, $F^{Counter\text{-}ion}$); *m/z* (LRMS, ESI-MS)$^+$ 397.20 [**3.16**-PF_6]$^+$ and [**3.17**-PF_6]$^+$ ($C_{18}H_{18}{}^{35}ClO_2{}^{96}Ru^+$ requires 397.20).

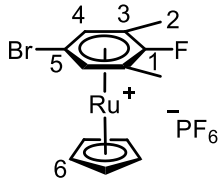

[Ru(η^6-5-bromo-2-fluoro-1,3-dimethylbenzene)(η^5-cyclopentadienyl)]PF_6 ***(3.18)***

Tris(acetonitrile)cyclopentadienylruthenium(II) hexafluorophosphate (100 mg, 0.236 mmol, 1 eq.) was dissolved in anhydrous 1,2-DCE (8 mL). 5-bromo-2-fluoro-1,3-dimethylbenzene (50 µL, 0.253 mmol, 1.1 eq.) was added and the reaction was stirred at reflux under inert atmosphere overnight. The reaction mixture was cooled to room temperature, filtered and the filtrate dried in *vacuo* to give a brown solid. The crude product was dissolved in a minimum of acetonitrile, then added dropwise to diethyl ether (10 mL). The liquid phase was decanted off and the resulting solid dried to give the title compound as a brown solid (109 mg, 0.212 mmol, 90 %).

^{1}H NMR (599 MHz, Acetone-D_6) δ 6.91 (2H, d, *J* = 3.0 Hz, H^4), 5.65 (5H, s, H^6), 2.53 (6H, d, *J* = 1.8 Hz, H^2), ^{13}C NMR (151 MHz, Acetone-D_6) δ 134.7 (d, *J* = 272.4 Hz, C^1), 93.4 (d, *J* = 20.1 Hz, C^2), 90.1 (s, C^5), 89.7 (d, *J* = 4.3 Hz, C^4), 84.1 (, 13.9 (d, *J* = 1.2 Hz, C^2), ^{19}F NMR (376 MHz, Acetone-D_6) δ -72.41 (d, *J* = 707.8 Hz, $F^{Counter\text{-}ion}$), -147.26 (s, F^{Arene}), ^{31}P (acetone-D_6) δ -144.3 (sept., $J_{P\text{-}F}$ 707 Hz, $P^{Counter\text{-}ion}$); *m/z* (HRMS, ESI-MS)$^+$ [M-PF_6]$^+$ 362.9268 ($C_{13}H_{13}{}^{79}BrF^{96}Ru^+$ requires 362.9261).

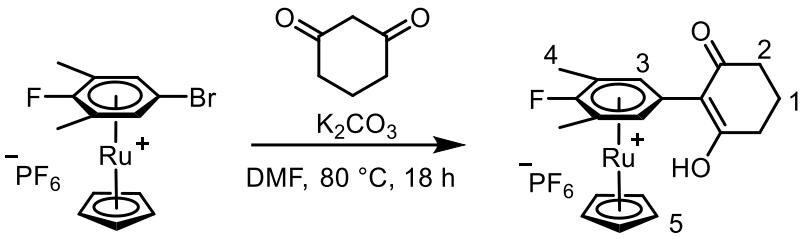

[Ru(η^6-4'-fluoro-6-hydroxy-3',5'-dimethyl-4,5-dihydro-[1,1'-biphenyl]-2(3H)-one)(η^5-cyclopentadienyl)]PF_6 ***(3.19)***

To a flame-dried Schlenk flask, **3.18** (20 mg, 0.039 mmol, 1 eq.), cyclohexanedione (4 mg, 0.040 mmol, 1 eq.) and K_2CO_3 (12 mg, 0.08 mmol, 2 eq.) were combined in anhydrous DMF (3 mL). The mixture was stirred at 80 °C for 24 hours, then the solvent was removed under reduced pressure. The crude brown residue was triturated with CH_2Cl_2 (3 x 3 mL) and concentrated to dryness under reduced pressure. Analysis of the brown residue by ^{1}H NMR spectroscopy and mass spectrometry indicated formation of complex **3.19** exclusively.

^{1}H NMR (400 MHz, Acetone-D_6) δ 7.03 (2H, d, $J_{H\text{-}F}$ = 4.0 Hz, H^3), 5.17 (5H, s, H^5), 2.38 (3H, d, $J_{H\text{-}F}$ = 1.7 Hz, H^4) 2.30 – 2.19 (4H, m, H^2), 1.76 (2H, tt, J = 7.2, 5.7 Hz, H^1), ^{19}F NMR (376 MHz, Acetone-D_6) δ -72.41 (d, J = 707.8 Hz, $F^{Counter\text{-}ion}$), -147.26 (s, F^{Arene}), ^{31}P (acetone-D_6) δ -155.1 (sept., $J_{P\text{-}F}$ 707 Hz, $P^{Counter\text{-}ion}$); *m/z* (LRMS, ESI-MS)$^+$ [M-PF_6]$^+$ 395.20 ($C_{19}H_{20}FO_2{}^{96}Ru^+$ requires 395.20).

Dione Scope for Enolate S_NAr - General Experimental

Potassium carbonate (9.5 mg, 0.068 mmol, 2 eq.), dione (0.040 mmol, 1.1 eq.), [CpRu(η^6-2-chlorotoluene)]PF_6 (**2b**, 15 mg, 0.034 mmol, 1 eq.) and anhydrous DMF were combined in an oven-dried Schlenk flask and stirred at 75 °C for 18 h. The reaction mixture was evaporated to dryness in *vacuo*, then the resulting brown residue was triturated with dichloromethane (3x5 mL) and filtered. The filtrate was dried under reduced pressure, then the brown solid was dissolved in a minimum of dichloromethane and the solution added dropwise to diethyl ether (5 mL). The solvents were decanted and the residue dried to give the complex as a brown/yellow solid.

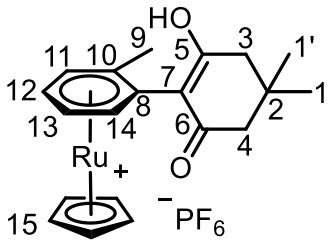

[Ru(η^6-2-(2-tolyl)(5,5'-dimethyl)cyclopentane-1,3-dione)(η^5-cyclopentadienyl)]PF_6 ***(3.20)***

Synthesised via general experimental 2, using 5,5'-dimethylcyclohexane1,3-dione (5.4 mg, 0.038 mmol, 1.1 eq.). The title compound was isolated as a brown solid (11.3 mg, 0.021 mmol, 61 %).

^{1}H NMR (599 MHz, CD_3OD) δ 6.10 (1H, d, *J* = 5.6 Hz, H^{11}), 5.98 – 5.95 (1H, m, H^{13}), 5.94 – 5.92 (1H, m, H^{14}), 5.91 (1H, td, *J* = 5.6, 1.0 Hz, H^{12}), 5.26 (5H, s, H^{15}), 2.29 (4H, s, $H^{3,\ 4}$), 2.15 (3H, s, H^9), 1.12 (3H, s, H^1), 1.09 (3H, s, $H^{1'}$), $^{13}C\{^1H\}$ NMR (151 MHz, CD_3OD) δ 193.4 (s, $C^{5/6}$), 192.2 (s, $C^{5/6}$), 106.9 (s, C^8), 106.2 (s, C^7), 103.9 (s, C^{10}), 90.3 (s, C^{14}), 87.6 (s, C^{11}), 84.3 (s, C^{13}), 83.7 (s, C^{12}), 81.1 (s, C^{15}), 51.7 (s, $C^{3/4}$), 51.1 (s, $C^{3/4}$), 32.2 (s, C^2), 29.3 (s, $C^{1/1'}$), 28.5 (s, $C^{1/1'}$), 20.5 (s, C^9), ^{31}P NMR (243 MHz, CD_3OD) δ -132.06 – -156.07 (m, $p^{Counter\text{-}ion}$), ^{19}F NMR δ -72.58 (d, *J* = 707 Hz, $F^{Counter\text{-}ion}$); *m/z* (HRMS, ESI-MS)$^+$ 391.0772 [M-PF6] ($C_{20}H_{23}O_2{}^{96}Ru^+$ requires 391.0774).

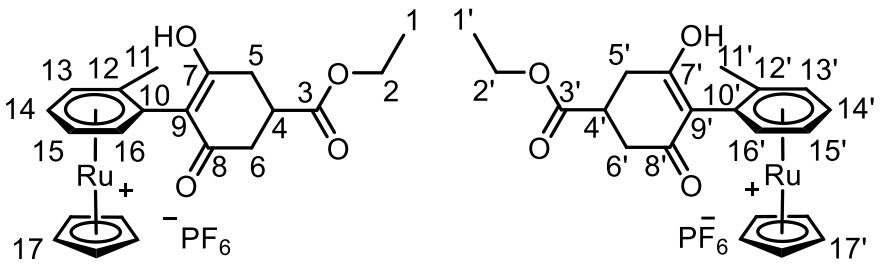

*[Ru(η^6-2-(2-tolyl)(5-ethylacetyl)cyclopentane-1,3-dione)(η^5-cyclopentadienyl)]PF_6 (1:1 mixture of diastereomers) (**3.21**)*

Synthesised via general experimental 2, using 5-(ethylacetyl)cyclohexane1,3-dione (7.1 mg, 0.038 mmol, 1.1 eq.). The title compound was isolated as an impure brown solid (12.5 mg, 0.022 mmol, 63 %).

^{1}H NMR (599 MHz, CD_3OD) δ 6.07 (1H, dd, *J* = 8.7, 5.7 Hz, $H^{13/13'}$), 5.97 – 5.86 (3H, m, $H^{14/14', 15/15', 16/16'}$), 5.23 (5H, d, *J* = 8.5 Hz, $H^{17/17'}$), 4.14 (2H, dq, *J* = 14.1, 7.1 Hz, $H^{2/2'}$), 3.09 – 3.03 (1H, m, $H^{5/5' \text{ or } 6/6'}$), 2.78 – 2.68 (1H, m, $H^{5/5' \text{ or } 6/6'}$), 2.63 – 2.54 (3H, m, $H^{4/4', 5/5', 6/6'}$), 2.10 (3H, d, *J* = 34.2 Hz, $H^{11/11'}$), 1.25 (3H, dt, *J* = 10.5, 7.1 Hz, $H^{1/1'}$), $^{13}C\{^1H\}$ NMR (151 MHz, CD_3OD) δ 190.4 (s, $C^{7/7' \text{ or } 8/8'}$), 190.2 (s, $C^{7/7' \text{ or } 8/8'}$), 189.2 (s, $C^{7/7' \text{ or } 8/8'}$), 189.0 (s, $C^{7/7' \text{ or } 8/8'}$), 174.2 (s, $C^{3/3'}$), 174.0 (s, $C^{3/3'}$), 105.7 (s, $C^{9/9'}$), 105.4 (s, $C^{9/9'}$), 104.9 (s, $C^{10/10'}$), 102.5 (s, $C^{12/12'}$), 88.7 (s, $C^{15/15'}$), 88.6 (s, $C^{15/15'}$), 86.4 (s, $C^{13/13'}$), 86.2 (s, $C^{13/13'}$), 83.0 (s, $C^{14/14'}$), 82.5 (s, $C^{16/16'}$), 82.4 (s, $C^{16/16'}$), 79.7 (d, *J* = 2.4 Hz, $C^{17/17'}$), 60.5 (s, $C^{2/2'}$), 60.4 (s, $C^{2/2'}$), 38.3 (s, $C^{4/4' \text{ or } 5/5' \text{ or } 6/6'}$), 38.2 (s, $C^{4/4' \text{ or } 5/5' \text{ or } 6/6'}$), 37.9 (s, $C^{4/4' \text{ or } 5/5' \text{ or } 6/6'}$), 37.8 (s, $C^{4/4' \text{ or } 5/5' \text{ or } 6/6'}$), 37.7 (s, $C^{4/4' \text{ or } 5/5' \text{ or } 6/6'}$), 37.5 (s, $C^{4/4' \text{ or } 5/5' \text{ or } 6/6'}$), 19.0 (s, $C^{11/11'}$), 18.9 (s, $C^{11/11'}$), 13.1 (s, $C^{1/1'}$), 13.1 (s, $C^{1/1'}$), ^{31}P NMR (243 MHz, CD_3OD) δ -132.06 – -156.07 (m, $p^{\text{Counter-ion}}$), ^{19}F NMR δ -74.65 (d, *J* = 707.8 Hz, $F^{\text{Counter-ion}}$); *m/z* (HRMS, ESI-MS)$^+$ 435.0764 [M-PF6] ($C_{21}H_{23}O_4{}^{96}Ru^+$ requires 435.0672)

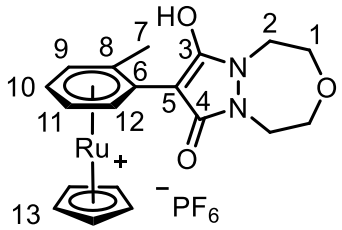

[Ru(η^6-8-(2-tolyl)-1,2,4,5-tetrahydropyrazolo[1,2-d][1,4,5]oxadiazepine-7,9-dione)(η^5-cyclopentadienyl)]PF_6 ***(3.22)***

Synthesised via general experimental 2, using 1,2,4,5-tetrahydropyrazolo[1,2-d][1,4,5]oxadiazepine-7,9-dione (6.6 mg, 0.038 mmol, 1.1 eq.). The title compound was isolated as a yellow foam (14.2 mg, 0.023 mmol, 68 %).

^{1}H NMR (599 MHz, CD_3OD) δ 6.22 (1H, dd, *J* = 6.0, 0.9 Hz, H^{12}), 6.12 (1H, d, *J* = 5.8 Hz, H^9), 6.01 (1H, td, *J* = 5.9, 0.9 Hz, H^{11}), 5.93 (1H, td, *J* = 5.7, 0.9 Hz, H^{10}), 5.32 (5H, s, H^{13}), 3.88 – 3.85 (4H, m, H^1), 3.82 – 3.80 (4H, m, H^2), 2.38 (3H, s, H^7), ^{13}C{^{1}H} NMR (151 MHz, CD_3OD) δ 167.1 (s, $C^{3,4}$), 101.8 (s, C^6), 100.5 (s, C^8), 86.7 (s, C^9), 86.3 (s, C^{12}), 83.5 (s, C^{11}), 82.5 (s, C^{10}), 79.5 (s, C^{13}), 79.2 (s, C^5), 69.7 (s, C^1), 47.7 (s, C^2), 19.1 (s, C^7), ^{31}P NMR (243 MHz, CD_3OD) δ -132.06 – -156.07 (m, $p^{Counter\text{-}ion}$), ^{19}F NMR δ -72.63 (d, *J* = 707 Hz, $F^{Counter\text{-}ion}$); *m/z* (HRMS, ESI-MS)$^+$ 421.0261 [M-PF6] ($C_{19}H_{21}N_2O_3{}^{96}Ru^+$ requires 421.0268)

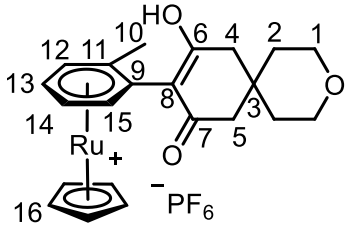

[Ru(η^6-9-(2-tolyl)-3-oxaspiro[5.5]undecane-8,10-dione)(η^5-cyclopentadienyl)]PF_6 ***(3.23)***

Synthesised via general experimental 2, using 3-oxaspiro[5.5]undecane (6.6 mg, 0.038 mmol, 1.1 eq.). The title compound was isolated as a brown solid (14.4 mg, 0.024 mmol, 70 %).

^{1}H NMR (599 MHz, CD_3OD) δ 6.11 (1H, d, *J* = 5.7 Hz, H^{12}), 5.98 (1H, t, *J* = 5.7 Hz, H^{14}), 5.95 – 5.89 (2H, m, $H^{13,15}$), 5.27 (5H, s, H^{16}), 3.73 (4H, t, *J* = 5.5 Hz, H^1), 2.48 (2H, dd, *J*

= 16.6, 2.7 Hz, $H^{4/5}$), 2.42 (2H, dd, *J* = 16.4, 2.6 Hz, $H^{4/5}$), 2.14 (3H, s, H^{10}), 1.64 (4H, dt, *J* = 33.9, 5.4 Hz, $H^{2, 2'}$), $^{13}C\{^{1}H\}$ NMR (151 MHz, CD_3OD) δ 192.1 (s, $C^{5/6}$), 190.9 (s, $C^{5/6}$), 106.5 (s, $C^{8/9}$), 106.5 (s, $C^{8/9}$), 103.8 (s, C^{11}), 90.2 (s, C^{15}), 87.6 (s, C^{12}), 84.4 (s, C^{14}), 83.8 (s, C^{13}), 81.1 (s, C^{16}), 64.7 (s, C^{1}), 64.6 (s, $C^{1'}$), 48.8 (s, $C^{4/5}$), 48.1 (s, $C^{4/5}$), 38.2 (s, C^{2}), 37.5 (s, $C^{2'}$), 32.8 (s, C^{3}), 20.5 (s, C^{10}), ^{31}P NMR (243 MHz, CD_3OD) δ -132.06 – -156.07 (m, $p^{Counter\text{-}ion}$), ^{19}F NMR δ -72.72 (d, *J* = 707 Hz, $F^{Counter\text{-}ion}$); *m/z* (HRMS, ESI-MS)$^+$ 433.0874 [M-PF6] ($C_{22}H_{25}O_3{}^{96}Ru^+$ requires 433.0880).

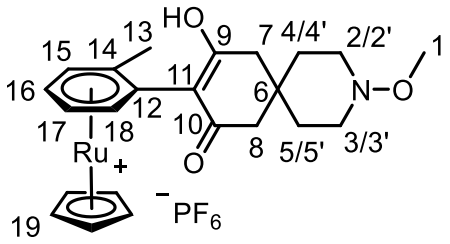

[Ru(η^6-9-(2-tolyl)-3-methoxy-3-azaspiro[5.5]undecane-8,10-dione)(η^5-cyclopentadienyl)]PF_6 ***(3.24)***

Synthesised via general experimental 2, using 3-methoxy-3-azaspiro[5.5]undecane-8,10-dione (8.3 mg, 0.038 mmol, 1.1 eq.). The title compound was isolated as a brown solid (18 mg, 0.030 mmol, 63 %).

^{1}H NMR (599 MHz, CD_3OD) δ 6.08 (1H, d, *J* = 5.7 Hz, H^{15}), 5.95 (1H, t, *J* = 5.7 Hz, H^{17}), 5.92 – 5.88 (2H, m, $H^{16, 18}$), 5.25 (5H, s, H^{19}), 3.50 (3H, s, H^{1}), 3.20-3.12 (2H, m, $H^{7/8}$), 2.68-2.60 (2H, m, $H^{7/8}$), 2.54 (1H, d, *J* = 16.5 Hz, H^{3}), 2.40 (1H, d, *J* = 16.7 Hz, H^{2}), 2.31-2.24 (2H, m, $H^{2', 3'}$), 2.11 (3H, s, H^{13}), 1.95-1.85 (1H, m, H^{4}), 1.83-1.74 (1H, m, H^{5}), 1.60-1.50 (2H, m, $H^{4', 5'}$), $^{13}C\{^{1}H\}$ NMR (151 MHz, CD_3OD) δ 191.1 (s, $C^{9/10}$), 189.8 (s, $C^{9/10}$), 105.4 (s, $C^{11/12}$), 104.9 (s, $C^{11/12}$), 102.4 (s, C^{14}), 88.8 (s, C^{18}), 86.2 (s, C^{15}), 82.9 (s, C^{17}), 82.4 (s, C^{16}), 79.7 (s, C^{19}), 57.6 (s, C^{1}), 50.6 (s, $C^{7/8}$), 50.5 (s, $C^{7/8}$), 35.0 (s, C^{5}), 34.2 (s, C^{4}), 31.4 (s, C^{6}), 19.1 (s, C^{13}), $^{31}P\{^{1}H\}$ NMR (243 MHz, CD_3OD) δ -132.06 – -156.07 (m, $p^{Counter\text{-}ion}$), ^{19}F NMR δ -74.76 (d, *J* = 707 Hz, $F^{Counter\text{-}ion}$); *m/z* (HRMS, ESI-MS)$^+$ 462.1140 [M-PF6] ($C_{23}H_{28}NO_3{}^{96}Ru^+$ requires 462.1145)

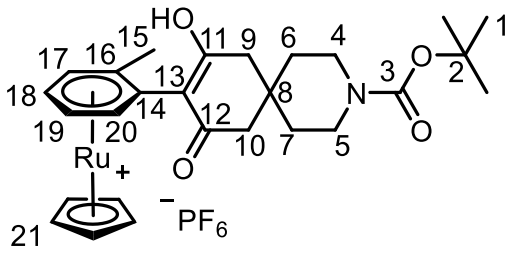

[Ru(η^6-9-(2-tolyl)-tert-butyl-8,10-dioxo-3-azaspiro[5.5]undecane-3-carboxylate)(η^5-cyclopentadienyl)]PF_6 ***(3.25)***

Synthesised via general experimental 2, using tert-butyl-8,10-dioxo-3-azaspiro[5.5]undecane-3-carboxylate (11 mg, 0.038 mmol, 1.1 eq.). The title compound was isolated as a brown solid (19.5 mg, 0.029 mmol, 61 %).

^{1}H NMR (599 MHz, CD_3OD) δ 6.09 (1H, d, *J* = 5.7 Hz, H^{17}), 5.96 (1H, t, *J* = 5.7 Hz, H^{19}), 5.92 – 5.88 (2H, m, $H^{18, 20}$), 5.25 (5H, s, H^{21}), 3.50-3.42 (4H, m, $H^{4, 5}$), 2.42 (2H, dd, *J* = 16.4, 5.9 Hz, $H^{9/10}$), 2.36 (2H, dd, *J* = 16.4, 2.8 Hz, $H^{9/10}$), 2.12 (3H, s, H^{15}), 1.59 (2H, t, *J* = 5.9 Hz, $H^{6/7}$), 1.53 (2H, t, *J* = 6.0 Hz, $H^{6/7}$), 1.45 (9H, s, H^1), ^{13}C{^{1}H} NMR (151 MHz, CD_3OD) δ 190.7 (s, $C^{11/12}$), 189.5 (s, $C^{11/12}$), 155.1 (s, C^3), 105.0 (s, $C^{13, 14}$), 102.4 (s, C^{16}), 88.8 (s, C^{20}), 86.2 (s, C^{17}), 83.0 (s, C^{19}), 82.4 (s, C^{18}), 79.7 (s, C^{21}), 79.5 (s, C^2), 78.3 (s, $C^{4/5}$), 77.0 (s, $C^{4/5}$), 47.0 (s, $C^{9/10}$), 46.2 (s, $C^{9/10}$), 35.9 (s, $C^{6/7}$), 35.1 (s, $C^{6/7}$), 32.2 (s, C^8), 27.2 (3C, s, C^1), 19.1 (s, C^{15}), ^{31}P NMR (243 MHz, CD_3OD) δ -132.06 – -156.07 (m, $p^{Counter-ion}$), ^{19}F NMR δ -72.65 (d, *J* = 707 Hz, $F^{Counter-ion}$); *m/z* (HRMS, ESI-MS)$^+$ 532.1567 [M-PF6] ($C_{27}H_{34}NO_4{}^{96}Ru^+$ requires 532.1564).

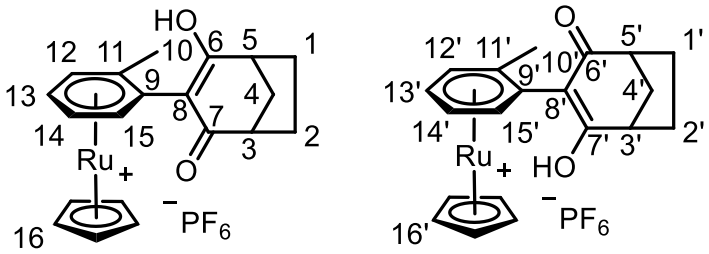

*[Ru(η^6-3-(2-tolyl)-1,3-bicyclo[3.2.1]octane-2,4-dione)(η^5-cyclopentadienyl)]PF_6 (1:1 mixture of diastereomers) (**3.26**)*

Synthesised via general experimental 2, using 1,3-bicyclo[3.2.1]octane-2,4-dione (6.4 mg, 0.038 mmol, 1.1 eq.). The title compound was isolated as an impure brown oil.

^{1}H NMR (599 MHz, CD_3OD) δ 6.06 (1H, dd, *J* = 9.5, 5.7 Hz, $H^{15/15'}$), 5.93 (1H, q, *J* = 5.6 Hz, $H^{12/12'}$), 5.88 (2H, ddd, *J* = 14.6, 9.4, 5.7 Hz, $H^{13/13', 14/14'}$), 5.27 – 5.21 (5H, m, $H^{16/16'}$), 2.83 – 2.74 (2H, m, $H^{1/1' \text{ or } 2/2'}$), 2.16 and 2.08 (3H, s, $H^{10/10'}$), 2.13 – 2.07 (3H, m, $H^{4/4' \text{ and } 3/3' \text{ or } 5/5'}$), 1.74 (2H, dd, *J* = 21.0, 6.6 Hz, $H^{1/1' \text{ or } 2/2'}$), 1.55 (1H, ddt, *J* = 23.9, 10.9, 4.3 Hz, $H^{5/5' \text{ or } 3/3'}$), $^{13}C\{^1H\}$ NMR (151 MHz, CD_3OD) δ 198.9 (s, $C^{6/6' \text{ or } 7/7'}$), 198.3 (s, $C^{6/6' \text{ or } 7/7'}$), 197.3 (s, $C^{6/6' \text{ or } 7/7'}$), 197.2 (s, $C^{6/6' \text{ or } 7/7'}$), 105.2 (s, $C^{8/8'}$), 104.7 (s, $C^{8/8'}$), 102.6 (s, $C^{9/9'}$), 102.2 (s, $C^{9/9'}$), 101.2 (s, $C^{11/11'}$), 100.7 (s, $C^{11/11'}$), 88.9 (s, $C^{13/13' \text{ or } 14/14'}$), 88.1 (s, $C^{13/13' \text{ or } 14/14'}$), 86.3 (s, $C^{15/15'}$), 86.1 (s, $C^{15/15'}$), 83.0 (s, $C^{12/12'}$), 82.9 (s, $C^{12/12'}$), 82.3 (s, $C^{13/13' \text{ or } 14/14'}$), 79.6 (s, $C^{16/16'}$), 79.6 (s, $C^{16/16'}$), 49.5 (s, $C^{1/1' \text{ or } 2/2'}$), 49.4 (s, $C^{1/1' \text{ or } 2/2'}$), 48.9 (s, $C^{1/1' \text{ or } 2/2'}$), 48.8 (s, $C^{1/1' \text{ or } 2/2'}$), 36.8 (s, $C^{5/5' \text{ or } 3/3'}$), 36.3 (s, $C^{5/5' \text{ or } 3/3'}$), 28.1 and 28.1 (s, $C^{1/1' \text{ or } 2/2'}$), 27.9 and 27.8 (s, $C^{4/4'}$), 19.0 (s, $C^{10/10'}$), 18.3 (s, $C^{10/10'}$), ^{31}P NMR (243 MHz, CD_3OD) δ -132.06 – -156.07 (m, $p^{\text{Counter-ion}}$), ^{19}F NMR δ -72.5 (d, *J* = 707 Hz, $F^{\text{Counter-ion}}$); *m/z* (HRMS, ESI-MS)$^+$ 389.0602 [M-PF6] ($C_{22}H_{25}O_3{}^{96}Ru^+$ requires 389.0618).

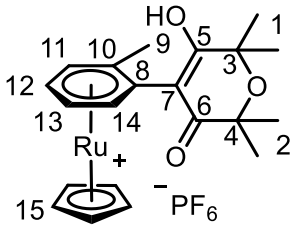

[Ru(η^6-2,2',6,6'-tetramethyl-4-(2-tolyl)-oxane-3,5-dione)(η^5-cyclopentadienyl)]PF_6 ***(3.27)***

Synthesised via general experimental 2, using 2,2',6,6'-tetramethyl-4-(2-tolyl)-oxane-3,5-dione (6.6 mg, 0.038 mmol, 1.1 eq.). The title compound was isolated as an impure brown oil.

^{1}H NMR (400 MHz, CD_3OD) δ 6.02 (1H, d, *J* = 5.7 Hz, H^{Arene}), 5.89 (2H, dd, *J* = 3.0, 0.9 Hz, H^{Arene}), 5.83 (1H, ddd, *J* = 5.7, 3.9, 2.6 Hz, H^{Arene}), 5.17 (5H, s, H^{15}), 1.30-1.19 (12H, m, $H^{1,2}$), *m/z* (HRMS, ESI-MS)$^+$ 421.0875 [M-PF_6] ($C_{21}H_{25}O_3{}^{96}Ru^+$ requires 421.0880).

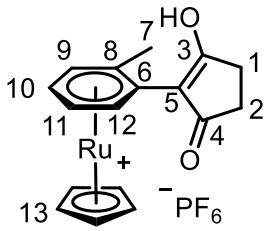

[Ru(η^6-2-(2-tolyl)-cyclopentane-1,3-dione)(η^5-cyclopentadienyl)]PF_6 ***(3.28)***

Synthesised via general experimental 2, using cyclopentane-1,3-dione (3.8 mg, 0.038 mmol, 1.1 eq.). The title compound was isolated as an impure brown solid (89%).

^{1}H NMR (599 MHz, CD_3OD) δ 6.12 (1H, d, *J* = 5.7 Hz, H^9), 6.02-5.96 (2H, m $H^{11,12}$), 5.95 (1H, t, *J* = 5.6 Hz, H^{10}), 5.32 (5H, s, H^{13}), 2.40 (4H, s, $H^{1,2}$), 2.23 (3H, s, H^7), $^{13}C\{^1H\}$ NMR (151 MHz, CD_3OD) δ 201.4 (s, $C^{3,4}$), 106.0 (s, C^5), 101.3 (s, C^6), 101.0 (s, C^8), 87.1 (s, C^{12}), 86.6 (s, C^9), 83.5 (s, C^{11}), 82.9 (s, C^{10}), 79.5 (s, C^{13}), 32.3 (s, $C^{1,2}$), 18.7 (s, C^7), ^{31}P NMR (243 MHz, CD_3OD) δ -132.06 – -156.07 (m, $p^{Counter\text{-}ion}$), ^{19}F NMR δ -72.54 (d, *J* = 707 Hz, $F^{Counter\text{-}ion}$); *m/z* (HRMS, ESI-MS)$^+$ 349.0314 [M-PF6] ($C_{17}H_{17}NO_4{}^{96}Ru^+$ requires 349.0305).

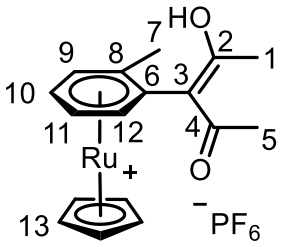

[Ru(η^6-3-(2-tolyl)-pentane-2,4-dione)(η^5-cyclopentadienyl)]PF_6 ***(3.29)***

Synthesised via general experimental 2, using acetylacetate (3.8 mg, 0.038 mmol, 1.1 eq.). The title compound was isolated as an impure brown oil (72%).

^{1}H NMR (400 MHz, Acetone) δ 6.11 (1H, d, *J* = 5.3 Hz, H^{Arene}), 6.01 (1H, d, *J* = 5.5 Hz, H^{Arene}), 5.98 – 5.90 (2H, m, H^{arene}), 5.29 (5H, s, H^{13}), 2.12 (3H, s, H^{7}), 2.07 (6H, q, *J* = 2.2 Hz, $H^{1, 5}$). m/z (LRMS, ESI-MS)$^+$ 351.20 [M-PF6] ($C_{17}H_{19}O_2{}^{96}Ru^+$ requires 351.04).

Photolytic Liberation of Ru π-Arene Complexes - General Experimental

The specified Ru complex (10 mg) was added to a vial and dissolved in 1.5 mL CD_3CN. The vial was placed in a Penn M2 photoreactor and irradiated with UV light (365 nm, 60 Hz) for a specified amount of time. The mixture was analysed by ^{1}H NMR spectroscopy after 1, 2, 5, 10 and 15 minutes. Formation of free arene was detected by observing disappearance of bound arene signals (ca. 5.8-7 ppm) and emergence of free arene signals (ca. 6.8-8 ppm)

Stacked Photolysis Spectra

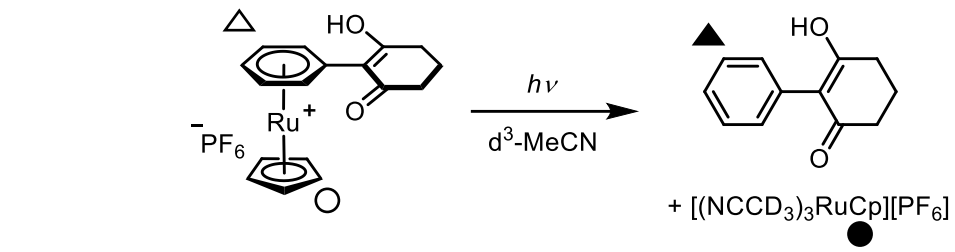

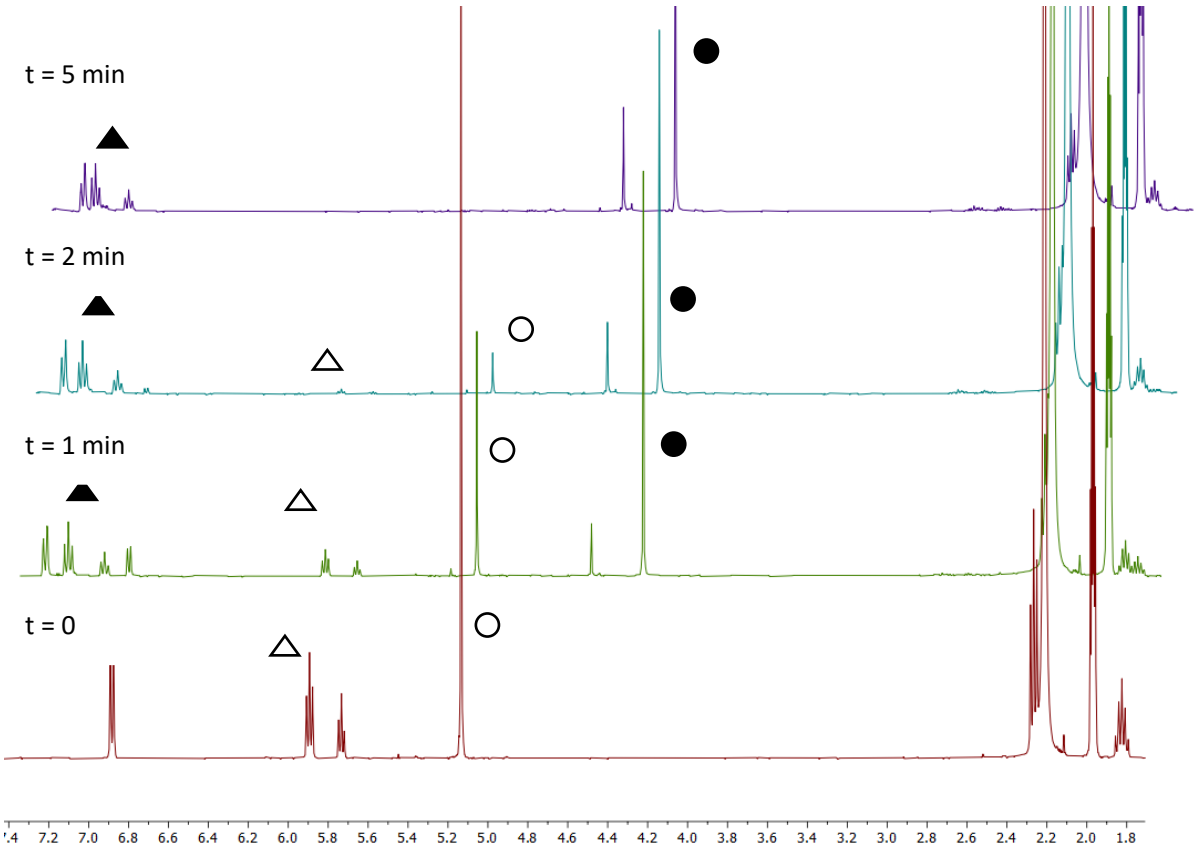

***Figure 7.1**. Stacked ^{1}H NMR spectra (CD_3CN, 298 K, 400 MHz) for the photolysis of the complex* [Ru(η^6-2-benzylcyclohexane-1,3-dione)(η^5-cyclopentadienyl)]PF_6

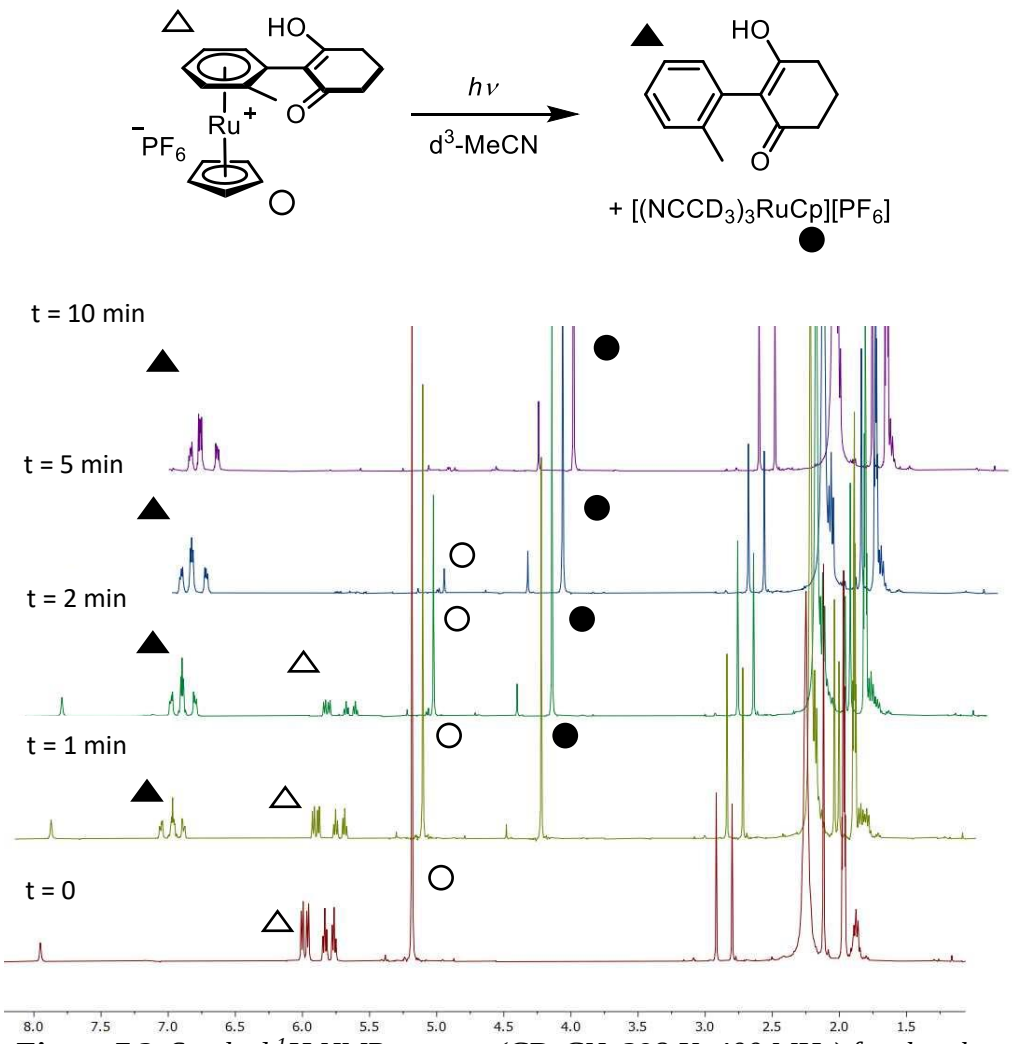

***Figure 7.2**. Stacked ^{1}H NMR spectra (CD_3CN, 298 K, 400 MHz) for the photolysis of the complex* [Ru(η^6-2-(2-tolyl)cyclohexane-1,3-dione)(η^5-cyclopentadienyl)]PF_6

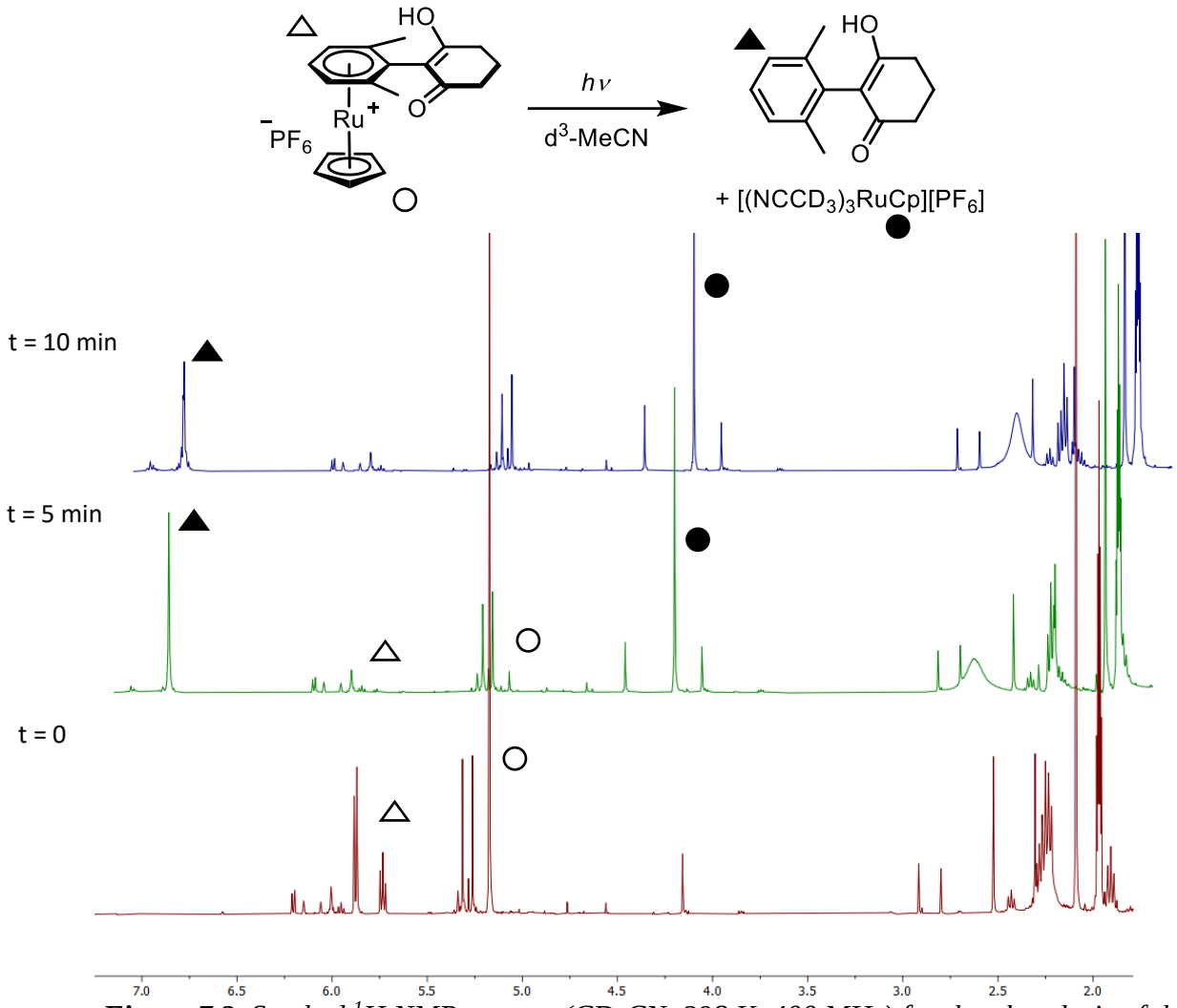

***Figure 7.3**. Stacked ^{1}H NMR spectra (CD_3CN, 298 K, 400 MHz) for the photolysis of the complex* [Ru(η^6-2-(2-m-xylene)cyclohexane-1,3-dione)(η^5-cyclopentadienyl)]PF_6

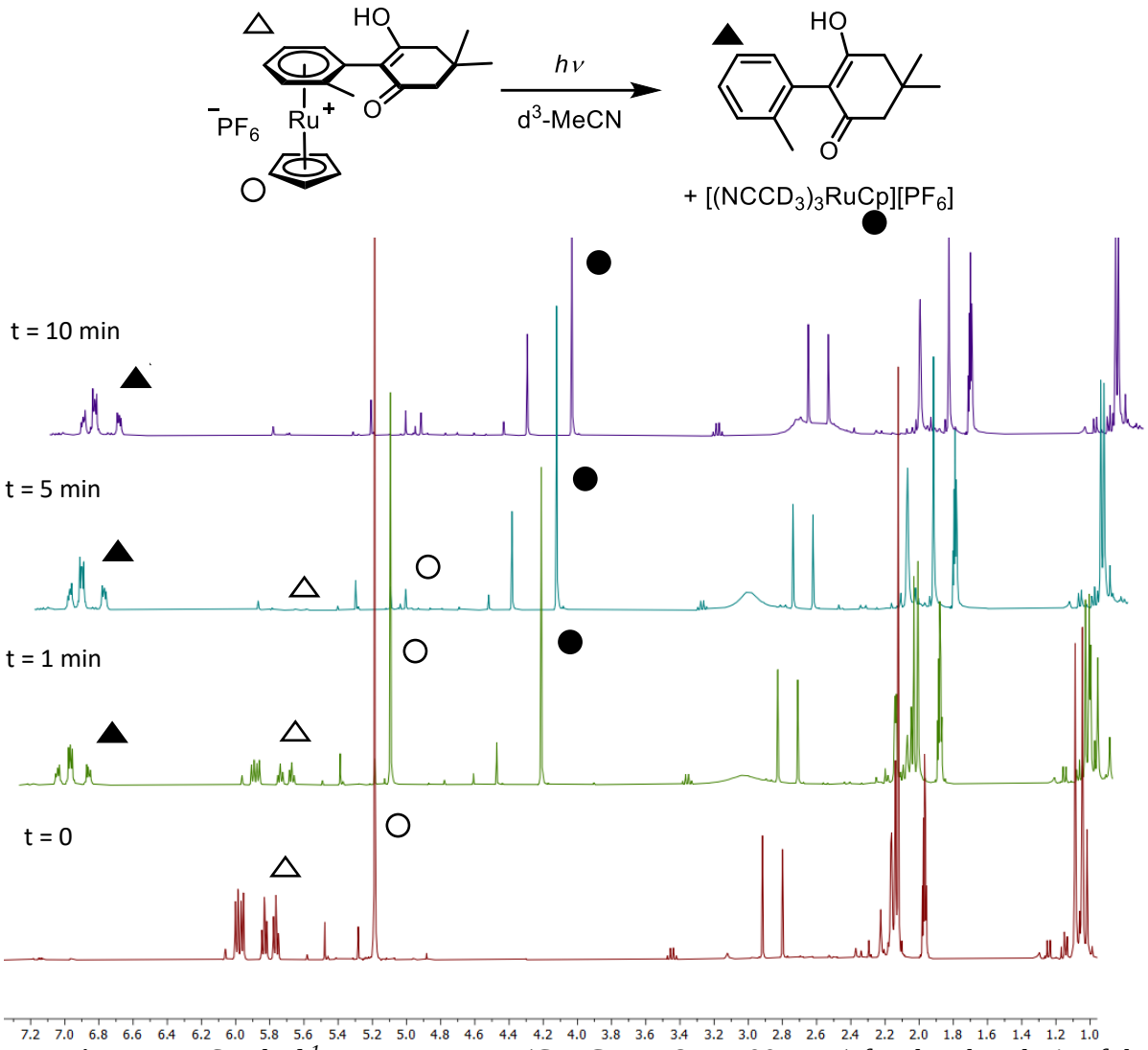

***Figure 7.4**. Stacked ^{1}H NMR spectra (CD_3CN, 298 K, 400 MHz) for the photolysis of the complex* [Ru(η^6-2-(2-tolyl)-5,5'-dimethylcyclohexane-1,3-dione)(η^5-cyclopentadienyl)]PF_6

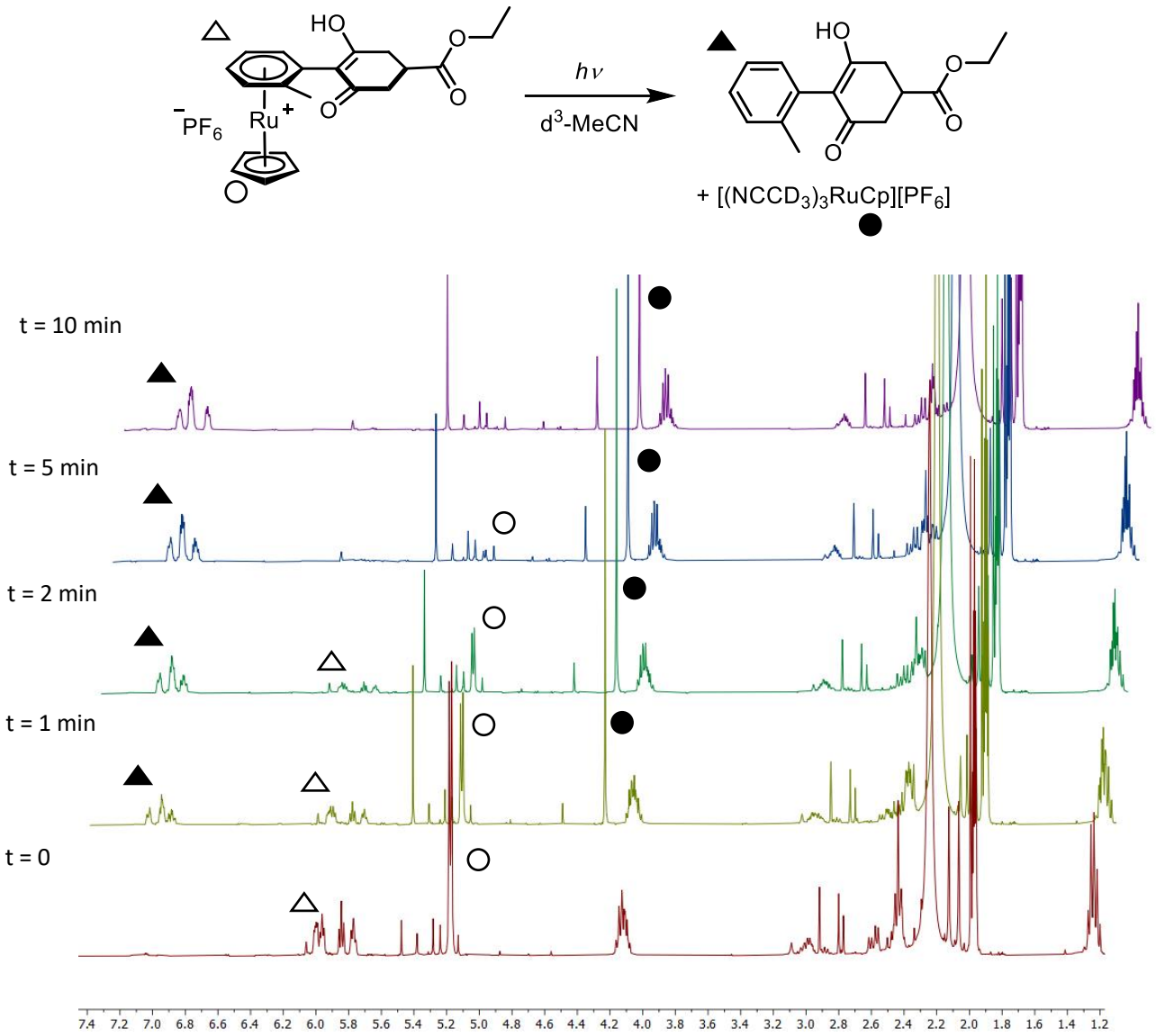

***Figure 7.5**. Stacked ^{1}H NMR spectra (CD_3CN, 298 K, 400 MHz) for the photolysis of the complex* [Ru(η^6-2-(2-tolyl)-(5-ethylacetyl)cyclohexane-1,3-dione)(η^5-cyclopentadienyl)]PF_6

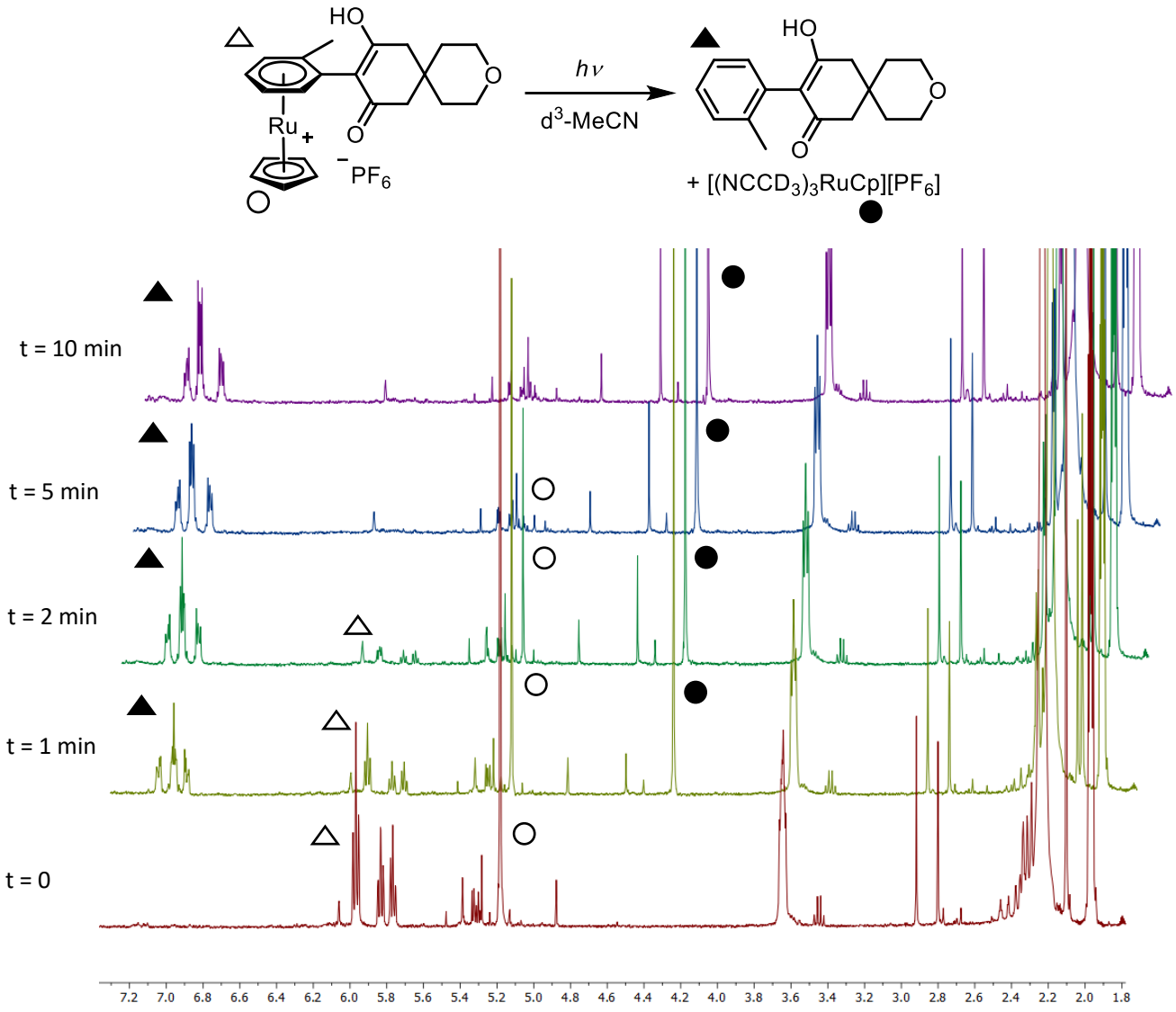

Figure 7.6. Stacked ^{1}H NMR spectra (CD_3CN, 298 K, 400 MHz) for the photolysis of the complex

[Ru(η^6-2-(2-tolyl)-3-oxaspiro[5.5]undecane-8,10-dione)(η^5-cyclopentadienyl)]PF_6

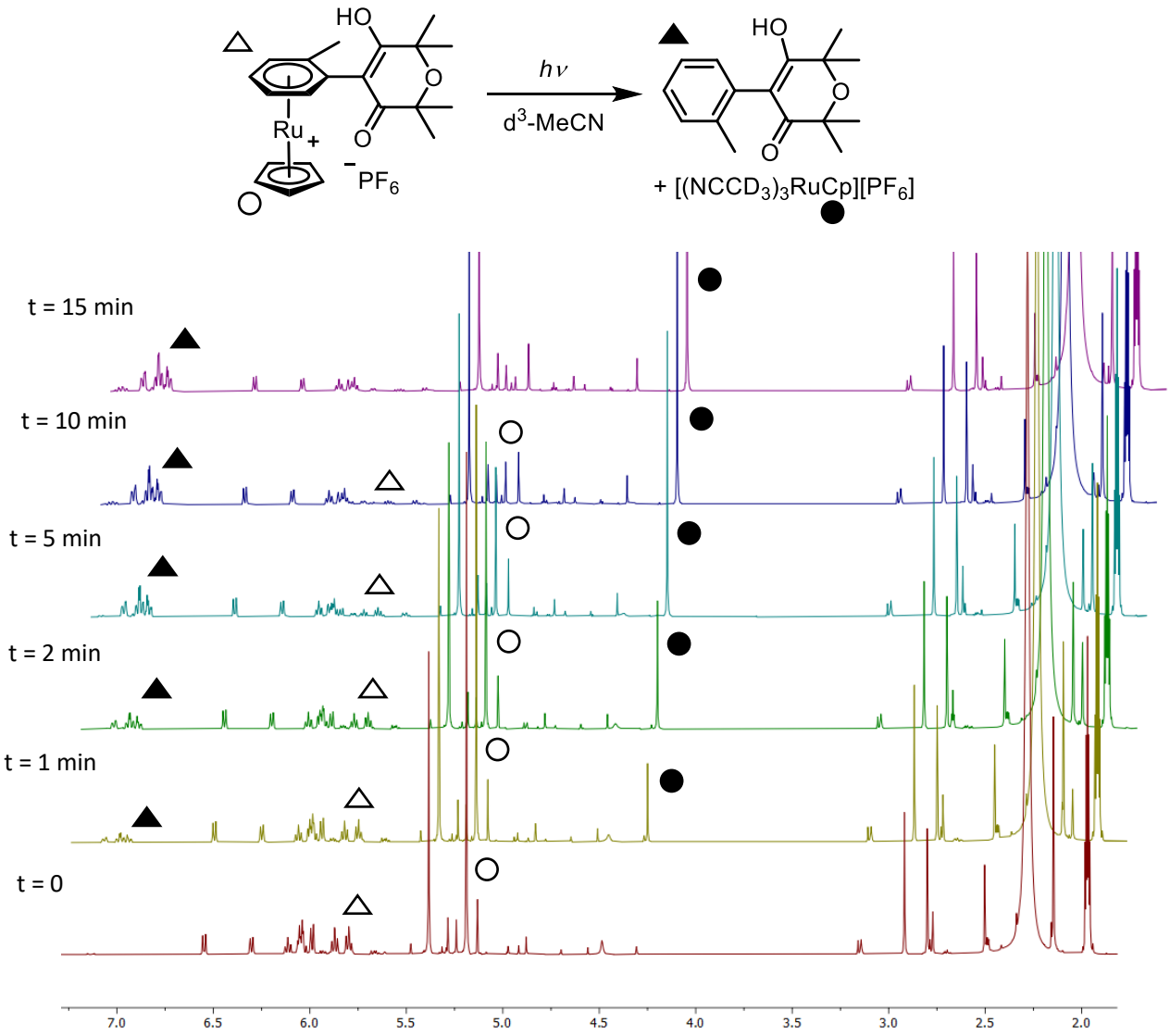

***Figure 7.7**. Stacked ^{1}H NMR spectra (CD_3CN, 298 K, 400 MHz) for the photolysis of the complex [Ru(η^6--2,2',6,6'-tetramethyl-4-(2-tolyl)-oxane-3,5-dione)(η^5-cyclopentadienyl)]PF_6*

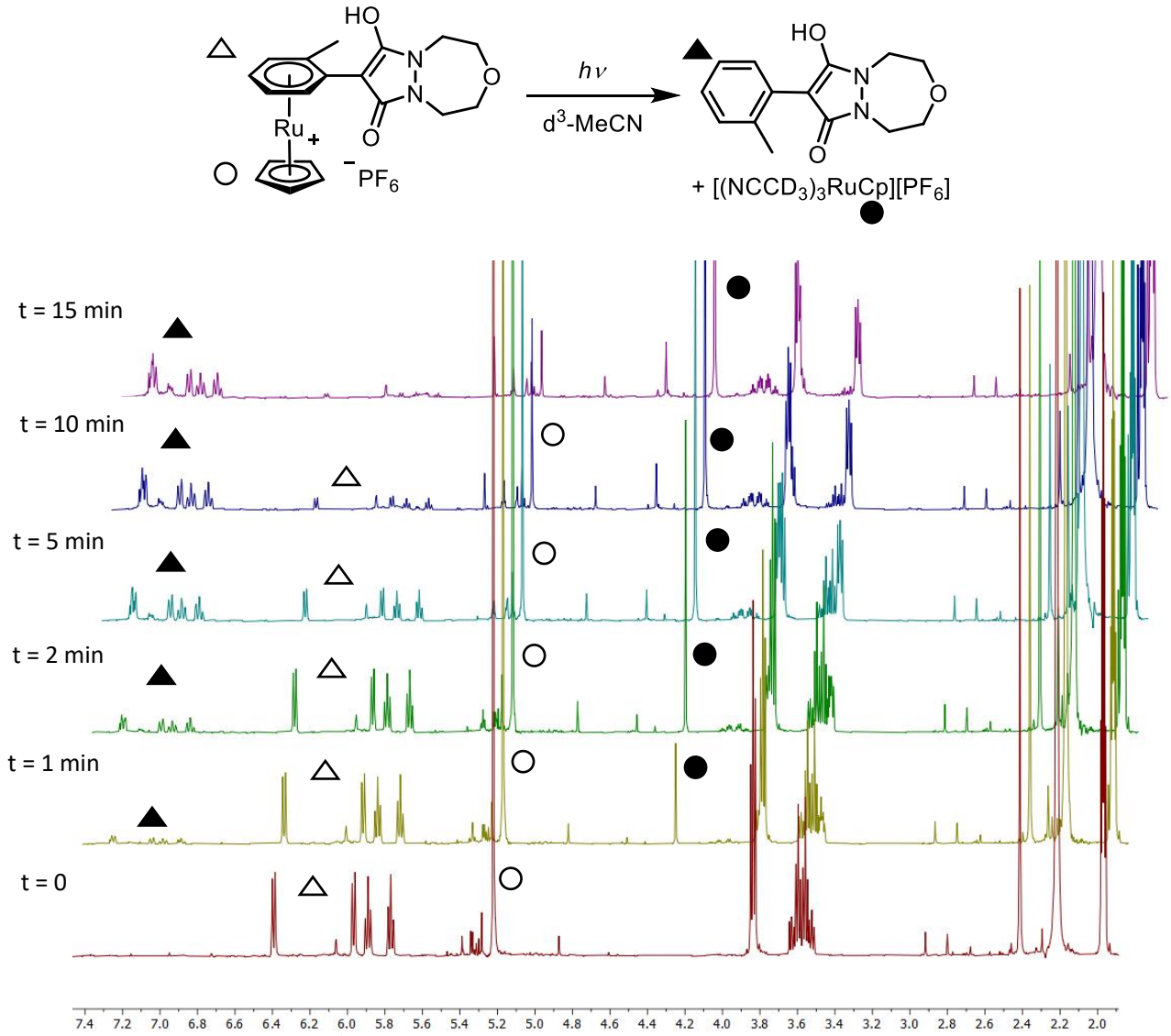

Figure 7.8. Stacked ^{1}H NMR spectra (CD_3CN, 298 K, 400 MHz) for the photolysis of the complex [Ru(η^6-8-(2-tolyl)-1,2,4,5-tetrahydropyrazolo[1,2-d][1,4,5]oxadiazepine-7,9-dione)(η^5-cyclopentadienyl)]PF_6

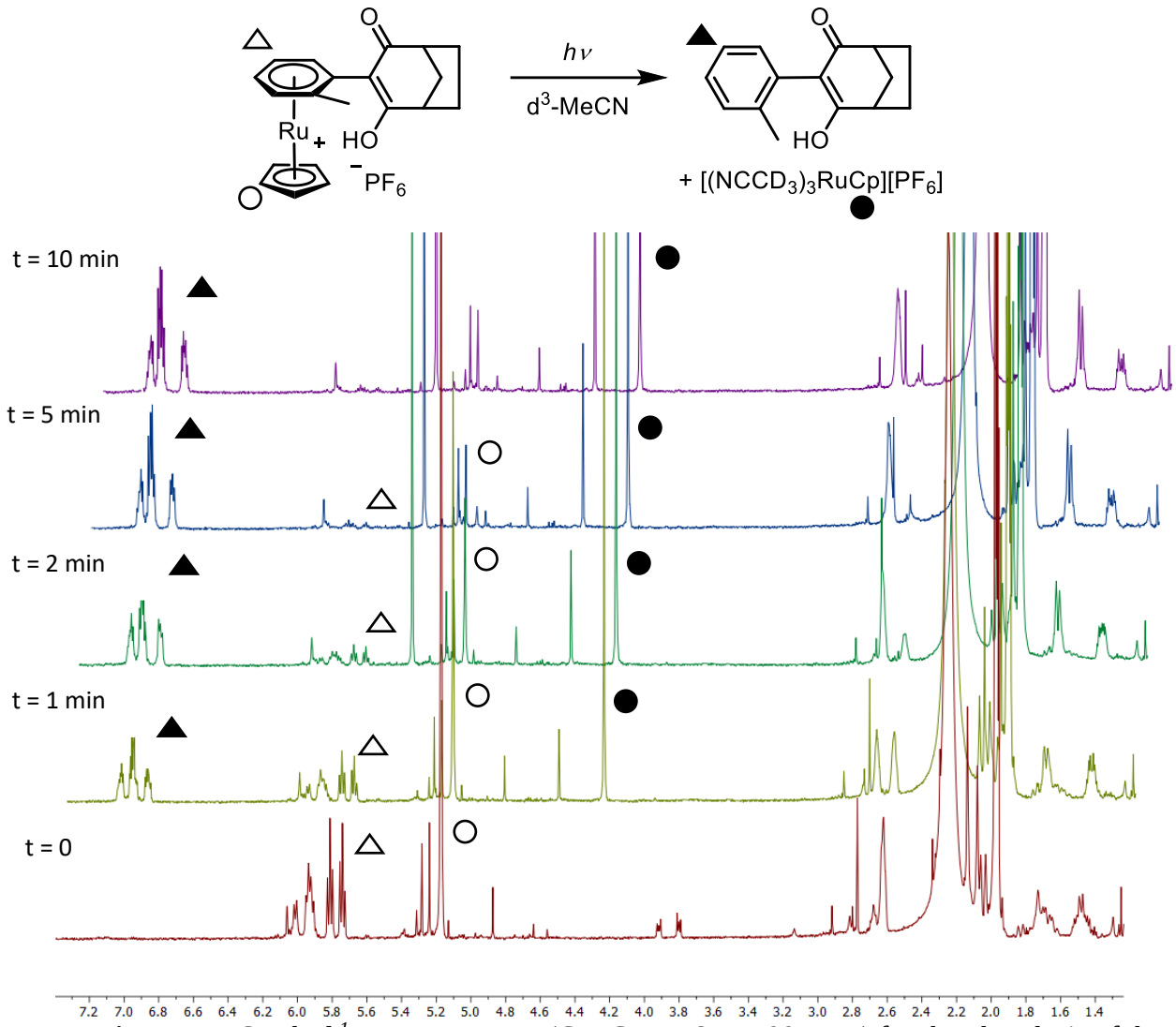

***Figure 7.9**. Stacked ^{1}H NMR spectra (CD_3CN, 298 K, 400 MHz) for the photolysis of the complex [Ru(η^6-3-(2-tolyl)-1,3-bicyclo[3.2.1]octane-2,4-dione)(η^5-cyclopentadienyl)]PF_6*

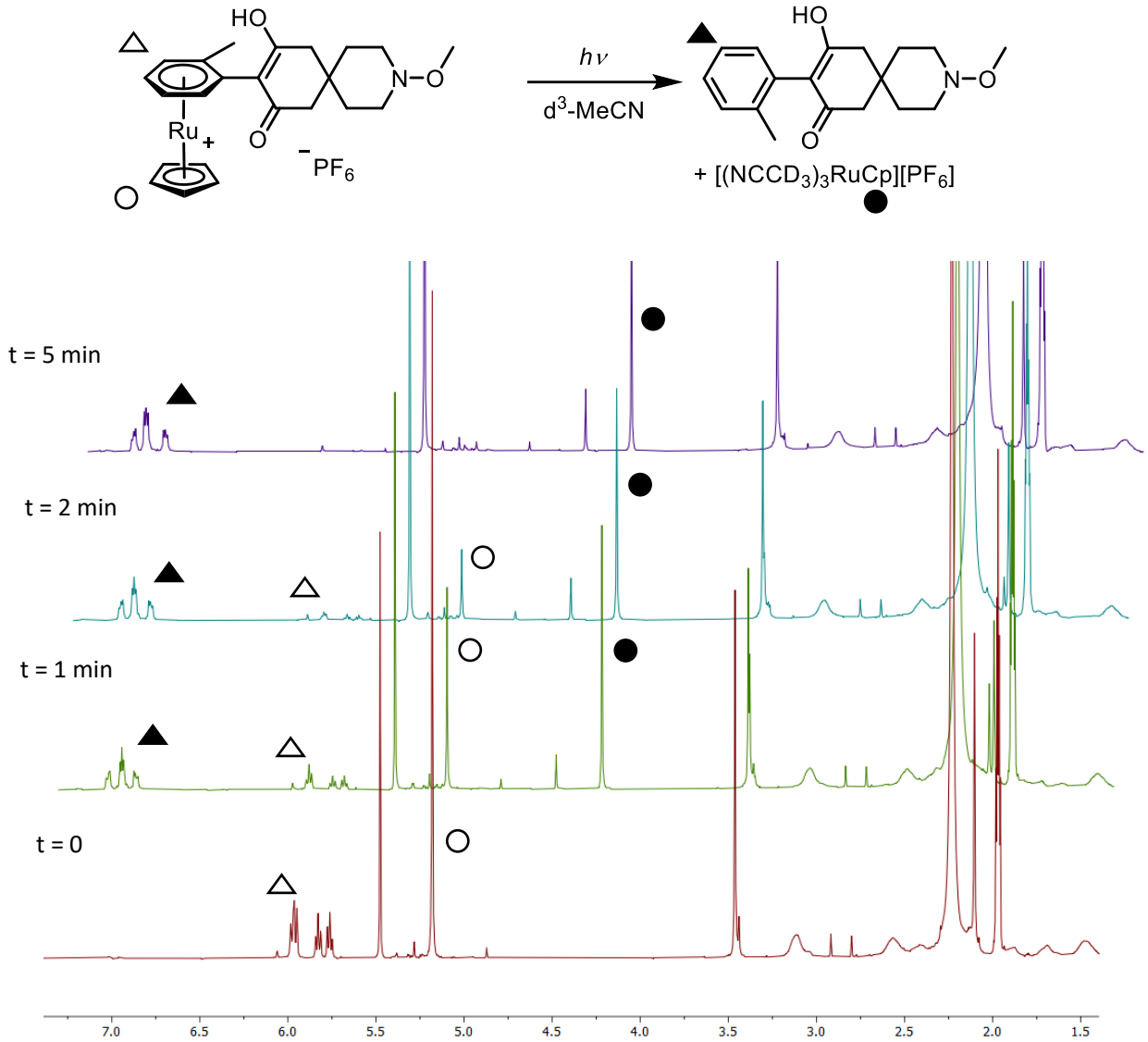

***Figure 7.10**. Stacked ^{1}H NMR spectra (CD_3CN, 298 K, 400 MHz) for the photolysis of the complex [Ru(η^6-9-(2-tolyl)-3-methoxy-3-azaspiro[5.5]undecane-8,10-dione)(η^5-cyclopentadienyl)]PF_6*

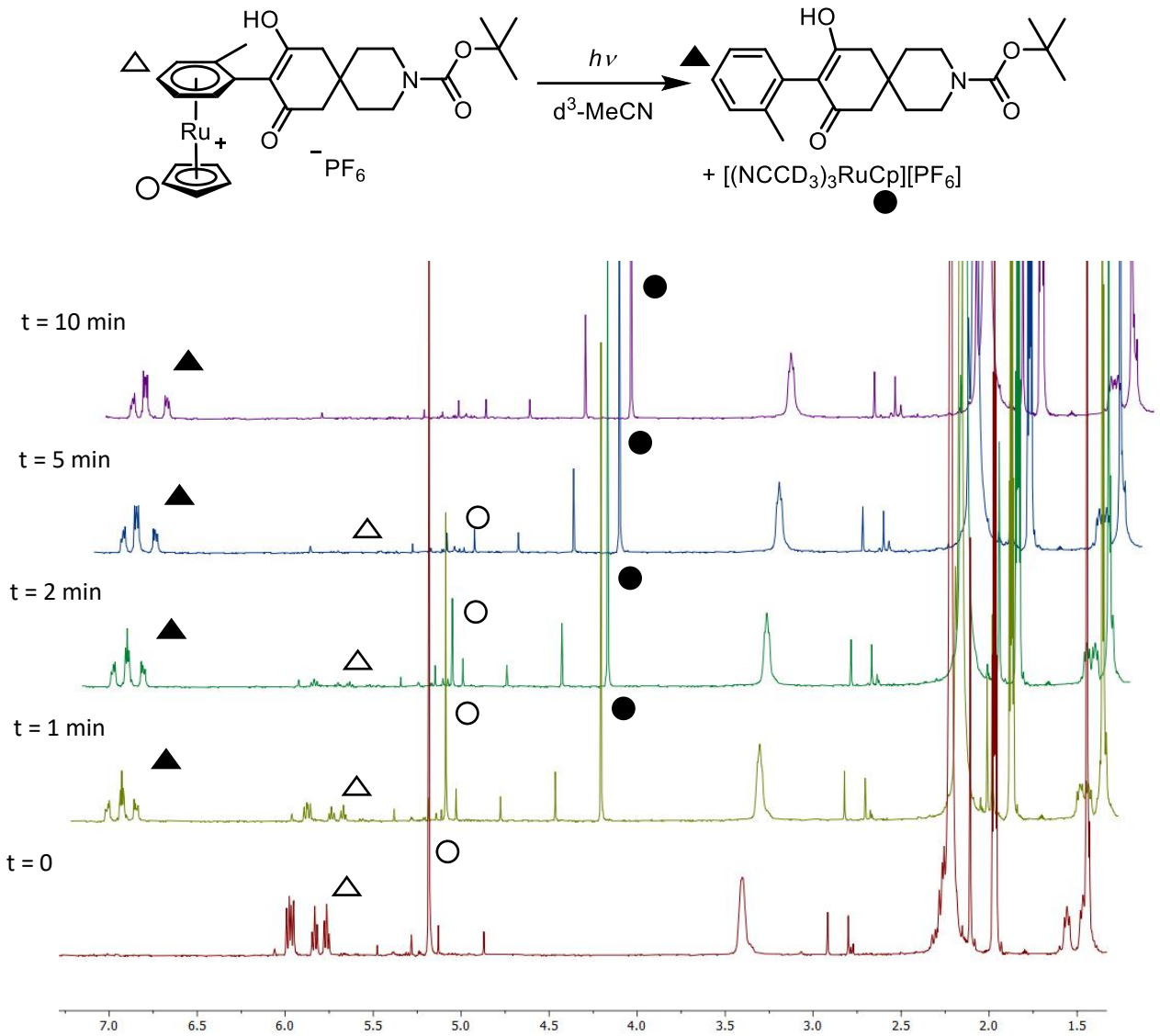

Figure 7.11. *Stacked ^{1}H NMR spectra (CD_3CN, 298 K, 400 MHz) for the photolysis of the complex [Ru(η^6-9-(2-tolyl)-tert-butyl-8,10-dioxo-3-azaspiro[5.5]undecane-3-carboxylate)(η^5-cyclopentadienyl)]PF_6*

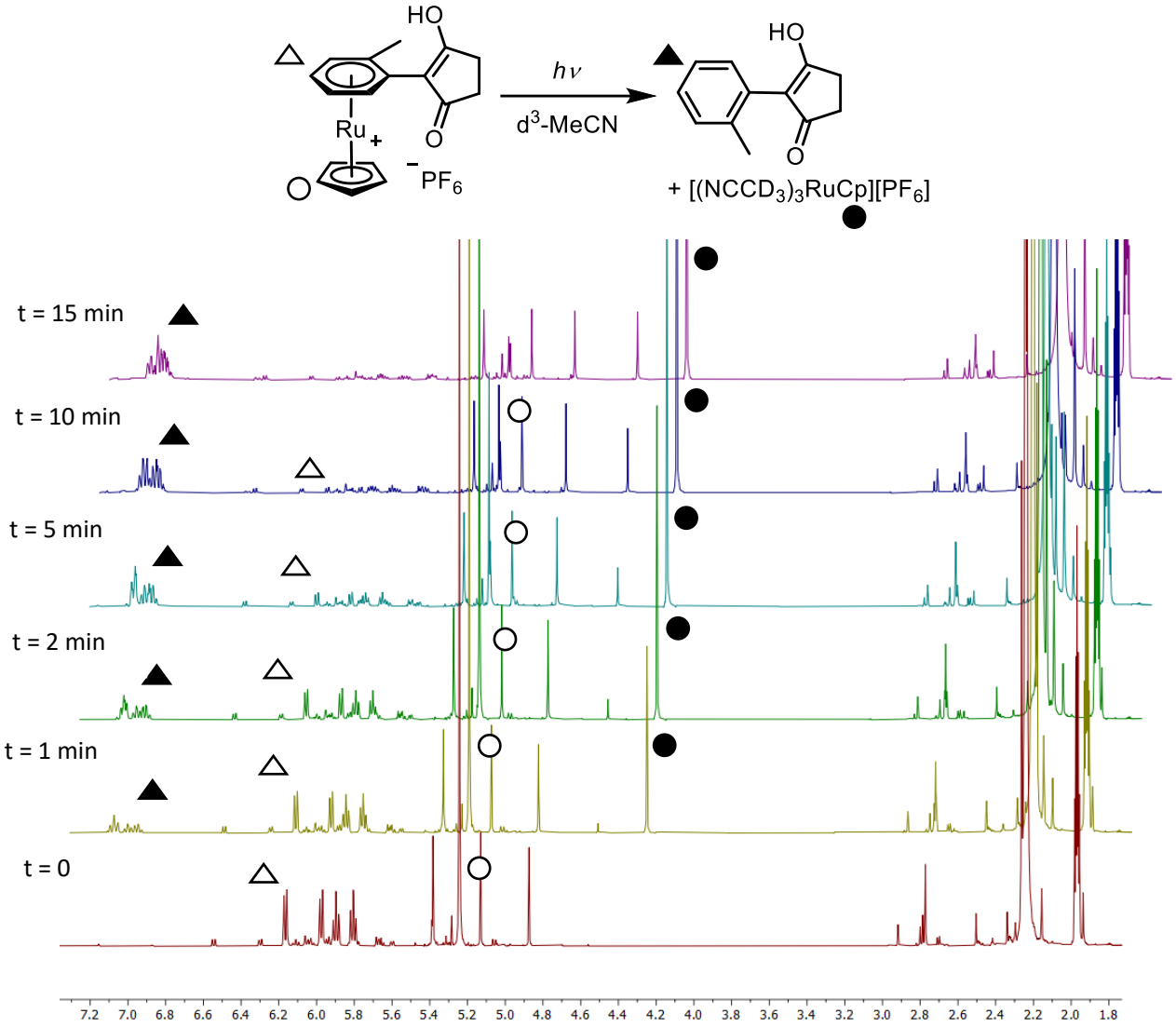

***Figure 7.12**. Stacked ^{1}H NMR spectra (CD_3CN, 298 K, 400 MHz) for the photolysis of the complex [Ru(η^6-2-(2-tolyl)cyclopentanedione)(η^5-cyclopentadienyl)]PF_6*

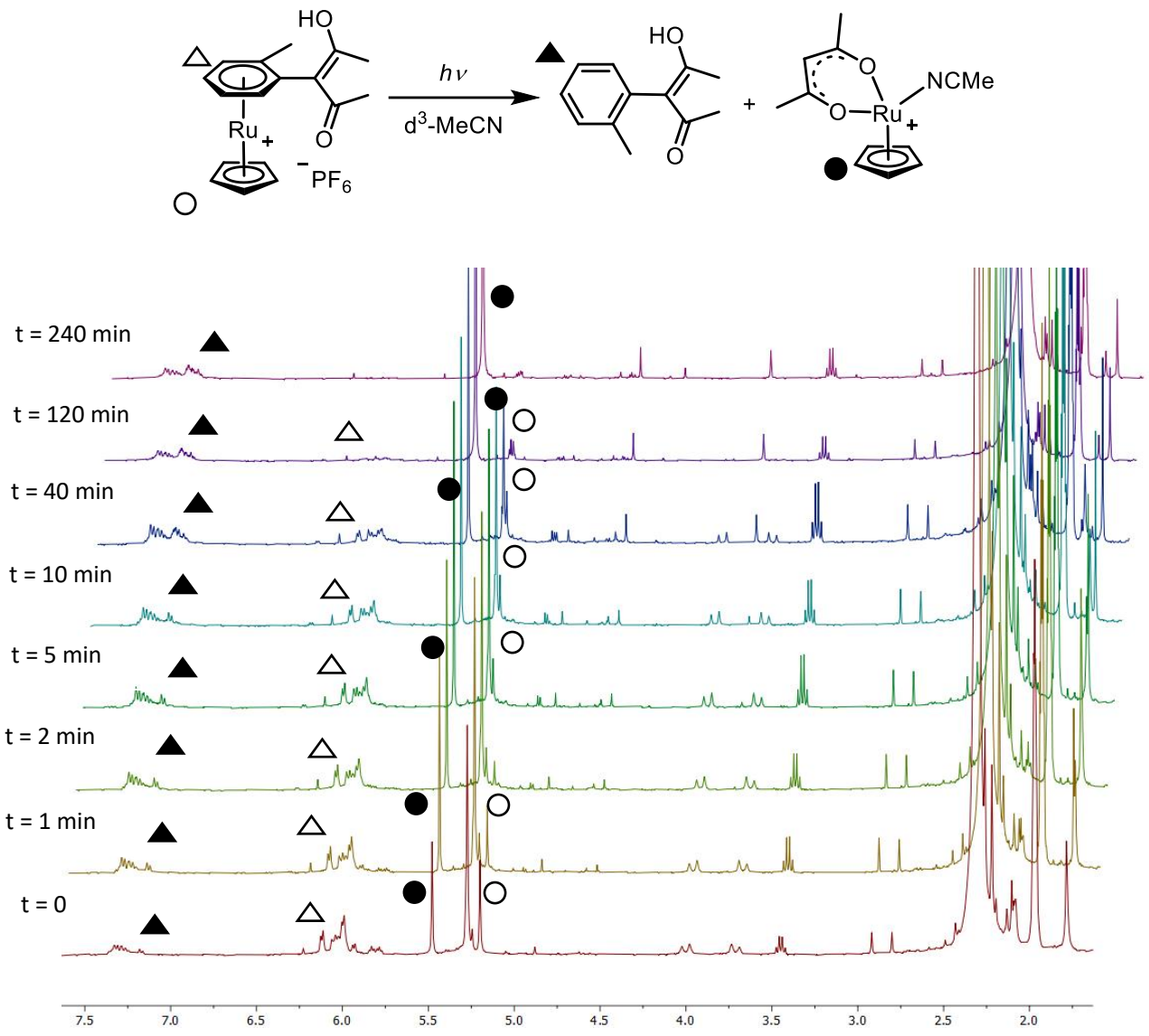

***Figure 7.13**. Stacked ^{1}H NMR spectra (CD_3CN, 298 K, 400 MHz) for the photolysis of the complex [Ru(η^6-2-(2-tolyl)acetylacetone)(η^5-cyclopentadienyl)]PF_6*

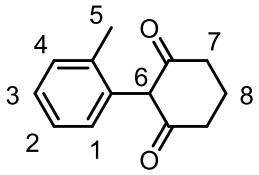

*2-tolylcyclohexane-1,3-dione (**3.30**)*

[Ru(η^6-6-hydroxy-4,5-dihydro-[1,1'-biphenyl]-2(3H)-one)(η^5-cyclopentadienyl)]PF_6 (80 mg, 0.16 mmol, 1 eq.) was dissolved in deuterated acetonitrile under inert atmosphere and irradiated with UV (365 nm) light for 30 minutes. The crude reaction mixture was diluted to 10 mL with dichloromethane, then filtered and extracted with water (3 x 5 mL), before the pH was decreased to 1 by adding HCl (5 mL, 2M in water), which was washed with dichloromethane (3 x 10 mL). The organic phase was dried over $MgSO_4$, then evaporated to dryness to give the title compound as a pale yellow solid (29 mg, 0.15 mmol, 92%).

^{1}H NMR (400 MHz, Methanol-D_4) δ 7.21 – 7.08 (3H, m, $H^{2, 3, 4}$), 6.94 (1H, dd, *J* = 7.2, 1.8 Hz, H^1), 2.55 (4H, t, *J* = 6.5 Hz, H^7), 2.12-2.06 (5H, m, $H^{5, 8}$); *m/z* (LRMS, ESI-MS)$^+$ 203.30 $[M+H]^+$ - $C_{13}H_{15}O_2^+$ requires 203.20

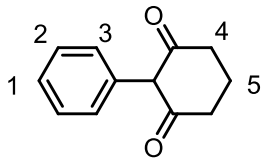

*2-phenylcyclohexane-1,3-dione (**3.31**)*

[Ru(η^6-6-hydroxy-4,5-dihydro-[1,1'-biphenyl]-2(3H)-one)(η^5-cyclopentadienyl)]PF_6 (80 mg, 0.16 mmol, 1 eq.) was dissolved in deuterated acetonitrile under inert atmosphere and irradiated with UV (365 nm) light for 30 minutes. The crude reaction mixture was diluted to 10 mL with dichloromethane, then filtered and dried under vacuum to give the crude product as a brown oil. Purification by column chromatography (SiO_2, 1% MeOH in CH_2Cl_2 eluent) gave the title compound as a yellow solid (27 mg, 0.14 mmol, 90%).

^{1}H NMR (400 MHz, Methanol-D_4) δ 7.37 – 7.26 (2H, m, H^2), 7.25 – 7.19 (1H, m, H^1), 7.17 – 7.07 (2H, m, H^3), 2.55 (4H, t, *J* = 6.4 Hz, H^4), 2.12 – 2.02 (2H, m, H^5); *m/z* (LRMS, ESI-MS)$^+$ 189.20 $[M+H]^+$ - $C_{12}H_{13}O_2^+$ 189.09

Stepwise Ru-Catalysed Synthesis of 2-(2-tolyl)1,3-cyclohexanedione from 2-chlorotoluene

To a flame-dried Schlenk flask were added tris(acetonitrile)cyclopentadienyl ruthenium(II) hexafluorophosphate (50 mg, 0.115 mmol, 1 eq.), 2-chlorotoluene (14 μL, 0.13 mmol, 1.1 eq.) and MeCN-d_3 (5 mL). The mixture was stirred at 80 °C for 18 h and the progress monitored by ^{1}H NMR spectroscopy. Then, 1,3-cyclohexanedione (14 mg, 0.17 mmol, 1.1 eq.) and K_2CO_3 (30 mg, 0.230 mmol, 2 eq.) were added and the reaction was stirred at 75 °C for 18 h. After observing the formation of the bound aromatic product *via in-situ* ^{1}H NMR spectroscopy, the reaction mixture was subjected to irradiation conditions (365 nm, *ca.* 5 cm) for 20 minutes. The free product, 2-(2-tolyl)-1,3-cyclohexanedione was observed by ^{1}H NMR spectroscopy (*ca.* 23% conversion with respect to the starting 2-chlorotoluene) as well as the deuterated form of the initial piano-stool complex [(MeCN-d_3)RuCp]$^+$.

7.2.3. Chapter 4 – Arene Exchange of Ru Sandwich Complexes

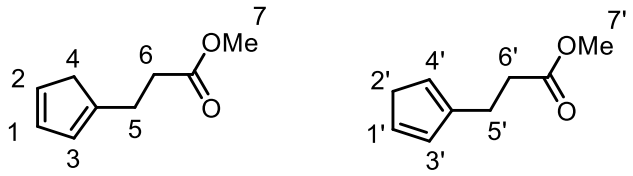

Methyl 3-(cyclopenta-1,3-dien-1-yl)propanoate and
*methyl 3-(cyclopenta-1,4-dien-1-yl) propanoate (**4.18A+B**)*

Methyl-3-bromopropionate (0.9 mL, 8.40 mmol, 1 eq.) was dissolved in anhydrous THF (10 mL) before being cooled to -78 °C. To this solution, NaCp (5 mL, 2.4 M solution in THF, 1.1 eq.) was added dropwise and the mixture was stirred for 18 h, during which time the reaction was allowed to warm to 25 °C. The resulting suspension was filtered through a plug of celite using CH_2Cl_2 (30 mL), before the filtrate was dried under reduced pressure to give a 1:1 mixture of the title compounds as a yellow oil (1.10 g, 7.24 mmol, 86%).

^{1}H NMR (400 MHz, $CDCl_3$) δ 6.50 – 5.91 (3H, m, $H^{1/1', 2/2', 3/3'}$), 3.69 (3H, s, $H^{7/7'}$), 2.96-2.87 (2H, m, $H^{4/4'}$), 2.76-2.65 (2H, m, $H^{5/5'}$), 2.63 – 2.55 (2H, m, $H^{6/6'}$).

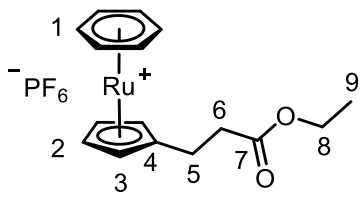

[Ru(η^6-benzene)(η^5-ethyl 3-(cyclopentadienyl)propanoate)]PF_6 ***(4.2)***

Sodium carbonate (350 mg, 3.29 mmol, 10 eq.) was added to an oven-dried 2-neck round-bottom flask and was further dried by heating under reduced pressure. Subsequently, benzeneruthenium chloride dimer (165 mg, 0.33 mmol, 1 eq.), a 1:1 mixture of Methyl 3-(cyclopenta-1,3-dien-1-yl)propanoate and methyl 3-(cyclopenta-1,4-dien-1-yl) propanoate (500 mg, 3.29 mmol, 10 eq.) and anhydrous ethanol (15 mL)were added and the reaction mixture was heated to reflux under inert atmosphere for 24 h. The reaction mixture was then filtered, and the filtrate concentrated under reduced pressure to 2 mL. To the resulting brown liquid was added an aqueous solution of ammonium hexafluorophosphate (130 mg, 0.80 mmol, 2.5 eq.). The resulting brown residue was extracted with CH_2Cl_2 (4 x 20 mL) and the organic fractions were combined and dried over $MgSO_4$, then the solvent was removed under reduced pressure. The resulting dark brown residue was dissolved in a minimum of acetonitrile, then Et_2O (15 mL) was added. The liquid phase was decanted to give the title compound as a brown oil (108 mg, 0.22 mmol, 33%).

^{1}H NMR (599 MHz, acetone-D_6) δ 6.34 (6H, s, H^1), 5.59-5.55 (2H, m, H^3), 5.44-5.40 (2H, m, H^2), 4.09 (2H, q, *J* = 7.1 Hz, H^8), 2.67 (2H, t, *J* = 7.5 Hz, H^5), 2.59 – 2.52 (2H, m, H^6), 1.19 (3H, t, *J* = 7.1 Hz, H^9), ^{13}C{^{1}H} NMR (151 MHz, acetone-D_6) δ 171.5 (s, C^7), 103.1 (s, C^4), 86.5 (s, C^1)F, 80.6 (s, C^3), 79.7 (s, C^2), 60.1 (s, C^8), 34.0 (s, C^6), 22.9 (s, C^5). 13.5 (s, C^9), ^{19}F NMR (376 MHz, Acetone-D_6) δ -72.5 (d, *J* = 707 Hz, $F^{Counter\text{-}ion}$), ^{31}P (acetone-D_6) δ -145.7 (sept., $J_{P\text{-}F}$ 707 Hz, $P^{Counter\text{-}ion}$); *m/z* (HRMS, ESI-MS)$^+$ 339.0466 [M-PF_6] ($C_{16}H_{19}O_2{}^{96}Ru^+$ requires 339.0461).

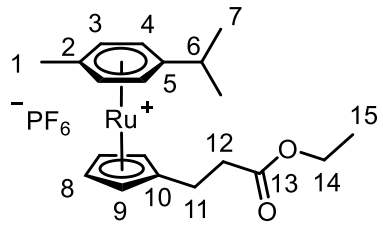

*[Ru(η^6-p-cymene)(η^5-ethyl 3-(cyclopentadienyl)propanoate)]PF_6 (**4.8**)*

Sodium carbonate (350 mg, 3.29 mmol, 10 eq.) was added to an oven-dried 2-neck round-bottom flask and was further dried by heating under reduced pressure. Subsequently, p-cymene ruthenium chloride dimer (200 mg, 0.33 mmol, 1 eq.), a 1:1 mixture of methyl 3-(cyclopenta-1,3-dien-1-yl)propanoate and methyl 3-(cyclopenta-1,4-dien-1-yl) propanoate (500 mg, 3.29 mmol, 10 eq.) and anhydrous ethanol (15 mL)were added and the reaction mixture was heated to reflux under inert atmosphere for 24 h. The reaction mixture was then filtered, and the filtrate concentrated under reduced pressure to 2 mL. To the resulting brown liquid was added an aqueous solution of ammonium hexafluorophosphate (130 mg, 0.8 mmol, 2.5 eq.). The resulting brown residue was extracted with CH_2Cl_2 (4 x 20 mL) and the organic fractions were combined and dried over $MgSO_4$, then the solvent was removed under reduced pressure. The resulting dark brown residue was dissolved in a minimum of acetonitrile, then Et_2O (15 mL) was added. The liquid phase was decanted to give the title compound as a brown oil (250 mg, 0.46 mmol, 70%).

^{1}H NMR (599 MHz, acetone-D_6) δ 6.27 (4H, br. s, $H^{3,4}$), 5.48-5.44 (2H, m, $H^{8/9}$), 5.40 – 5.37-5.33 (2H, m, $H^{8/9}$), 4.09 (2H, q, *J* = 7.2 Hz, H^{14}), 2.87 – 2.75 (1H, m, H^6), 2.63 (2H, td, *J* = 7.2, 1.2 Hz, H^{11}), 2.60 – 2.51 (2H, m, H^{12}), 2.38 (3H, s, H^1), 1.29 (6H, d, *J* = 6.9 Hz, H^7), 1.19 (3H, t, *J* = 7.1 Hz, H^{15}), ^{13}C{^{1}H} NMR (151 MHz, acetone-D_6) δ 171.5 (s, C^{13}), 112.3 (s, C^5), 102.2 (s, C^{10}), 101.3 (s, C^2), 86.9 (s, C^3) , 84.5 (s, C^4), 80.9 (s, C^9), 79.9 (s, C^8), 60.1 (s, C^{14}), 34.3 (s, C^{11}), 31.7 (s, C^6), 22.7 (s, C^{12}), 22.6 (s, C^7), 18.7 (s, C^1), 13.5 (s, C^{15}), ^{19}F NMR (376 MHz, Acetone-D_6) δ -72.50 (d, *J* = 707 Hz, $F^{Counter\text{-}ion}$), ^{31}P (acetone-D_6) δ -145.7 (sept., $J_{P\text{-}F}$ 707 Hz, $P^{Counter\text{-}ion}$); *m/z* (HRMS, ESI-MS)$^+$ 395.0916 [M-PF_6] ($C_{20}H_{27}O_2{}^{96}Ru^+$ requires 395.0987)

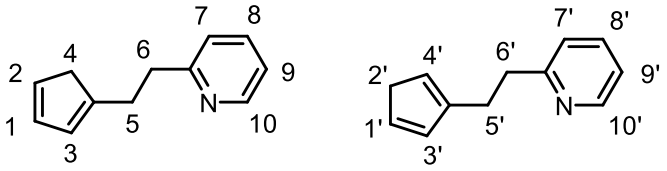

2-[2-(Cyclopenta-1,3-dien-1-yl)ethyl]pyridine and
*2-[2-(cyclopenta-1,4-dien-1-yl)ethyl] pyridine (**4.21A+B**)*

Method 1: PPh_3 (6.98 g, 26.6 mmol, 1.3 eq.), CBr_4 (8.82 g, 26.6 mmol, 1.3 eq.) and 2-pyridineethanol (2.0 mL, 17.8 mmol, 1 eq.) were combined in anhydrous THF (40 mL) and the mixture was stirred at 25 °C for 24 h. The mixture was filtered and cooled to -78 °C and a solution of NaCp (2.4 M in THF, 8.9 mL) was added dropwise. The resulting mixture was stirred under an inert atmosphere for 18 h, during which time the temperature was increased to 25 °C. The solvent was removed under reduced pressure to give a brown residue, which was triturated with Et_2O (5 x 10 mL) and the resulting solution was passed through a plug of silica. The filtrate was dried under reduced pressure to give a 1:1 mixture of the title compounds contaminated with triphenylphosphine oxide, as an orange oil, which was used without further purification (2.76 g).

Method 2: 2-pyridineethanol (1.20 mL, 10.6 mmol, 1 eq.), methanesulfonic anhydride (2.77 g, 25.9 mmol, 1.5 eq.) and DIPEA (4.6 mL, 26.5 mmol, 2.5 eq.) were combined in anhydrous THF (15 mL) and stirred at 25 °C for 2 hours. The reaction mixture was then dried under reduced pressure and the yellow residue dissolved in CH_2Cl_2 (20 mL). The organic layer was washed with water (3 x 15 mL), then dried over $MgSO_4$ before the solvent was removed under reduced pressure to give 2-(pyridin-2-yl)ethyl methanesulfonate as a pale yellow oil. The 2-(pyridin-2-yl)ethyl methanesulfonate was then dissolved in anhydrous THF (10 mL) before being cooled to -78 °C. To this solution, NaCp (4.8 mL, 2.4 M solution in THF, 1.1 eq.) was added dropwise and the mixture was stirred for 18 h, during which time the reaction was allowed to warm to 25 °C. The resulting suspension was filtered through a plug of celite using CH_2Cl_2 (30 mL), before the filtrate was dried under reduced pressure to give a 1:1 mixture of the title compounds as a yellow oil (1.40 g, 8.20 mmol, 77%).

Mesylate (4.22): ^{1}H NMR (400 MHz, Chloroform-*D*) δ 8.48 (1H, dq, *J* = 4.9, 1.0 Hz, $H^{Pyridyl}$), 7.66 – 7.44 (1H, m, $H^{Pyridyl}$), 7.23 – 6.97 (2H, m, $H^{Pyridyl}$), 4.68 – 4.47 (2H, m, H^{Ethyl}), 3.23 – 3.07 (2H, m, H^{Ethyl}), 2.82 (3H, s, $H^{Mesityl}$); m/z (LRMS, ESI-MS)$^{+}$ 202.229 $[M+H]^{+}$ $C_8H_{12}NO_3S$

Cyclopentadiene isomers (4.21A+B): ^{1}H NMR (400 MHz, $CDCl_3$) δ 8.57 – 8.43 (1H, m, $H^{10/10'}$), 7.60 – 7.48 (1H, m, $H^{8/8'}$), 7.13 – 7.01 (2H, m, $H^{7/7', 9/9'}$), 6.54 – 5.89 (3H, m, $H^{1/1', 2/2'. 3/3'}$), 3.08 – 2.97 (2H, m, $H^{6/6'}$), 2.97 – 2.87 (2H, m, $H^{4/4'}$), 2.85 – 2.73 (2H, m, $H^{5/5'}$), *m/z* (HRMS, ESI-MS)$^{+}$ 172.1136 $[M+H]^{+}$ ($C_{12}H_{14}N^{+}$ requires 172.1126).

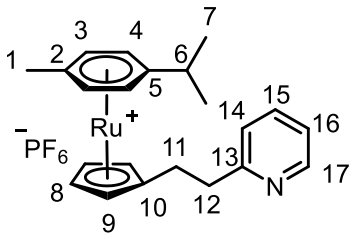

[Ru(η^{6}-p-cymene)(2-[2-(η^{5}-cyclopentadienyl)ethyl]pyridine)]PF_6 ***(4.5)***

Sodium carbonate (350 mg, 3.29 mmol, 10 eq.) was added to an oven-dried 2-neck round-bottom flask and was further dried by heating under reduced pressure. Subsequently, p-cymene ruthenium chloride dimer (200 mg, 0.33 mmol, 1 eq.), a 1:1 mixture of 2-[2-(Cyclopenta-1,3-dien-1-yl)ethyl]pyridine and 2-[2-(cyclopenta-1,4-dien-1-yl)ethyl] pyridine (562 mg, 3.29 mmol, 10 eq.) and anhydrous ethanol (15 mL) were added and the reaction mixture was heated to reflux under inert atmosphere for 24 h. The reaction mixture was then filtered, and the filtrate concentrated under reduced pressure to 2 mL. To the resulting brown solution was added an aqueous solution of ammonium hexafluorophosphate (130 mg, 0.8 mmol, 2.5 eq.). The resulting brown residue was extracted with CH_2Cl_2 (4 x 20 mL) and the organic fractions were combined and dried over $MgSO_4$, then the solvent was removed under reduced pressure. The resulting dark brown residue was dissolved in a minimum of acetonitrile, then Et_2O (15 mL) was added. The liquid phase was decanted to give the title compound as a brown oil (212 mg, 0.388 mmol, 56%). Where necessary, triphenylphosphine oxide was removed by column chromatography (2% MeOH in CH_2Cl_2).

^{1}H NMR (599 MHz, acetone-D_6) δ 8.52 (1H, d, *J* = 4.8 Hz, H^{17}), 7.68 (1H, td, *J* = 7.6, 1.9 Hz, H^{15}), 7.23 (1H, d, *J* = 7.8 Hz, H^{14}), 7.21 – 7.18 (1H, m, H^{16}), 6.27 (4H, br. s, $H^{3, 4}$), 5.41-5.37 (2H, m, $H^{8/9}$), 5.37-5.33 (2H, m, $H^{8/9}$), 3.00 (2H, dd, *J* = 8.7, 6.7 Hz, H^{12}), 2.83 – 2.75 (3H, m, $H^{6, 11}$), 2.39 (3H, s, H^{1}), 1.29 (6H, d, *J* = 6.9 Hz, H^{7}), ^{13}C{^{1}H} NMR (151 MHz, acetone-D_6) δ 159.9 (s, C^{13}), 149.2 (s, C^{17}), 136.3 (s, C^{15}), 122.9 (s, C^{14}), 121.4 (s, C^{16}), 112.2 (s, C^{5}), 103.2 (s, C^{10}), 101.4 (s, C^{2}), 86.9 (s, $C^{3/4}$), 84.5 (s, $C^{3/4}$), 80.8 (s, $C^{8/9}$), 79.8 (s, $C^{8/9}$), 38.3 (s, C^{12}), 31.7 (s, C^{6}), 26.9 (s, C^{11}), 22.6 (s, C^{7}), 18.8 (s, C^{1}), ^{19}F NMR (376 MHz, Acetone-D_6) δ -72.50 (d, *J* = 707.7 Hz, $F^{Counter\text{-}ion}$), ^{31}P (acetone-D_6) δ -145.7 (sept., $J_{P\text{-}F}$ 707 Hz, $P^{Counter\text{-}ion}$); *m/z* (HRMS, ESI-MS)$^{+}$ 400.1148 [M-PF_6] ($C_{22}H_{26}N^{96}Ru^{+}$ requires 400.1141).

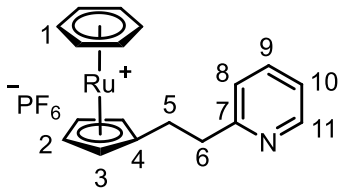

[Ru(η^{6}-benzene)(2-[2-(η^{5}-cyclopentadienyl)ethyl]pyridine)]PF_6 ***(4.7)***

Sodium carbonate (350 mg, 3.29 mmol, 10 eq.) was added to an oven-dried 2-neck round-bottom flask and was further dried by heating under reduced pressure. Subsequently, benzene ruthenium chloride dimer (165 mg, 0.33 mmol, 1 eq.), a 1:1 mixture of 2-[2-(Cyclopenta-1,3-dien-1-yl)ethyl]pyridine and
2-[2-(cyclopenta-1,4-dien-1-yl)ethyl] pyridine (562 mg, 3.29 mmol, 10 eq.) and anhydrous ethanol (15 mL)were added and the reaction mixture was heated to reflux under inert atmosphere for 24 h. The reaction mixture was then filtered, and the filtrate concentrated under reduced pressure to 2 mL. To the resulting brown liquid was added an aqueous solution of ammonium hexafluorophosphate (130 mg, 0.8 mmol, 2.5 eq.). The resulting brown residue was extracted with CH_2Cl_2 (4 x 20 mL) and the organic fractions were combined and dried over $MgSO_4$, then the solvent was removed under reduced pressure. The resulting dark brown residue was dissolved in a minimum of acetonitrile, then Et_2O (15 mL) was added. The liquid phase was decanted to give the title compound as a brown solid (99 mg, 0.20 mmol, 30%).

^{1}H NMR (599 MHz, acetone-D_6) δ 8.42 – 8.29 (1H, m, H^{11}), 7.60 – 7.46 (1H, m, H^{9}), 7.14 – 7.00 (2H, m, $H^{8, 10}$), 6.24 (6H, s, H^{1}), 5.42 – 5.31 (2H, m, $H^{2/3}$), 5.28 – 5.20 (2H, m, $H^{2/3}$), 2.90 – 2.79 (2H, m, H^{6}), 2.76 – 2.61 (2H, m, H^{5}), ^{13}C{^{1}H} NMR (151 MHz, acetone-D_6) δ 159.3 (s, C^{7}), 148.5 (s, C^{11}), 135.6 (s, C^{9}), 122.2 (s, $C^{8/10}$), 120.7 (s, $C^{8/10}$), 103.4 (s, C^{4}), 85.7 (s, C^{1}), 79.9 (s, $C^{2/3}$), 78.9 (s, $C^{2/3}$), 37.4 (s, C^{6}), 26.5 (s, C^{5}), ^{19}F NMR (376 MHz, Acetone-D_6) δ -72.50 (d, J = 707 Hz, $F^{\text{Counter-ion}}$), ^{31}P (acetone-D_6) δ -145.7 (sept., $J_{P\text{-}F}$ 707 Hz, $P^{\text{Counter-ion}}$); *m/z* (HRMS, ESI-MS)$^{+}$ 344.0522 [M-PF_6] ($C_{18}H_{18}N^{96}Ru^{+}$ requires 344.0515).

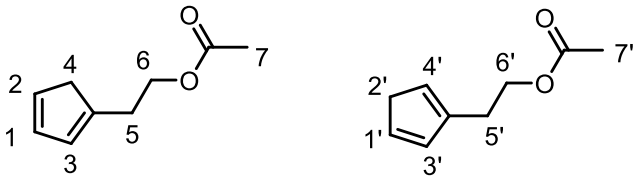

2-(cyclopenta-1,3-dien-1-yl)ethyl acetate and 2-(cyclopenta-1,4-dien-1-yl)ethyl acetate ***(4.24A+B)***

2-Bromoethyl acetate (0.9 mL, 8.40 mmol, 1 eq.) was dissolved in anhydrous THF (10 mL) before being cooled to -78 °C. To this solution, NaCp (4.5 mL, 9.80 mmol, 2.4 M solution in THF, 1.1 eq.) was added dropwise and the mixture was stirred for 18 h, during which time the reaction was allowed to warm to 25 °C. The resulting suspension was filtered through a plug of celite using CH_2Cl_2 (30 mL), before the filtrate was dried under reduced pressure to give a 1:1 mixture of the title compounds as a yellow oil (1.05 g, 6.90 mmol, 82%).

^{1}H NMR (400 MHz, Acetone-D^{6}) δ 6.58 – 5.91 (3H, m, $H^{1/1', 2/2', 3/3'}$), 4.39 – 4.00 (2H, m, $H^{6/6'}$), 2.95-2.87 (2H, m, $H^{4/4'}$), 2.69-2.60 (2H, m, $H^{5/5'}$), 2.05 – 1.94 (2H, m, $H^{7/7'}$).

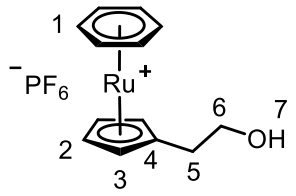

[Ru(η^6-benzene)(2-[2-(η^5-cyclopentadienyl)ethanol)]PF_6 ***(4.9)***

Sodium carbonate (350 mg, 3.29 mmol, 10 eq.) was added to an oven-dried 2-neck round-bottom flask and was further dried by heating under reduced pressure. Subsequently, benzeneruthenium chloride dimer (165 mg, 0.33 mmol, 1 eq.), a 1:1 mixture of 2-(cyclopenta-1,3-dien-1-yl)ethyl acetate and 2-(cyclopenta-1,4-dien-1-yl)ethyl acetate (500 mg, 3.29 mmol, 10 eq.) and anhydrous ethanol (15 mL)were added and the reaction mixture was heated to reflux under inert atmosphere for 24 h. The reaction mixture was then filtered, and the filtrate concentrated under reduced pressure to 2 mL. To the resulting brown liquid was added an aqueous solution of ammonium hexafluorophosphate (130 mg, 0.80 mmol, 2.5 eq.). The resulting brown residue was extracted with CH_2Cl_2 (4 x 20 mL) and the organic fractions were combined and dried over $MgSO_4$, then the solvent was removed under reduced pressure. The resulting dark brown residue was dissolved in a minimum of acetonitrile, then Et_2O (15 mL) was added. The liquid phase was decanted to give the title compound as a brown oil (105 mg, 0.24 mmol, 37%).

^{1}H NMR (599 MHz, acetone-D_6) δ 6.31 (6H, s, H^1), 5.58-5.56 (2H, m, H^3), 5.47-5.45 (2H, m, H^2), 3.87 (1H, t, *J* = 5.2 Hz, H^7), 3.72 – 3.65 (2H, m, H^6), 2.56 (2H, t, *J* = 6.1 Hz, H^5), ^{13}C{^{1}H} NMR (151 MHz, acetone-D_6) δ 102.3 (s, C^4), 86.3 (s, C^1), 81.1 (s, C^3), 79.5 (s, C^2), 61.2 (s, C^6), 30.9 (s, C^5), ^{19}F NMR (376 MHz, Acetone-D_6) δ -72.5 (d, *J* = 707 Hz, $F^{Counter\text{-}ion}$), ^{31}P{^{1}H} (acetone-D_6) δ -145.7 (sept., $J_{P\text{-}F}$ 707 Hz, $P^{Counter\text{-}ion}$); *m/z* (HRMS, ESI-MS)$^+$ 283.0209 [M-PF_6] ($C_{13}H_{15}O^{96}Ru^+$ requires 283.0199).

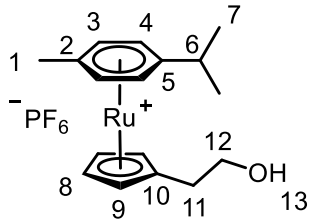

[Ru(η^6-p-cymene)(2-[2-(η^5-cyclopentadienyl)ethanol)]PF_6 ***(4.10)***

Sodium carbonate (350 mg, 3.29 mmol, 10 eq.) was added to an oven-dried 2-neck round-bottom flask and was further dried by heating under reduced pressure. Subsequently, *p*-cymene ruthenium chloride dimer (200 mg, 0.33 mmol, 1 eq.), a 1:1 mixture of 2-(cyclopenta-1,3-dien-1-yl)ethyl acetate and 2-(cyclopenta-1,4-dien-1-yl)ethyl acetate (500 mg, 3.29 mmol, 10 eq.) and anhydrous ethanol (15 mL)were added and the reaction mixture was heated to reflux under inert atmosphere for 24 h. The reaction mixture was then filtered, and the filtrate concentrated under reduced pressure to 2 mL. To the resulting brown liquid was added an aqueous solution of ammonium hexafluorophosphate (130 mg, 0.80 mmol, 2.5 eq.). The resulting brown residue was extracted with CH_2Cl_2 (4 x 20 mL) and the organic fractions were combined and dried over $MgSO_4$, then the solvent was removed under reduced pressure. The resulting dark brown residue was dissolved in a minimum of acetonitrile, then Et_2O (15 mL) was added. The liquid phase was decanted to give the title compound as a brown oil (200 mg, 0.40 mmol, 62%).

^{1}H NMR (599 MHz, acetone-D_6) δ 6.32-6.24 (4H, m, $H^{3,4}$), 5.47-5.42 (2H, m, H^9), 5.39-5.34 (2H, m, H^8), 3.94 (1H, t, *J* = 5.1 Hz, H^{13}), 3.69 (2H, td, *J* = 6.2, 4.0 Hz, H^{12}), 2.82 – 2.77 (1H, m, H^6), 2.51 (2H, t, *J* = 6.1 Hz, H^{11}), 2.37 (3H, s, H^1), 1.29 (6H, d, *J* = 6.9 Hz, H^7), ^{13}C{^{1}H} NMR (151 MHz, acetone-D_6) δ 112.1 (s, C^5), 101.4 (s, C^{10}), 101.2 (s, C^2), 86.8 (s, C^3), 84.4 (s, C^4), 81.3 (s, C^9), 79.7 (s, C^8), 61.3 (s, C^{12}), 31.7 (s, C^6), 30.7 (s, C^{11}), 22.6 (s, C^7), 18.8 (s, C^1), ^{19}F NMR (376 MHz, Acetone-D_6) δ -72.50 (d, *J* = 707 Hz, $F^{Counter-ion}$), ^{31}P NMR (acetone-D_6) δ -145.7 (sept., J_{P-F} 707 Hz, $P^{Counter-ion}$); *m/z* (HRMS, ESI-MS)$^+$ 339.0825 [M-PF_6] ($C_{17}H_{23}O^{96}Ru^+$ requires 339.0825).

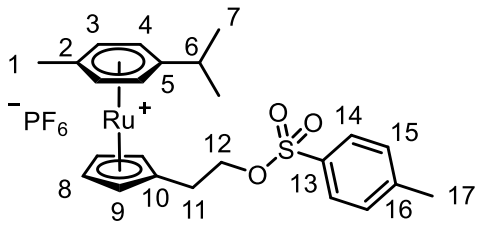

[Ru(η^6-p-cymene)(2-[2-cyclopentadienylethyl 4-methylbenzenesulfonate)]PF_6 ***(4.25)***

To an oven-dried Schlenk flask were added [Ru(η^6-p-cymene)(2-[2-(η^5-cyclopentadienyl)ethanol)]PF_6 (30 mg, 0.061 mmol, 1 eq.) and tosyl chloride (26 mg, 0.12 mmol, 2 eq.), then dissolved in anhydrous CH_2Cl_2 (3 mL). The solution was cooled to 0 °C, then pyridine (10 μL, 0.12 mmol, 2 eq.) was added and the mixture was stirred for 16 hours. The mixture was then filtered and the filtrate concentrated to dryness under vacuum. The crude brown residue was dissolved in a minimum of acetone, then added to diethyl ether (10 mL), resulting in formation of a brown precipitate. The solution phase was decanted off and the solid washed with diethyl ether (3 x 5 mL) to give the title compound as a light brown solid (35 mg, 0.054 mmol, 89%).

^{1}H NMR (599 MHz, acetone-D_6) δ 7.76 (2H, d, *J* = 8.3 Hz, H^{14}), 7.48 (2H, d, *J* = 8.0 Hz, H^{15}), 6.25 (4H, d, *J* = 1.4 Hz, H$^{3, 4}$), 5.44.-5.42 (2H, m, H^9), 5.38-5.35 (2H, m, H^8), 4.21 (2H, t, *J* = 6.0 Hz, H^{12}), 2.77 – 2.72 (3H, m, H$^{6, 11}$), 2.45 (3H, s, H^{17}), 2.36 (3H, s, H^1), 1.27 (6H, d, *J* = 7.0 Hz, H^7), ^{13}C{^{1}H} NMR (151 MHz, acetone-D_6) δ 145.2 (s, C^{16}), 132.9 (s, C^{13}), 130.1 (s, C^{15}), 127.8 (s, C^{14}), 112.4 (s, C^5), 101.6 (s, C^2), 98.2 (s, C^{10}), 87.0 (s, C^3), 84.7 (s, C^4), 81.2 (s, C^9), 80.1 (s, C^8), 69.7 (s, C^{12}), 31.7 (s, C^6), 27.2 (s, C^{11}), 22.6 (s, C^7), 20.6 (s, C^{17}), 18.7 (s, C^1), ^{19}F NMR (376 MHz, Acetone-D_6) δ -72.5 (d, *J* = 707 Hz, F$^{Counter-ion}$), ^{31}P NMR (acetone-D_6) δ -145.7 (sept., J_{P-F} 707 Hz, P$^{Counter-ion}$); *m/z* (HRMS, ESI-MS)$^+$ 493.0917 [M-PF_6] ($C_{24}H_{29}O_3S^{96}Ru^+$ requires 493.0913).

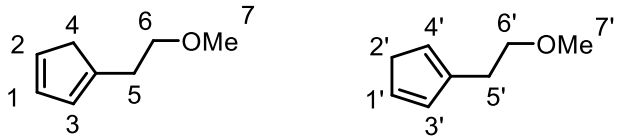

*1-(2-methoxyethyl)cyclopenta-1,3-diene and 2-(2-methoxyethyl)cyclopenta-1,3-diene (**4.28A+B**)*

2-Bromoethyl methyl ether (1.0 mL, 10.6 mmol, 1 eq.) was dissolved in anhydrous THF (10 mL) before being cooled to -78 °C. To this solution, NaCp (4.5 mL, 2.4 M solution in THF, 1 eq.) was added dropwise and the mixture was stirred for 18 h, during which time the reaction was allowed to warm to 25 °C. The resulting suspension was filtered through a plug of celite using CH_2Cl_2 (30 mL), before the filtrate was dried under reduced pressure to give a 1:1 mixture of the title compounds as a yellow oil (1.17 g, 9.43 mmol, 89%).

^{1}H NMR (400 MHz, $CDCl_3$) δ 6.51 – 6.06 (3H, m, $H^{1/1', 2/2', 3/3'}$), 3.60 – 3.51 (2H, m, $H^{6/6'}$), 3.38 – 3.33 (3H, m, $H^{7/7'}$), 2.97 – 2.86 (2H, m, $H^{4/4'}$), 2.73 – 2.55 (2H, m, $H^{5/5'}$).

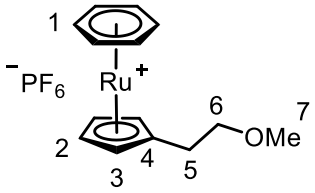

*[Ru(η^6-benzene)(2-[2-(η^5-(1-(2-methoxyethyl)cyclopentadienyl)]PF_6 (**4.11**)*

Sodium carbonate (350 mg, 3.29 mmol, 10 eq.) was added to an oven-dried 2-neck round-bottom flask and was further dried by heating under reduced pressure. Subsequently, p-cymene ruthenium chloride dimer (165 mg, 0.33 mmol, 1 eq.), a 1:1 mixture of 1-(2-methoxyethyl)cyclopenta-1,3-diene and 2-(2-methoxyethyl)cyclopenta-1,3-diene (408 mg, 3.29 mmol, 10 eq.) and anhydrous ethanol (15 mL)were added and the reaction mixture was heated to reflux under inert atmosphere for 24 h. The reaction mixture was then filtered, and the filtrate concentrated under reduced pressure to 2 mL. To the resulting brown liquid was added an aqueous solution of ammonium hexafluorophosphate (130 mg, 0.80 mmol, 2.5 eq.). The resulting brown residue was extracted with CH_2Cl_2 (4 x 20 mL) and the organic fractions were combined and dried over $MgSO_4$, then the solvent was removed under reduced pressure. The resulting dark brown residue was dissolved in a minimum of

acetonitrile, then Et_2O (15 mL) was added. The liquid phase was decanted to give the title compound as a brown solid (140 mg, 0.31 mmol, 48%).

^1H NMR (599 MHz, acetone-D_6) δ 6.32 (6H, s, H^1), 5.55-5.41 (2H, m, H^3), 5.41-5.38 (2H, m, H^2), 3.51 (2H, t, *J* = 6.1 Hz, H^6), 3.30 (3H, s, H^7), 2.62 (2H, t, *J* = 6.0 Hz, H^5), $^{13}C\{^1H\}$ NMR (151 MHz, acetone-D_6) δ 102.0 (s, C^4), 86.4 (s, C^1), 80.9 (s, C^3), 79.5 (s, C^2), 71.3 (s, C^6), 57.6 (s, C^7), 27.9 (s, C^5), ^{19}F NMR (376 MHz, Acetone-D_6) δ -72.5 (d, *J* = 707 Hz, $F^{Counter\text{-}ion}$), ^{31}P (acetone-D_6) δ -145.7 (sept., $J_{P\text{-}F}$ 707 Hz, $P^{Counter\text{-}ion}$); *m/z* (HRMS, ESI-MS)$^+$ 297.0368 [M-PF_6] ($C_{14}H_{17}O^{96}Ru^+$ requires 297.0355).

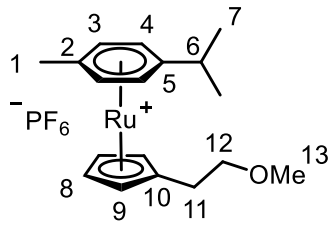

[Ru(η^6-p-cymene)(2-[2-(η^5-(1-(2-methoxyethyl)cyclopentadienyl)]PF_6 ***(4.12)***

Sodium carbonate (350 mg, 3.29 mmol, 10 eq.) was added to an oven-dried 2-neck round-bottom flask and was further dried by heating under reduced pressure. Subsequently, p-cymene ruthenium chloride dimer (200 mg, 0.33 mmol, 1 eq.), a 1:1 mixture of 1-(2-methoxyethyl)cyclopenta-1,3-diene and 2-(2-methoxyethyl)cyclopenta-1,3-diene (408 mg, 3.29 mmol, 10 eq.) and anhydrous ethanol (15 mL)were added and the reaction mixture was heated to reflux under inert atmosphere for 24 h. The reaction mixture was then filtered, and the filtrate concentrated under reduced pressure to 2 mL. To the resulting brown liquid was added an aqueous solution of ammonium hexafluorophosphate (130 mg, 0.80 mmol, 2.5 eq.). The resulting brown residue was extracted with CH_2Cl_2 (4 x 20 mL) and the organic fractions were combined and dried over $MgSO_4$, then the solvent was removed under reduced pressure. The resulting dark brown residue was dissolved in a minimum of acetonitrile, then Et_2O (15 mL) was added. The liquid phase was decanted to give the title compound as a brown oil (225 mg, 0.44 mmol, 68%).

^{1}H NMR (599 MHz, acetone-D_6) δ 6.25 – 6.20 (4H, m, $H^{3,4}$), 5.42-5.40 (2H, m, H^{9}), 5.35-5.33 (2H, m, H^{8}), 3.50 (2H, t, *J* = 6.1 Hz, H^{12}), 3.29 (3H, s, H^{13}), 2.82 – 2.76 (1H, m, H^{6}), 2.57 (2H, t, *J* = 6.1 Hz, H^{11}), 2.36 (3H, s, H^{1}), 1.29 (6H, d, *J* = 6.9 Hz, H^{7}), ^{13}C{^{1}H} NMR (151 MHz, acetone-D_6) δ 112.1 (s, C^{5}), 101.3 (s, C^{2}), 101.1 (s, C^{10}), 86.9 (s, C^{3}), 84.5 (s, C^{4}), 81.2 (s, C^{9}), 79.8 (s, C^{8}), 71.5 (s, C^{12}), 57.6 (s, C^{13}), 31.7 (s, C^{6}), 27.7 (s, C^{11}), 22.6 (s, C^{7}), 18.7 (s, C^{1}), ^{19}F NMR (376 MHz, Acetone-D_6) δ -72.50 (d, *J* = 707 Hz, $F^{Counter\text{-}ion}$), ^{31}P (acetone-D_6) δ -145.7 (sept., $J_{P\text{-}F}$ 707 Hz, $P^{Counter\text{-}ion}$); *m/z* (HRMS, ESI-MS)$^{+}$ 353.0997 [M-PF_6] ($C_{18}H_{25}O^{96}Ru^{+}$ requires 353.0981).

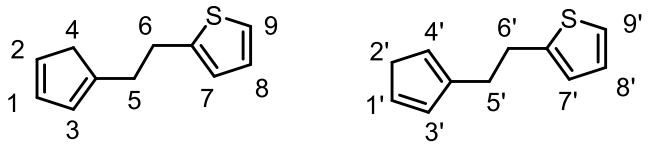

*2-(2-(cyclopenta-1,3-dien-1-yl)ethyl)thiophene and 2-(2-(cyclopenta-1,4-dien-1-yl)ethyl)thiophene (**4.30A+B**)*

2-Thiopheneethanol (0.93 mL, 8.40 mmol, 1 eq.), methanesulfonic anhydride (2.19 g, 12.6 mmol, 1.5 eq.) and DIPEA (2.93 mL, 16.8 mmol, 2 eq.) were combined in anhydrous THF (15 mL) and stirred at 25 °C for 2 hours. The reaction mixture was then dried under reduced pressure and the yellow residue dissolved in CH_2Cl_2 (20 mL). The organic layer was washed with water (3 x 15 mL), then dried over $MgSO_4$ before the solvent was removed under reduced pressure to give 2-(pyridin-2-yl)ethyl methanesulfonate as a pale yellow oil. The 1:1 mixture 2-(thiophene-2-yl)ethyl methanesulfonate isomers were then dissolved in anhydrous THF (10 mL) before being cooled to -78 °C. To this solution, NaCp (3.9 mL, 2.4 M solution in THF, 1.1 eq.) was added dropwise and the mixture was stirred for 18 h, during which time the reaction was allowed to warm to 25 °C. The resulting suspension was filtered through a plug of celite using CH_2Cl_2 (30 mL), before the filtrate was dried under reduced pressure to give a 1:1 mixture of the title compounds as a yellow oil (1.38 g, 7.90 mmol, 94%).

^{1}H NMR (400 MHz, $CDCl_3$) δ 7.13 – 7.06 (1H, m, $H^{9/9'}$), 6.93 – 6.88 (1H, m, $H^{8/8'}$), 6.82 – 6.77 (1H, m, $H^{7/7'}$), 6.48 – 6.03 (3H, m, $H^{1/1',2/2',3/3'}$), 3.07 (2H, dddd, *J* = 9.2, 6.7, 6.0, 1.0 Hz, $H^{6/6'}$), 2.93 (2H, dq, *J* = 25.4, 1.5 Hz, H^{4}), 2.82 – 2.71 (2H, m, $H^{5/5'}$).

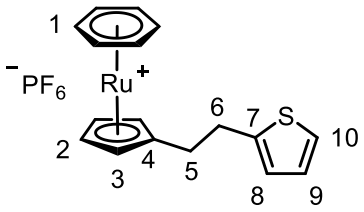

[Ru(η^6-benzene)(2-[2-[η^5-(cyclopentadienyl)ethy)lthiophenel]]PF_6 ***(4.14)***

Sodium carbonate (300 mg, 2.84 mmol, 10 eq.) was added to an oven-dried 2-neck round-bottom flask and was further dried by heating under reduced pressure. Subsequently, benzeneruthenium chloride dimer (142 mg, 0.28 mmol, 1 eq.), a 1:1 mixture of 2-(2-(cyclopenta-1,3-dien-1-yl)ethyl)thiophene and 2-(2-(cyclopenta-1,4-dien-1-yl)ethyl)thiophene (500 mg, 2.84 mmol, 10 eq.) and anhydrous ethanol (15 mL)were added and the reaction mixture was heated to reflux under inert atmosphere for 24 h. The reaction mixture was then filtered, and the filtrate concentrated under reduced pressure to 2 mL. To the resulting brown liquid was added an aqueous solution of ammonium hexafluorophosphate (115 mg, 0.71 mmol, 2.5 eq.). The resulting brown residue was extracted with CH_2Cl_2 (4 x 20 mL) and the organic fractions were combined and dried over $MgSO_4$, then the solvent was removed under reduced pressure. The resulting dark brown residue was dissolved in a minimum of acetonitrile, then Et_2O (15 mL) was added. The liquid phase was decanted to give the title compound as a brown solid (136 mg, 0.27 mmol, 48%).

^{1}H NMR (599 MHz, acetone-D_6) δ 7.25 (1H, dd, *J* = 5.1, 1.2 Hz, H^{10}), 6.92 (1H, dd, *J* = 5.1, 3.4 Hz, H^9), 6.86 (1H, dd, *J* = 3.4, 1.1 Hz, H^8), 6.31 (6H, s, H^1), 5.51-5.50 (2H, m, H^2), 5.42-5.39 (2H, m, H^3), 3.06 (2H, ddd, *J* = 8.9, 6.8, 0.9 Hz, H^6), 2.77 – 2.73 (2H, m, H^5), ^{13}C{^{1}H} NMR (151 MHz, acetone-D_6) δ 142.9 (s, C^7), 126.8 (s, C^9), 125.0 (s, C^8), 123.5 (s, C^{10}), 103.0 (s, C^4), 86.4 (s, C^1), 80.7 (s, C^3), 79.7 (s, C^2), 30.3 (s, C^6), 29.9 (s, C^5), ^{19}F NMR (376 MHz, Acetone-D_6) δ -72.5 (d, *J* = 707 Hz, $F^{Counter\text{-}ion}$), ^{31}P (acetone-D_6) δ -145.7 (sept., $J_{P\text{-}F}$ 707 Hz, $P^{Counter\text{-}ion}$); *m/z* (HRMS, ESI-MS)$^+$ 349.0140 [M-PF_6] ($C_{17}H_{17}S^{96}Ru^+$ requires 349.0127).

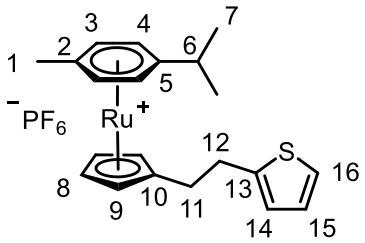

[Ru(η^6-p-cymene)(2-[2-[η^5-(cyclopentadienyl)ethy)lthiophene]]PF_6 ***(4.14)***

Sodium carbonate (300 mg, 2.84 mmol, 10 eq.) was added to an oven-dried 2-neck round-bottom flask and was further dried by heating under reduced pressure. Subsequently, p-cymene ruthenium chloride dimer (174 mg, 0.28 mmol, 1 eq.), a 1:1 mixture of 2-(2-(cyclopenta-1,3-dien-1-yl)ethyl)thiophene and 2-(2-(cyclopenta-1,4-dien-1-yl)ethyl)thiophene (500 mg, 2.84 mmol, 10 eq.) and anhydrous ethanol (15 mL)were added and the reaction mixture was heated to reflux under inert atmosphere for 24 h. The reaction mixture was then filtered, and the filtrate concentrated under reduced pressure to 2 mL. To the resulting brown liquid was added an aqueous solution of ammonium hexafluorophosphate (115 mg, 0.71 mmol, 2.5 eq.). The resulting brown residue was extracted with CH_2Cl_2 (4 x 20 mL) and the organic fractions were combined and dried over $MgSO_4$, then the solvent was removed under reduced pressure. The resulting dark brown residue was dissolved in a minimum of acetonitrile, then Et_2O (15 mL) was added. The liquid phase was decanted to give the title compound as a brown oil (190 mg, 0.34 mmol, 60%).

^{1}H NMR (599 MHz, acetone-D_6) δ 7.26 (1H, dd, *J* = 5.2, 1.2 Hz, H^{16}), 6.93 (1H, dd, *J* = 5.2, 3.4 Hz, H^{15}), 6.86 – 6.83 (1H, m, H^{14}), 6.26 (4H, s, $H^{3, 4}$), 5.42-5.40 (2H, m, H^9), 5.37-5.36 (2H, m, H^8), 3.07 (2H, td, *J* = 7.6, 0.9 Hz, H^{12}), 2.84 – 2.76 (1H, m, H^6), 2.72 (2H, dd, *J* = 8.5, 6.9 Hz, H^{11}), 2.38 (3H, s, H^1), 1.29 (6H, d, *J* = 7.0 Hz, H^7), ^{13}C{^{1}H} NMR (151 MHz, acetone-D_6) δ 142.8 (s, C^{13}), 126.8 (s, C^{15}), 125.7 (s, C^{14}), 123.6 (s, C^{16}), 112.2 (s, C^5), 102.1 (s, C^{10}), 101.4 (s, C^2), 86.9 (s, C^3), 84.5 (s, C^4), 80.9 (s, C^9), 79.9 (s, C^8), 31.7 (s, C^6), 30.5 (s, C^{12}), 29.8 (s, C^{11}), 22.6 (s, C^7), 18.8 (s, C^1), ^{19}F NMR (376 MHz, Acetone-D_6) δ -72.50 (d, *J* = 707 Hz, $F^{Counter\text{-}ion}$), ^{31}P (acetone-D_6) δ -145.7 (sept., $J_{P\text{-}F}$ 707 Hz, $P^{Counter\text{-}ion}$); *m/z* (HRMS, ESI-MS)$^+$ 405.0768 [M-PF_6] ($C_{21}H_{25}S^{96}Ru^+$ requires 405.0753).

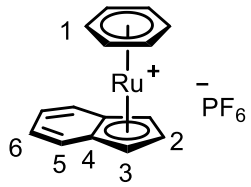

[Ru(η^6-benzene)(2-[2-(η^5-indenyl)]PF_6 ***(4.15)***

Sodium hydroxide (131 mg, 3.29 mmol, 10 eq.) was added to an oven-dried 2-neck round-bottom flask and was further dried by heating under reduced pressure. Subsequently, benzeneruthenium chloride dimer (165 mg, 0.33 mmol, 1 eq.), indene (0.38 mL, 3.29 mmol, 10 eq.) and anhydrous ethanol (15 mL)were added and the reaction mixture was heated to reflux under inert atmosphere for 24 h. The reaction mixture was then filtered, and the filtrate concentrated under reduced pressure to 2 mL. To the resulting brown liquid was added an aqueous solution of ammonium hexafluorophosphate (130 mg, 0.80 mmol, 2.5 eq.). The resulting brown residue was extracted with CH_2Cl_2 (4 x 20 mL) and the organic fractions were combined and dried over $MgSO_4$, then the solvent was removed under reduced pressure. The resulting dark brown residue was dissolved in a minimum of acetonitrile, then Et_2O (15 mL) was added. The liquid phase was decanted to give the title compound as a brown solid (50 mg, 0.11 mmol, 17%).

^{1}H NMR (599 MHz, acetone-D_6) δ 7.64 (2H, dd, *J* = 6.7, 3.0 Hz, H^5), 7.30 (2H, dd, *J* = 6.8, 3.0 Hz, H^6), 6.23 (2H, d, *J* = 2.4 Hz, H^3), 6.00 (6H, s, H^1), 5.49 (1H, t, *J* = 2.5 Hz, H^2), ^{13}C{^{1}H} NMR (151 MHz, acetone-D_6) δ 129.0 (s, C^6), 125.5 (s, C^5), 98.3 (s, C^4), 86.2 (s, C^1), 80.6 (s, C^2), 74.6 (s, C^3), ^{19}F NMR (376 MHz, Acetone-D_6) δ -72.50 (d, *J* = 707 Hz, $F^{Counter\text{-}ion}$), ^{31}P (acetone-D_6) δ -145.7 (sept., $J_{P\text{-}F}$ 707 Hz, $P^{Counter\text{-}ion}$); *m/z* (HRMS, ESI-MS)$^+$ 289.0098 [M-PF_6] ($C_{15}H_{13}{}^{96}Ru^+$ requires 289.0093).

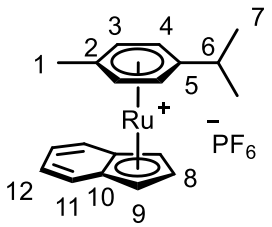

[Ru(η^6-p-cymene)(2-[2-(η^5-indenyl)]PF_6 ***(4.16)***

Sodium hydroxide (131 mg, 3.29 mmol, 10 eq.) was added to an oven-dried 2-neck round-bottom flask and was further dried by heating under reduced pressure. Subsequently, *p*-cymene ruthenium chloride dimer (200 mg, 0.33 mmol, 1 eq.), indene (0.38 mL. 3.29

mmol, 10 eq.) and anhydrous ethanol (15 mL)were added and the reaction mixture was heated to reflux under inert atmosphere for 24 h. The reaction mixture was then filtered, and the filtrate concentrated under reduced pressure to 2 mL. To the resulting brown liquid was added an aqueous solution of ammonium hexafluorophosphate (130 mg, 0.80 mmol, 2.5 eq.). The resulting brown residue was extracted with CH_2Cl_2 (4 x 20 mL) and the organic fractions were combined and dried over $MgSO_4$, then the solvent was removed under reduced pressure. The resulting dark brown residue was dissolved in a minimum of acetonitrile, then Et_2O (15 mL) was added. The liquid phase was decanted to give the title compound as a brown solid (180 mg, 0.36 mmol, 55%).

^{1}H NMR (599 MHz, acetone) δ 7.56 (2H, dd, *J* = 6.8, 3.0 Hz, H^{11}), 7.37 (2H, dd, *J* = 6.8, 3.0 Hz, H^{12}), 6.15 (2H, d, *J* = 2.3 Hz, H^9), 6.06 (2H, d, *J* = 5.6 Hz, H^4), 5.82 (2H, d, *J* = 5.7 Hz, H^3), 5.44 (1H, t, *J* = 2.3 Hz, H^8), 2.60-2.56 (1H, m, *J* = 6.9 Hz, H^6), 1.92 (3H, s, H^1), 1.24 (6H, d, *J* = 6.9 Hz, H^7), ^{13}C{^{1}H} NMR (151 MHz, acetone-D_6) δ 128.8 (s, C^{12}), 125.0 (s, C^{11}), 109.6 (s, C^5), 99.5 (s, C^2), 97.9 (s, C^{10}), 86.9 (s, C^3), 84.0 (s, C^4), 81.6 (s, C^8), 74.7 (s, C^9), 31.1 (s, C^6), 22.2 (s, C^7), 16.9 (s, C^1), ^{19}F NMR (376 MHz, Acetone-D_6) δ -72.5 (d, *J* = 707 Hz, $F^{Counter\text{-}ion}$), ^{31}P (acetone-D_6) δ -145.7 (sept., $J_{P\text{-}F}$ 707 Hz, $P^{Counter\text{-}ion}$); *m/z* (HRMS, ESI-MS)$^+$ 345.0718 [M-PF_6] ($C_{19}H_{21}{}^{96}Ru^+$ requires 345.0719).

Arene Exchange Studies

General Procedure Heat-Assisted Arene Exchange

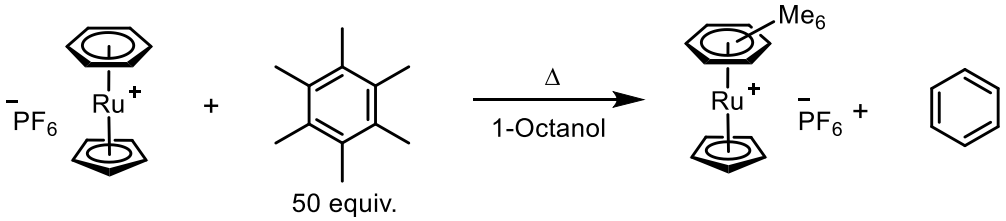

To a flame-dried Schlenk flask was added complex [(η^6-C_6H_6)RuCp][PF_6] (1 mg, 2.5 μmol, 1 equiv.), hexamethyl benzene (21 mg, 0.15 mmol, 60 equiv.) and 1-octanol (1 mL), then the mixture was left to stir for 48 hours at 120, 150 or 180 °C. Aliquots of the reaction mixture were taken at certain time points and analysed by ESI-MS on a Waters QTOF spectrometer. Data analysis was done by comparing relative integrals of peaks corresponding to each complex, and then calculating the % of starting complex remaining at each time point, then plotting % of complex [(η^6-C_6H_6)RuCp][PF_6] against time.

General Procedure for Photocatalytic Heat-Assisted Arene Exchange

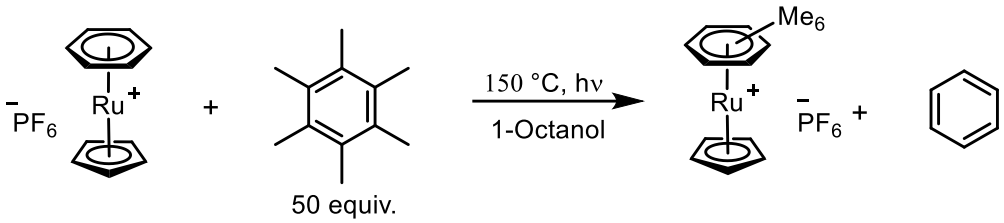

To a flame-dried Schlenk flask was added complex [(η^6-C_6H_6)RuCp][PF_6] (1 mg, 2.5 μmol, 1 equiv.), hexamethyl benzene (21 mg, 0.15 mmol, 60 equiv.) and 1-octanol (1 mL), then the mixture was left to stir for 48 hours while exposed to 365 nm light (ca. 5 cm) at rt. Aliquots of the reaction mixture were taken at certain time points and analysed by ESI-MS on a Waters QTOF spectrometer.

Data Analysis of Arene Exchange Reactions

The following procedure, using MestReNova version 14.2.1 was used to determine all arene exchange conversions.

Open the MS file in MestReNova > select 'mass analysis' > 'New mass chromatogram' > 'Manually' > The range of mass selected was 2 Da either side of the major monoisotopic mass for each complex. Once the new chromatogram is generated, select 'properties' > 'peaks', 'show second line label' > 'area'. The relative areas of the two peaks were used to calculate a % conversion at any given time. Conversion was calculated using the equation:

$$\%\, Conversion\ = 100\left(\frac{[B]}{[A]+[B]}\right) \qquad \text{(Equation 1)}$$

Where [A] is the relative integral (concentration) of the starting complex; and [B] is the relative integral (concentration) of the exchange product.

The % conversions were plotted against time in MS excel. Assuming a first order rate law, the half life for the exchange was calculated according to the equations:

$$[A] = [A]_0 e^{-kt} \qquad \text{(Equation 2)}$$

$$t_{1/2} = \frac{Ln(2)}{k} \qquad \text{(Equation 3)}$$

Where [A] is the concentration of the starting complex at a given time; $[A]_0$ = initial concentration of the starting complex; t = time; and $t_{1/2}$ = half life of the exchange reaction. All calculations performed here use the assumption that the precursor and product Ru complexes behave identically in the ESI-MS spectrometer.

7.2.4. Chapter 5 – Ruthenium-Catalysed Aromatic Transformations *via* Transient η^6Arene Complexes

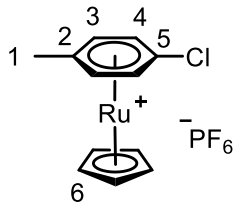

[Ru(η^6-4-chlorotoluene)(η^5-cyclopentadienyl)]PF_6 ***(4.5)***

Tris(acetonitrile)cyclopentadienylruthenium(II) hexafluorophosphate (100 mg, 0.236 mmol, 1 eq.) was dissolved in anhydrous 1,2-DCE (8 mL). 4-chlorotoluene (32 mg, 30 µL, 0.253 mmol, 1.1 eq.) was added and the reaction was stirred at reflux under inert atmosphere overnight. The reaction mixture was cooled to room temperature, filtered and the filtrate dried in *vacuo* to give a brown solid. The crude product was dissolved in a minimum of acetonitrile, then added dropwise to diethyl ether (10 mL). The liquid phase was decanted off and the resulting solid dried to give the title compound as a brown solid (94 mg, 0.222 mmol, 93 %).

^{1}H NMR (599 MHz, acetone-D_6) δ 6.74 (2H, d, *J* = 6.3 Hz, H^4), 6.48 (2H, d, *J* = 6.2 Hz, H^3), 5.60 (5H, s, H^6), 2.39 (3H, s, H^1), ^{13}C{^{1}H} NMR (151 MHz, acetone-D_6) δ 104.3 (s, C^5), 102.3 (s, C^2), 87.0 (s, C^3), 86.9 (s, C^4), 82.6 (s, C^6), 18.9 (s, C^1), ^{19}F NMR δ -72.6 (d, *J* = 707 Hz, $F^{Counter\text{-}ion}$), ^{31}P NMR (acetone-D_6) δ -145.7 (sept., $J_{P\text{-}F}$ 707 Hz, $P^{Counter\text{-}ion}$); *m/z* (HRMS, ESI-MS)$^+$ 286.9707 [M-PF_6] ($C_{12}H_{12}{}^{35}Cl^{96}Ru^+$ requires 286.9703).

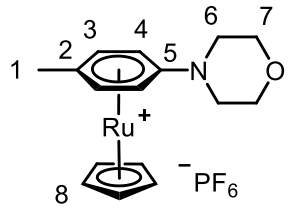

[Ru(η^6-4-(p-tolyl)morpholine)(η^5-cyclopentadienyl)]PF_6 ***(5.4)***

To a flame-dried Schlenk flask was added [CpRu(η^6-4-chlorotoluene)][PF_6] (60 mg, 0.137 mmol, 1 eq.), morpholine (24 mg, 24 µL, 0.274 mmol, 2 eq.) and degassed N,N-DMF (3 mL), then the solution was stirred at 60 ºC for 16 hours. The crude mixture was filtered, dried in *vacuo* and dissolved in a minimum of MeCN (0.2 mL), then added dropwise to Et_2O (4 mL) to give a brown solid. Further purification was achieved by eluting the crude compound through a silica plug (2 % MeOH in CH_2Cl_2), then subsequent precipitation from Et_2O (3 mL) to give the title compound as a white solid (50 mg, 87%).

^{1}H NMR (700 MHz, Acetone-D_6) δ 6.13 (2H, d, J = 6.8 Hz, H^3), 6.04 (2H, d, J = 6.8 Hz, H^4), 5.46 (5H, s, H^8), 3.80-3.75 (4H, m, H^7), 3.10-3.06 (4H, m, H^6), 2.35 (3H, s, H^1), ^{13}C NMR (Hz, Acetone-D_6) δ 124.5 (s, C^5), 98.2 (s, C^2), 84.8 (s, C^3), 78.6 (s, C^8), 69.4 (s, C^4), 65.4 (s, C^7), 47.2 (s, C^6), 18.8 (s, C^1), ^{19}F NMR -72.6 (d, J = 707 Hz, PF_6), ^{31}P NMR (acetone-D_6) δ -145.7 (sept., $J_{P\text{-}F}$ 707 Hz, $P^{Counter\text{-}ion}$); *m/z* (HRMS, ESI-MS)$^+$ 338.0641 [M-PF_6]$^+$ ($C_{16}H_{20}NO^{96}Ru^+$ requires 338.0652)

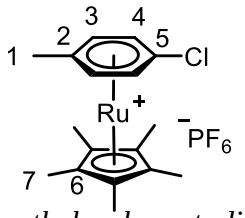

[Ru(η^6-4-chlorotoluene)(η^5-pentamethylcyclopentadienyl)]PF_6 ***(5.7)***

Tris(acetonitrile)pentamethylcyclopentadienylruthenium(II) hexafluorophosphate (80 mg, 0.157 mmol, 1 eq.) was dissolved in anhydrous 1,2-DCE (8 mL). 4-chlorotoluene (23 mg, 21 µL, 0.179 mmol, 1.1 eq.) was added and the reaction was stirred at reflux under inert atmosphere overnight. The reaction mixture was cooled to room temperature, filtered and the filtrate dried in *vacuo* to give a brown solid. The crude product was dissolved in a minimum of acetonitrile, then added dropwise to diethyl ether (10 mL). The liquid phase

was decanted off and the resulting solid dried to give the title compound as an off-white solid (75 mg, 0.149 mmol, 93%).

^{1}H NMR (600 MHz, Acetone-D_6) δ 6.32 (2H, d, J 6.2 Hz, H^4), 6.07 (2H, d, J 6.2 Hz, H^3), , 2.35 (3H, s, H^1), 2.01 (15H, s, H^7) ^{13}C{^{1}H} NMR (151 MHz, Acetone-D_6) δ 105.2 (s, C^6) 103.2 (s, C^5), 100.8, (s, C^2) 97.1 (s, C^5), 88.5 (s, $C^{3/4}$), 88.4 (s, $C^{3/4}$), 16.8 (s, C^1), 9.6 (s, C^7), ^{19}F NMR δ -72.6(d, *J* = 707 Hz, $F^{Counter\text{-}ion}$), ^{31}P NMR (acetone-D_6) δ -145.7 (sept., $J_{P\text{-}F}$ 707 Hz, $P^{Counter\text{-}ion}$); *m/z* (HRMS, ESI-MS)$^+$ 357.0454 [M-PF_6] ($C_{17}H_{22}{}^{35}Cl^{96}Ru^+$ requires 357.0486).

Heat Assisted Ru-Catalysed SNAr Amination

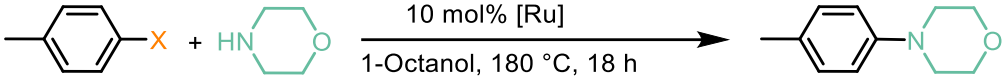

General Procedure

To a flame dried Schlenk flask were added *p*-chlorotoluene (40 µL, 0.34 mmol, 1.0 eq.), or *p*-fluorotoluene, morpholine (84 µL, 1 mmol, 3 eq.) the Ru catalyst (10 mol%) and solvent (0.7 mL). The mixture was heated at 180 °C for 18 hours. Conversion (%) was measured using ^{1}H NMR spectroscopy by comparing the aromatic peaks of the product (*ca*. 6.8 and 7.0 ppm) and starting material (*ca*. 7.0 and 7.2 ppm).

Light Assisted Ru-Catalysed SNAr Amination

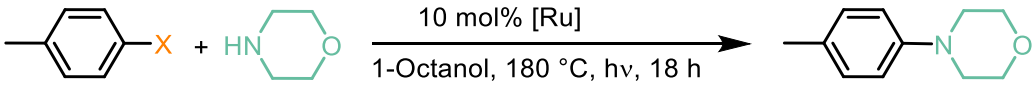

General Procedure

To a flame dried Schlenk flask were added *p*-chlorotoluene (1.0 eq.), morpholine (3 eq.) the Ru catalyst (10 mol%) and solvent (0.7 mL). The mixture was heated at 120, 150 or 180 °C, with irradiation by 420, 380 or 360 nm light for 18 hours. Conversion (%) was measured using ^{1}H NMR spectroscopy by comparing the aromatic peaks of the product (ca. 6.8 and 7.0 ppm) and starting material (ca. 7.0 and 7.2 ppm).

Ruthenium-Catalysed Hydrodeiodination

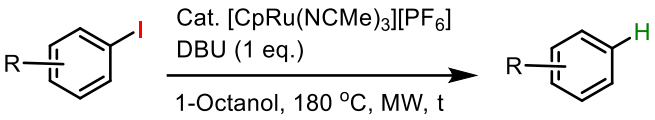

General Procedure for Ru-catalysed Hydrodeiodination

To a 2 mL microwave vial were added an iodoarene (1.0 eq.), $[CpRu(NCMe)_3][PF_6]$ (5 or 10 mol %), DBU (1.0 eq.) and degassed 1-octanol (1 mL), then the vial was sealed and the mixture heated in a microwave reactor at 180 °C for a specified period of time. Conversion (%) was measured using ^1H NMR spectroscopy by comparing the aromatic peaks of the product (ca. 6.8 and 7.0 ppm) and starting material (ca. 7.0 and 7.2 ppm).

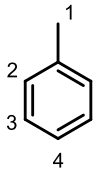

*Toluene (**5.8**)*

^1H NMR (400 MHz, $CDCl_3$) δ 7.20-7.14 (2H, m, H^3), 7.13-7.03 (3H, m, H^2 and H^4), 2.28 (3H, s, H^1).

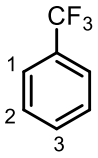

*α,α,α-Trifluorotoluene (**5.9**)*

^1H NMR (400 MHz, $CDCl_3$) δ 7.60-7.54 (2H, m, H^1), 7.54-7.47 (1H, m, H^3), 7.47-7.40 (2H, m, H^2).

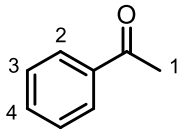

*Acetophenone (**5.10**)*

^{1}H NMR (400 MHz, $CDCl_3$) δ 7.87 (2H, d, J 7.6 Hz, H^2), 7.48 (1H, t, J 7.5 Hz, H^4), 7.37 (2H, t, J 7.6 Hz, H^3), 2.52 (3H, s, H^1).

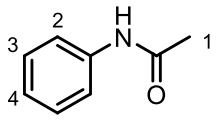

*N-Phenylacetamide (**5.11**)*

^{1}H NMR (400 MHz, $CDCl_3$) δ 7.51 (2H, d, J 7.5 Hz, H^2), 7.34-7.29 (2H, m, H^3), 7.10 (1H, t, J 7.4, H^4), 2.18 (3H, s, H^1).

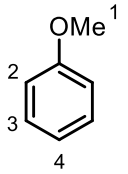

*Anisole (**5.12**)*

^{1}H NMR (400 MHz, $CDCl_3$) δ 7.20 (2H, dd, J 8.6, 7.2 Hz, H^3), 6.90-6.77 (3H, m, H^2 and H^4), 3.73 (3H, s, H^1).

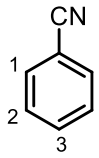

*Benzonitrile (**5.13**)*

^{1}H NMR (400 MHz, $CDCl_3$) δ 2.63 (2H, d, J 7.7 Hz, H^1), 7.58 (1H, t, J 7.7 Hz, H^3), 7.15 (2H, t, J 7.7 Hz, H^2).

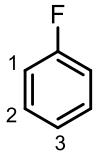

*Fluorobenzene (**5.14**)*

^{1}H NMR (400 MHz, $CDCl_3$) δ 7.65-7.59 (2H, m, H^2), 7.36-7.28 (1H, m, H^3), 7.14-7.09 (2H, m, H^1).

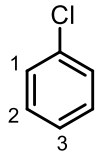

*Chlorobenzene (**5.15**)*

^{1}H NMR (400 MHz, $CDCl_3$) 7.35-7.26 (4H, m, H^1 and H^2), 7.25-7.19 (1H, m, H^3)

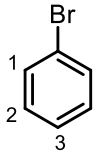

*Bromobenzene (**5.16**)*

^{1}H NMR (400 MHz, $CDCl_3$) δ 7.49 (2H, d, J 8.3 Hz, H^1), 7.32-7.26 (1H, m, H^3), 7.23 (2H, t, J 8.5 Hz, H^2).

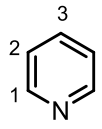

*Pyridine (**5.17**)*

^{1}H NMR (400 MHz, $CDCl_3$) δ 8.56-8.47 (2H, m, H^1), 7.65 (1H, t, J 7.7 Hz, H^3), 7.30-7.22 (2H, m, H^2).

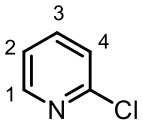

*2-Chloropyridine (**5.18**)*

^{1}H NMR (400 MHz, $CDCl_3$) δ 8.28 (1H, d, J 4.9 Hz, H^1), 7.59 (1H, t, J 7.9 Hz, H^3), 7.26-7.22 (1H, m, H^4), 7.15 (1H, dd, J 7.4, 5.1 Hz, H^2).

Data Analysis for Ru-Catalysed Hydrodeiodination

Data analysis was performed using MestReNova version 10.0.0. Open the ^{1}H NMR spectrum of the reaction mixture at a given time > select 'baseline' > 'Baseline correction' > 'Whittaker smoother'. Integrals were converted to % conversions according to equation 1.

In MS excel, the hammett parameter, σ, was plotted against % conversion and a trendline was generated to observe any correlation between EWG potential of the substituent, R, and % conversion.

References

1 E. O. Fischer and W. Hafner, *Über Aromatenkomplexe von Met. I*, 1955, **10**, 665–668.

2 K. Kündig, E. Peter, Semmelhack, M. F, Chlenov, A, Pape, A, Harman, W. D, Uemura, M, Schmalz, H. G, Gotov, B, Bottcher, A, Rigby, J. H, Kondratenkov, M, A, Munizz, *Transition Metal Arene Pi-Complexes in Organic Synthesis and Catalysis*, Springer, Berlin, 2004.

3 J. W. Walton and L. A. Wilkinson, *Organomet. Chem.*, 2019, **42**, 125–171

4 S. Takemoto and H. Matsuzaka, *Tetrahedron Lett.*, 2018, **59**, 697–703.

5 L. J. Williams, Y. Bhonoah, L. A. Wilkinson and J. W. Walton, *Chem. - A Eur. J.*, 2021, **27**, 3650–3660.

6 C. A. L. Mahaffy and P. L. Pauson, *Reagents Transit. Met. Complex Organomet. Synth.*, 1990, **28**, 136–191.

7 M. Tamm, T. Bannenberg, R. Fröhlich, S. Grimme and M. Gerenkamp, *J. Chem. Soc. Dalt. Trans.*, 2004, **4**, 482–491.

8 M. F. Semmelhack, W. Seufert and L. Keller, *J. Am. Chem. Soc.*, 1980, **102**, 6584–6586.

9 M. F. Semmelhack, J. Bisaha and M. Czarny, *J. Am. Chem. Soc.*, 1979, **101**, 768–770.

10 R. P. Houghton, M. Voyle and R. Price, *J. Organomet. Chem.*, 1983, **259**, 183–188.

11 P. Ricci, K. Krämer, X. C. Cambeiro and I. Larrosa, *J. Am. Chem. Soc.*, 2013, **135**, 13258–13261.

12 D. Whitaker, J. Burés and I. Larrosa, *J. Am. Chem. Soc.*, 2016, **138**, 8384–8387.

13 P. Ricci, K. Krämer and I. Larrosa, *J. Am. Chem. Soc.*, 2014, **136**, 18082–18086.

14 R. E. Banks, S. N. Mohialdin-Khaffaf, G. S. Lal, I. Sharif and R. G. Syvret, *J. Chem. Soc. Chem. Commun.*, 1992, 595–596.

15 S. L. Mukerjee, R. F. Lang, T. Ju, G. Kiss and C. D. Hoff, *Inorg. Chem.*, 1992, **31**, 4885–4889.

16 E. P. Kündig, C.-H. Fabritius, G. Grossheimann, P. Romanens, H. Butenschön and H. G. Wey, *Organometallics*, 2004, **23**, 3741–3744.

17 A. J. Pearson and P. R. Bruhn, *J. Org. Chem.*, 1991, **56**, 7092–7097.

18 A. J. Pearson, J. G. Park and P. Y. Zhu, *J. Org. Chem.*, 1992, **57**, 3583–3589.

19 A. J. Pearson and H. Shin, *J. Org. Chem.*, 1994, **59**, 2314–2323.

20 A. J. Pearson and H. Shin, *Tetrahedron*, 1992, **48**, 7527–7538.

21 A. J. Pearson and H. Shin, *J. Org. Chem.*, 1994, **59**, 2314–2323.

22 Y. K. Chung, H. S. Choi and D. A. Sweigart, 1982, 4245–4247.

23 A. Eloi, F. Rose-Munch, E. Rose, A. Pille, P. Lesot and P. Herson, *Organometallics*, 2010, **29**, 3876–3886.

24 D. Cetiner, L. Norel, J. P. Tranchier, F. Rose-Munch, E. Rose and P. Herson, *Organometallics*, 2010, **29**, 1778–1788.

25 W. H. Miles, C. M. Madison, C. Y. Kim, D. J. Sweitzer, S. D. Valent and D. M. Thamattoor, *J. Organomet. Chem.*, 2017, **851**, 218–224.

26 R. Alberto, G. Meola and D. H. Valdés, *Adv. Bioorganometallic Chem.*, 2018, 215–241.

27 G. Meola, H. Braband, D. Hernández-Valdés, C. Gotzmann, T. Fox, B. Spingler and R. Alberto, *Inorg. Chem.*, 2017, **56**, 6297–6301.

28 D. Hernández-Valdés, F. Avignon, P. Müller, G. Meola, B. Probst, T. Fox, B. Spingler and R. Alberto, *Dalt. Trans.*, 2020, **49**, 5250–5256.

29 E. P. Kündig, P. Jeger and G. Bernardinelli, *Inorganica Chim. Acta*, 2004, **357**, 1909–1919.

30 M. P. Luecke, D. Porwal, A. Kostenko, Y. P. Zhou, S. Yao, M. Keck, C. Limberg, M. Oestreich and M. Driess, *Dalt. Trans.*, 2017, **46**, 16412–16418.

31 B. M. Trost and C. M. Older, *Organometallics*, 2002, **21**, 2544–2546.

32 E. Kayahara, V. K. Patel, A. Mercier, E. P. Kündig and S. Yamago, *Angew. Chemie - Int. Ed.*, 2016, **55**, 302–306.

33 J. M. Cross, T. R. Blower, N. Gallagher, J. H. Gill, K. L. Rockley and J. W. Walton, *Chempluschem*, 2016, **81**, 1276–1280.

34 J. W. Walton and J. M. J. Williams, *Chem. Commun.*, 2015, **51**, 2786–2789.

35 R. G. Sutherland, A. Piorko, U. S. Gill and C. C. Lee, *J. Heterocycl. Chem.*, 1981, **19**, 801–803.

36 R. C. Cambie, S. J. Janssen, P. S. Rutledge and P. D. Woodgate, *J. Organomet. Chem.*, 1991, **420**, 387–418.

37 R. C. Cambie, G. R. Clark, S. L. Coombe, S. A. Coulson, P. S. Rutledge and P. D. Woodgate, *J. Organomet. Chem.*, 1996, **507**, 1–21.

38 J. P. Storm and C. M. Andersson, *J. Org. Chem.*, 2000, **65**, 5264–5274.

39 T. Ruhland, K. S. Bang and K. Andersen, *J. Org. Chem.*, 2002, **67**, 5257–5268.

40 F. Christopher Pigge, J. J. Coniglio and S. Fang, *Organometallics*, 2002, **21**, 4505–4512.

41 F. C. Pigge, J. J. Coniglio and N. P. Rath, *Org. Lett.*, 2003, **5**, 2011–2014.

42 F. C. Pigge, J. J. Coniglio and R. Dalvi, *J. Am. Chem. Soc.*, 2006, **128**, 3498–3499.

43 F. Christopher Pigge, R. Dhanya and D. C. Swenson, *Organometallics*, 2009, **28**, 3869–3875.

44 C. N. Neumann, J. M. Hooker and T. Ritter, *Nature*, 2016, **534**, 369–373.

45 M. H. Beyzavi, D. Mandal, M. G. Strebl, C. N. Neumann, E. M. D'Amato, J. Chen, J. M. Hooker and T. Ritter, *ACS Cent. Sci.*, 2017, **3**, 944–948.

46 J. A. Pike and J. W. Walton, *Chem. Commun.*, 2017, **53**, 9858–9861.

47 L. A. Wilkinson, J. A. Pike and J. W. Walton, *Organometallics*, 2017, **36**, 4376–4381.

48 H. Boennemann, R. Goddard, J. Grub, R. Mynott, E. Raabe and S. Wendel, *Organometallics*, 1989, **8**, 1941–1958.

49 A. R. Kudinov, E. V. Mutseneck and D. A. Loginov, *Coord. Chem. Rev.*, 2004, **248**, 571–585.

50 S. D. Pike, A. L. Thompson, A. G. Algarra, D. C. Apperley, S. A. Macgregor and A. S. Weller, *Science*, 2012, **337**, 1648–1651.

51 S. D. Pike, M. R. Crimmin and A. B. Chaplin, *Chem. Commun.*, 2017, **53**, 3615–3633.

52 L. I. Goryunov, N. M. Romanova, G. S. Zhilovskii and V. D. Shteingarts, *Russ. J. Org. Chem.*, 2007, **43**, 1765–1772.

53 E. M. D'Amato, C. N. Neumann and T. Ritter, *Organometallics*, 2015, **34**, 4626–4631.

54 M. F. Semmelhack, A. Chlenov and D. M. Ho, *J. Am. Chem. Soc.*, 2005, **127**, 7759–7773.

55 T. G. Traylor and K. Stewart, *Organometallics*, 1984, **3**, 325–327.

56 T. G. Traylor, K. J. Stewart and M. J. Goldberg, *Organometallics*, 1986, **5**, 2062–2067.

57 T. G. Traylor, K. J. Stewart and M. J. Goldberg, *J. Am. Chem. Soc.*, 1984, **106**, 4445–4454.

58 Z. C.L., S. S.L., R. S.A. and W. B.R., *J. Chem. Res., Synop.*, 1980, **108**, 1289–1297.

59 P. L. PAUSON and C. A. L. MAHAFFY, *J. Chem. Res., Synop.*, 1977, 1752–1775.

60 B. R. Jagirdar and K. J. Klabunde, *J. Coord. Chem.*, 1995, **34**, 31–43.

61 D. S. Perekalin and A. R. Kudinov, *Coord. Chem. Rev.*, 2014, **276**, 153–173.

62 A. I. Konovalov, E. E. Karslyan, D. S. Perekalin, Y. V. Nelyubina, P. V. Petrovskii and A. R. Kudinov, *Mendeleev Commun.*, 2011, **21**, 163–164.

63 T. Shibasaki, N. Komine, M. Hirano and S. Komiya, *J. Organomet. Chem.*, 2007, **692**, 2385–2394.

64 D. S. Perekalin, E. E. Karslyan, P. V. Petrovskii, A. O. Borissova, K. A. Lyssenko and A. R. Kudinov, *Eur. J. Inorg. Chem.*, 2012, 1485–1492.

65 M. Rioja, P. Hamon, T. Roisnel, S. Sinbandhit, M. Fuentealba, K. Letelier, J. Y. Saillard, A. Vega and J. R. Hamon, *Dalt. Trans.*, 2015, **44**, 316–329.

66 J. M. Lynam, L. M. Milner, N. S. Mistry, J. M. Slattery, S. R. Warrington and A. C. Whitwood, *Dalt. Trans.*, 2014, **43**, 4565–4572.

67 R. Makhoul, J. A. Shaw-Taberlet, H. Sahnoune, V. Dorcet, S. Kahlal, J. F. Halet, J. R. Hamon and C. Lapinte, *Organometallics*, 2014, **33**, 6023–6032.

68 A. Decken, J. F. Britten and M. J. McGlinchey, *J. Am. Chem. Soc.*, 1993, **115**, 7275–7284.

69 R. T. C. Pays-bas, E. P. Kündig, M. Kondratenko and P. Romanens, *Angew. Chemie - Int. Ed.*, 1998, 3146–3148.

70 M. F. Semmelhack, A. Chlenov, L. Wu and D. Ho, *J. Am. Chem. Soc.*, 2001, **123**, 8438–8439.

71 R. J. Lavallee and C. Kutal, *J. Organomet. Chem.*, 1998, **562**, 97–104.

72 A. J. Pearson, J. G. Park, S. H. Yang and Y.-H. Chuang, *J. Chem. Soc. Chem. Commun.*, 1989, 1363–1364.

73 K. R. Mann and T. P. Gill, *Inorg. Chem.*, 1983, **22**, 1986–1991.

74 T. P. Gill and K. R. Mann, *Inorg. Chem.*, 1980, **19**, 3007–3010.

75 M. G. Choi, T. C. Ho and R. J. Angelici, *Organometallics*, 2008, **27**, 1098–1105.

76 E. E. Karslyan, D. S. Perekalin, P. V. Petrovskii, A. O. Borisova and A. R. Kudinov, *Russ. Chem. Bull. Int. Ed.*, 2009, **58**, 585–588.

77 K. R. Mann, A. M. Blough, J. L. Schrenk, R. S. Koefod, D. A. Freedman and J. R. Matachek, *Pure Appl. Chem.*, 1995, **67**, 95–101.

78 R. P. Houghton, M. Voyle and R. Price, *J. Chem. Soc. Perkin Trans. 1*, 1984, 925–931.

79 M. Otsuka, K. Endo and T. Shibata, *Chem. Commun.*, 2010, **46**, 336–338.

80 B. R. J. Mueller and N. D. Schley, *Dalt. Trans.*, 2020, **49**, 10114–10119.

81 M. Otsuka, H. Yokoyama, K. Endo and T. Shibata, *Synlett*, 2010, 2601–2606.

82 Q. K. Kang, Y. Lin, Y. Li and H. Shi, *J. Am. Chem. Soc.*, 2020, **142**, 3706–3711.

83 Q. K. Kang, Y. Lin, Y. Li, L. Xu, K. Li and H. Shi, *Angew. Chemie - Int. Ed.*, 2021, **60**, 20391–20399.

84 A. I. Konovalov, E. O. Gorbacheva, F. M. Miloserdov and V. V. Grushin, *Chem. Commun.*, 2015, **51**, 13527–13530.

85 D. Astruc, J. R. Hamon, E. Roman and P. Michaud, *J. Am. Chem. Soc.*, 1981, **103**, 7502–7514.

86 S. Takemoto, E. Shibata, M. Nakajima, Y. Yumoto, M. Shimamoto and H. Matsuzaka, *J. Am. Chem. Soc.*, 2016, **138**, 14836–14839.

87 M. Utsunomiya and J. F. Hartwig, *J. Am. Chem. Soc.*, 2004, **126**, 2702–2703.

88 J. Takaya and J. F. Hartwig, *J. Am. Chem. Soc.*, 2005, **127**, 5756–5757.

89 M. Otsuka, H. Yokoyama, K. Endo and T. Shibata, *Org. Biomol. Chem.*, 2012, **10**, 3815–3818.

90 A. G. Sergeev and J. F. Hartwig, *Science*, 2011, **332**, 439–443.

91 N. I. Saper and J. F. Hartwig, *J. Am. Chem. Soc.*, 2017, **139**, 17667–17676.

92 B. Sawatlon, T. Wititsuwannakul, Y. Tantirungrotechai and P. Surawatanawong, *Dalt. Trans.*, 2014, **43**, 18123–18133.

93 F. Zhu and Z. X. Wang, *Adv. Synth. Catal.*, 2013, **355**, 3694–3702.

94 T. Harada, Y. Ueda, T. Iwai and M. Sawamura, *Chem. Commun.*, 2018, **54**, 1718–1721.

95 T. L. Gianetti, R. G. Bergman and J. Arnold, *Chem. Sci.*, 2014, **5**, 2517–2524.

96 N. C. Tomson, J. Arnold and R. G. Bergman, *Dalt. Trans.*, 2011, **40**, 7718–7729.

97 J. M. O'Connor, S. J. Friese and B. L. Rodgers, *J. Am. Chem. Soc.*, 2005, **127**, 16342–16343.

98 T. P. Lockhart, P. B. Comita and R. G. Bergman, *J. Am. Chem. Soc*, 1981, **I**, 4082–4090.

99 K. Müller, C. Faeh and F. Diederich, *Science*, 2007, **317**, 1881–1886.

100 P. Jeschke, *ChemBioChem*, 2004, 5, 570–589.

101 R. Berger, G. Resnati, P. Metrangolo, E. Weber and J. Hulliger, *Chem. Soc. Rev.*, 2011, 40, 3496–3508.

102 D. O'Hagan, *Chem. Soc. Rev.*, 2008, **37**, 308–319.

103 S. Purser, P. R. Moore, S. Swallow and V. Gouverneur, *Chem. Soc. Rev.*, 2008, **37**, 320–330.

104 L. E. Forslund and N. Kaltsoyannis, *New J. Chem.*, 2003, **27**, 1108–1114.

105 D. M. Lemal, *J. Org. Chem.*, 2004, 69, 1–11.

106 G. S. Lal, G. P. Pez and R. G. Syvret, *Chem. Rev.*, 2002, **96**, 1737–1756.

107 S. Singh, D. D. DesMarteu, S. S. Zuberi, M. Witz and H. Huang, *J. Am. Chem. Soc.*, 1987, **109**, 7194–7196.

108 E. Differding and H. Ofner, *Synlett*, 1991, 187–189.

109 W. E. barnette, *J. Am. Chem. Soc.*, 1984, **106**, 452–454.

110 S. H. Lee and J. Schwartz, *J. Am. Chem. Soc.*, 1986, **108**, 2445–2447.

111 T. Umemoto and G. Tomizawa, *Preparation of 2-Fluoropyridines via Base-Induced Decomposition of N-Fluoropyridinium Salts1*, 1989, vol. 54.

112 L. Strekowski and A. S. Kiselyov, in *Advances in Heterocyclic Chemistry*, 1995, vol. 62, pp. 1–17.

113 R. E. Banks, R. A. Du Boisson, W. D. Morton and E. Tsiliopoulos, *J. Chem. Soc., Perkin Trans. 1*, 2004, 2805–2811.

114 R. E. Banks, R. A. Du Boisson and E. Tsiliopoulos, *J. Fluor. Chem.*, 1986, **32**, 461–466.

115 C. I. Tewksbury, B. C. I. Tewksbury and H. M. Haendler, *J. Am. Chem. Soc.*, 1949, **71**, 2336–2337.

116 A. I. Vogel, J. Leicester and W. A. T. Macey, in *Organic Syntheses*, John Wiley & Sons, Inc., 2003, pp. 40–40.

117 C. G. Bergstrom, R. T. Nicholson and R. M. Dodson, *J. Org. Chem.*, 1963, **28**, 2633–2640.

118 G. A. Olah, J. T. Welch, Y. D. Vankar, M. Nojima, I. Kerekes and J. A. Olah, *J. Org. Chem.*, 1979, **44**, 3872–3881.

119 G. Balz and G. Schiemann, *Eur. J. Inorg. Chem.*, 1927, 1186–1190.

120 D. T. Flood, *Org. Synth.*, 1933, **13**, 46–50.

121 T. Mohy El Dine, O. Sadek, E. Gras and D. M. Perrin, *Chem. - A Eur. J.*, 2018, **24**, 14933–14937.

122 P. S. Fier and J. F. Hartwig, *Science*, 2013, **342**, 956–960.

123 P. S. Fier and J. F. Hartwig, *J. Am. Chem. Soc.*, 2014, **136**, 10139–10147.

124 A. P. Lothian and C. A. Ramsden, *Synlett*, 1993, **10**, 753–755.

125 P. S. Fier and J. F. Hartwig, *J. Am. Chem. Soc.*, 2012, **134**, 10795–10798.

126 H. G. Lee, P. J. Milner and S. L. Buchwald, *J. Am. Chem. Soc.*, 2014, **136**, 3792–3795.

127 B. T. Loughrey, B. V. Cunning, P. C. Healy, C. L. Brown, P. G. Parsons and M. L. Williams, *Chem. - An Asian J.*, 2012, **7**, 112–121.

128 J. A. Pike and J. W. Walton, *Chem. Commun.*, 2017, **53**, 9858–9861.

129 R. M. Moriarty, Y. Y. Ku and U. S. Gill, *Organometallics*, 1988, **7**, 660–665.

130 G. K. S. Prakash and Z. Zhang, *New Nucleophilic Fluoroalkylations*, Elsevier Inc., 2017.

131 E. Buncel, J. M. Dust and F. Terrier, *Chem. Rev.*, 1995, **95**, 2261–2280.

132 N. Selvakumar, B. Y. Reddy, G. S. Kumar and J. Iqbal, *Tetrahedron Lett.*, 2002, **43**, 4125.

133 R. J. Snow, T. Butz, A. Hammach, S. Kapadia, T. M. Morwick, A. S. Prokopowicz, H. Takahashi, J. D. Tan, M. A. Tschantz and X. J. Wang, *Tetrahedron Lett.*, 2002, **43**, 7553–7556.

134 N. J. Lawrence, C. A. Davies and M. Gray, *Org. Lett.*, 2004, **6**, 4957–4960.

135 G. Islas-Gonzalez, M. Bois-Choussy and J. Zhu, *Org. Biomol. Chem.*, 2003, **1**, 30–32.

136 K. C. Nicolaou, H. Li, C. N. C. Boddy, J. M. Ramanjulu, T. Y. Yue, S. Natarajan, X. J. Chu, S. Bräse and F. Rübsam, *Chem. - A Eur. J.*, 1999, **5**, 2584–2601.

137 K. C. Nicolaou, C. N. C. Boddy, H. Li, A. E. Koumbis, R. Hughes, S. Natarajan, N. F. Jain, J. M. Ramanjulu, S. Bräse and M. E. Solomon, *Chem. - A Eur. J.*, 1999, **5**, 2602–2621.

138 M. Bella, S. Kobbelgaard and K. A. Jørgensen, *J. Am. Chem. Soc.*, 2005, **127**, 3670–3671.

139 T. Smejkal, V. Gopalsamuthiram, S. K. Ghorai, A. M. Jawalekar, D. Pagar, K. Sawant, S. Subramanian, J. Dallimore, N. Willetts, J. N. Scutt, L. Whalley, M. Hotson, A. M. Hogan and G. Hodges, *Org. Process Res. Dev.*, 2017, **21**, 1625–1632.

140 J. M. Fox, X. Huang, A. Chieffi and S. L. Buchwald, *J. Am. Chem. Soc.*, 2000, **122**, 1360–1370.

141 A. M. Wilders, J. Henle, M. C. Haibach, R. Swiatowiec, J. Bien, R. F. Henry, S. O. Asare, A. L. Wall and S. Shekhar, *ACS Catal.*, 2020, **10**, 15008–15018.

142 J. N. Scutt, S. A. M. Jeanmart, C. J. Mathews, M. Muehlebach, T. Smejkal, S. C. Smith, H. Smits, J. S. Wailes, W. G. Whittingham and N. J. Willetts, *ACS Symp. Ser.*, 2015, **1204**, 291–304.

143 J. Morgan and J. T. Pinhey, *J. Chem. Soc., Perkin Trans 1*, 1990, 715–720.

144 F. C. Pigge and S. Fang, *Tetrahedron Lett.*, 2001, **42**, 17–20.

145 V. Gupta and K. S. Carroll, *Chem. Sci.*, 2016, **7**, 400–415.

146 F. M. Wong, J. R. Keeffe and W. Wu, *Tetrahedron Lett.*, 2002, **43**, 3561–3564.

147 P. F. Vogt and J. J. Gerulis, *A Compr. Guid. to Hazard. Prop. Chem. Subst.*, 2006, **2**, 699–718.

148 E. Vitaku, D. T. Smith and J. T. Njardarson, *J. Med. Chem.*, 2014, **57**, 10257–10274.

149 P. A. Forero-Cortés and A. M. Haydl, *Org. Process Res. Dev.*, 2019, **23**, 1478–1483.

150 M. Kosugi, M. Kameyama and T. Migita, *Chem. Lett.*, 1983, 927–928.

151 L. Dale Boger and J. S. Panek, *Tetrahedron Lett.*, 1984, **25**, 3175–3178.

152 F. Paul, J. Patt and J. F. Hartwig, *J. Am. Chem. Soc.*, 1994, 5969–5970.

153 S. L. Buchwald and A. S. Guram, *J. Am. Chem. Soc.*, 1994, **116**, 7901–7902.

154 J. Louie and J. F. Hartwig, *Tetrahedron Lett.*, 1995, **36**, 3609–3612.

155 A. S. Guram, R. A. Rennels and S. L. Buchwald, *Angew. Chemie Int. Ed. English*, 1995, **34**, 1348–1350.

156 M. S. Driver and J. F. Hartwig, *J. Am. Chem. Soc.*, 1996, **118**, 7217–7218.

157 J. P. Wolfe, S. Wagaw and S. L. Buchwald, *J. Am. Chem. Soc.*, 1996, **118**, 7215–7216.

158 J. Louie, M. S. Driver, B. C. Hamann and J. F. Hartwig, *J. Org. Chem.*, 1997, **62**, 1268–1273.

159 K. W. Anderson, R. E. Tundel, T. Ikawa, R. A. Altman and S. L. Buchwald, *Angew. Chemie - Int. Ed.*, 2006, **45**, 6523–6527.

160 T. Ikawa, T. E. Barder, M. R. Biscoe and S. L. Buchwald, *J. Am. Chem. Soc.*, 2007, **129**, 13001–13007.

161 Q.-L. Yang, X.-Y. Wang, J.-Y. Lu, L.-P. Zhang, P. Fang and T.-S. Mei, *J. Am. Chem. Soc.*, 2018, **140**, 11487–11494.

162 D. G. Brown and J. Boström, *J. Med. Chem.*, 2016, **59**, 4443–4458.

163 F. Alonso, I. P. Beletskaya and M. Yus, *Chem. Rev.*, 2002, **102**, 4009–4091.

164 E. C. Kendall, *J. Am. Med. Assoc*, 1915, **LXIV**, 2042–2043.

165 M. Yus, *Chem. Soc. Rev.*, 1996, **25**, 155–161.

166 N. Rot and F. Bickelhaupt, *Organometallics*, 1997, **16**, 5027–5031.

167 C. Ferrayoli, E. Austin, R. A. Alonso and R. A. Rossi, *Tetrahedron*, 1993, **49**, 4495–4502.

168 A. A. M. Lapis, O. C. Kreutz, A. R. Pohlmann and V. E. U. Costa, *Tetrahedron Asymmetry*, 2001, **12**, 557–561.

169 M. S. Hong, L. He, B. E. Dale and K. C. Donnelly, *Environ. Sci. Technol.*, 1995, **29**, 702–708.

170 A. M. El Massry, A. Amer and C. U. Pittman, *Synth. Commun.*, 1990, **20**, 1091–1094.

171 H. Nishiyama, K. Isaka, K. Itoh, K. Ohno, H. Nagase, K. Matsumoto and H. Yoshiwara, *J. Org. Chem.*, 1992, **57**, 407–410.

172 M. Abarbri, J. Thibonnet, L. Bérillon, F. Dehmel, M. Rottländer and P. Knochel, *J. Org. Chem.*, 2000, **65**, 4618–4634.

173 R. A. O'Brien, T. Chen and R. D. Rieke, *J. Org. Chem.*, 1992, **57**, 2667–2677.

174 H. M. Walborsky and C. Hamdouchi, *J. Org. Chem.*, 1993, **58**, 1187–1193.

175 N. A. Cortese and R. F. Heck, *J. Org. Chem.*, 1977, **42**, 3491–3494.

176 A. Ramanathan and L. S. Jimenez, *Synthesis (Stuttg).*, 2010, 217–220.

177 A. Dewanji, C. Mück-Lichtenfeld and A. Studer, *Angew. Chemie - Int. Ed.*, 2016, **55**, 6749–6752.

178 T. Hokamp, A. Dewanji, M. Lübbesmeyer, C. Mück-Lichtenfeld, E. U. Würthwein and A. Studer, *Angew. Chemie - Int. Ed.*, 2017, **56**, 13275–13278.

179 J. Broggi, T. Terme and P. Vanelle, *Angew. Chemie Int. Ed.*, 2014, **53**, 384–413.

180 T. Naito, A. Saito, M. Ueda and O. Miyata, *Heterocycles*, 2005, **65**, 18571869.

181 C. A. Merlic, M. M. Miller, B. N. Hietbrink and K. N. Houk, *J. Am. Chem. Soc.*, 2001, **123**, 4904–4918.

Appendices

1. Crystallography Data

The X-ray single crystal data have been collected using λMoKα radiation (λ =0.71073Å) on an Agilent XCalibur (Sapphire-3 CCD detector, fine-focus sealed tube, graphite monochromator) diffractometer equipped with a Cryostream (Oxford Cryosystems) open-flow nitrogen cryostat at the temperature 120.0(2)K. The structure was solved by direct method and refined by full-matrix least squares on F^2 for all data using Olex2 [3] and SHELXTL [4] software. All non-hydrogen atoms were refined anisotropically, hydrogen atoms were placed in the calculated positions and refined in riding mode. Crystal data and parameters of refinement are listed in Tables S1-S5. Crystallographic data for the structure have been deposited with the Cambridge Crystallographic Data Centre as supplementary publication CCDC-2170169 (**3.1A**), 2170171 (**3.1B**), 2170174 (**3.2A**), 2170175 (**3.2B**), 2170173 (**3.3A**), 2170172 (**3.3B**) and 2170170 (**3.3C**).

1a. Complex 2.14/3.1B

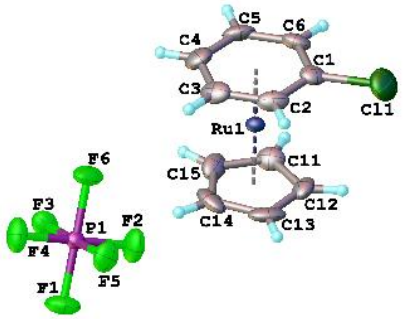

Table 1. Crystal data and structure refinement for Ru complex **2.14/3.1B**

Empirical formula	$[C_{11}H_{10}ClRu]PF_6$
Formula weight	423.68
Temperature/K	120.0
Crystal system	monoclinic
Space group	$P2_1/n$
a/Å	9.0165(4)
b/Å	13.3485(6)
c/Å	10.9347(5)
α/°	90
β/°	91.0311(18)
γ/°	90
Volume/Å^3	1315.85(10)
Z	4
ρ_{calc}g/cm^3	2.139
μ/mm^{-1}	1.572
F(000)	824.0
Crystal size/mm^3	0.19 × 0.11 × 0.07
Radiation	MoKα (λ = 0.71073)
2Θ range for data collection/°	4.816 to 58.994
Index ranges	$-12 \leq h \leq 12$, $-18 \leq k \leq 18$, $-15 \leq l \leq 15$
Reflections collected	20662
Independent reflections	3659 [R_{int} = 0.0316, R_{sigma} = 0.0228]
Data/restraints/parameters	3659/0/181
Goodness-of-fit on F^2	1.028
Final R indexes [I>=2σ (I)]	R_1 = 0.0189, wR_2 = 0.0398
Final R indexes [all data]	R_1 = 0.0261, wR_2 = 0.0417
Largest diff. peak/hole / e Å^{-3}	0.39/-0.40

1b. Complex 2.16/3.1A

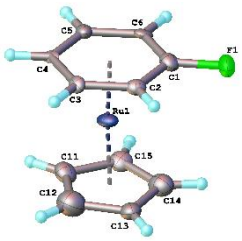

Table 2. Crystal data and structure refinement for Ru complex **2.16/3.1A**

Empirical formula	$[C_{11}H_{10}FRu]PF_6$
Formula weight	407.23
Temperature/K	120.0
Crystal system	monoclinic
Space group	C2
a/Å	8.9922(2)
b/Å	9.5814(3)
c/Å	7.2372(2)
α/°	90
β/°	96.5700(10)
γ/°	90
Volume/$Å^3$	619.45(3)
Z	2
$\rho_{calc}g/cm^3$	2.183
μ/mm^{-1}	1.467
F(000)	396.0
Crystal size/mm^3	0.14 × 0.12 × 0.06
Radiation	Mo Kα (λ = 0.71073)
2Θ range for data collection/°	5.666 to 59.986
Index ranges	$-12 \leq h \leq 12, -13 \leq k \leq 13, -10 \leq l \leq 10$
Reflections collected	6340
Independent reflections	1782 [R_{int} = 0.0196, R_{sigma} = 0.0190]
Data/restraints/parameters	1782/67/126
Goodness-of-fit on F^2	1.089
Final R indexes [I>=2σ (I)]	R_1 = 0.0210, wR_2 = 0.0507
Final R indexes [all data]	R_1 = 0.0215, wR_2 = 0.0511
Largest diff. peak/hole / e $Å^{-3}$	0.60/-0.43
Flack parameter	0.57(7)

3c. Complex 3.2A

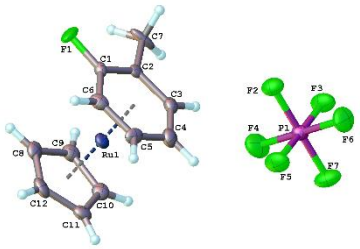

Table 3. Crystal data and structure refinement for Ru complex **3.2A**

Empirical formula	$[C_{12}H_{12}FRu]PF_6$
Formula weight	421.26
Temperature/K	120.00
Crystal system	monoclinic
Space group	$P2_1/n$
a/Å	9.0446(3)
b/Å	14.1266(4)
c/Å	10.6960(3)
α/°	90
β/°	90.0265(11)
γ/°	90
Volume/Å^3	1366.62(7)
Z	4
ρ_{calc}g/cm^3	2.047
μ/mm^{-1}	1.334
F(000)	824.0
Crystal size/mm^3	0.14 × 0.09 × 0.06
Radiation	Mo Kα (λ = 0.71073)
2Θ range for data collection/°	4.776 to 58.996
Index ranges	$-12 \leq h \leq 12$, $-19 \leq k \leq 19$, $-14 \leq l \leq 14$
Reflections collected	27182
Independent reflections	3817 [R_{int} = 0.0388, R_{sigma} = 0.0251]
Data/restraints/parameters	3817/96/240
Goodness-of-fit on F^2	1.069
Final R indexes [I>=2σ (I)]	R_1 = 0.0292, wR_2 = 0.0676
Final R indexes [all data]	R_1 = 0.0369, wR_2 = 0.0714
Largest diff. peak/hole / e Å^{-3}	0.99/-0.54

3d. Complex 3.2B

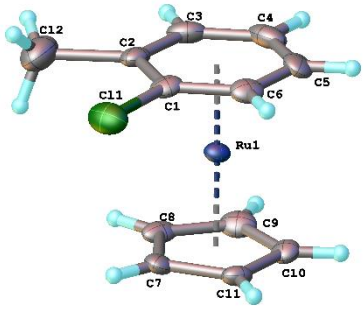

Table 4. Crystal data and structure refinement for Ru complex **3.2B**

Empirical formula	$[C_{12}H_{12}ClRu]PF_6$
Formula weight	437.71
Temperature/K	120
Crystal system	triclinic
Space group	P-1
a/Å	13.8713(6)
b/Å	13.8734(6)
c/Å	14.9953(7)
α/°	89.4442(16)
β/°	79.4373(16)
γ/°	89.6981(16)
Volume/Å^3	2836.7(2)
Z	8
ρ_{calc}g/cm^3	2.050
μ/mm^{-1}	1.462
F(000)	1712.0
Crystal size/mm^3	0.208 × 0.132 × 0.124
Radiation	MoKα (λ = 0.71073)
2Θ range for data collection/°	2.762 to 59.998
Index ranges	-19 ≤ h ≤ 19, -19 ≤ k ≤ 19, -21 ≤ l ≤ 21
Reflections collected	60601
Independent reflections	16458 [R_{int} = 0.0428, R_{sigma} = 0.0439]
Data/restraints/parameters	16458/0/758
Goodness-of-fit on F^2	1.059
Final R indexes [I>=2σ (I)]	R_1 = 0.0457, wR_2 = 0.1077
Final R indexes [all data]	R_1 = 0.0658, wR_2 = 0.1230
Largest diff. peak/hole / e Å^{-3}	1.06/-1.20

3e. Complex 3.3A

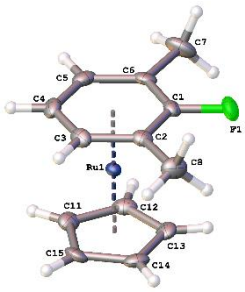

Table 5. Crystal data and structure refinement for Ru complex **3.3A**

Empirical formula	$[C_{13}H_{14}FRu]PF_6$
Formula weight	435.28
Temperature/K	120.00
Crystal system	monoclinic
Space group	$P2_1/c$
a/Å	7.0290(2)
b/Å	15.3782(5)
c/Å	13.9470(5)
α/°	90
β/°	103.0623(12)
γ/°	90
Volume/Å^3	1468.57(8)
Z	4
ρ_{calc}g/cm^3	1.969
μ/mm^{-1}	1.244
F(000)	856.0
Crystal size/mm^3	0.15 × 0.07 × 0.02
Radiation	Mo Kα (λ = 0.71073)
2Θ range for data collection/°	4 to 59.998
Index ranges	$-9 \le h \le 9$, $-21 \le k \le 21$, $-19 \le l \le 19$
Reflections collected	26106
Independent reflections	4275 [R_{int} = 0.0320, R_{sigma} = 0.0220]
Data/restraints/parameters	4275/24/222
Goodness-of-fit on F^2	1.089
Final R indexes [I>=2σ (I)]	R_1 = 0.0244, wR_2 = 0.0552
Final R indexes [all data]	R_1 = 0.0276, wR_2 = 0.0565
Largest diff. peak/hole / e Å^{-3}	1.35/-0.53

3f. Complex 3.3B

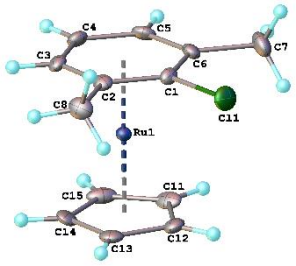

Table 6. Crystal data and structure refinement for Ru complex **3.3B**

Empirical formula	$[C_{13}H_{14}ClRu]PF_6$
Formula weight	451.73
Temperature/K	120.0
Crystal system	monoclinic
Space group	$P2_1$
a/Å	6.9414(2)
b/Å	15.3352(4)
c/Å	7.3463(2)
α/°	90
β/°	104.6140(10)
γ/°	90
Volume/Å^3	756.70(4)
Z	2
ρ_{calc}g/cm^3	1.983
μ/mm^{-1}	1.373
F(000)	444.0
Crystal size/mm^3	0.13 × 0.11 × 0.06
Radiation	Mo Kα (λ = 0.71073)
2Θ range for data collection/°	5.312 to 57.988
Index ranges	$-9 \le h \le 9$, $-20 \le k \le 20$, $-10 \le l \le 10$
Reflections collected	18388
Independent reflections	3986 [R_{int} = 0.0299, R_{sigma} = 0.0240]
Data/restraints/parameters	3986/1/202
Goodness-of-fit on F^2	1.047
Final R indexes [I>=2σ (I)]	R_1 = 0.0211, wR_2 = 0.0511
Final R indexes [all data]	R_1 = 0.0223, wR_2 = 0.0517
Largest diff. peak/hole / e Å^{-3}	2.02/-0.53
Flack parameter	0.51(4)

3g. Complex 3.3C

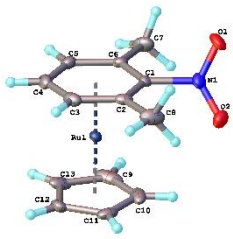

Table 7. Crystal data and structure refinement for Ru complex **3.3C**

Empirical formula	$[C_{13}H_{14}NO_2Ru]PF_6$
Formula weight	462.29
Temperature/K	120.0
Crystal system	monoclinic
Space group	$P2_1/c$
a/Å	16.7069(7)
b/Å	14.2729(6)
c/Å	14.1391(6)
α/°	90
β/°	112.2030(10)
γ/°	90
Volume/Å^3	3121.6(2)
Z	8
ρ_{calc}g/cm^3	1.967
μ/mm^{-1}	1.179
F(000)	1824.0
Crystal size/mm^3	0.23 × 0.2 × 0.15
Radiation	MoKα (λ = 0.71073)
2Θ range for data collection/°	3.882 to 60
Index ranges	$-23 \leq h \leq 23$, $-20 \leq k \leq 20$, $-19 \leq l \leq 19$
Reflections collected	52996
Independent reflections	9078 [R_{int} = 0.0295, R_{sigma} = 0.0214]
Data/restraints/parameters	9078/67/470
Goodness-of-fit on F^2	1.046
Final R indexes [I>=2σ (I)]	R_1 = 0.0249, wR_2 = 0.0572
Final R indexes [all data]	R_1 = 0.0293, wR_2 = 0.0593
Largest diff. peak/hole / e Å^{-3}	0.85/-0.77

1h. Complex 5.4

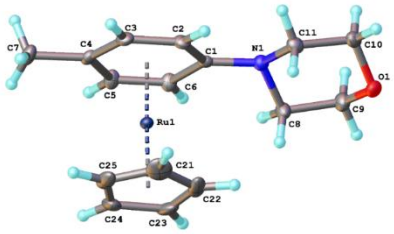

Table 8 Crystal data and structure refinement for complex **5.4**.

Empirical formula	$[C_{16}H_{20}NORu]PF_6$
Formula weight	488.37
Temperature/K	120.0
Crystal system	monoclinic
Space group	$P2_1/c$
a/Å	7.5415(9)
b/Å	21.148(2)
c/Å	11.1990(13)
α/°	90
β/°	95.700(4)
γ/°	90
Volume/Å^3	1777.3(4)
Z	4
ρ_{calc}g/cm^3	1.825
μ/mm^{-1}	1.037
F(000)	976.0
Crystal size/mm^3	0.26 × 0.24 × 0.13
Radiation	MoKα (λ = 0.71073)
2Θ range for data collection/°	5.31 to 59.996
Index ranges	$-10 \leq h \leq 10$, $-29 \leq k \leq 29$, $-15 \leq l \leq 15$
Reflections collected	38568
Independent reflections	5178 [R_{int} = 0.0316, R_{sigma} = 0.0176]
Data/restraints/parameters	5178/0/236
Goodness-of-fit on F^2	1.038
Final R indexes [I>=2σ (I)]	R_1 = 0.0199, wR_2 = 0.0476
Final R indexes [all data]	R_1 = 0.0235, wR_2 = 0.0489
Largest diff. peak/hole / e Å^{-3}	0.57/-0.48

References:

1 Dolomanov, O. V.; Bourhis, L. J.; Gildea, R. J.; Howard, J. A. K.; Puschmann, H. J. Appl. Crystallogr. 2009, 42, 339.

2 Sheldrick, G. M. Acta Crystallogr. Sect. A Found. Crystallogr. 2008, 64, 112

List of Publications

1. ‘As Nice as π: Aromatic Reactions Activated by π-Coordination to Transition Metals’, **L. J. Williams**, Y. Bhonoah, L. A. Wilkinson and J. W. Walton, *Chem. - A Eur. J.*, 2021, **27**, 3650–3660, DOI: 10.1002/chem.202004621

2. ‘Novel ruthenium complexes bearing bipyridine-based and N-heterocyclic carbene-supported pyridine (NCN) ligands: the influence of ligands on catalytic transfer hydrogenation of ketones’, A. Piyasaengthong, **L. J. Williams**, D. S. Yufit and J. W. Walton, *Dalt. Trans.*, 2022, **51**, 340–351, DOI: 10.1039/D1DT03240B

3. ‘Enolate S_NAr of Unactivated Arenes *via* $[(\eta^6\text{-arene})RuCp]^+$ Intermediates’, **L. J. Williams**, Y. Bhonoah and J. W. Walton, *Chem. Commun.*, 2022, DOI: 10.1039/D2CC02508F.